Validating Pathogen Reduction in Ozone-Biofiltration Water Reuse Applications

Samantha Hogard

Dissertation submitted to the faculty of the Virginia Polytechnic Institute and State University in partial fulfillment of the requirements for the degree of

Doctor of Philosophy

In

Civil Engineering

William R. Knocke, Chair

Charles B. Bott, Co-chair

Amy Pruden

Marc A. Edwards

December 8, 2023

Blacksburg, Virginia

Keywords: Water reuse, ozone, biologically activated carbon filtration, bromate, NDMA, 1,4-dioxane, oxidation, disinfection, virus, *Cryptosporidium, Giardia*

Validating Pathogen Reduction in Ozone-Biofiltration Water Reuse Applications

Samantha Hogard

Abstract

Advanced water treatment (AWT)/reuse has become a necessity for many utilities across the globe as the quantity and quality of water resources has been diminished. In some locations including California, the full-advanced treatment (FAT) train is mandated including membrane filtration, reverse osmosis, and UV advanced oxidation. The application of carbon-based treatment has emerged as a cost-effective alternative to FAT in locations that cannot manage brine disposal. However, considering the relative novelty of this treatment technology for water reuse, the process still requires full-scale validation of treatment goals including pathogen reduction. While there are many constituents of concern in water reuse, exposure to pathogens remains the greatest acute health risk. The studies described herein examine pathogen and microbial surrogate reduction both full-scale and pilot-scale floc/sed-ozone-biofiltration advanced water treatment facility. Both culture and molecular-based methods were used to demonstrate removal in this case and pilot challenge testing was employed to address the shortcomings of full-scale monitoring and to address additional research objectives.

The reduction of *Cryptosporidum, Giardia*, enteric viruses, pathogenic bacteria and their corresponding surrogate microorganisms (e.g. spore forming bacteria, coliphage) was quantified across the upstream wastewater treatment process and the AWT. In general, the removal of surrogate microorganisms was less than or equal that of the pathogens of interest thereby justifying their use in full-scale monitoring. Several limitations of full-scale monitoring were noted including low starting concentrations which resulted in large sample volume required to demonstrate log-reduction. Additionally, while molecular methods were sufficient to demonstrate reduction by physical treatment steps, they are unable to demonstrate inactivation. Therefore, ozone pilot testing was performed to evaluate the use of capsid integrity PCR for showing inactivation by ozonation. Additional testing was also performed to relate the LRV shown with culture methods to the LRV shown with PCR so as to create a relationship that can be used in future monitoring.

While pathogen inactivation is a major concern in water reuse, these objectives must also be balanced with the formation of disinfection byproducts (DBPs) through ozonation. Given the elevated concentration of dissolved organic matter, relatively higher ozone doses are required in reuse applications when compared with water treatment applications in order to achieve the desired treatment goals (oxidation, disinfection). Pilot scale ozone testing was performed to evaluate ozone disinfection performance in unfiltered secondary effluent while balancing the

formation of bromate and oxidation of trace organic contaminants (TrOCs). Two chemical bromate control methods were compared including preformed monochloramine (NH_2Cl), and hydrogen peroxide (H_2O_2). Neither of these bromate control methods had any demonstrable impact on virus or coliform inactivation, however H_2O_2 eliminated measurable ozone exposure which is necessary for the inactivation of more resistant spore forming bacteria. Additionally, NH_2Cl was shown to suppress *OH exposure and thus negatively impacted the oxidation of ozone resistant TrOCs, while H_2O_2 marginally improved TrOC oxidation.

Finally, the use of H_2O_2 for bromate control necessitates the validation of an alternative framework for ozone process control. The existing ozone Ct framework has been shown to be prohibitively conservative especially for virus inactivation. In this study, the applied specific ozone dose (O3:TOC) and the change in UV_{254} absorbance were evaluated as ozone monitoring frameworks across a range of water quality characteristics. Elevated temperature and pH were shown to significantly impact ozone decay kinetics, and only marginally impact virus inactivation. Both frameworks that were evaluated were shown to be valid across all water quality conditions evaluated.

Validating pathogen reduction across carbon-based reuse treatment trains is imperative in order to allow for more widespread application and regulatory confidence in the technology. Coagulation, floc/sed, ozone, and biofiltration were shown to be robust barriers for pathogen and surrogate reduction and recommended concentration and quantification methods are presented herein. The ozone challenge testing results also provide guidance to utilities using ozone for disinfection while controlling DBPs and enhancing organics oxidation in water reuse applications.

Validating Pathogen Reduction in Ozone-Biofiltration Water Reuse Applications

Samantha Hogard

General Audience Abstract

Water reuse has become a necessity for many utilities across the globe as the quantity and quality of water resources has been diminished. In some locations including California, the full-advanced treatment (FAT) train is required including membrane filtration, reverse osmosis, and UV advanced oxidation. The application of carbon-based treatment has emerged as a cost-effective alternative to FAT in locations that cannot manage brine disposal. However, considering the relative novelty of this treatment technology for water reuse, the process still requires full-scale validation of treatment goals including pathogen reduction. While there are many constituents of concern in water reuse, exposure to pathogens remains the greatest acute health risk. The studies described herein examine pathogen and microbial surrogate reduction both full-scale and pilot-scale floc/sed-ozone-biofiltration advanced water treatment facility. Both culture and molecular-based methods were used to demonstrate removal in this case and pilot challenge testing was employed to address the shortcomings of full-scale monitoring and to address additional research objectives.

The reduction of protozoa, viruses, bacteria and their corresponding surrogate microorganisms was quantified across the upstream wastewater treatment process and the water reuse treatment train. In general, the removal of surrogate microorganisms was less than or equal that of the pathogens of interest thereby justifying their use in full-scale monitoring. Several limitations of full-scale monitoring were noted including low starting concentrations which resulted in large sample volume required to demonstrate log-reduction. Additionally, while molecular methods were sufficient to demonstrate reduction by physical treatment steps, they are unable to demonstrate inactivation. Therefore, ozone pilot testing was performed to evaluate several methods to adapt these methods to reflect inactivation.

While pathogen inactivation is a major concern in water reuse, these objectives must also be balanced with the formation of disinfection byproducts through ozonation. Given the elevated concentration of dissolved organic matter, relatively higher ozone doses are required in reuse applications when compared with water treatment applications in order to achieve the desired treatment goals (oxidation, disinfection). Pilot scale ozone testing was performed to evaluate ozone disinfection performance in wastewater effluent while balancing the formation of byproducts and oxidation of trace organic contaminants. Two chemical byproduct control methods were compared including preformed monochloramine, and hydrogen peroxide. Neither of these bromate control methods had any demonstrable impact on virus or coliform inactivation, however

H_2O_2 eliminated measurable ozone exposure which is necessary for the inactivation of more resistant spore forming bacteria. Additionally, monochloramine was shown to suppress hydroxyl radical exposure and thus negatively impacted the oxidation of ozone resistant organic contaminants, while hydrogen peroxide marginally improved oxidation.

Finally, the use of hydrogen peroxide for bromate control necessitates the validation of an alternative framework for ozone process control. The existing framework that relies on ozone exposure has been shown to be conservative especially for virus inactivation. In this study, the applied specific ozone dose and the change in UV_{254} absorbance were evaluated as ozone monitoring frameworks across a range of water quality characteristics. Elevated temperature and pH were shown to impact ozone decay kinetics and virus inactivation to varying degrees. Both frameworks that were evaluated were shown to be valid across all water quality conditions evaluated.

Validating pathogen reduction across carbon-based reuse treatment trains is imperative in order to allow for more widespread application and regulatory confidence in the technology. Coagulation, flocculation/sedimentation, ozone, and biofiltration were shown to be robust barriers for pathogen and surrogate reduction and recommended concentration and quantification methods are presented herein. The ozone challenge testing results also provide guidance to utilities using ozone for disinfection while controlling disinfection byproducts and enhancing organics oxidation in water reuse applications.

Acknowledgements

First and foremost, I would like to express my gratitude to the members of my committee, Dr. William Knocke, Dr. Charles Bott, Dr. Amy Pruden, and Dr. Marc Edwards, for the guidance and invaluable input over the years. Most of all, thank you to Charles and HRSD for the incredible opportunities that this program has afforded me. It has been the privilege of my life to contribute to the SWIFT program.

Thank you to the HRSD and SWIFT team especially Mack Pearce who assisted with every pilot test and kept me motivated along the way. Thanks also to Kat Yetka, Raul Gonzalez, and the wonderful ladies of the HRSD pathogen lab who helped make every experimental idea a reality. Also, to all current and former HRSD coworkers and Virginia Tech classmates, I would not have finished without your support.

Finally, I would not be here without the love and support of my dear friends and family. Hillary and Niki, thank you for being my support system for the last six years (and before that). To all the friends who have come along on this journey with me, and those I made along the way- your unwavering support has meant the world to me. And to my parents for their unparalleled love and encouragement- I owe my success to you. My success is your success.

Preface

The experiments described herein were performed at the Hampton Roads Sanitation District's (HRSD) 1-MGD carbon-based indirect potable reuse demonstration facility and the ozone/biofiltration pilots housed within. The overarching objective of this work is to validate and optimize the ozone-biofiltration treatment process for water reuse. Chapters 2 and 3 are published, Chapter 4 has been submitted for publication, and Chapter 5 is in preparation for publication. The work done in Chapters 3 and 4 represents in kind contributions to Water Research Foundation Project 5035 and 5129 respectively. The appendices include published review papers and research studies on the topic of ozone disinfection and bromate control.

Chapter 1 provides a brief literature review and introduction to ozone/biofiltration for water reuse.

Chapter 2 is an evaluation of carbon-based advanced water treatment for managed aquifer recharge at the 1-MGD scale. A wide range of performance indicators were considered including bulk organics removal, biofilter performance during acclimation, DBP formation, and trace organic contaminant removal.

Hogard, S., Salazar-Benites, G., Pearce, R., Nading, T., Schimmoller, L., Wilson, C., Heisig-Mitchell, J., & Bott, C. (2021). Demonstration-scale evaluation of ozone–biofiltration–granular activated carbon advanced water treatment for managed aquifer recharge. Water Environment Research, 1–16. https://doi.org/10.1002/wer.1525

- Hogard: data collection, analysis, writing lead
- Pearce: writing support
- Salazar-Benites, Nading, Schimmoller, Wilson, Mitchell, Bott: writing/review

Chapter 3 examines the balance between disinfection using ozonation and the formation of disinfection byproducts. Multiple bromate control methods are evaluated and the benefits/drawbacks related to disinfection and trace organic contaminant oxidation and are presented. A framework for utilities using ozone with various treatment goals is provided.

Hogard, S., Pearce, R., Gonzalez, R., Yetka, K., & Bott, C. (2023). Optimizing Ozone Disinfection in Water Reuse: Controlling Bromate Formation and Enhancing Trace Organic Contaminant Oxidation. Environmental Science and Technology. https://doi.org/10.1021/acs.est.3c00802

- Hogard: experimental design, data collection, analysis, writing lead
- Pearce: input on experimental design, assistance with data collection, writing support
- Gonzalez, Yetka: input on experimental design, writing support
- Bott: writing/review

Chapter 4 provides alternative approaches to validating ozone disinfection for water reuse. Both applied specific ozone dose (O3:TOC corrected for NO2) and change in UV254 absorbance were evaluated as alternative monitoring approaches. Several variables were examined including temperature, pH, TOC, TSS, and hydrogen peroxide addition. Both the impact on ozone exposure and ozone disinfection performance is summarized in this manuscript.

Hogard, S., Pearce, R., Gonzalez, R., Yetka, K., & Bott, C. (2023). Virus inactivation in low ozone exposure water reuse applications. Under review Water Research.

- Hogard: experimental design, data collection, analysis, writing lead

- Pearce: input on experimental design, assistance with data collection, writing support
- Gonzalez, Yetka: input on experimental design, writing support
- Bott: writing/review

Chapter 5 summarizes years of pathogen and pathogen surrogate monitoring data across a wastewater treatment plant as well as the carbon-based advanced water treatment process. These data can be used to validate LRV values for wastewater treatment and advanced water treatment processes. Additionally, capsid integrity PCR was investigated as a method to determine viral inactivation across ozonation.

Hogard, S., Yetka, K., Thompson, H., Pearce, R., Gonzalez, R., & Bott, C. (2023). Validating Pathogen Reduction in Flocculation/Sedimentation, Ozone, and Biofiltration Water Reuse Treatment Trains. In preparation for submission to Water Research.

- Hogard: experimental design, data collection, analysis, writing lead
- Yetka, Thompson, Gonzalez: input on experimental design, assistance with data collection, writing support
- Curtis: assistance with statistical analysis
- Pearce, Bott: writing support and review

Chapter 6 will briefly summarize the conclusions of the entire study and the implications for water reuse engineering.

Appendices:

A. Ozone disinfection of waterborne pathogens and their surrogates: A critical review

Morrison, C. M., Hogard, S., Pearce, R., Gerrity, D., von Gunten, U., & Wert, E. C. (2022). Ozone disinfection of waterborne pathogens and their surrogates: A critical review. Water Research, 214(November 2021), 118206. https://doi.org/10.1016/j.watres.2022.118206

- Morrison: literature review, data collection, analysis, writing lead
- Hogard, Pearce: literature review, data collection, writing support
- Gerrity, von Gunten, Wert: writing support and review

B. Evaluation of preformed monochloramine for bromate control in ozonation for potable reuse

Pearce, R., Hogard, S., Buehlmann, P., Salazar-Benites, G., Wilson, C., & Bott, C. (2022). Evaluation of preformed monochloramine for bromate control in ozonation for potable reuse. Water Research, 211, 118049. https://doi.org/10.1016/j.watres.2022.118049

- Pearce: experimental design, data collection, analysis, writing lead
- Hogard, Buehlmann: assistance with data collection, writing support
- Salazar-Benites, Wilson, Bott: writing/review

C. Critical Review on Bromate Formation during Ozonation and Control Options for Its Minimization

Morrison, C. M., Hogard, S., Pearce, R., Mohan, A., Pisarenko, A. N., Dickenson, E. R. V., von Gunten, U., & Wert, E. C. (2023). Critical Review on Bromate Formation during Ozonation and Control Options for Its Minimization. Environmental Science and Technology. https://doi.org/10.1021/acs.est.3c00538

- Morrison: literature review, writing lead
- Hogard, Pearce, Mohan, Pisarenko: literature review, writing support
- Dickenson, von Gunten, Wert: writing support and review

Table of Contents

List of Figures

Chapter 5

List of Tables

Chapter 1. Introduction

Water reuse projects have been implemented worldwide with many purposes including irrigation, drinking water source augmentation, and groundwater replenishment (EPA, 2017; Gerrity et al., 2013). Water reuse schemes typically include a combination of membrane filtration and reverse osmosis (RO), however non-RO treatment trains have become more common in recent years (Funk et al., 2019). The shift to non-RO treatment technologies may be attributed to the potential cost savings they provide, especially to land-locked utilities with no convenient option for brine disposal. Ozone in combination with biofiltration has emerged as an effective alternative to RO treatment for water reuse. These treatment schemes are able to meet nearly every advanced water treatment goal with the major drawback being limited capacity for organics removal. However, ozone and biofiltration, often in combination with granular activated carbon, provide pathogen reduction, as well as both trace and bulk organics removal at a lower cost when compared with RO (Gerrity et al., 2011; Sundaram et al., 2014). Ozone has been implemented for decades for drinking water disinfection as it is highly effective in inactivating viral and bacterial pathogens. The primary drawback to ozone treatment is the formation of disinfection byproducts (DBPs) such as bromate. Optimizing ozone/biofiltration treatment in water reuse applications is important in order to limit DBP formation and enhance organics removal, while maintaining efficient disinfection.

Maintaining the microbial safety of treated water remains the greatest acute health concern associated with water reuse. For this reason, it is important to validate and demonstrate pathogen removal via indicator microorganisms and monitoring frameworks. In California, indirect potable reuse plants must achieve log removal values (LRVs) for pathogens including 12-log removal of enteric viruses, and 10-log removal of both *Cryptosporidium* and *Giardia*. Pathogen LRVs are credited to each treatment process according to the validation performed by the equipment manufacturer or regulatory guidance manuals for drinking water treatment that have been extended to water reuse applications. Although ozone and filtration are well established technologies for pathogen inactivation/removal in water treatment, there have been limited studies investigating the validation of these frameworks for use in water reuse applications. In fact, validating and improving disinfection in ozone/biofiltration water reuse treatment trains will be the topic of an upcoming Water Research Foundation request for proposals, highlighting the importance of this topic (WRF, 2021). Current frameworks for monitoring ozone disinfection in drinking water applications require a dissolved ozone residual to be maintained (to achieve a target CT), however this may be difficult to achieve when ozonating wastewater with a much

greater ozone demand. In the context of wastewater reuse, there is interest in developing alternative frameworks that do not rely on ozone exposure. In addition to creating new monitoring frameworks, it is also important to have representative indigenous microorganisms that can be used to routinely monitor pathogen removal in the advanced treatment process.

Disinfection credit for physical removal of pathogens is allocated differently depending on whether the treatment plant implements conventional filtration or direct filtration. The elimination of the settling step in direct filtration results in less virus removal credit which must be made up in subsequent treatment processes. With the inclusion of ozonation in a direct filtration treatment process, it would not be difficult to make up this virus removal credit. However, the tertiary removal of solids prior to ozonation has been shown to have an impact on ozone disinfection efficacy. The effect of upstream wastewater treatment process performance and tertiary removal of organics/suspended solids on ozone/biofiltration in conventional and direct filtration configurations in water reuse must be considered.

Ozone disinfection in water reuse and wastewater treatment

Historically, the primary purpose for applying ozone treatment has been water and wastewater disinfection (von Gunten, 2003). Ozone is extremely effective in inactivating bacterial and viral pathogens as well as chlorine resistant protozoa such as *Cryptosporidium parvum* (Rennecker et al., 1999). Increasing stringency in water treatment disinfection regulations and increased monitoring requirements for pathogens and disinfection byproducts (DBPs) imposed on utilities in the United States, has resulted in the shift away from chlorine as a primary disinfectant (EPA, 1999). The use of ozone for water and wastewater disinfection is also common in countries such as France, Germany and Japan (Loeb et al., 2012). Ozone is also implemented in water reuse to simultaneously eliminate trace organic contaminants of emerging concern (CECs) via oxidation (Gerrity & Snyder, 2011).

Ozone inactivates viruses and bacteria very efficiently with relatively high reaction rates (von Gunten, 2003). Ozone disinfection kinetics are typically represented with some variation of the Chick-Watson equation shown below, where N is the number of viable microorganisms, k is the reaction rate constant, and c is the disinfectant concentration at a given time, t (Equation 1). Using this rate law, the integrated ozone exposure can be used to predict the log-inactivation of a given microorganism. The EPA Surface Water Treatment Rule (SWTR) utilizes a conservative estimate of pathogen inactivation corresponding to a single point concentration*time (CT) measurement at various temperatures.

Equation 1. $\log (N/N_0) = -kc^n t$

It is generally accepted that molecular ozone is primarily responsible for disinfection, however there are several studies that speculate as to the role of hydroxyl radicals (OH*) in disinfection (Cho et al., 2002; Miguel et al., 2016). One study reported greater inactivation of *Bacillus subtilis* spores at an elevated pH while maintaining the same ozone exposure, therefore owing the additional removal to OH* (Cho et al., 2002). Another study found the removal of *Clostridium perfringens* to be enhanced with the addition of hydrogen peroxide during ozonation, which indicates that OH* may play a role in this inactivation mechanism (Hijnen et al., 2004). However, other studies have suggested that it is molecular ozone that is responsible for microorganism inactivation as evidenced by comparable inactivation with and without the addition of OH* scavengers (Hunt & Marinas, 1997).

Hunt & Mariñas (1999) reported a first order reaction rate of $1.04*10^5$ $M^{-1}s^{-1}$ of molecular ozone with *Escherichia coli*. The rapid reaction of ozone with viruses has made it difficult to ascertain accurate kinetic data for these microorganisms. Wolf et al., (2018) created a bench testing apparatus to quantify relatively low ozone exposures and thus allowed for the measurement of kinetic virus inactivation data. This study identified first order reaction rates for a suite of five enteric viruses and four bacteriophages ranging from 10^5-10^6 $M^{-1}s^{-1}$. In addition to these bench scale tests, there have been many pilot-scale and full-scale validation studies that demonstrate the efficacy of ozone disinfection. In a pilot study conducted on an ozone/BAC wastewater reuse treatment train, >2-log reduction of total coliforms and >3-log reduction of fecal coliform was reported by ozone alone (Gerrity et al., 2011). In this study they also performed challenge testing where they spiked the male specific coliphage (MS2) and measured greater than 6.5 log reduction by ozone. Similar results have been obtained elsewhere with variations observed for different sources water characteristics. The reaction of ozone with protozoa is not as rapid due to the protective cyst structure. The disinfection kinetics for *Cryptosporidium* and *Giardia* can be characterized by a lag-phase followed by pseudo first order decay. This is often modeled according to delayed Chick Watson kinetic models (Hunt & Mariñas, 1999).

Impact of water quality on ozone disinfection

There are many water quality parameters which influence the ozone treatment process including organic carbon, nitrite, dissolved metals, pH, and temperature. The transferred ozone dose is the critical design parameter in these disinfection systems and therefore, the impact of the water matrix on ozone decay rate is an important consideration. This presents a challenge in wastewater ozonation as the water matrix is typically composed of much greater concentrations of organics

and other ozone demanding compounds (M.-O. Buffle et al., 2006). The source water pH and temperature are important to consider since ozone decay rate increases greatly at elevated pH and temperature, resulting in decreased ozone exposure for a given applied ozone dose (Rennecker et al., 2001). Wolf et al., (2018) showed that the reaction rate of viruses depends weakly on both temperature and pH. Temperature and pH were shown increases the reactivity of ozone with microorganisms but will also increase the ozone decay rate (Driedger et al., 2001; Hirata et al., 2001; Wolf et al., 2018).

Lazarova et al. (2014) demonstrated the impact of suspended solids and organic carbon on the ozone demand and thus the ozone dose required for pathogen inactivation. In addition to the impact on ozone decay, this study also showed the capacity for suspended solids to shield microorganisms from disinfection by ozone. The influence of upstream wastewater treatment processes was also investigated in this study, which showed that the extended aeration compared with high-rate wastewater treatment marginally decreased the ozone demand. For water reuse applications in California, the use of ozone for disinfection is only conditionally accepted with a prerequisite turbidity requirement. This often requires the implementation of tertiary filtration prior to ozonation to meet turbidity/TSS requirements for disinfection (CDPH, 2018). It remains to be determined if there is any significant benefit of tertiary solids removal if relatively high-quality secondary effluent is achieved at the upstream wastewater treatment plant (WWTP) (low TSS, low turbidity).

Disinfection byproduct formation

The major drawback to ozone application is the formation of DBPs in the presence of precursors. Bromate is the primary DBP of concern in the ozonation process (von Gunten et al., 1995). This compound is regulated in the US with a maximum contaminant level (MCL) of 10 ug/L (US EPA, 1998). Bromate forms by the oxidation of bromide via direct reactions with molecular ozone, and indirect reactions with OH* (von Gunten, 2003). Bromate formation during wastewater ozonation is of particular concern due to the potential for introduction of external bromide sources to wastewater plants and higher overall ozone demand. Additionally, during wastewater treatment, ozone reacts with organic matter in reactions which result in the propagation of OH* (Buffle & von Gunten, 2006; Nöthe et al., 2009). This can result in greater bromate formation via the indirect pathway. This has led to extensive research into bromate control methods in water treatment and wastewater treatment applications.

Other DBPs that are formed during ozonation include aldehydes and N-nitrosodimethylamine (NDMA) (Gerrity et al., 2015; Schechter & Singer, 2008). Aldehydes form as a result of the

oxidation of hydrophobic organic compounds by ozone. NDMA forms by reactions of precursors with both ozone and monochloramine and is recognized as potentially toxic at concentrations greater than 10 ng/L (CDPH, n.d.). NDMA precursors including personal care products, pesticides, and amine based polymers, to name a few, are prevalent in treated wastewater (Sgroi et al., 2018). Therefore, the formation of NDMA is a major concern in water reuse applications utilizing ozone or monochloramine.

Disinfection byproduct control methods

Both NDMA and aldehydes that form during ozonation have been shown to be susceptible to biological degradation in downstream biofiltration (Sundaram et al., 2014). Therefore, the implementation of BAFs after ozonation has been shown to be an important barrier for the elimination of ozonation byproducts. Bromate however, is not susceptible to aerobic biological degradation, and therefore other measures must be implemented to limit its formation. The first two options are lowering the applied ozone dose or eliminating extraneous bromide sources. The former is not always feasible in situations where ozone is used for disinfection because an elevated ozone dose is typically required to achieve a certain level of disinfection. Therefore, if bromide sources cannot be reduced, chemical control measures can be used to modify and interrupt the bromate formation pathway. In drinking water applications, pH adjustment and/or ammonia addition are often used to control bromate formation (von Gunten, 2003).

These methods may be insufficient to limit bromate formation in water reuse scenarios where bromide concentrations are higher and ozone demand is greater. Chlorine and subsequent ammonia addition has been used in full scale applications to promote the preoxidation of bromide to hypobromous acid, followed by the formation of bromamine (M. O. Buffle et al., 2004; Wert et al., 2007). Bromamine is slowly oxidized by ozone at a negligible rate which makes this compound a reservoir for bromide. Preformed monochloramine can also be used to limit bromate formation by quenching OH* which play a role in bromate formation (Soltermann et al., 2017). Hydroxyl radicals also play an important role in trace organic contaminant oxidation, and therefore this bromate control method can have a negative impact on overall ozone performance. Monochloramine also reacts with bromide to form other haloamines such as bromochloramine, which is a stable intermediate compound that sequesters bromide (Ling et al., 2020). Another auxiliary impact of monochloramine addition is the potential formation of NDMA or other byproducts.

Another widely used bromate control method in water treatment is hydrogen peroxide addition (von Gunten & Oliveras, 1998). Hydrogen peroxide reacts with hypobromous acid to reduce it to bromide while simultaneously rapidly decomposing ozone. These two mechanisms result in limited bromate formation overall. One study reported bromate formation below the MCL with the addition of 3.5 mg/L of H_2O_2 while feeding 5 mg/L of ozone (Gerrity et al., 2011). The major drawback associated with using hydrogen peroxide is the absence of a dissolved ozone residual. As mentioned previously, ozone disinfection frameworks require an ozone residual to be maintained to calculate a CT value. Therefore, it is important to balance treatment goals such as disinfection with DBP formation and control in these scenarios.

Pathogen removal by physical treatment

Physical treatment processes such as flocculation, sedimentation, and filtration also provide barriers for the removal of pathogens (James K. Edzwald, 2011). The SWTR accounts for pathogen removal credit for these processes according to the type of filtration achieved, e.g. conventional filtration is credited with greater pathogen removal credit than direct filtration (US EPA, 1999). Many studies have demonstrated removal of indicator bacteria via coagulation and sedimentation (Hokajärvi et al., 2018; Sha et al., 2019). Additionally, there have been studies performed which demonstrate the potential virucidal characteristics of aluminum coagulants (Matsui et al., 2003). Biofiltration has also been shown to effectively remove indicator bacteria and pathogens (Maurya et al., 2020). It is also well documented that ozonation prior to filtration improves particle removal significantly. This is due to the microflocculation and coagulation that occurs as a result of ozone reacting with organics and suspended solids in the water (Becker & O'Melia, 2001; Edwards & Benjamin, 1991). The impact of ozonation on the removal of pathogens by biofiltration has not been specifically investigated. The level of pathogen removal achieved by physical treatment determines the required level of treatment by chemical or UV disinfection.

Contaminants of emerging concern

Ozone itself is an extremely powerful oxidant, and upon decomposition, ozone forms hydroxyl radicals (OH*), which are recognized as the strongest oxidant in water. The combination of ozone application and OH* formation has been shown to result in efficient CEC oxidation in water treatment and water reuse. Reactions of ozone with dissolved organic matter can result in both OH* propagation and quenching (Buffle & von Gunten, 2006; Nöthe et al., 2009). Due to the great amount of OH* formed, wastewater ozonation itself is considered an advanced oxidation process (M. O. Buffle et al., 2006). Lee et al., (2013) categorized CECs based on their reactivity with molecular ozone and OH*. The majority of CECs are removed efficiently at low to moderate ozone doses. There are however multiple CECs such as flame retardants and pesticides that are

extremely recalcitrant to ozone oxidation. Many of these compounds are more effectively removed via other advanced oxidation processes such as ozone in combination with hydrogen peroxide (Bourgin et al., 2018). For compounds which are resistant to oxidative treatment entirely (e.g. perfluorinated organics), water reuse plants must rely on some other treatment barrier such as biological treatment, or GAC adsorption.

Indicator microorganisms

Reliable pathogen indicators are very useful for routine monitoring purposes. A good indicator microorganism is present when the pathogen of interest is present and ideally originates from the intestinal tract of warm-blooded animals. Additionally, it should be easier and less expensive to cultivate than the target pathogen. Finally, it must be removed at a similar or more conservative rate when compared with the pathogen of interest (Metcalf & Eddy; et al., 2007). The coliform group of bacteria belong to a group of microorganisms termed fecal indicator bacteria (FIB) and they are frequently used as an indicator of fecal contamination as they are excreted by humans on a daily basis (EPA, 2017). *E. coli* belong to this category of fecal coliform bacteria which are typically not harmful to humans, but some strains are pathogenic. Total coliform or fecal coliform bacteria can both be used as indicators of ozone disinfection of bacterial pathogens, but they are inactivated at a much greater rate than protozoa or viruses (Facile et al., 2000).

Clostridium perfringens are a species of anaerobic spore forming bacteria (SFB) which are present at sufficiently high concentrations in wastewater effluent and they are more resistant to treatment than other bacteria, and therefore they are a useful indicator of ozone disinfection of other resistant pathogens (Stelma, 2018). In the United States, the only state to adopt this microorganism as a treatment indicator so far is North Carolina (EPA, 2017). The inactivation of *C. perfringens* by ozone has been studied extensively in wastewater treatment applications (Hijnen et al., 2004; Lanao et al., 2008; Lazarova et al., 2014). Hijnen et al., (2004) investigated the impact of organic matter concentration on the inactivation of *C. perfringens* and found that a high DOC concentration does not necessarily impact the inactivation efficiency. Another study found that ozone in combination with hydrogen peroxide resulted in greater inactivation of *C. perfringens* when compared with ozone alone (Lanao et al., 2008). This suggests that perhaps OH* play a role in the inactivation of these bacteria. Similarly, *Bacillus subtilis* and other species of aerobic spore forming bacteria, display similar resistance to ozone treatment as protozoan pathogens such as *Cryptosporidium* and *Giardia*. These bacteria are generally accepted as a suitable surrogate microorganism to represent protozoa inactivation in ozone lab experiments

(Facile et al., 2000). The merits of using aerobic or anerobic SFB as indicators of ozone disinfection has been contested in recent studies (Stelma, 2018).

Bacteriophages, or viruses that infect bacteria, also serve as useful indicators of the presence of viruses. Coliphages are viruses that infect coliform bacteria specifically, and therefore their presence indicates the presence of coliforms as well. Coliphages are useful indicators for viruses in water reuse treatment schemes because they are similar in morphology and resistant to ozone treatment when compared with human viruses (EPA, 2017). Other viruses which are numerous in nature and useful indicators of treatment effectiveness are pepper mild mottle virus (PMMoV), Bacteroides bacteriophage, crAssphage, as well as tobacco mosaic virus (Tandukar et al., 2020). PMMoV is ubiquitous in wastewater effluents at relatively high concentrations, and it is resistant virus which makes it an ideal conservative indicator (Kitajima et al., 2018). Similarly, crAssphage was identified in 2014 as the most abundant virus in the human gut and is also detected in most wastewater effluents (Dutilh et al., 2014; R. A. Edwards, 2019).

Methods for determining microbial inactivation

The most common methods for measuring microbial inactivation include both molecular and culture-based methods. Quantitative PCR (qPCR) is a useful method for determining the presence or absence of a certain genome but does not inform about infectivity. Culture-based methods more accurately measure the inactivation of viruses and bacteria as only viable microorganisms can be cultured (Metcalf & Eddy; et al., 2007). These methods have several drawbacks including excessive time requirements and cost. Additionally, culture methods do not yet exist for some important human viruses, including human norovirus (Rockey et al., 2020). Recent studies have investigated the correlation between loss of infectivity and genome damage as measured by PCR. The relationship between change in infectivity and genome damage is unique to each disinfectant that has different mechanisms of inactivation (Gerba et al., 2018). Pecson et al., (2011) demonstrated that this relationship between infectivity and genome damage is consistent and useful when evaluating UV disinfection, but further research is needed to evaluate other modes of disinfection in natural waters. Several other studies have been performed to evaluate reduction in viral infectivity during free chlorine, ozone, and UV disinfection using qPCR (Rockey et al., 2020; Young et al., 2020). Another strategy to overcome the limitations of molecular methods is the use of intercalating dyes in combination with qPCR to evaluate the capsid integrity of a given virus (Canh et al., 2019). The dye is able to infiltrate a compromised cell or virion and bind covalently to the DNA thereby inhibiting the amplification of this DNA during

PCR. While this method does not explicitly inform about the “viability” of a virus, it does offer some information about the inactivation by a given disinfectant.

Surrogate frameworks for process monitoring

Disinfection credit in water reuse schemes is typically achieved via multiple treatment barriers to ensure pathogen removal is consistent and reliable. As mentioned previously, ozone disinfection credit is achieved by maintaining CT values according to methods defined in the EPA SWTR. However there have been several studies that suggest this may not be the most suitable framework to use in the case of wastewater disinfection (Xu et al., 2002). This is due to the high ozone demand of wastewater that will result in much higher applied ozone doses to achieve the same ozone exposure. Gerrity et al., (2012) demonstrated the usefulness of surrogate monitoring parameters such as the change in UV254 absorbance for predicting CEC oxidation, but the correlations were less consistent for microbial inactivation. Several studies have shown that significant bacterial and viral inactivation at low ozone doses or in the absence of a measurable ozone residual during the application of $O3/H_2O_2$ (Gamage et al., 2013; Ishida et al., 2008). Gamage et al. (2013) demonstrated the usefulness of ozone/TOC ratio and the change in UV254 absorbance and total fluorescence as surrogate parameters for monitoring MS2 bacteriophage and *B. subtilis* inactivation when no CT is achieved. Lee et al., (2016) investigated the use of ATP as a surrogate monitoring parameter and found that extracellular ATP increased upon ozonation as a result of intracellular ATP being released by the compromised cells, therefore intracellular ATP may be the most useful monitoring parameter. Carvajal et al., (2017) compared the results from these previous studies to their own experiments and analysis. This study suggested that the correlation with these non-CT parameters is site specific and therefore requires development at each treatment plant.

References

Becker, W. C., & O'Melia, C. R. (2001). Ozone: Its effect on coagulation and filtration. *Water Science and Technology: Water Supply*, *1*(4), 81–88. https://doi.org/10.2166/ws.2001.0070

Bourgin, M., Beck, B., Boehler, M., Borowska, E., Fleiner, J., Salhi, E., Teichler, R., von Gunten, U., Siegrist, H., & McArdell, C. S. (2018). Evaluation of a full-scale wastewater treatment plant upgraded with ozonation and biological post-treatments: Abatement of micropollutants, formation of transformation products and oxidation by-products. *Water Research*, *129*, 486–498. https://doi.org/10.1016/j.watres.2017.10.036

Buffle, M.-O., Schumacher, J., Meylan, S., Jekel, M., & von Gunten, U. (2006). Ozonation and Advanced Oxidation of Wastewater: Effect of O3 Dose, pH, DOM and HO Scavengers on Ozone Decomposition and HO Generation. *Ozone: Science and Engineering*, *28*(4), 247–259.

Buffle, M. O., Galli, S., & Von Gunten, U. (2004). Enhanced bromate control during ozonation: The chlorine-ammonia process. *Environmental Science and Technology*, *38*(19), 5187–5195. https://doi.org/10.1021/es0352146

Buffle, M. O., Schumacher, J., Meylan, S., Jekel, M., & Von Gunten, U. (2006). Ozonation and advanced oxidation of wastewater: Effect of O3 dose, pH, DOM and HO.-scavengers on ozone decomposition and HO . generation. *Ozone: Science and Engineering*, *28*(4), 247–259. https://doi.org/10.1080/01919510600718825

Buffle, M. O., & von Gunten, U. (2006). Phenols and amine induced HO. generation during the initial phase of natural water ozonation. *Environmental Science and Technology*, *40*(9), 3057–3063. https://doi.org/10.1021/es052020c

Canh, V. D., Kasuga, I., Furumai, H., & Katayama, H. (2019). Viability RT-qPCR Combined with Sodium Deoxycholate Pre-treatment for Selective Quantification of Infectious Viruses in Drinking Water Samples. *Food and Environmental Virology*, *11*(1), 40–51. https://doi.org/10.1007/s12560-019-09368-2

Carvajal, G., Branch, A., Michel, P., Sisson, S. A., Roser, D. J., Drewes, J. E., & Khan, S. J. (2017). Robust evaluation of performance monitoring options for ozone disinfection in water recycling using Bayesian analysis. *Water Research*, *124*, 605–617. https://doi.org/10.1016/j.watres.2017.07.079

CDPH. (n.d.). *Drinking Water Notification Levels*. Retrieved May 8, 2021, from https://www.waterboards.ca.gov/drinking_water/certlic/drinkingwater/NotificationLevels.html

Regulations related to recycled water, (2018).

Cho, M., Chung, H., & Yoon, J. (2002). *Effect of pH and Importance of Ozone initiated Radical Reactions In Inactivating Bacillus subtilis Spore*. *9512*. https://doi.org/10.1080/01919510208901605

Driedger, A. M., Staub, E., Pinkernell, U., Marinas, B., Koster, W., & von Gunten, U. (2001). INACTIVATION OF BACILLUS SUBTILIS SPORES AND FORMATION OF BROMATE DURING OZONATION. *Water Research*, *37*(12), 2950–2960. https://doi.org/10.1016/S0043-1354(02)00381-0

Dutilh, B. E., Cassman, N., McNair, K., Sanchez, S. E., Silva, G. G. Z., Boling, L., Barr, J. J., Speth, D. R., Seguritan, V., Aziz, R. K., Felts, B., Dinsdale, E. A., Mokili, J. L., & Edwards, R. A. (2014). A highly abundant bacteriophage discovered in the unknown sequences of

human faecal metagenomes. *Nature Communications*, *5*, 1–11. https://doi.org/10.1038/ncomms5498

Edwards, M., & Benjamin, M. M. (1991). Mechanistic study of ozone-induced particle destabilization. *Journal / American Water Works Association*, *83*(6), 96–105. https://doi.org/10.1002/j.1551-8833.1991.tb07169.x

Edwards, R. A. (2019). *Global phylogeography and ancient evolution of the widespread human gut virus crAssphage*. *4*(October).

EPA. (2017). *Potable Reuse Compendium*. 203. https://www.epa.gov/sites/production/files/2018-01/documents/potablereusecompendium_3.pdf

Facile, N., Barbeau, B., Prevost, M., & Koudjonou, B. (2000). Evaluating bacterial aerobic spores as a surrogate for giardia and cryptosporidium inactivation by ozone. *Water Research*, *34*(12), 3238–3246.

Funk, D., County, G., Hooper, J., Goldman, J., & Schulz, C. (2019). *Ozone Biofiltration Direct Potable Reuse Testing at Gwinnett County Ozone Biofiltration Direct Potable Reuse Testing at Gwinnett County*.

Gamage, S., Gerrity, D., Pisarenko, A. N., Wert, E. C., & Snyder, S. A. (2013). Evaluation of Process Control Alternatives for the Inactivation of Escherichia coli, MS2 Bacteriophage, and Bacillus subtilis Spores during Wastewater Ozonation. *Ozone: Science and Engineering*, *35*(6), 501–513. https://doi.org/10.1080/01919512.2013.833852

Gerba, C. P., Betancourt, W. Q., Kitajima, M., & Rock, C. M. (2018). Reducing uncertainty in estimating virus reduction by advanced water treatment processes. *Water Research*, *133*, 282–288. https://doi.org/10.1016/j.watres.2018.01.044

Gerrity, D., Gamage, S., Holady, J. C., Mawhinney, D. B., Quiñones, O., Trenholm, R. A., & Snyder, S. A. (2011). Pilot-scale evaluation of ozone and biological activated carbon for trace organic contaminant mitigation and disinfection. *Water Research*, *45*(5), 2155–2165. https://doi.org/10.1016/j.watres.2010.12.031

Gerrity, D., Gamage, S., Jones, D., Korshin, G. V., Lee, Y., Pisarenko, A., Trenholm, R. A., von Gunten, U., Wert, E. C., & Snyder, S. A. (2012). Development of surrogate correlation models to predict trace organic contaminant oxidation and microbial inactivation during ozonation. *Water Research*, *46*(19), 6257–6272. https://doi.org/10.1016/j.watres.2012.08.037

Gerrity, D., Pecson, B., Shane Trussell, R., & Rhodes Trussell, R. (2013). Potable reuse treatment trains throughout the world. *Journal of Water Supply: Research and Technology - AQUA*, *62*(6), 321–338. https://doi.org/10.2166/aqua.2013.041

Gerrity, D., Pisarenko, A. N., Marti, E., Trenholm, R. A., Gerringer, F., Reungoat, J., & Dickenson, E. (2015). Nitrosamines in pilot-scale and full-scale wastewater treatment plants with ozonation. *Water Research*, *72*, 251–261. https://doi.org/10.1016/j.watres.2014.06.025

Gerrity, D., & Snyder, S. (2011). Review of ozone for water reuse applications: Toxicity, regulations, and trace organic contaminant oxidation. *Ozone: Science and Engineering*, *33*(4), 253–266. https://doi.org/10.1080/01919512.2011.578038

Hijnen, W. A. M., Baars, E., Bosklopper, T. G. J., Van Der Veer, A. J., Meijers, R. T., & Medema, G. J. (2004). Influence of DOC on the inactivation efficiency of ozonation assessed with Clostridium perfringens and a lab-scale continuous flow system. *Ozone: Science and*

Engineering, *26*(5), 465–473. https://doi.org/10.1080/01919510490507784

Hirata, T., Shimura, A., Morita, S., Suzuki, M., Motoyama, N., Hoshikawa, H., Moniwa, T., & Kaneko, M. (2001). The effect of temperature on the efficacy of ozonation for inactivating Cryptosporidium parvum oocysts. *Water Science and Technology*, *43*(12), 163–166. https://doi.org/10.2166/wst.2001.0729

Hokajärvi, A., Pitkänen, T., Meriläinen, P., & Kauppinen, A. (2018). Determination of Removal Efficiencies for Coliphages in Unit Processes of Surface Waterworks for QMRA Applications. *Water*, *10*(1525). https://doi.org/10.3390/w10111525

Hunt, N. K., & Marinas, B. (1997). Kinetics of Escherichia coli inactivation with ozone. *Water Research*, *31*(6), 1355–1362.

Hunt, N. K., & Mariñas, B. J. (1999). Inactivation of Escherichia coli with ozone: Chemical and inactivation kinetics. *Water Research*, *33*(11), 2633–2641. https://doi.org/10.1016/S0043-1354(99)00115-3

Ishida, C., Salveson, A., Robinson, K., Bowman, R., & Snyder, S. (2008). Ozone disinfection with the HiPOX™ reactor: Streamlining an “old technology” for wastewater reuse. *Water Science and Technology*, *58*(9), 1765–1773. https://doi.org/10.2166/wst.2008.548

James K. Edzwald. (2011). *WATER QUALITY AND TREATMENT: A HANDBOOK ON DRINKING WATER, SIXTH EDITION*. American Water Works Association, American Society of Civil Engineers, McGraw-Hill.

Kitajima, M., Sassi, H. P., & Torrey, J. R. (2018). Pepper mild mottle virus as a water quality indicator. *Npj Clean Water*, *1*(1). https://doi.org/10.1038/s41545-018-0019-5

Lanao, M., Ormad, M. P., Ibarz, C., Miguel, N., & Ovelleiro, J. L. (2008). Bactericidal effectiveness of O3, O3/H 2O2 and O3/TiO2 on Clostridium perfringens. *Ozone: Science and Engineering*, *30*(6), 431–438. https://doi.org/10.1080/01919510802488003

Lazarova, V., Liechti, P. A., Savoye, P., & Hausler, R. (2014). Ozone disinfection: Main parameters for process design in wastewater treatment and reuse. *Journal of Water Reuse and Desalination*, *3*(4), 337–345. https://doi.org/10.2166/wrd.2013.007

Lee, Y., Gerrity, D., Lee, M., Bogeat, A. E., Salhi, E., Gamage, S., Trenholm, R. A., Wert, E. C., Snyder, S. A., & Von Gunten, U. (2013). Prediction of micropollutant elimination during ozonation of municipal wastewater effluents: Use of kinetic and water specific information. *Environmental Science and Technology*, *47*(11), 5872–5881. https://doi.org/10.1021/es400781r

Lee, Y., Imminger, S., Czekalski, N., von Gunten, U., & Hammes, F. (2016). Inactivation efficiency of Escherichia coli and autochthonous bacteria during ozonation of municipal wastewater effluents quantified with flow cytometry and adenosine tri-phosphate analyses. *Water Research*, *101*, 617–627. https://doi.org/10.1016/j.watres.2016.05.089

Ling, L., Deng, Z., Fang, J., & Shang, C. (2020). Bromate control during ozonation by ammonia-chlorine and chlorine-ammonia pretreatment: Roles of bromine-containing haloamines. *Chemical Engineering Journal*, *389*(August 2019). https://doi.org/10.1016/j.cej.2019.123447

Loeb, B. L., Thompson, C. M., Drago, J., Takahara, H., & Baig, S. (2012). *Worldwide Ozone Capacity for Treatment of Drinking Water and Wastewater : A Review*. 64–77. https://doi.org/10.1080/01919512.2012.640251

Matsui, Y., MATSUSHITA, T., SAKUMA, S., GOJO, T., MAMIYA, T., SUZUOKI, H., & Inoue, T. (2003). *Virus Inactivation in Aluminum and Polyaluminum Coagulation*. 5175–5180.

Maurya, A., Singh, M. K., & Kumar, S. (2020). *Biofiltration technique for removal of waterborne pathogens*. *January*.

Metcalf & Eddy;, Asano;, T., Burton;, F., & Leverenz., H. (2007). *Water Reuse: Issues, Technologies, and Applications*. McGraw Hill.

Miguel, N., Lanao, M., Valero, P., Mosteo, R., & Ormad, M. P. (2016). Enterococcus sp. Inactivation by Ozonation in Natural Water: Influence of H2O2 and TiO2 and Inactivation Kinetics Modeling. *Ozone: Science and Engineering*, *38*(6), 443–451. https://doi.org/10.1080/01919512.2016.1204223

Nöthe, T., Fahlenkamp, H., & Von Sonntag, C. (2009). Ozonation of wastewater: Rate of ozone consumption and hydroxyl radical yield. *Environmental Science and Technology*, *43*(15), 5990–5995. https://doi.org/10.1021/es900825f

Pecson, B. M., Ackermann, M., & Kohn, T. (2011). Framework for using quantitative PCR as a nonculture based method to estimate virus infectivity. *Environmental Science and Technology*, *45*(6), 2257–2263. https://doi.org/10.1021/es103488e

Rennecker, J. L., Kim, J. H., Corona-Vasquez, B., & Mariñas, B. J. (2001). Role of disinfectant concentration and pH in the inactivation kinetics of Cryptosporidium parvum oocysts with ozone and monochloramine. *Environmental Science and Technology*, *35*(13), 2752–2757. https://doi.org/10.1021/es010526z

Rennecker, J. L., Mariñas, B. J., Owens, J. H., & Rice, E. W. (1999). Inactivation of Cryptosporidium parvum oocysts with ozone. *Water Research*, *33*(11), 2481–2488. https://doi.org/10.1016/S0043-1354(99)00116-5

Rockey, N., Young, S., Kohn, T., Pecson, B., Wobus, C. E., Raskin, L., & Wigginton, K. R. (2020). UV Disinfection of Human Norovirus: Evaluating Infectivity Using a Genome-Wide PCR-Based Approach. *Environmental Science and Technology*, *54*(5), 2851–2858. https://doi.org/10.1021/acs.est.9b05747

Schechter, D. S., & Singer, P. C. (2008). Formation Of Aldehydes During Ozonation. *Ozone: Science & Engineering*, *9512*(1995), 53–69. https://doi.org/10.1080/01919519508547577

Sgroi, M., Vagliasindi, F. G. A., Snyder, S. A., & Roccaro, P. (2018). N-Nitrosodimethylamine (NDMA) and its precursors in water and wastewater: A review on formation and removal. *Chemosphere*, *191*, 685–703. https://doi.org/10.1016/j.chemosphere.2017.10.089

Sha, S., Noor, S., Azizan, F., & Akhir, F. N. (2019). *Removal effi ciency of Gram-positive and Gram-negative bacteria using a natural coagulant during coagulation , fl occulation , and sedimentation processes Muhamad Ali Muhammad Yuzir , Nor ' azizi Othman , Zuriati Zakaria ,*. 1787–1795. https://doi.org/10.2166/wst.2019.433

Soltermann, F., Abegglen, C., Tschui, M., Stahel, S., & von Gunten, U. (2017). Options and limitations for bromate control during ozonation of wastewater. *Water Research*, *116*, 76–85. https://doi.org/10.1016/j.watres.2017.02.026

Stelma, G. N. (2018). Use of bacterial spores in monitoring water quality and treatment. *Journal of Water and Health*, *16*(4), 491–500. https://doi.org/10.2166/wh.2018.013

Sundaram, V., Emerick, R. W., & Shumaker, S. E. (2014). Advanced Treatment Process for

Pharmaceuticals, Endocrine Disruptors, and Flame Retardants Removal. *Water Environment Research*, *86*(2), 111–122. https://doi.org/10.2175/106143013x13807328849053

Tandukar, S., Sherchan, S. P., & Haramoto, E. (2020). Applicability of crAssphage, pepper mild mottle virus, and tobacco mosaic virus as indicators of reduction of enteric viruses during wastewater treatment. *Scientific Reports*, *10*(1), 1–8. https://doi.org/10.1038/s41598-020-60547-9

The Water Research Foundation. (2021). *The Water Research Foundation Funds Three New Projects*. https://www.waterrf.org/news/water-research-foundation-funds-three-new-projects

US EPA. (1998). National Primary Drinking Water Regulations: Disinfectants and Disinfection Byproducts: 40 CFR 9, 141, 142. In *Federal Register* (Issue December).

US EPA. (1999). *Guidance Manual for Compliance with the Interim Enhanced Surface Water Treatment Rule: Turbidity Provisions* (p. 216).

von Gunten, U. (2003). Ozonation of drinking water: Part II. Disinfection and by-product formation in presence of bromide, iodide or chlorine. *Water Research*, *37*(7), 1469–1487. https://doi.org/10.1016/s0043-1354(02)00458-x

Von Gunten, U., Hoigne, J., & Bruchet, A. (1995). Bromate formation during ozonation of bromide-containing waters. *Water Supply*, *13*(1), 45–50.

von Gunten, U., & Oliveras, Y. (1998). Advanced oxidation of bromide-containing waters: Bromate formation mechanisms. *Environmental Science and Technology*, *32*(1), 63–70. https://doi.org/10.1021/es970477j

Wert, E. C., Neemann, J. J., Johnson, D., Rexing, D., & Zegers, R. (2007). Pilot-scale and full-scale evaluation of the chlorine-ammonia process for bromate control during ozonation. *Ozone: Science and Engineering*, *29*(5), 363–372. https://doi.org/10.1080/01919510701552883

Wolf, C., von Gunten, U., & Kohn, T. (2018). Kinetics of Inactivation of Waterborne Enteric Viruses by Ozone. *Environmental Science and Technology*, *52*(4), 2170–2177. https://doi.org/10.1021/acs.est.7b05111

Xu, P., Janex, M. L., Savoye, P., Cockx, A., & Lazarova, V. (2002). Wastewater disinfection by ozone: Main parameters for process design. *Water Research*, *36*(4), 1043–1055. https://doi.org/10.1016/S0043-1354(01)00298-6

Young, S., Torrey, J., Bachmann, V., & Kohn, T. (2020). Relationship Between Inactivation and Genome Damage of Human Enteroviruses Upon Treatment by UV254, Free Chlorine, and Ozone. *Food and Environmental Virology*, *12*(1), 20–27. https://doi.org/10.1007/s12560-019-09411-2

Chapter 2 Demonstration-scale evaluation of ozone–biofiltration–granular activated carbon advanced water treatment for managed aquifer recharge

Samantha Hogard[1,2], Germano Salazar-Benites[2], Robert Pearce[1,2], Tyler Nading[3], Larry Schimmoller[3], Chris Wilson[2], Jamie Heisig-Mitchell[2], Charles Bott[2]

[1]Civil and Environmental Engineering Department, Virginia Polytechnic Institute and State University, Blacksburg, VA, USA

[2]Hampton Roads Sanitation District, PO Box 5911, Virginia Beach, VA 23471-0911

[3] Jacob Engineering Group, Inc. Englewood, CO

Citation: Hogard, S., Salazar-Benites, G., Pearce, R., Nading, T., Schimmoller, L., Wilson, C., Heisig-Mitchell, J., & Bott, C. (2021). Demonstration-scale evaluation of ozone–biofiltration–granular activated carbon advanced water treatment for managed aquifer recharge. Water Environment Research, 1–16. https://doi.org/10.1002/wer.1525

16 pages

Water Environment Federation
the water quality people™

Demonstration-scale evaluation of ozone–biofiltration–granular activated carbon advanced water treatment for managed aquifer recharge

Samantha Hogard ,[1,*] Germano Salazar-Benites ,[2] Robert Pearce ,[1] Tyler Nading ,[3] Larry Schimmoller ,[3] Christopher Wilson ,[2] Jamie Heisig-Mitchell ,[2] Charles Bott [2]

[1] Civil and Environmental Engineering Department, Virginia Tech, Blacksburg, VA, USA

[2] Hampton Roads Sanitation District (HRSD), Virginia Beach, VA, USA

[3] Jacobs Engineering Group, Inc., Englewood, CO, USA

Received 26 October 2020; Revised 13 January 2021; Accepted 17 January 2021

Additional Supporting Information may be found in the online version of this article.

Correspondence to: Samantha Hogard, Civil and Environmental Engineering Department, Virginia Tech, Blacksburg, VA, USA.
Email: shogard@vt.edu

*WEF Member.

DOI: 10.1002/wer.1525

Abstract

The Sustainable Water Initiative for Tomorrow (SWIFT) program is the effort of the Hampton Roads Sanitation District to implement indirect potable reuse to recharge the depleted Potomac Aquifer. This initiative is being demonstrated at the 1-MGD SWIFT Research Center with a treatment train including coagulation/flocculation/sedimentation (floc/sed), ozonation, biofiltration (BAF), granular activated carbon (GAC) adsorption, and UV disinfection, followed by managed aquifer recharge. Bulk total organic carbon (TOC) removal occurred via multiple treatment barriers including, floc/sed (26% removal), ozone/BAF (30% removal), and adsorption by GAC. BAF acclimation was observed during the first months of plant operation which coincided with the establishment of biological nitrification and dissolved metal removal. Bromate formation during ozonation was efficiently controlled below 10 μg/L using preformed monochloramine and preoxidation with free chlorine. N-nitrosodimethylamine (NDMA) was formed at an average concentration of 53 ng/L post-ozonation and was removed >70% by the BAFs after several months of operation. Contaminants of emerging concern were removed by multiple treatment barriers including oxidation, biological degradation, and adsorption. The breakthrough of these contaminants and bulk TOC will likely determine the replacement interval of GAC. The ozone/BAC/GAC treatment process was shown to meet all defined treatment goals for managed aquifer recharge. © 2021 Water Environment Federation

Practitioner points

- Floc/sed, biofiltration, and GAC adsorption provide important barriers in carbon-based treatment trains for bulk TOC and trace organic contaminant removal.
- Biofilter acclimation was observed during the first three months of operation in each operating period as evidenced by the establishment of nitrification.
- Bromate was effectively controlled during ozonation of a high bromide water with monochloramine doses of 3–5 mg/L.
- NDMA was formed at an average concentration of 53 ng/L by ozonation and complete removal was achieved by BAFs after several months of biological acclimation.
- An average 25% removal of 1,4-dioxane was achieved via oxidation by hydroxyl radicals during ozonation.

Key words

1,4-dioxane; biofiltration; bromate; granular activated carbon; managed aquifer recharge; NDMA; ozone; total organic carbon

Introduction

Water reuse has been implemented in recent years to combat environmental challenges associated with overuse of water resources. Common drivers for these projects include combating water scarcity and augmenting existing ground/surface water resources (US EPA, 2017). While water reuse often relies on membrane-based technologies in conjunction with reverse osmosis (RO), especially at coastal locations with existing ocean disposal, ozone/biofiltration-based treatment has several advantages associated with lower operating cost and elimination of brine waste streams (Gerrity et al., 2014). This provides a major benefit to inland utilities with few options for brine disposal. Additionally, ozone/biofiltration treatment may produce water that is more suitable for groundwater recharge from a geochemical compatibility standpoint (Vaidya et al., 2019). While there have been numerous studies of ozone-biofiltration-based advanced water treatment, there have been few at a large scale. Several full-scale ozone-biofiltration reuse facilities that have been operated in the United States include Gwinnett County, Georgia (Funk et al., 2019), Rio Rancho, New Mexico (City of Rio Rancho, 2017), El Paso, Texas (Sheng, 2005), and Abilene, Texas (Enprotec/Hibbs & Todd Inc.) while many others are still in the pilot testing or planning phase. The primary drawback observed in these treatment schemes is the limited capacity for total organic carbon (TOC) and total dissolved solids removal (Hooper et al., 2020), and the need for reliable and efficient nitrogen removal in the upstream wastewater treatment facility. However, in many cases ozone-biofiltration treatment is able to meet nearly every other treatment goal, as well as efficient trace organic contaminant removal, at a lower cost when compared with other membrane/advanced oxidation-based treatments (Plumlee et al., 2014; Sundaram et al., 2014).

Ozone treatment provides many benefits in water reuse applications including oxidation of organics, dissolved metals, taste and odor-causing compounds, and pathogen inactivation. The treatment goals and operation of the ozone system vary widely depending on the application. For example, utilizing ozone for the purpose of disinfection can often require a higher dose and closer process control than other applications. Efficiently controlling the ozone system is integral to maintaining finished water quality. The primary drawback associated with the implementation of ozone oxidation/disinfection is the formation of disinfection by-products (DBPs). Bromate is a well-known DBP which forms by the ozonation of bromide containing waters. This compound is regulated with a maximum contaminant level (MCL) of 10 µg/L (US EPA, 1998). Bromate forms via multiple reaction pathways including direct reactions with ozone and indirect reactions with the secondary oxidant, hydroxyl radicals (Pinkernell & von Gunten, 2001). While there are many strategies that can be implemented to interrupt or modify these formation pathways, common bromate control methods applied in water and wastewater treatment include pH suppression, ammonia addition, hydrogen peroxide addition, and free chlorine or monochloramine addition (Buffle et al., 2004; Soltermann et al., 2017). These mechanisms for control are less understood in the context of wastewater ozonation due to the high bromide concentrations and increased radical scavenging capacity of wastewater. Pilot testing has shown the benefits of using monochloramine to suppress hydroxyl radical exposure and form intermediate compounds, such as bromamines, thereby limiting bromate formation by the indirect pathway (Buehlmann et al., 2017). This study will highlight the use of monochloramine and peroxidation with free chlorine to control bromate formation at a demonstration-scale ozone–biofiltration plant.

Ozone treatment is also a well-established treatment technology for the removal of contaminants of emerging concern (CECs), which includes a suite of pharmaceuticals, pesticides, personal care products, and flame retardants. Some of these CECs are highly reactive with molecular ozone while others are more susceptible to oxidation by hydroxyl radicals, which form as a by-product of ozone decomposition (Lee et al., 2013). One of the CECs that is regularly detected in treated wastewater is 1,4-dioxane. This compound was widely used as an industrial solvent stabilizer and is commonly detected in surface water, groundwater, and treated wastewater (Stepien et al., 2014). Graywater produced from laundry wash water has also been identified as a significant source of 1,4-dioxane as this compound is a constituent of many laundry detergents and bleach products (Szczuka et al., 2020; Tanabe & Kawata, 2008). Many states have established drinking water and groundwater limits for 1,4-dioxane, but it is not yet regulated at the federal level. For example, potable water reuse facilities in California must exhibit at least 0.5-log removal of 1,4-dioxane by the selected advanced oxidation process (AOP) (California Department of Public Health, 2014), and there exists a 1 µg/L treatment goal for drinking water treatment facilities (California Water Boards, 2010). Treatment techniques for 1,4-dioxane removal in water reuse applications include AOPs such as UV advanced oxidation or ozone with hydrogen peroxide (US EPA, 2007).

The operation of ozone systems has also been shown to directly impact the performance of the downstream biofiltration (Bourgin et al., 2018). Ozone produces assimilable organic carbon that is biodegraded in the biologically active filters (BAFs). BAFs can also potentially remove dissolved metals and CECs. N-nitrosodimethylamine (NDMA) is a CEC which belongs to a group of compounds called nitrosamines, which is commonly removed biologically through BAFs (Bourgin et al., 2018; Gerrity et al., 2015; Nawrocki & Andrzejewski, 2011; Sundaram et al., 2020; Zeng et al., 2016). NDMA is formed as a disinfection by-product of chloramination and ozonation with common precursors including nitrogen-containing organic compounds such as personal care products, pharmaceuticals, and pesticides (Krasner et al., 2013). The formation of NDMA may also be influenced by several water quality and operating parameters including ammonia concentration, bromide concentration, precursor concentration, pH, and applied ozone dose (Sgroi et al., 2014). One study investigating the relative contribution of NDMA precursors by different water sources suggested that nutrient removal wastewater effluent produced lower levels of NDMA upon ozonation when compared with conventional wastewater effluent (Zeng, Glover et al., 2016;

Zeng, Plewa et al., 2016). Marti et al. (2015) also showed that ozone reactive precursors react to form higher NDMA concentrations when ozonated in wastewater when compared with deionized water as a result of catalyzing reactions and hydroxyl radical scavenging. The acclimation of biomass and biological removal of NDMA in the BAFs requires several months of filter operation (Sundaram et al., 2020). This degradation likely occurs as a result of co-metabolism as no organisms have been identified which can use NDMA as a sole carbon source (Fournier et al., 2009). This study will examine the performance of the biofilters during plant startup and the parameters which influence the formation and biodegradation of NDMA.

Granular-activated carbon (GAC) adsorption is commonly implemented in water reuse as another barrier against the removal of CECs and total organic carbon (Sundaram & Pagilla, 2019). As mentioned previously, limited TOC removal is the primary drawback to ozone-BAF treatment processes. However, ozone and biofiltration implemented in combination with GAC provide a multiple barrier approach for bulk and trace organic contaminant removal. The removal of CECs remains a topic of great concern in water reuse applications due to the continual emergence of new contaminants such as perfluoroalkyl substances (PFAS), pharmaceuticals, and personal care products. Some of these compounds can serve as surrogates for treatment performance based on their chemical structure (Schimmoller et al., 2020). Monitoring the operation of the GAC is important to plant operation, as the replacement or regeneration of GAC media may represent a significant operations and maintenance cost at an ozone/BAF/GAC-based advanced water treatment facility.

The Sustainable Water Initiative for Tomorrow (SWIFT) is the effort of the Hampton Roads Sanitation District (HRSD) to provide sustainable water resources in the southeast Virginia region by implementing managed aquifer recharge through advanced water treatment. Pilot testing was conducted to compare the performance of membrane-based and ozone/BAF/GAC-based treatment technologies for this purpose. The results of this testing proved that the ozone/BAF/GAC treatment train was able to meet all defined treatment goals and produced water which was more compatible with the native groundwater when compared with membrane-based treatment (Vaidya et al., 2019). Therefore, the ozone/BAF/GAC treatment train was selected for further pilot testing. This treatment train includes coagulation–flocculation–sedimentation (floc/sed), ozone oxidation and disinfection, BAF, GAC adsorption, and ultraviolet (UV) disinfection (Figure 1). The pilot was operated from July 2016 to May 2018 to collect long-term monitoring data and to support the full-scale application of this treatment process (Vaidya et al., 2019). The next phase of the initiative included the construction and operation of the SWIFT Research Center (SRC) in Suffolk, Virginia which includes the 1-MGD demonstration advanced treatment train, recharge well, and monitoring wells. The monitoring data gathered during the startup and operation of this facility can be used to better understand the ozone/BAF/GAC-based treatment process as it is applied in large scale applications with the purpose of water supply augmentation and groundwater recharge. Operational challenges identified during startup include optimizing the operation of the ozone system while controlling disinfection by-product formation and maximizing trace organic contaminant removal, monitoring BAF acclimation and CEC biodegradation during plant startup, and optimizing GAC performance. The purpose of this study is to demonstrate the effectiveness of an ozone-BAF-GAC-based advanced water treatment plant with respect to bulk organics removal, disinfection by-product mitigation, nitrosamine removal, and trace organic contaminant oxidation and adsorption.

Methods

The SRC has been in operation and recharging the Potomac Aquifer since May 2018. This paper will present data from two distinct operating periods from May 2018 to December 2018 and April 2019 to May 2020 denoted as operating period one and two, respectively. This represents two periods of plant

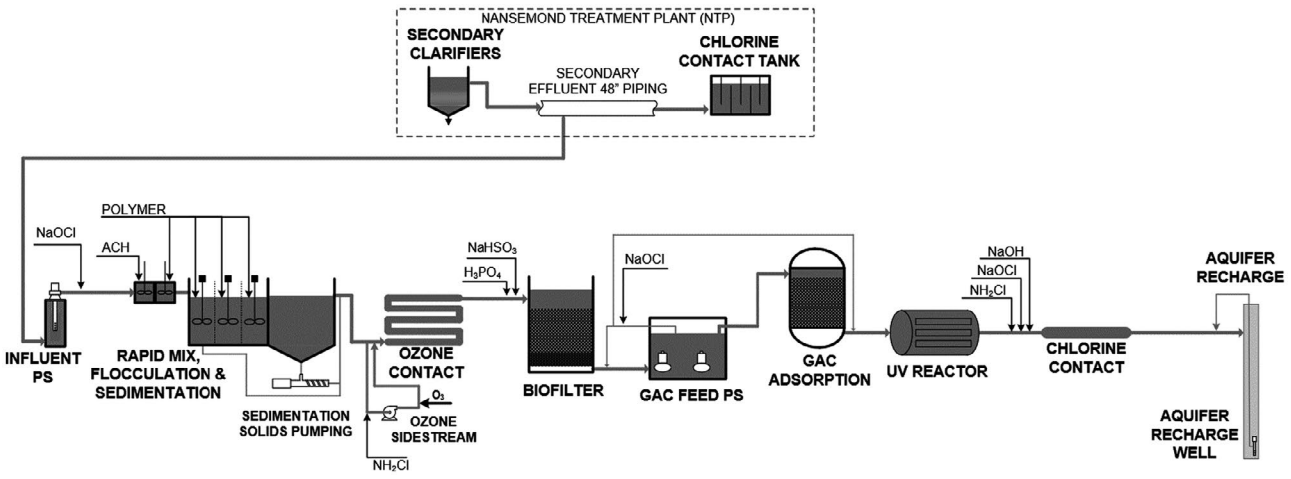

Figure 1. SRC process flow diagram.

startup that occurred due to warranty repairs that were made at the SRC from December 2018 to April 2019. During this period of time, the media in the BAFs was replaced with virgin activated carbon media and the media in the GAC vessels was also replaced.

The SRC treats secondary wastewater effluent (N < 4 mg/L, P < 0.3 mg/L) from the Nansemond Wastewater Treatment Plant (NTP), owned and operated by HRSD. NTP is a five-stage Bardenpho treatment process with typical effluent characteristics outlined in Table 1. The quality of the final treated water (referred to herein as SWIFT Water) at the SRC was highly dependent on the upstream wastewater plant operation. During times of stable operation, the SRC operated according to parameters outlined in Table 2. The SRC process flow diagram can be seen in Figure 1. The SRC was permitted to meet all primary drinking water maximum contaminant levels (MCLs) and total nitrogen (TN) and total organic carbon (TOC) limits. The finished water TOC treatment goals include a daily maximum of 6 mg/L and a monthly average of 4 mg/L. This limit is consistent with the equivalent chemical oxygen demand (COD) limit of 10 mg/L that is followed by other potable reuse facilities in Virginia, including Loudoun Water and Upper Occoquan Service Authority (US EPA, 2017). The TN treatment goals include a daily maximum of 8 mg/L and a monthly average of 5 mg/L. SWIFT Water also meets the "12/10/10" disinfection rule set forth in the California Department of Public Health's guidelines for indirect potable reuse (IPR) via groundwater recharge (12-log enteric virus removal, and 10-log removal of both *giardia* and *cryptosporidium*). The complete summary of how disinfection credits are achieved at the SRC can be found in Table S1.

The coagulant, aluminum chlorohydrate (ACH), was fed with a cationic polymer to rapid mix ahead of floc/sed. There was also an optional sodium hypochlorite addition point ahead of floc/sed to pre-oxidize organics at times of elevated ozone demand. Prechlorination was only used on several occasions for short periods of time and it was controlled manually. The floc/sed process is operated with two inclined plate trains in parallel (equipment provided by Meurer Research Inc., Golden, CO). Preformed monochloramine was fed to the settled water at a dose of 3–5 mg/L Cl_2 to control DBP formation during ozonation. This dose was determined during pilot testing and preliminary testing at the SRC. Preformed monochloramine was formed inline by the injection of ammonia followed by the injection of chlorine. Softened water was used for carrier water in this system.

Table 1. Average NTP SCE characteristics

	MIN	MAX	AVERAGE	ST DEV
TKN (mg-N/L)	1.24	5.11	1.83	0.53
NO_3^- (mg-N/L)	0.20	3.34	1.50	0.58
NO_2^- (mg-N/L)	0.01	0.16	0.03	0.03
TOC (mg/L)	8.01	16.6	10.7	1.55
Total Mn (µg/L)	11.6	454	34.0	50.0
Bromide (mg/L)	0.11	1.49	0.41	0.21
1,4-dioxane (µg/L)	0.39	1.39	0.62	0.13
NDMA (ng/L)	3.33	72.9	15.1	14.3
NMOR (ng/L)	<2	283	50.7	70.6

The ozone system, supplied by Xylem-Wedeco (Herford, Germany), was a side stream system in which approximately 50% of the flow was ozonated and subsequently combined with the bulk flow in a custom built 316 stainless steel pipeline contactor with a residence time of approximately 8 min. This residence time was sufficient for complete ozone decay during normal operating conditions. The ozone generators had a capacity of 92 kg/day at 12% weight ozone gas concentration. The ozone residual concentration was monitored at different locations in the ozone contactor using an Orbisphere C1100 dissolved ozone probe (Hach, Loveland, CO), and the applied ozone dose was adjusted automatically to achieve at least 3-log virus removal and 1.5-log giardia removal as calculated through single-point CT measurement and automated ozone dose control using Table C-13 from the EPA Guidance Manual for Disinfection Profiling and Benchmarking (recreated in SI as Table S2).

After ozonation, monochloramine was quenched with sodium bisulfite to prevent any detrimental impact to the biofilters. The flow was split evenly to the four BAFs (Xylem-Wedeco, Herford, Germany) in parallel with a design empty bed contact time of 9.4 min with one filter out of service (12 min with all filters in service). The activated carbon media in the BAFs was Calgon Filtrasorb816 (Pittsburgh, PA). Phosphorus was identified as a limiting nutrient in the BAFs, and therefore, during the second operating period, phosphoric acid was added prior to the filters. Backwashing was performed periodically based on head loss or turbidity breakthrough. Due to the high dissolved oxygen concentration in the ozone effluent, there was gas binding observed in the filters which resulted in artificially high head loss after short periods of operation. For this reason, a resting period protocol was established in which flow was stopped to the filter for approximately 10 min to allow for gas bubble release.

The next step in the treatment process was GAC adsorption in which the flow was split between two GAC contactors (WesTech, Salt Lake City, UT). The operation of the GAC adsorbers was flexible, allowing for parallel or series operation with variable flow split possible for each vessel. The GAC carbon media was Calgon Filtrasorb400M (Pittsburgh, PA). Finally, the water was processed through the UV disinfection system (Xylem-Wedeco) which was designed and validated to provide 4 logs of virus inactivation at a dose of 186 mJ/cm^2. After this, sodium hydroxide was added to adjust the pH to match that of the native groundwater, and either preformed monochloramine or free chlorine was added to prevent biofouling to the wellhead.

Analytical methods

Sampling was performed daily during times of aquifer recharge for constituents including bromide, bromate, and nitrogen species. Bromate was analyzed according to EPA method 300.1 with a Dionex 5000 plus with IC columns AS19 and AS24. Bromide was analyzed by EPA method 300 using a Dionex Integrion HPIC and column AS27. Samples were collected weekly for nitrosamines

Table 2. Operating parameters

PARAMETER	VALUE
ACH dose (as product)	25 mg/L
Cationic floc-aid polymer dose	0.75 mg/L
NH_2Cl dose	3–5 mg/L Cl_2
Ozone dose control	Residual control to achieve >3-log virus removal and >1.5-log giardia removal by CT per Disinfection Profiling and Benchmarking Guidance Manual
Average O3:TOC	0.8 ± 0.2[1]
Average applied ozone dose	5.4 ± 1 mg/L[1]
BAF EBCT	12 min
GAC EBCT	15–30 min
Design UV dose	4-log virus = 186 mJ/cm^2

[1]Average and standard deviation for startup 2.

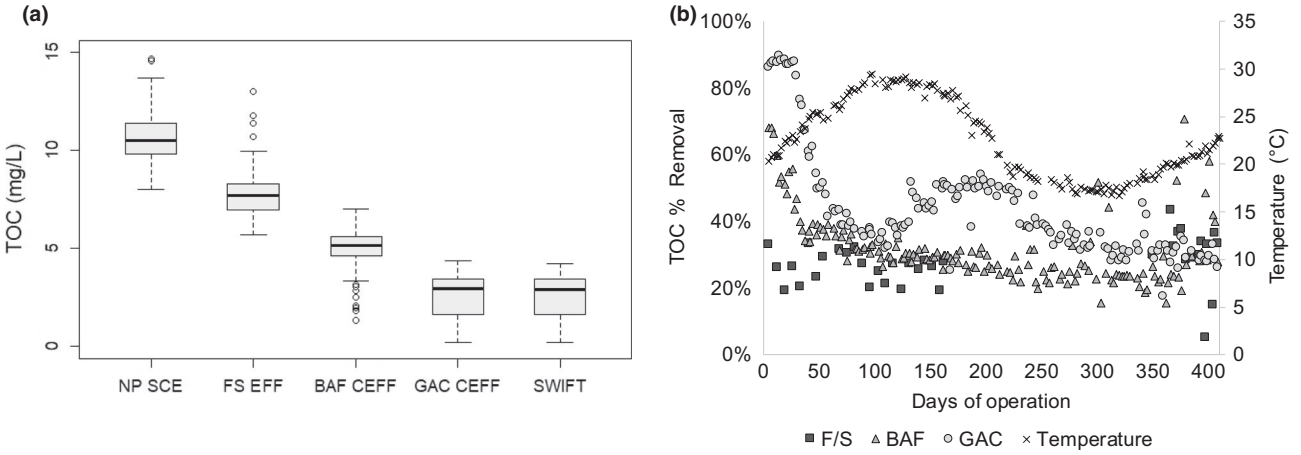

Figure 2. (a) TOC data represented by box and whisker plots—box represents interquartile range with the middle line denoting the mean, whiskers represent minimum and maximum if they are within the bounds of ±1.5 * IQR, any value greater than this is shown as an outlier with an open symbol. (b) Percent removal of TOC during Startup 2.

(NDMA, NMOR) and 1,4-dioxane. These compounds were analyzed according to EPA method 521 and 522, respectively, using an Agilent 7010B GC/MS Triple Quadrupole (Santa Clara, CA). Total organic carbon (TOC) was analyzed three times per week according to Standard Method 5310 using a Shimadzu TOC 4200. Total manganese and iron were analyzed weekly according to EPA method 200.7. Haloacetic acids (HAAs) and trihalomethanes (THMs) were analyzed monthly according to EPA methods 552.2 and 524.2, respectively. All of the aforementioned analyses were performed by HRSD's Central Environmental Laboratory. A suite of 96 CECs was analyzed quarterly by Eurofins Eaton Analytical (Monrovia, CA) by liquid chromatography with tandem mass spectrometry (LC-MS-MS). In addition to these, there is a list of unregulated chemicals including those which are considered public health or treatment efficacy indicator compounds, which are listed on the Contaminant Candidate Lists (CCLs) and the Unregulated Contaminant Monitoring Rule (UCMR) that were also monitored quarterly. A complete list of the compounds which were monitored, the respective analytical methods and rationale for monitoring can be found in Table S3.

Results and discussion

Total organic carbon

TOC was measured across the SRC process train to quantify performance of floc/sed, BAF, and GAC. This multiple barrier approach ensures efficient TOC removal at several stages in the process. Influent TOC fluctuations may be attributed to changes in treatment performance at NTP or varying inputs of refractory organic material from industrial, commercial, or domestic sources into the raw wastewater influent. Box plots showing the average range of TOC data throughout the SWIFT process are presented in Figure 2a.

The percent TOC removal achieved by each treatment process is summarized for the second operating period in Figure 2b. The apparent increase in TOC removal by GAC when temperature decreased was due to the operation of the GAC vessels changing. Floc/sed was consistently responsible for approximately 20%–30% TOC removal. After this, ozone oxidation produced organic carbon which may be amenable to biodegradation and subsequently removed through

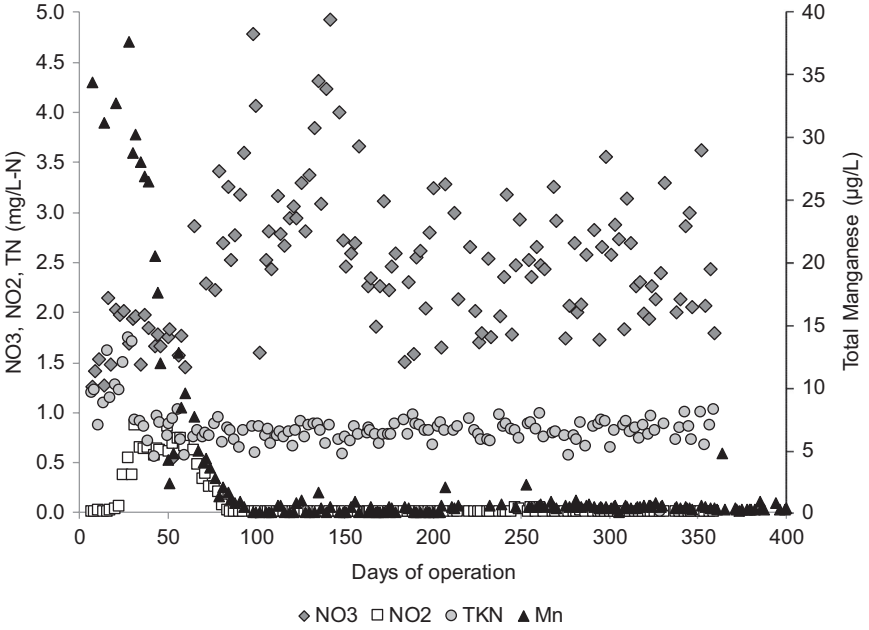

Figure 3. BAF effluent nitrogen and manganese during acclimation (Startup 2).

biofiltration. At the beginning of plant operation, however, the elevated TOC removal provided by the BAF was most likely due to adsorption by virgin GAC media. After several months of operation, TOC removal can be attributed to the biological degradation of assimilable organic carbon. TOC removal by BAF levelled off at approximately 30% and this was only slightly decreased during winter months. This removal is consistent with removal reported for biofilters with exhausted media in previous studies (Sundaram & Pagilla, 2019). It was found during the second startup that phosphorus was likely a limiting nutrient in the BAFs based on the low concentrations in ozone effluent, and therefore, phosphoric acid was fed to the BAF influent beginning on day 190 of operation.

GAC adsorption was the final treatment barrier which provides TOC removal. The primary mechanism of TOC removal through GAC is adsorption while some biological growth and removal may also be occurring. GAC effluent TOC is important to monitor to understand when the adsorption capacity of the carbon media is exhausted and when GAC reactivation will be required to remain in compliance with the TOC and trace organic contaminant treatment objectives. During the first operating period, the two GAC vessels were operated in parallel for the entire duration of plant operation. After GAC media was replaced in GAC vessel 1, it was operated alone at the beginning of the second operating period. As TOC breakthrough was observed approaching the 4 mg/L treatment objective, GAC vessel 2 was put into service as well. The GAC vessels have since been operated in parallel with variable flow splits in order to achieve a target TOC of 4 mg/L. The flow split variations are shown in Figure S1a. GAC breakthrough curves for both periods of operation are shown in Figure S1b. As the removal is observed through GAC plateaus, it can be assumed that the adsorption capacity has been exhausted and biological removal is occurring. Theoretically, TOC removal by adsorption should only depend on the number of BV processed and should be independent of empty bed contact time (EBCT) (beyond the mass transfer zone). However, during the second startup, TOC removal by GAC 1 can be seen to have a dependence on EBCT exhibited by the disjointed breakthrough curve observed in Figure S1b as a result of changing flow. This suggests the likely development of biological activity in the GAC well prior to exhaustion of adsorption capacity. Both continuing to monitor the performance of GAC and optimizing TOC removal upstream is critical in successfully operating this ozone-BAF-GAC treatment train in order to meet SWIFT Water treatment goals.

Ammonia oxidation

Nitrogen compounds (NO_2, NO_3, NH_3, TKN) have been monitored throughout the treatment process during both startup periods. There was no mechanism for significant nitrogen removal in the process, but the transformation of nitrogen reveals important information about the biological acclimation of the biofilters. With the addition of monochloramine prior to ozone, there was an added ammonia residual (0.5–1 mg/L-N) which reaches the biofilters. As the filters start to accumulate biomass, they begin to nitrify ammonia. Nitrification occurs in two steps, first ammonia is oxidized to nitrite and then nitrite is oxidized to nitrate. This transition is seen clearly by the increase in nitrite which occurred one month after startup, followed by the shift to full nitrification approximately two months after this (Figure 3). This was observed on the pilot scale as well, and the occurrence of nitrification was used as an indicator for biological activity (Vaidya et al., 2020). Other studies have also noted the usefulness of biofiltration after ozonation due to the capacity for BAFs to oxidize ammonia (Wert et al., 2007).

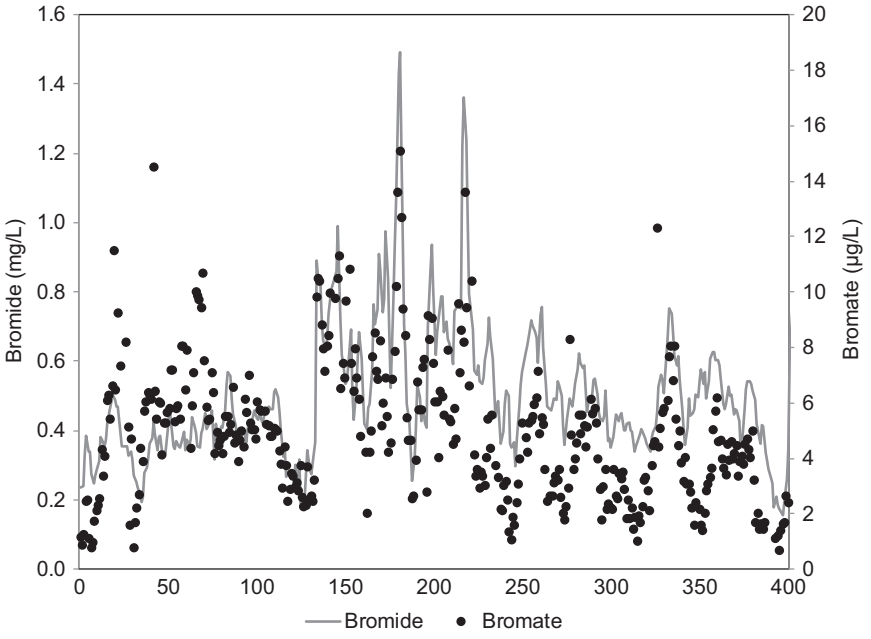

Figure 4. NTP SCE bromide and ozone effluent bromate. NH_2Cl dose was increased from 3 to 5 mg/L when bromide spiked on day 134.

Dissolved metals removal

Metals concentrations are also monitored throughout the process in order to quantify removal and to adhere to secondary MCLs. Both iron and manganese are regulated with secondary MCLs of 0.3 and 0.05 mg/L, respectively. Each of these compounds is related to esthetic concerns including color and taste of the treated water. Manganese is also potentially related to health concerns, and for this reason, it is regulated with a maximum acceptable concentration (MAC) of 0.12 mg/L in Canada (Health Canada, 2019). Oxidized metals removal is also important at the SRC to prevent fouling of downstream equipment and clogging of the recharge well. The majority of iron removal occurs physiochemically during flocculation/sedimentation (~70% removal observed) and biofiltration serves as a biological treatment barrier in this process. Most iron measurements throughout the treatment process were below the method reporting limit during the second operating period (Figures S2). It is hypothesized that the residual iron remaining in SWIFT water is complexed with organics and therefore cannot be removed via oxidation and filtration. This is a challenge often associated with the treatment of drinking water with high levels of iron and organics (Munter et al., 2005). Reckhow et al. (1991) also demonstrated the detrimental impact of organics concentration on the oxidation of iron by ozone. Excursions in the influent iron concentration can be attributed to periods of time where NTP was feeding ferric sulfate to promote chemical phosphorus precipitation upstream.

Removal of manganese is primarily achieved through chemical and biological oxidation and precipitation/adsorption in the ozone-BAF treatment step. The biological removal requires a period of acclimation which was consistent with the establishment of nitrification in the biofilters. The complete removal of manganese was observed just after the time where complete nitrification was established (Figure 3). This is consistent with expectations and observations of other studies which showed biological removal of manganese after complete oxidation of ammonia due to the necessary change in oxidation–reduction potential (ORP) (Hasan et al., 2012). The simultaneous biological oxidation of ammonium, manganese, and iron has been shown to be influenced by several parameters including the respective concentration of each constituent, dissolved oxygen, ORP, and pH (Cheng et al., 2017; Tekerlekopoulou et al., 2013). The factors which influence dissolved metal removal and re-dissolution in the biofilters are still under investigation at the SRC.

Bromate formation and control

Bromide concentrations measured daily in the NTP effluent during the second operating period are presented in Figure 4. The bromide concentration in the NTP effluent ranged widely from 0.15 to 1.49 mg/L (average = 0.50 ± 0.19 mg/L). The cause of this broad variation is the variable flow rate of landfill leachate that is discharged to NTP which introduces the primary source of bromide. During the second operating period, it was also found that there was a strong tidal influence on bromide concentration as a result of seawater inflow and infiltration. At times when all other bromide loads were constant, there was found to be a direct correlation (R^2 = 0.63) between conductivity and bromide due to this tidal influence (Figure S3b). Therefore, online conductivity measurements became an important surrogate parameter that was used to monitor bromide real time.

Due to this elevated background bromide concentration, there was a need to consistently monitor and control bromate formation at the SRC. The resulting bromate concentration depends on several operating parameters including applied

ozone dose, influent bromide concentration, and monochloramine dose. Applied monochloramine dose, NTP SCE bromide, ozone effluent bromate data are summarized for the second operating period in Figure 4. During the second startup period, testing was performed to understand a manageable level of landfill leachate, and resulting bromide load, which can be accepted at NTP. This testing showed that a bromide concentration of 0.3–0.5 mg/L was sustainable for plant operations and bromate was able to be controlled below the MCL while using preformed monochloramine to limit formation. Bromate formation was measured for a range of applied ozone doses and chloramine doses during this startup period while the bromide was increasing. Figure 5 shows that bromate could be controlled below the MCL at a leachate flow that resulted in bromide = 0.37 mg/L and applied ozone dose of 6 mg/L (0.74 O3:TOC) with a chloramine dose of 3 mg/L-Cl_2.

During times of relatively stable bromide concentration, it was found that bromate formation depended mostly on the applied ozone dose. This relationship between ozone dose and bromate formation motivated testing to reduce ozone demand by preoxidizing the NTP SCE with free chlorine. Testing at the SRC has shown that preoxidation ahead of floc/sed is effective in reducing the ozone demand and thereby suppressing bromate formation. In one instance, sodium hypochlorite was fed at a dose of 4 mg/L-Cl_2 which decreased the ozone demand, and thus, the applied ozone dose required to achieve the same CT, by approximately 2 mg/L. The applied chlorine dose did not exceed the 1.5-h chlorine demand of the NTP SCE. As a result, bromate formation decreased by about 90%. Similar results have been observed in several studies, which demonstrated the benefits of feeding free chlorine to control bromate formation (Buffle et al., 2004; Wert et al., 2007). The major drawback associated with using chlorine to control bromate is the potential formation of disinfection by-products such as trihalomethanes (THMs) and haloacetic acids (HAAs). This concern is elevated when chlorinating treated wastewater effluent due to the higher bromide and organics/precursor concentrations (Krasner et al., 2009). During testing at the SRC, THMs and HAAs were formed with the addition of free chlorine to the SCE, and however, the concentrations were below the respective MCLs. Additionally, these compounds were effectively removed in the BAFs (Figure 6). Previous studies have shown that HAAs are somewhat amenable to biological removal in BAFs, but the same has not typically been observed for THMs (Arnold et al., 2018; Zeng, Glover, et al., 2016; Zeng, Plewa, et al., 2016). The mechanism by which THMs were removed by BAFs was not determined as a part of this study.

Bromate removal by GAC. During each startup period, bromate removal was observed on virgin GAC media. This may be attributed to the capacity of the surface of the virgin GAC media to catalytically reduce bromate to bromide (Asami et al., 1999; Siddiqui et al., 1999). The reduction of bromate by GAC provided a temporary barrier against bromate MCL exceedances and allowed flexibility in ozone operation during each startup period. This bromate reduction capacity was completely exhausted ($C/C_0 = 1$) after approximately 8000 GAC bed volumes in each startup period (Figure 7). This shows that GAC only provides short-term bromate removal and other control methods should be employed when needed. In previous studies, the bromate removal rate of virgin GAC decreased after three months of operation when the media became biologically active (Asami et al., 1999). Low (<0.5) C/C_0 values observed at higher bed volumes can most likely be attributed to the

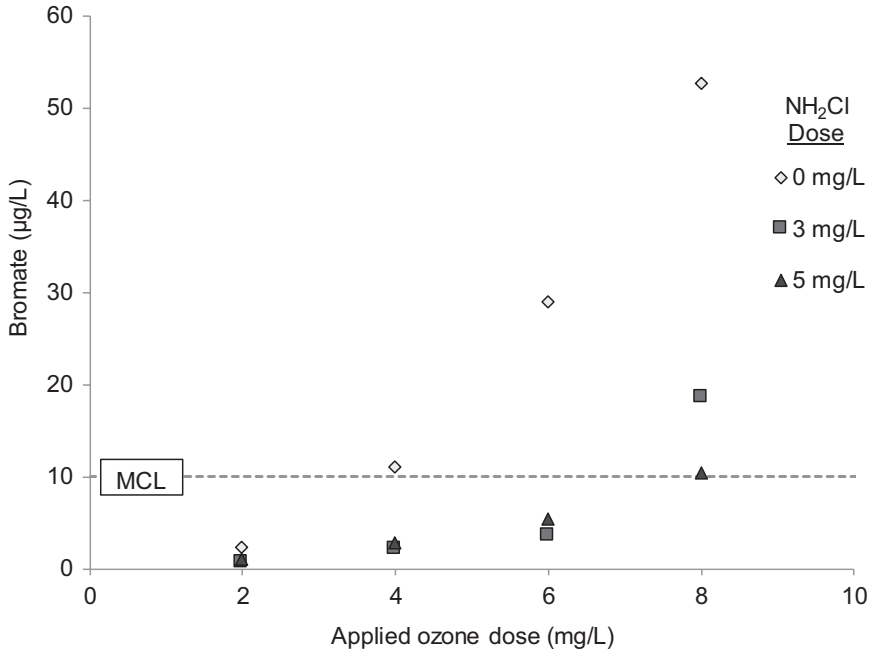

Figure 5. Bromate formation while bromide = 0.37 mg/L.

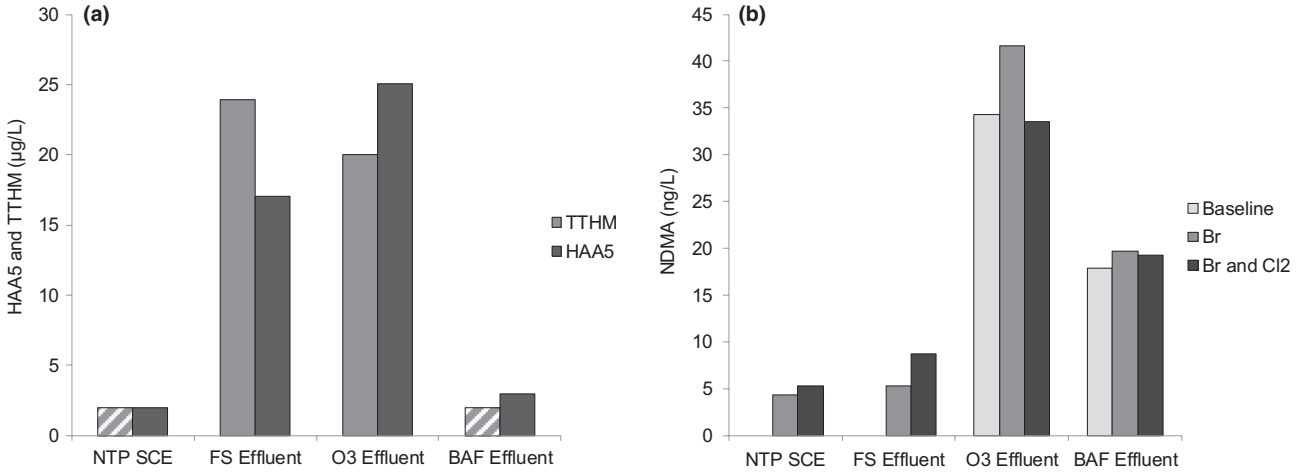

Figure 6. DBP formation and removal during prechlorination (4 mg/L Cl_2) and bromide spiking (spiked + 0.3 mg/L bromide) in NTP SCE, floc/sed effluent, ozone effluent, and BAF effluent. Values below the detection limit are shown at half of the detection limit value, and those bars are hatched. NDMA data was collected while adding 0.4 mg/L bromide and 4 mg/L Cl_2.

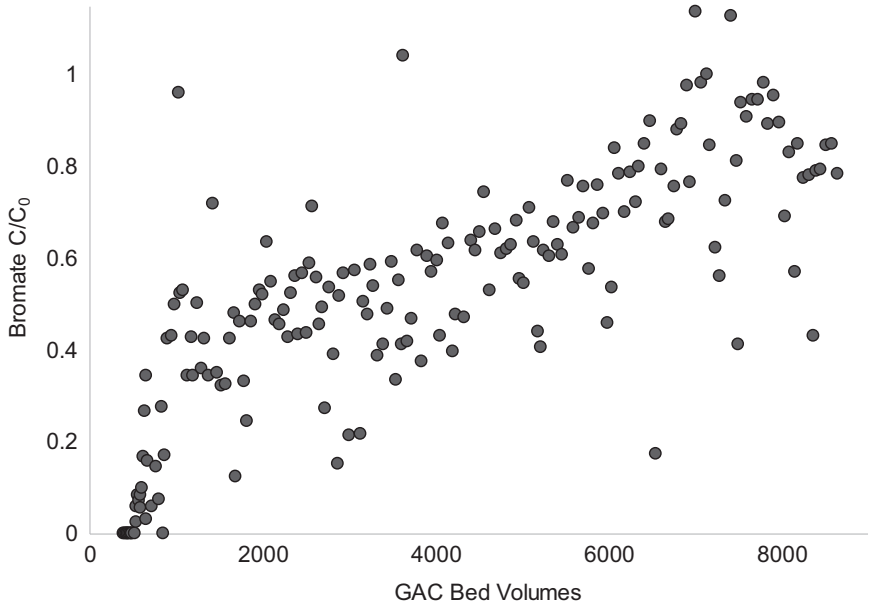

Figure 7. Bromate removal by GAC (Startup 1). GAC bed volumes are represented as flow weighted values according to the GAC flow split at the time of sampling.

extended residence time between ozone effluent and GAC effluent sample points which may result in an apparent decrease in bromate where there was none.

Optimizing ozone addition. During the period of time when warranty repairs were being made at the SRC, one notable design modification that was made was the relocation of the ozone injection point. Originally, the sidestream residence time was approximately 30 s, during which significant bromate formation and ozone decay occurred. The bromate formation in the sidestream was likely due to both the elevated ozone to bromide and ozone to TOC ratios that are achieved in the sidestream. Studies have shown that bromate formation in the sidestream can be problematic if the residence time exceeds the design guidelines of 3 s (Wert et al., 2016). Testing during SRC startup showed that roughly half of the total bromate formation occurred in the extended sidestream piping (data not shown). Minimizing this sidestream residence time is particularly important when using ozone to achieve disinfection credit because ozone contact time in the sidestream before degassing is not included for CT credit (US EPA, 2010). For this reason, design guidelines also recommend minimizing this time as much as possible to reduce uncredited disinfection. After the injector was moved at the SRC, the residence time in the sidestream was reduced to ~1.2 s. This resulted in an approximately 24% lower average O3:TOC dose to meet the

same disinfection treatment goals. As a result, bromate control was also feasible during the second startup period with 160% higher average bromide concentration when compared with the first operating period (startup 1 average bromide = 0.19 ± 0.04, startup 2 bromide = 0.50 ± 0.19).

Nitrosamines

NDMA. The NTP SCE NDMA concentration varied from 3 to 73 ng/L (average = 15.4 ± 14.6 ng/L). This variation may have been due to variable influent sources of NDMA or this might reflect changes in NTP operation. Several studies have shown the impact of WWTP operation on NDMA formation/removal upstream of advanced water treatment plant (Krasner et al., 2009). The impact of NTP SCE bromide concentration on NDMA formation was investigated at the SRC due to the potential for bromide to enhance NDMA formation in the presence of specific precursors (von Gunten et al., 2010). No significant difference in NDMA formation was observed as a function of bromide concentration (correlation not shown). One study by Marti et al. (2016) showed the potential for chlorine to pre-oxidize ozone reactive NDMA precursors, but no significant difference in NDMA formation was observed during preoxidation at the SRC (Figure 6). This demonstrates the dependence of NDMA formation on ozone exposure rather than applied ozone dose, which was variable in this case to achieve the same CT disinfection credit. Additionally, preoxidation had no impact on short-term biological NDMA removal downstream. During normal operating conditions, NDMA was measured at an average concentration of 53 ± 21 ng/L after ozonation. These data are summarized in Figure 8 for both the first and second operating periods. Although chloramine was fed prior to ozonation, testing has shown that chloramine does not contribute to or inhibit NDMA formation at the typical operating ozone doses (Figure S4). This was likely due to the short residence time and potentially the concurrent oxidation of chloramine reactive precursors by ozone which has been noted by several studies (Chen et al., 2018; Lee et al., 2007). The limited impact of monochloramine addition and resulting hydroxyl radical quenching, on NDMA formation also supports the claims of Pisarenko et al. (2015) that hydroxyl radicals do not contribute to NDMA formation. Additionally, preformed monochloramine was used at the SRC instead of in situ monochloramine addition in order to avoid dichloramine formation, which has been shown to form higher concentrations of NDMA (McCurry et al., 2017). At lower ozone doses, the addition of chloramine appears to contribute to marginally higher NDMA formation (Figure S4). It was also observed that there was no increased NDMA formation by ozone beyond the ozone dose where there was a measurable ozone residual. This was likely due to the maximum NDMA formation potential being reached for most precursors at this point (Marti et al., 2015).

NDMA was primarily removed in the process via cometabolic biological degradation in the BAFs and by UV photolysis at high doses. The establishment of sustained NDMA biodegradation in the BAFs may require several months of acclimation (Sundaram et al., 2020). The removal observed by BAFs immediately following the first startup can most likely be attributed to short-term adsorption of NDMA on virgin GAC media. After this, the occurrence of NDMA removal was concurrent with the development of nitrification and removal of dissolved Mn in the biofilters during both startup periods suggesting there was biological removal occurring at this time. Greater than 70% NDMA removal was achieved in one to three months for both operating periods. During the first startup operating period, there were several occurrences of decreased biological removal of NDMA (less than 50%) which may be attributed to short-term shutdowns of the filters prior to sampling (indicated by X symbols in Figure 8). The length of biofilter shutdown ranged from 18 to 72 h. There was no observed decrease in TOC or

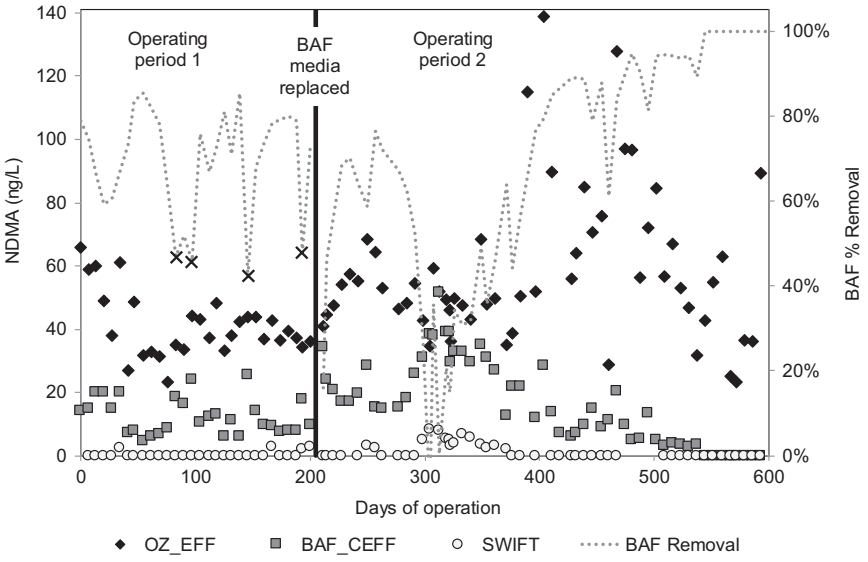

Figure 8. NDMA throughout the duration of plant operation. X symbols represent instances of poor NDMA removal attributed to BAF shutdown events during operating period 1. Vertical line represents the beginning of operating period 2 where BAF media was replaced.

dissolved metal removal after these events. Two months after the second BAF startup, approximately 80% biological NDMA removal was achieved. Several weeks after this, the removal of NDMA through the biofilters decreased to <10%. It was identified that sodium bisulfite was being fed in excess of the concentration which is required to quench residual monochloramine after ozonation. The toxic effect of bisulfite was clearly exhibited by the poor NDMA removal, and however, there was no other indication of reduced biological activity at this time. Neither the TOC removal nor the oxidation of ammonia and dissolved metals was affected by the overfeeding of $NaHSO_4$. The opposite result was observed on the pilot scale, where nitrification was inhibited by overdosing sodium bisulfite but NDMA removal was not impacted (Vaidya, 2020). After the $NaHSO_4$ dose was decreased at the SRC (beginning on day 298 on Figure 8), biological removal of NDMA began to recover almost immediately and >70% removal was established again after approximately three months of operation. Therefore, it can be determined that consistently maintaining the appropriate dose of sodium bisulfite for complete dechlorination is crucial in order to ensure biological activity is sustained.

During times when there was detectable NDMA after the BAFs, the additional removal observed was due to direct photolysis by UV irradiation. The actual UV dose during startup was in excess of the required value with new lamps, minimal sleeve fouling, and high UVT as a result of efficient TOC removal by virgin GAC. The maximum NDMA removal observed by UV was 90% at an average UV dose of 495 mJ/cm^2 and GAC effluent UVT equal to 94.4%. Considering the high UV dose required for NDMA photolysis, this was only considered a temporary NDMA removal mechanism. The primary concern with respect to NDMA removal during startup of this treatment process was that biological removal must be established in the BAFs prior to the point when the UV system was unable to deliver the relatively high dose required for efficient NDMA photolysis (based on GAC removal of TOC).

NMOR. N-nitrosomorpholine (NMOR) is another nitrosamine frequently detected in water reuse applications. Although no regulatory standard exists for NMOR in the United States, drinking water reuse guidelines have been established in Germany and Australia of 10 and 1 ng/L, respectively (NHMRC, 2008; Planas et al., 2008). NTP SCE NMOR concentrations observed during the second startup operating period varied widely (Figure S5). After approximately two months of operation, the influent concentration increased to approximately 300 ng/L. Following the time when this maximum concentration was observed, the influent NMOR concentration began to decrease over a period of a few weeks. Generally, this compound is not considered a disinfection byproduct like NDMA, but instead exists in wastewater effluent from anthropogenic sources (Glover et al., 2019; Krauss et al., 2009). The most common treatment technology for removal of NMOR is RO or photolysis by UV (Glover et al., 2019). There was marginal removal observed through ozonation and adsorption in GAC, and however, the majority of NMOR removal at the SRC was achieved by photolysis during UV treatment. At the time that the concentration began decreasing, desorption of NMOR from the BAF and GAC was observed due to the change in concentration gradient. Up to 41% NMOR removal was observed by ozone at an O3:TOC ratio of 0.93 in the absence of monochloramine. This is well aligned with the maximum removal noted in literature of 36% at O3:DOC of 1.16 (Hollender et al., 2009). GAC breakthrough of NMOR was observed after approximately 7000 GAC bed volumes. Additionally, greater than 2-log removal was observed through

Table 3. SWIFT water DBPs, CECs, and performance indicators

	SAMPLING EVENTS (*N*)	NUMBER OF DETECTIONS	MDL	MIN	MAX	AVERAGE	ST DEV
HAA5 (μg/L)	22	14	0.2[1]	0.64	13.4	4.41	3.65
TTHM (μg/L)	22	4	4	4.4	10.7	7.62	2.34
Chlorate (mg/L)	10	9	0.01	0.04	1.37	0.74	0.34
Perchlorate (μg/L)	9	4	0.5	0.52	0.84	0.70	0.12
Acetaldehyde (μg/L)	8	7	5	2	5.9	3.37	1.28
Formaldehyde (μg/L)	10	7	5	18	41	32.3	8.29
Quinoline (ng/L)	9	3	5	8.1	11	10	1.37
Sucralose (ng/L)	9	4	5	270	12,000	6012	5501
Iohexol (ng/L)	9	4	10	22	160	70.3	53.9
Primidone (ng/L)	9	2	5	9.7	11	10.4	–
Cotinine (ng/L)	9	1	10	26	26	–	–
Caffeine (ng/L)	9	1	5	22	22	–	–
Acetaminophen (ng/L)	9	1	5	9.6	9.6	–	–
Ketorolac (ng/L)	9	1	5	2.3	2.3	–	–
Diltiazem	9	1	5	7.2	7.2	–	–
4-nonylphenol (ng/L)	9	1	100	1400	1400	–	–
PFOA (ng/L)	10	2	2	5.3	5.7	5.5	–

[1]The MDL is variable for each of the five HAAs.

UV photolysis at a dose of 280 mJ/cm^2 which exceeds removals reported elsewhere (Glover et al., 2019; Shah et al., 2013). The source of NMOR was not determined as a part of this study.

Other disinfection by-products

In an effort to prevent biofouling in the SWIFT Water piping to the wellhead, the final disinfectant was changed from monochloramine to free chlorine after several low-level total coliform detections on SWIFT Water. As a result of this, chlorinated DBPs (HAAs and TTHMs) were formed at concentrations below their respective MCLs while they were not detected during periods of monochloramination (Table 3). Another noted benefit of ozone–biofiltration treatment is the reduction in DBP formation potential which allows for flexibility in final disinfectant selection and protects against MCL exceedances (Selbes et al., 2017; de Vera et al., 2016). Furthermore, pilot scale testing at HRSD has demonstrated the efficacy of soil aquifer treatment to abate these contaminants below detection limits (Pradhan, 2018).

Chlorate was also regularly detected in the finished water at concentrations ranging from 0.04 to 1.37 mg/L. Measurable concentrations of chlorate are indicative of sodium hypochlorite aging and the concentration formed often depends on parameters such as storage time, pH, concentration, ionic strength, and temperature (Stanford et al., 2011). Perchlorate also forms as a degradation product of aged hypochlorite solutions at concentrations typically lower than chlorate. Perchlorate has been measured in the finished water at an average concentration of 0.7 ± 0.12 µg/L. Neither of these compounds is regulated in the United States at the national level, and however, chlorate has a drinking water notification level of 800 µg/L in California and perchlorate has an established EPA health advisory and California MCL of 15 and 6 µg/L, respectively. In an effort to reduce the concentration formed of each of these compounds, efforts have been made to reduce the storage time of hypochlorite on site at the SRC. Additionally, air conditioning was installed in the hypochlorite storage rooms at NTP (maximum temperature = 22°C) during the second operating period to prevent degradation that results due to high temperatures. The installation of air conditioning at NTP will provide an opportunity to assess the impact of temperature on chlorate and perchlorate concentrations in the finished water.

Both acetaldehyde and formaldehyde are also consistently detected on the finished water at average concentrations of 3.37 and 32.3 µg/L, respectively. While there are no MCLs for either of these compounds, there is a drinking water notification limit of 100 µg/L for formaldehyde in California. These compounds are well-known by-products that form as a result of ozone reacting with natural organic matter (Schechter & Singer, 2008). Typically, aldehydes are well removed via biofiltration (Sundaram et al., 2014; Weinberg et al., 1993), and however, these compounds have been frequently detected in SWIFT Water at concentrations higher than those measured in the NTP SCE. Therefore, it was assumed that these compounds are either not being well removed biologically after ozonation, or they are being formed by another mechanism later in the treatment process. Aldehydes can also form during final chlorination as a result of reaction of free chlorine or monochloramine with amino acids (Froese et al., 1999).

Contaminants of emerging concern

In addition to the aforementioned contaminants, a suite of unregulated compounds was monitored due to their well-known occurrence in wastewater. These compounds are monitored with the purpose of both protecting public health and monitoring treatment efficacy (Crook et al., 2013). A summarized list of these compounds and rationale for monitoring can be seen in Table S4, and a complete list of these compounds can be found in Table S3. The majority of these compounds have not been detected in the SWIFT Water for the duration of plant operation, compounds which have been detected are summarized in Table 3. In general, previous studies have found that ozone is effective in mitigating a large number of these compounds at O3:TOC of 0.25–1 (Gerrity et al., 2014). However, compounds which are more ozone-resistant require a higher applied O3:TOC or a different treatment technology to be mitigated. In order to make general conclusions about the removal a large group of structurally diverse compounds by ozone, Lee et al. (2013) summarized trace organic contaminants into groups based on their reaction rate constant with both molecular ozone and hydroxyl radicals.

Compounds with high reactivity with ozone and OH*. Compounds which are known to have high or moderate reaction rates with ozone have not been frequently detected in the SWIFT Water. Those which have been measured above the detection limit on one occasion (caffeine, acetaminophen, etc.) were likely detected as a result of sample contamination. Sulfamethoxazole has been proposed to be used as an indicator of oxidation efficacy due to its wide use as an antibiotic and common detection in wastewater effluent samples (Schimmoller et al., 2020). This compound is highly susceptible to ozone oxidation with removal of >99% reported when an ozone residual is achieved (Huber et al., 2005; Wert et al., 2009). Sulfamethoxazole has been detected in the NTP SCE during every sampling event, and it has never been detected in SWIFT Water. This is aligned with expectations as the SRC operates with an average O3:TOC of 0.8 to achieve an ozone residual for CT credit, and therefore, complete oxidation was likely achieved. Other compounds which also exhibit a relatively high reaction rate with ozone and are regularly detected in the NTP SCE, but never in SWIFT Water include diclofenac, gemfibrozil, naproxen, triclosan, and carbamazepine.

Compounds with moderate to high reactivity with OH*. Compounds which have a low reaction rate with molecular ozone and a moderate reaction rate with hydroxyl radicals are removed partially during ozonation and potentially during later treatment steps as well. An exemplary compound in this category is 1,4-dioxane. The concentration of 1,4-dioxane measured throughout the duration of the second operating period is presented in Figure S6. The influent concentration of 1,4-dioxane averages 0.62 ± 0.13 µg/L. During the second

startup, an average of 25% removal of 1,4-dioxane was observed across the SWIFT process, and this was primarily attributed to oxidation by hydroxyl radicals during ozonation, k_{OH} = 2.5–3.1 * 10^8 M^{-1} s^{-1} (von Sonntag & von Gunten, 2012). The production of hydroxyl radicals during wastewater ozonation occurs as a result of rapid reactions of ozone with organic matter that produce OH* as ozone decomposes (Nöthe et al., 2009). It should be noted that 1,4-dioxane is not particularly susceptible to oxidation by molecular ozone, k_{O3} = 0.32 M^{-1} s^{-1} (von Sonntag & von Gunten, 2012). Therefore, the addition of monochloramine to control bromate formation by suppressing hydroxyl radical exposure results in decreased removal of 1,4-dioxane. This can be seen in Figure 9 where the open symbols represent samples taken without NH_2Cl, and closed symbols represent samples taken with NH_2Cl addition. The maximum 1,4-dioxane removal observed without NH_2Cl was 54% at an O3:TOC of 0.9 and this decreased to 37% with NH_2Cl addition. This was clear evidence of NH_2Cl quenching hydroxyl radicals during ozonation. A similar effect was observed with respect to NMOR removal by ozone, due to the high reactivity of NMOR with hydroxyl radicals, k = 1.75 * 10^9 (Mezyk et al., 2007). NMOR removal decreased from 41% to 17% with the addition of monochloramine at O3:TOC of 0.9. These compounds can be used as treatment indicators to understand hydroxyl radical exposure and expected removal for compounds with similar reactivity. Further testing with alternative bromate control methods such as ozone-hydrogen peroxide is needed to optimize bromate control and to minimize the impact on CEC oxidation. There was also a short-term adsorption of 1,4-dioxane observed in the GAC during both startup periods (data not shown). This adsorption capacity was quickly exhausted after approximately 1500 GAC bed volumes and short-term desorption was observed after this where the SWIFT Water concentration exceeded ozone effluent. Other treatment options for 1,4-dioxane that have been considered for future implementation include biological treatment via cometabolic degradation in the BAFs and UV-AOP.

Iohexol also belongs to the group of compounds which reacts primarily with hydroxyl radicals during ozonation (k_{OH^*} = 5.73 * 108 M^{-1} s^{-1}, Hu et al., 2019), and however, biological removal and adsorption have also been reported. This compound is an x-ray contrasting agent which can be used as an indicator of treatment efficacy due to its frequent detection in wastewater effluent. Given that there have been no operational changes made with regard to the ozone or biofilter operations, the detection of iohexol can be used as an indicator of GAC breakthrough of compounds with similar chemical structure. Partial breakthrough of iohexol was observed during the second operating period after approximately 6000 bed volumes treated by GAC unit 1. Sucralose is an artificial sweetener which is so ubiquitous in wastewater effluents, it has been proposed to be used as an indicator of wastewater loading to other water sources (Oppenheimer et al., 2011). Considering that sucralose is relatively resistant to oxidative and biological treatment, it serves as an indicator for GAC adsorption capacity of water soluble low molecular weight non-polar compounds in this treatment scheme (Schimmoller et al., 2020). During the second operating period, sucralose began to breakthrough after 6000-bed volumes treated by GAC unit 1. Monitoring for primidone and cotinine was conducted to understand removal of representative low molecular weight partially charged cyclic compounds which are frequently detected in treated wastewater. Primidone is removed to some extent by hydroxyl radical oxidation (k_{OH^*} = 6.7 * 109 M^{-1} s^{-1}, Lee et al., 2013) and GAC adsorption. Partial breakthrough was observed after 25,000 and 3000 GAC bed volumes for unit 1 and 2, respectively. The single detection of cotinine was

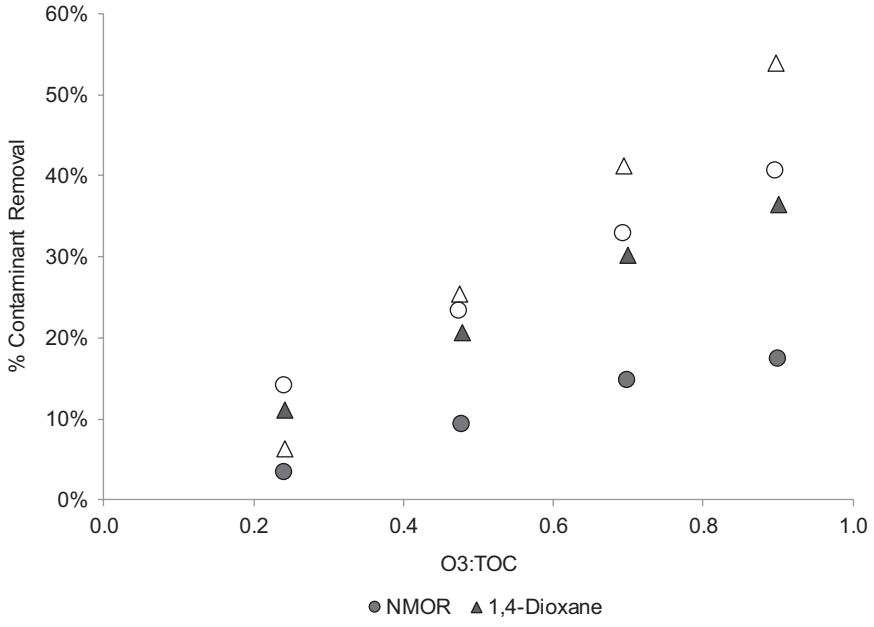

Figure 9. 1,4-dioxane and NMOR oxidation by ozone. Open symbols represent samples taken without NH_2Cl.

assumed to be a result of sample contamination as it is a common metabolite of tobacco.

Conclusions

The objective of this study was to evaluate the performance of a demonstration-scale ozone–biofiltration–GAC advanced water reuse treatment plant. This evaluation highlighted the operational challenges encountered during startup related to bulk TOC removal, ammonia oxidation, dissolved metals removal, controlling bromate formation, nitrosamine formation and removal, and CEC removal.

- Floc/sed, biofiltration, and GAC adsorption provide important barriers in carbon-based treatment trains for TOC removal. Greater than 20% TOC removal was achieved by BAFs consistently even during cold weather conditions.
- Biofilter acclimation was observed during the first three months of operation in each startup period. Acclimation and biological activity were clearly demonstrated by the onset of nitrification and manganese removal.
- Bromate was effectively controlled by managing the influent bromide load and optimizing chemical control measures of monochloramination and prechlorination (up to 81% and 90% reduction in bromate formed, respectively). Prechlorination resulted in some halogenated DBP formation (HAAs/THMs), and however, these compounds were well removed by the BAFs.
- Virgin GAC media provided a short-term barrier for bromate removal during plant startup. This capacity was completely exhausted after 8000 BV during both operating periods.
- Nitrosamines, NDMA and NMOR, were both detected in the NTP SCE. NDMA was formed at an average concentration of 53 ng/L by ozonation. NDMA was effectively biodegraded in the BAFs with >70% removal achieved after approximately one to three months of operation during each startup period. Multiple parameters that influence NDMA formation and removal were identified.
- Aldehyde formation was observed although the mechanism for formation and removal was not identified. Halogenated disinfection by-product formation was observed in the finished water when free chlorination was used to prevent biofouling to the wellhead. Chlorate and perchlorate were also detected frequently in the finished water indicating that efforts should be made to reduce hypochlorite age and temperature.
- The maximum 1,4-dioxane removal observed was 54% at an O3:TOC of 0.9 which was attributed to oxidation by hydroxyl radicals formed during ozonation. This removal was decreased to 37% with the addition of monochloramine for bromate control due to the hydroxyl radical scavenging capacity of monochloramine.
- The multiple barrier approach of ozone oxidation, biofiltration, GAC adsorption, and UV photolysis provided sufficient removal of trace contaminants and indicator compounds. The breakthrough of these compounds and bulk TOC will likely determine the regeneration frequency of GAC.

This study provides important insights about the operation and optimization of ozone/biofiltration/GAC-based advanced water treatment plants for managed aquifer recharge. Demonstrating the efficacy of this treatment process at a larger scale will further support the use of non-RO based treatment for water reuse applications in the future. The shift to non-RO based advanced water treatment is of great research interest as municipalities seek more cost-effective options for water reuse. The data presented herein suggest that ozone/biofiltration/GAC-based treatment can meet all defined treatment goals set forth for managed aquifer recharge. The lessons learned in the first years of operation of the SRC have also helped inform the design of future full-scale SWIFT facilities to be constructed at HRSD wastewater treatment plants.

Acknowledgments

The authors would like to thank HRSD for providing the funding and support for this project. They would also like to thank the NTP and SWIFT team staff for assisting in plant operations, and HRSD Central Environmental Laboratory staff for their hard work performing laboratory analyses. The authors would also like to thank Jacobs Engineering and Hazen and Sawyer for their support during startup of the SRC.

Author contributions

Samantha Hogard: Data curation (lead); methodology (lead); writing-original draft (lead). **Germano Salazar-Benites**: Writing-review & editing (equal). **Robert Pearce**: Writing-review & editing (equal). **Tyler Nading**: Data curation (supporting); writing-review & editing (equal). **Larry Schimmoller**: Writing-review & editing (supporting). **Chris Wilson**: Writing-review & editing (supporting). **Jamie Heisig-Mitchell**: Writing-review & editing (supporting). **Charles Bott**: Project administration (equal); supervision (equal); writing-review & editing (equal).

References

Arnold, M., Batista, J., Dickenson, E., & Gerrity, D. (2018). Use of ozone-biofiltration for bulk organic removal and disinfection byproduct mitigation in potable reuse applications. *Chemosphere*, *202*, 228–237. https://doi.org/10.1016/j.chemosphere.2018.03.085

Asami, M., Magara, Y., Nishijima, W., Aizawa, T., Tabata, A., & Morioka, T. (1999). Bromate removal during transition from new granular activated carbon (GAC) to biological activated carbon (BAC). *Water Research*, *33*(12), 2797–2804. https://doi.org/10.1016/s0043-1354(98)00504-1

Bourgin, M., Beck, B., Boehler, M., Borowska, E., Fleiner, J., Salhi, E., Teichler, R., von Gunten, U., Siegrist, H., & McArdell, C. S. (2018). Evaluation of a full-scale wastewater treatment plant upgraded with ozonation and biological post-treatments: Abatement of micropollutants, formation of transformation products and oxidation by-products. *Water Research*, *129*, 486–498. https://doi.org/10.1016/j.watres.2017.10.036

Buehlmann, P. H., Salazar-Benites, G., Wilson, C. A., & Bott, C. (2017). Ozonation of domestic wastewater for indirect potable reuse: Bromate control and related issues. In *IOA world congress, Washington DC.*

Buffle, M. O., Galli, S., & Von Gunten, U. (2004). Enhanced bromate control during ozonation: The chlorine-ammonia process. *Environmental Science and Technology*, *38*(19), 5187–5195. https://doi.org/10.1021/es0352146

California Department of Public Health (2014). *California Department of Public Health regulations related to recycled water* (pp. 1–33). Public Health.

California Water Boards (2010). *Drinking water notification levels*. Retrieved from https://www.waterboards.ca.gov/drinking_water/certlic/drinkingwater/NotificationLevels.html

Canada, H. (2019). Guidelines for Canadian drinking water quality. In *National meeting - American Chemical Society, Division of Environmental Chemistry* (Vol. *24*, Issue 2).

Chen, W. H., Huang, T. H., & Wang, C. Y. (2018). Impact of pre-oxidation on nitrosamine formation from a source to drinking water: A perspective on cancer risk assessment. *Process Safety and Environmental Protection*, *113*, 424–434. https://doi.org/10.1016/j.psep.2017.11.016

Cheng, Q., Nengzi, L., Bao, L., Wang, Y., Yang, J., & Zhang, J. (2017). Interactions between ammonia, iron and manganese removal using pilot-scale biofilters. *Journal of Water Supply: Research and Technology - AQUA*, *66*(3), 157–165. https://doi.org/10.2166/aqua.2017.089

City of Rio Rancho (2017). Injection Newsletter. Retrieved from https://rrnm.gov/DocumentCenter/View/69831/Injection-Newsletter_03062017?bidId=

Crook, J., Bull, R., Collins, H. F., Cotruvo, J. A., & Jakubowski, W. (2013). *Examining the criteria for direct potable reuse*. WateReuse Research Foundation. Retrieved from https://watereuse.org/watereuse-research/examining-the-criteria-for-direct-potable-reuse/

de Vera, G. A., Keller, J., Gernjak, W., Weinberg, H., & Farré, M. J. (2016). Biodegradability of DBP precursors after drinking water ozonation. *Water Research*, *106*, 550–561. https://doi.org/10.1016/j.watres.2016.10.022

Enprotec/Hibbs & Todd Inc. City of Abilene Hamby Water Reclamation Facility and Indirect Reuse Project. Retrieved from https://e-ht.com/our-services/waste-water/wastewater-treatment/city-of-abilene-hamby-water-reclamation-facility-and-indirect-reuse-project/

Fournier, D., Hawari, J., Halasz, A., Streger, S. H., McClay, K. R., Masuda, H., & Hatzinger, P. B. (2009). Aerobic biodegradation of N-nitrosodimethylamine by the propanotroph *Rhodococcus ruber* ENV425. *Applied and Environmental Microbiology*, *75*(15), 5088–5093. https://doi.org/10.1128/AEM.00418-09

Froese, K. L., Wolanski, A., & Hrudey, S. E. (1999). Factors governing odorous aldehyde formation as disinfection by-products in drinking water. *Water Research*, *33*(6), 1355–1364. https://doi.org/10.1016/S0043-1354(98)00357-1

Funk, D., County, G., Hooper, J., Goldman, J., & Schulz, C. (2019). *Ozone biofiltration direct potable reuse testing at Gwinnett County (reuse-15-11/4777)*. Water Research Foundation.

Gerrity, D., Owens-Bennett, E., Venezia, T., Stanford, B. D., Plumlee, M. H., Debroux, J., & Trussell, R. S. (2014). Applicability of ozone and biological activated carbon for potable reuse. *Ozone: Science and Engineering*, *36*(2), 123–137. https://doi.org/10.1080/01919512.2013.866886

Gerrity, D., Pisarenko, A. N., Marti, E., Trenholm, R. A., Gerringer, F., Reungoat, J., & Dickenson, E. (2015). Nitrosamines in pilot-scale and full-scale wastewater treatment plants with ozonation. *Water Research*, *72*, 251–261. https://doi.org/10.1016/j.watres.2014.06.025

Glover, C. M., Verdugo, E. M., Trenholm, R. A., & Dickenson, E. R. V. (2019). N-nitrosomorpholine in potable reuse. *Water Research*, *148*, 306–313. https://doi.org/10.1016/j.watres.2018.10.010

Hasan, H. A., Sheikh Abdullah, S. R., Tan Kofli, N., & Kamarudin, S. K. (2012). Effective microbes for simultaneous bio-oxidation of ammonia and manganese in biological aerated filter system. *Bioresource Technology*, *124*, 355–363. https://doi.org/10.1016/j.biortech.2012.08.055

Hollender, J., Zimmermann, S. G., Koepke, S., Krauss, M., Mcardell, C. S., Ort, C., Singer, H., Von Gunten, U., & Siegrist, H. (2009). Elimination of organic micropollutants in a municipal wastewater treatment plant upgraded with a full-scale post-ozonation followed by sand filtration. *Environmental Science and Technology*, *43*(20), 7862–7869. https://doi.org/10.1021/es9014629

Hooper, J., Funk, D., Bell, K., Noibi, M., Vickstrom, K., Schulz, C., Machek, E., & Huang, C. H. (2020). Pilot testing of direct and indirect potable water reuse using multi-stage ozone-biofiltration without reverse osmosis. *Water Research*, *169*, 115178. https://doi.org/10.1016/j.watres.2019.115178

Hu, C. Y., Hou, Y. Z., Lin, Y. L., Deng, Y. G., Hua, S. J., Du, Y. F., Chen, C. W., & Wu, C. H. (2019). Kinetics and model development of iohexol degradation during UV/H2O2 and UV/S2O82− oxidation. *Chemosphere*, *229*, 602–610. https://doi.org/10.1016/j.chemosphere.2019.05.012

Huber, M. M., Göbel, A., Joss, A., Hermann, N., Löffler, D., McArdell, C. S., Ried, A., Siegrist, H., Ternes, T. A., & Von Gunten, U. (2005). Oxidation of pharmaceuticals during ozonation of municipal wastewater effluents: A pilot study. *Environmental Science and Technology*, *39*(11), 4290–4299. https://doi.org/10.1021/es048396s

Krasner, S. W., Mitch, W. A., McCurry, D. L., Hanigan, D., & Westerhoff, P. (2013). Formation, precursors, control, and occurrence of nitrosamines in drinking water: A review. *Water Research*, *47*(13), 4433–4450. https://doi.org/10.1016/j.watres.2013.04.050

Krasner, S. W., Westerhoff, P., Chen, B., Rittmann, B. E., & Amy, G. (2009). Occurrence of disinfection byproducts in United States wastewater treatment plant effluents. *Environmental Science and Technology*, *43*(21), 8320–8325. https://doi.org/10.1021/es901611m

Krauss, M., Longrée, P., Dorusch, F., Ort, C., & Hollender, J. (2009). Occurrence and removal of N-nitrosamines in wastewater treatment plants. *Water Research*, *43*(17), 4381–4391. https://doi.org/10.1016/j.watres.2009.06.048

Lee, C., Schmidt, C., Yoon, J., & Von Gunten, U. (2007). Oxidation of N-nitrosodimethylamine (NDMA) precursors with ozone and chlorine dioxide: Kinetics and effect on NDMA formation potential. *Environmental Science and Technology*, *41*(6), 2056–2063. https://doi.org/10.1021/es062484q

Lee, Y., Gerrity, D., Lee, M., Bogeat, A. E., Salhi, E., Gamage, S., Trenholm, R. A., Wert, E. C., Snyder, S. A., & Von Gunten, U. (2013). Prediction of micropollutant elimination during ozonation of municipal wastewater effluents: Use of kinetic and water specific information. *Environmental Science and Technology*, *47*(11), 5872–5881. https://doi.org/10.1021/es400781r

Marti, E. J. (2016). *Ozonation in water reuse: Formation and mitigation of N-nitrosodimethylamine Marti*. May 2016. (Doctoral Dissertation). University of Nevada Las Vegas. Retrieved from https://digitalscholarship.unlv.edu/thesesdissertations/2707/

Marti, E. J., Pisarenko, A. N., Peller, J. R., & Dickenson, E. R. V. (2015). N-nitrosodimethylamine (NDMA) formation from the ozonation of model compounds. *Water Research*, *72*, 262–270. https://doi.org/10.1016/j.watres.2014.08.047

McCurry, D. L., Ishida, K. P., Oelker, G. L., & Mitch, W. A. (2017). Reverse osmosis shifts chloramine speciation causing re-formation of NDMA during potable reuse of wastewater. *Environmental Science and Technology*, *51*(15), 8589–8596. https://doi.org/10.1021/acs.est.7b01641

Mezyk, S. P., Landsman, N. A., Swancutt, K. L., Bradford, C. N., Cox, C. R., Kiddle, J. J., & Clore, T. J. (2007). Free radical chemistry of advanced oxidation process removal of nitrosamines in waters. *Environmental Science and Technology*, *41*(16), 5818–5823. https://doi.org/10.1021/bk-2008-0995.ch022

Munter, R., Ojaste, H., & Sutt, J. (2005). Complexed iron removal from groundwater. *Journal of Environmental Engineering*, *131*(7), 1014–1020. https://doi.org/10.1061/(asce)0733-9372(2005)131:7(1014)

National Health and Medical Research Council (2008). *Australian guidelines for water recycling*. Water, Phase 2.

Nawrocki, J., & Andrzejewski, P. (2011). Nitrosamines and water. *Journal of Hazardous Materials*, *189*(1–2), 1–18. https://doi.org/10.1016/j.jhazmat.2011.02.005

Nöthe, T., Fahlenkamp, H., & Von Sonntag, C. (2009). Ozonation of wastewater: Rate of ozone consumption and hydroxyl radical yield. *Environmental Science and Technology*, *43*(15), 5990–5995. https://doi.org/10.1021/es900825f

Oppenheimer, J., Eaton, A., Badruzzaman, M., Haghani, A. W., & Jacangelo, J. G. (2011). Occurrence and suitability of sucralose as an indicator compound of wastewater loading to surface waters in urbanized regions. *Water Research*, *45*(13), 4019–4027. https://doi.org/10.1016/j.watres.2011.05.014

Otto, M., & Nagaraja, S. (2007). Treatment technologies for 1,4-Dioxane: Fundamentals and field applications. *Remediation Journal*, *17*(3), 81–88. https://doi.org/10.1002/rem.20135

Pinkernell, U., & von Gunten, U. (2001). Bromate minimization during ozonation: Mechanistic considerations. *Environmental Science and Technology*, *35*(12), 2525–2531. https://doi.org/10.1021/es001502f

Pisarenko, A. N., Marti, E. J., Gerrity, D., Peller, R., & Dickenson, E. R. V. (2015). Effects of molecular ozone and hydroxyl radical on formation of N -nitrosamines and perfluoroalkyl acids during ozonation of treated wastewaters. *Environmental Science: Water Research and Technology*, *1*(5), 668–678. https://doi.org/10.1039/c5ew00046g

Planas, C., Palacios, Ó., Ventura, F., Rivera, J., & Caixach, J. (2008). Analysis of nitrosamines in water by automated SPE and isotope dilution GC/HRMS. Occurrence in the different steps of a drinking water treatment plant, and in chlorinated samples from a reservoir and a sewage treatment plant effluent. *Talanta*, *76*(4), 906–913. https://doi.org/10.1016/j.talanta.2008.04.060

Plumlee, M. H., Stanford, B. D., Debroux, J. F., Hopkins, D. C., & Snyder, S. A. (2014). Costs of advanced treatment in water reclamation. *Ozone: Science and Engineering*, *36*(5), 485–495. https://doi.org/10.1080/01919512.2014.921565

Pradhan, P. (2018). *Evaluation of soil aquifer treatment in a lab scale soil column experiment* (Masters Thesis). Virginia Tech. Retrieved from http://hdl.handle.net/10919/98749

Reckhow, D. A., Knocke, W., Kearney, M. J., & Parks, C. A. (1991). Oxidation of iron and manganese by ozone. *Ozone: Science & Engineering*, *13*(6), 675–695. https://doi.org/10.1080/01919512.1991.10555708

Schechter, D. S., & Singer, P. C. (2008). Formation of aldehydes during ozonation. *Ozone: Science & Engineering*, *9512*(1995), 53–69. https://doi.org/10.1080/01919519508547577

Schimmoller, L., Lozier, J., Mitch, W., & Snyder, S. (2020). *Characterizing and controlling organics in direct potable reuse projects (reuse-15-04/4771)*. Water Research Foundation.

Selbes, M., Brown, J., Lauderdale, C., & Karanfil, T. (2017). Removal of selected C- and N-DBP precursors in biologically active filters. *Journal - American Water Works Association*, *109*(3), E73–E84. https://doi.org/10.5942/jawwa.2017.109.0014

Sgroi, M., Roccaro, P., Oelker, G. L., & Snyder, S. A. (2014). N -nitrosodimethylamine formation upon ozonation and identification of precursors source in a municipal wastewater treatment plant. *Environmental Science and Technology*, *48*(17), 10308–10315. https://doi.org/10.1021/es5011658

Shah, A. D., Dai, N., & Mitch, W. A. (2013). Application of ultraviolet, ozone, and advanced oxidation treatments to washwaters to destroy nitrosamines, nitramines, amines, and aldehydes formed during amine-based carbon capture. *Environmental Science and Technology*, *47*(6), 2799–2808. https://doi.org/10.1021/es304893m

Sheng, Z. (2005). An aquifer storage and recovery system with reclaimed wastewater to preserve native groundwater resources in El Paso, Texas. *Journal of Environmental Management*, *75*(4 SPEC., ISS.), 367–377. https://doi.org/10.1016/j.jenvman.2004.10.007

Siddiqui, M. S., Zhai, W., Amy, G., & Mysore, C. (1999). Bromate ion removal by activated carbon. *Water Research*, *30*(7), 1651–1660.

Soltermann, F., Abegglen, C., Tschui, M., Stahel, S., & von Gunten, U. (2017). Options and limitations for bromate control during ozonation of wastewater. *Water Research*, *116*, 76–85. https://doi.org/10.1016/j.watres.2017.02.026

Stanford, B. D., Pisarenko, A. N., Snyder, S. A., & Gordon, G. (2011). Perchlorate, bromate, and chlorate in hypochlorite solutions: Guidelines for utilities. *Journal - American*

Water Works Association, *103*(6), 71–83. https://doi.org/10.1002/j.1551-8833.2011.tb11474.x

Stepien, D. K., Diehl, P., Helm, J., Thoms, A., & Püttmann, W. (2014). Fate of 1,4-dioxane in the aquatic environment: From sewage to drinking water. *Water Research*, *48*(1), 406–419. https://doi.org/10.1016/j.watres.2013.09.057

Sundaram, V., Emerick, R. W., & Shumaker, S. E. (2014). Advanced treatment process for pharmaceuticals, endocrine disruptors, and flame retardants removal. *Water Environment Research*, *86*(2), 111–122. https://doi.org/10.2175/106143013x13807328849053

Sundaram, V., & Pagilla, K. (2019). Trace and bulk organics removal during ozone–biofiltration treatment for potable reuse applications. *Water Environment Research*, *92*(3), 430–440. https://doi.org/10.1002/wer.1202

Sundaram, V., Pagilla, K., Guarin, T., Li, L., Marfil-Vega, R., & Bukhari, Z. (2020). Extended field investigations of ozone-biofiltration advanced water treatment for potable reuse. *Water Research*, *172*, 115513. https://doi.org/10.1016/j.watres.2020.115513

Szczuka, A., Chuang, Y.-H., Chen, F. C., Zhang, Z., Desormeaux, E., Flynn, M., Parodi, J., & Mitch, W. A. (2020). Removal of pathogens and chemicals of emerging concern by pilot-scale FO-RO hybrid units treating RO concentrate, graywater, and sewage for centralized and decentralized potable reuse. *ACS ES&T Water*, *1*(1), 89–100. https://doi.org/10.1021/acsestwater.0c00006

Tanabe, A., & Kawata, K. (2008). Determination of 1,4-dioxane in household detergents and cleaners. *Journal of AOAC International*, *91*(2), 439–444. https://doi.org/10.1093/jaoac/91.2.439

Tekerlekopoulou, A. G., Pavlou, S., & Vayenas, D. V. (2013). Removal of ammonium, iron and manganese from potable water in biofiltration units: A review. *Journal of Chemical Technology and Biotechnology*, *88*(5), 751–773. https://doi.org/10.1002/jctb.4031

US EPA (2017). *Potable reuse compendium*. (Issue 203). Retrieved from https://www.epa.gov/sites/production/files/2018-01/documents/potablereusecompendium_3.pdf

US EPA (1998). *National primary drinking water regulations: Disinfectants and disinfection byproducts* (Issue 241). https://www.epa.gov/ground-water-and-drinking-water/national-primary-drinking-water-regulations

US EPA (2010). *Long term 2 enhanced surface water treatment rule toolbox guidance manual*. Retrieved from http://water.epa.gov/lawsregs/rulesregs/sdwa/lt2/basicinformation.cfm

Vaidya, R. (2020). *Removal of total organic carbon and emerging contaminants in an advanced water treatment process using ozone-BAC-GAC*. Virginia Polytechnic Institute and State University.

Vaidya, R., Buehlmann, P. H., Salazar-Benites, G., Schimmoller, L., Nading, T., Wilson, C. A., Bott, C., Gonzalez, R., & Novak, J. T. (2019). Pilot plant performance comparing carbon-based and membrane-based potable reuse schemes. *Environmental Engineering Science*, *36*(11), 1369–1378. https://doi.org/10.1089/ees.2018.0559

Vaidya, R., Wilson, C., Salazar-Benites, G., Pruden, A., & Bott, C. (2020). Factors affecting removal of NDMA in an ozone-biofiltration process for water reuse. *Chemosphere*, *264*, 128333. https://doi.org/10.1016/j.chemosphere.2020.128333

von Gunten, U., Salhi, E., Schmidt, C. K., & Arnold, W. A. (2010). Kinetics and mechanisms of N -nitrosodimethylamine formation upon ozonation of N, N -dimethylsulfamide-containing waters: Bromide catalysis. *Environmental Science and Technology*, *44*(15), 5762–5768. https://doi.org/10.1021/es1011862

von Sonntag, C., & von Gunten, U. (2012). *Chemistry of ozone in water and wastewater treatment: From basic principles to applications*. https://doi.org/10.2166/9781780400839

Weinberg, H. S., Glaze, W. H., Krasner, S. W., & Sclimenti, M. J. (1993). Formation and removal of aldehydes in plants that use ozonation. *Journal - American Water Works Association*, *85*(5), 72–85. https://doi.org/10.1002/j.1551-8833.1993.tb05988.x

Wert, E. C., Lew, J., & Rakness, K. L. (2016). *Effect of ozone dissolution on bromate formation, disinfection credit, and operating cost*. [Project #4588].

Wert, E. C., Neemann, J. J., Johnson, D., Rexing, D., & Zegers, R. (2007). Pilot-scale and full-scale evaluation of the chlorine-ammonia process for bromate control during ozonation. *Ozone: Science and Engineering*, *29*(5), 363–372. https://doi.org/10.1080/01919510701552883

Wert, E. C., Rosario-Ortiz, F. L., & Snyder, S. A. (2009). Effect of ozone exposure on the oxidation of trace organic contaminants in wastewater. *Water Research*, *43*(4), 1005–1014. https://doi.org/10.1016/j.watres.2008.11.050

Zeng, T., Glover, C. M., Marti, E. J., Woods-Chabane, G. C., Karanfil, T., Mitch, W. A., & Dickenson, E. R. V. (2016). Relative importance of different water categories as sources of N-nitrosamine precursors. *Environmental Science and Technology*, *50*(24), 13239–13248. https://doi.org/10.1021/acs.est.6b04650

Zeng, T., Plewa, M. J., & Mitch, W. A. (2016). N-Nitrosamines and halogenated disinfection byproducts in U.S. Full Advanced Treatment trains for potable reuse. *Water Research*, *101*, 176–186. https://doi.org/10.1016/j.watres.2016.03.062

Chapter 2 Supplementary Information
Demonstration-scale evaluation of ozone-biofiltration-granular activated carbon advanced water treatment for managed aquifer recharge

Table SI-1. Disinfection Credit at SWIFTRC

	Floc/Sed (+BAF)	Ozone	UV	Cl_2	Total AWT[1]	SAT[2]	Total + SAT[3]
Enteric Viruses	2	3	4	4	13	6	15
Cryptosporidium	4	-	6	-	10	6	16
Giardia	2.5	1.5	6	-	10	6	16

Note: [1]Due to the availability of tasting water at the SWIFT RC, it is required to meet disinfection goals at the facility, additional pathogen removal is credited for soil aquifer treatment (SAT)
[2]1-log of removal is credited for each month of aquifer travel time, up to 6 months (CDPH, 2014)
[3]The total credits achieved for the injected SWIFT water do not include the virus credit achieved by free chlorination. These credits are only applied to the tasting system which is only a fraction of the flow that is diverted before aquifer injection.

Table SI-2. Disinfection Profiling and Benchmarking Guidance Manual Table C-13
CT Values for Inactivation of Viruses by Ozone

Temperature (°C)	Virus log inactivation		
	2	3	4
1	0.9	1.4	1.8
2	0.83	1.28	1.65
3	0.75	1.15	1.5
4	0.68	1.03	1.35
5	0.6	0.9	1.2
6	0.58	0.88	1.16
7	0.56	0.86	1.12
8	0.54	0.84	1.08
9	0.52	0.82	1.04
10	0.5	0.8	1
11	0.46	0.74	0.92
12	0.42	0.68	0.84
13	0.38	0.62	0.76
14	0.34	0.56	0.68
15	0.3	0.5	0.6
16	0.29	0.48	0.58
17	0.28	0.46	0.56
18	0.27	0.44	0.54

19	0.26	0.42	0.52
20	0.25	0.4	0.5
21	0.23	0.37	0.46
22	0.21	0.34	0.42
23	0.19	0.31	0.38
24	0.17	0.28	0.34
25	0.15	0.25	0.3

Table SI-3. SWIFT Water monitored parameters, rationale for monitoring, and analytical method

Parameter	Rationale for Monitoring	Method	Laboratory
Total Nitrogen (TN)		Calculation	
NO_3	PMCL	Calculation	HRSD
NO_2	PMCL	10-107-04-1-C	HRSD
NOx		10-107-04-1-A	HRSD
TKN		10-107-06-2-I	HRSD
Total Organic Carbon (TOC)	Indicator	SM 5310B/C	HRSD
Total Nitrogen (TN) by Combustion			HRSD
Microorganisms			
Total Coliform	PMCL	SM 9223B (Colilert 18)	HRSD
E. coli	PMCL	SM 9223B (Colilert 18)	HRSD
Legionella	PMCL	IDEXX	HRSD
Disinfection Byproducts			
Bromate	PMCL	EPA 302.0	HRSD
Chlorite	PMCL	EPA 300.0	HRSD
Trihalomethanes		EPA 524.2 (GC-MS)	
Bromodichloromethane	PMCL		HRSD
Bromoform	PMCL		HRSD
Chloroform	PMCL		HRSD
Dibromochloromethane	PMCL		HRSD
HAAs			
Dichloroacetic acid	PMCL	EPA 552.2 (GC)	HRSD
Trichloroacetic acid	PMCL	EPA 552.2 (GC)	HRSD
Monochloroacetic acid	PMCL	EPA 552.2 (GC)	HRSD
Bromoacetic acid	PMCL	EPA 552.2 (GC)	HRSD
Dibromoacetic acid	PMCL	EPA 552.2 (GC)	HRSD
Bromochloroacetic acid	UCMR4	EPA 552.2 (GC)	HRSD
Bromodichloroacetic acid	UCMR4	EPA 552.2 (GC)	HRSD
Dibromochloroacetic acid	UCMR4	EPA 552.2 (GC)	HRSD
Tribromoacetic acid	UCMR4	EPA 552.2 (GC)	HRSD
Inorganic Chemical			
Antimony	PMCL	EPA 200.8	HRSD
Arsenic	PMCL	EPA 200.8	HRSD
Barium	PMCL	EPA 200.7	HRSD

Parameter		Rationale for Monitoring	Method	Laboratory
	Beryllium	PMCL	EPA 200.8	HRSD
	Cadmium	PMCL	EPA 200.8	HRSD
	Chromium (total)	PMCL	EPA 200.8	HRSD
	Copper	PMCL	EPA 200.7	HRSD
	Cyanide (total)	PMCL	10-204-00-1-X	HRSD
	Fluoride	PMCL	EPA 300.0	HRSD
	Lead	PMCL	EPA 200.8	HRSD
	Mercury	PMCL	EPA 245.1	HRSD
	Selenium	PMCL	EPA 200.8	HRSD
	Thallium	PMCL	EPA 200.8	HRSD
VOCs				
	Benzene	PMCL	EPA 524.2 (GC-MS)	HRSD
	Chlorobenzene	PMCL	EPA 524.2 (GC-MS)	HRSD
	Carbon Tetrachloride	PMCL	EPA 524.2 (GC-MS)	HRSD
	o-Dichlororbenzene	PMCL	EPA 524.2 (GC-MS)	HRSD
	p-Dichlorobenzene	PMCL	EPA 524.2 (GC-MS)	HRSD
	1,2-Dichloroethane	PMCL	EPA 524.2 (GC-MS)	HRSD
	1,1-Dichlororethylene	PMCL	EPA 524.2 (GC-MS)	HRSD
	cis-1,2-Dichloroehtylene	PMCL	EPA 524.2 (GC-MS)	HRSD
	trans-1,2-Dichloroethylene	PMCL	EPA 524.2 (GC-MS)	HRSD
	Dichloromethane	PMCL	EPA 524.2 (GC-MS)	HRSD
	1,2-Dichloropropane	PMCL	EPA 524.2 (GC-MS)	HRSD
	Ethylbenzene	PMCL	EPA 524.2 (GC-MS)	HRSD
	Styrene	PMCL	EPA 524.2 (GC-MS)	HRSD
	Tetrachloroethylene	PMCL	EPA 524.2 (GC-MS)	HRSD
	Toluene	PMCL	EPA 524.2 (GC-MS)	HRSD
	1,2,4-Trichlorobenzene	PMCL	EPA 524.2 (GC-MS)	HRSD
	1,1,1-Trichloroethane	PMCL	EPA 524.2 (GC-MS)	HRSD
	1,1,2-Trichloroethane	PMCL	EPA 524.2 (GC-MS)	HRSD
	Trichloroethylene	PMCL	EPA 524.2 (GC-MS)	HRSD
	Vinyl Chloride	PMCL	EPA 524.2 (GC-MS)	HRSD
	p/m-Xylene	PMCL	EPA 524.2 (GC-MS)	HRSD
	o-Xylene	PMCL	EPA 524.2 (GC-MS)	HRSD
	Total Xylene	PMCL	EPA 524.2 (GC-MS)	HRSD

Parameter	Rationale for Monitoring	Method	Laboratory
DBCP	PMCL	EPA 504.1 (GC)	HRSD
Ethylene Dibromide	PMCL	EPA 504.1 (GC)	HRSD
Radionuclides			
Uranium	PMCL	EPA 200.8	HRSD
Virginia Groundwater Protection Standards			
Kepone	VA GWPS	EPA 8081	HRSD
Disinfection Byproducts			
Chlorate	UCMR3	EPA 300.1	HRSD
Indicators			
NDMA/NMOR		EPA 521 (GC-QQQ/SPE)	HRSD
1,4-dioxane		EPA 522 (GC-QQQ/SPE)	HRSD
Other			
Bromide	UCMR4	EPA 300.0	HRSD
Cobalt	CCL4	EPA 200.8	HRSD
Germanium	CCL4/UCMR4	EPA 200.8	HRSD
Manganese	UCMR4	EPA 200.8	HRSD
Molybdenum	CCL4	EPA 200.8	HRSD
Tellurium	CCL4	EPA 200.8	HRSD
Vanadium	CCL4	EPA 200.8	HRSD
Aniline	CCL3/CCL4	EPA 625 (GC-MS)	HRSD
Nitrobenzene	CCL3/CCL4	EPA 625 (GC-MS)	HRSD
n-Nitrosodiethylamine (NDEA)	CCL3/CCL4	EPA 521 (GC-QQQ/SPE)	HRSD
n-Nitrosodi-n-propylamine (NDPA)	CCL3/CCL4	EPA 521 (GC-QQQ/SPE)	HRSD
n-Nitrosodiphenylamine	CCL3/CCL4	EPA 625 (GC-MS)	HRSD
n-Nitrosopyrrolidine (NPYR)	CCL3/CCL4	EPA 521 (GC-QQQ/SPE)	HRSD
Nonylphenol	CCL4	ASTM D7065-06 (GC-MS)	HRSD
Propylbenzene	CCL3/CCL4	EPA 624 (GC-MS)	HRSD
Volatile Organics			
1,1,2,2-Tetrachloroethane	CCL3/CCL4	EPA 624 (GC-MS)	HRSD
Acrolein	CCL3/CCL4	EPA 624 (GC-MS)	HRSD
Hexane	CCL3/CCL4	EPA 624 (GC-MS)	HRSD
Methanol	CCL3/CCL4	EPA 624 (GC-MS)	HRSD
Methyl tert-Butyl Ether	CCL3/CCL4	EPA 624 (GC-MS)	HRSD

Parameter	Rationale for Monitoring	Method	Laboratory
sec-Butylbenzene	CCL3/CCL4	EPA 624 (GC-MS)	HRSD
Pathogens			
Adenovirus	CCL4		HRSD
Campylobacter jejuni	CCL4		HRSD
Norovirus GI			HRSD
Norovirus GII			HRSD
Enterovirus	CCL4		HRSD
Rotavirus			HRSD
Pepper Mild Mottle Virus			HRSD
Male Specific Coliphages			HRSD
Somatic Coliphages			HRSD
Non-regulatory Parameters with Aquifer Compatibility Focus			
Aluminum, dissolved		EPA 200.7	HRSD
Aluminum, total		EPA 200.7	HRSD
Arsenic, dissolved		EPA 200.8	HRSD
Iron, dissolved		EPA 200.7	HRSD
Iron, total		EPA 200.7	HRSD
Manganese, dissolved		EPA 200.8	HRSD
Magnesium, total		EPA 200.7	HRSD
Potassium, total		EPA 200.7	HRSD
Sodium, total		EPA 200.7	HRSD
Calcium, total		EPA 200.7	HRSD
Sulfate		EPA 300.0	HRSD
Chloride		EPA 300.0	HRSD
Alkalinity		10-303-31-1-A	HRSD
Silica as SiO2		EPA 200.7	HRSD
Dissolved Organic Carbon		SM 5310 B/C-2011	HRSD
Total Phosphorus		10-115-01-1-E	HRSD
Orthophosphate as P		10-115-01-1-A	HRSD
Total Dissolved Solids		SM 2540 C-2011	HRSD
Ammonia as N		10-107-06-1-J	HRSD
COD		Hach 8000	HRSD
Pesticides:			

Parameter	Rationale for Monitoring	Method	Laboratory
Chlordane	PMCL	EPA 505 (GC)	Eurofins
Endrin	PMCL	EPA 505 (GC)	Eurofins
Heptachlor	PMCL	EPA 505 (GC)	Eurofins
Heptachlor Epoxide	PMCL	EPA 505 (GC)	Eurofins
Lindane	PMCL	EPA 505 (GC)	Eurofins
Methoxychlor	PMCL	EPA 505 (GC)	Eurofins
Toxaphene	PMCL	EPA 505 (GC)	Eurofins
PCBs-AR1016,1221,1232,1242,1248,1254,1260	PMCL	EPA 505 (GC)	Eurofins
Herbicides:			
2,4-D	PMCL	EPA 515.4 (GC)	Eurofins
Dalapon	PMCL	EPA 515.4 (GC)	Eurofins
Picloram	PMCL	EPA 515.4 (GC)	Eurofins
Silvex	PMCL	EPA 515.4 (GC)	Eurofins
Dinoseb	PMCL	EPA 515.4 (GC)	Eurofins
Pentachlorophenol	PMCL	EPA 515.4 (GC)	Eurofins
Semi-VOC:			
Alachlor	PMCL	EPA 525.2 (GC-MS/SPE)	Eurofins
Atrazine	PMCL	EPA 525.2 (GC-MS/SPE)	Eurofins
Benzo(a)pyrene (PAHs)	PMCL	EPA 525.2 (GC-MS/SPE)	Eurofins
Di(2-ethylhexyl) adipate	PMCL	EPA 525.2 (GC-MS/SPE)	Eurofins
Di(2-ethylhexyl) phthalate	PMCL	EPA 525.2 (GC-MS/SPE)	Eurofins
Hexachlorocyclopentadiene	PMCL	EPA 525.2 (GC-MS/SPE)	Eurofins
Hexachlorobenzene	PMCL	EPA 525.2 (GC-MS/SPE)	Eurofins
Simazine	PMCL	EPA 525.2 (GC-MS/SPE)	Eurofins
Others:			
Acrylamide	PMCL	MWH/LCMSMS	Eurofins
Carbofuran	PMCL	EPA 531.2 (HPLC)	Eurofins
Oxamyl (Vydate)	PMCL	EPA 531.2 (HPLC)	Eurofins
Dioxin (2,3,7,8-TCDD)	PMCL	EPA 1613 (HRGC-HRMS)	Eurofins
Diquat	PMCL	EPA 549.2 (HPLC)	Eurofins
Endothall	PMCL	EPA 548.1 (GC-MS/IEE)	Eurofins
Glycophosphate	PMCL	EPA 547 (HPLC)	Eurofins
Epichlorohydrin	PMCL	EPA 524.2 (GC-MS)	Eurofins

Parameter	Rationale for Monitoring	Method	Laboratory
Asbestos	PMCL	EPA 100.2	Eurofins
Radionuclides			
alpha particles	PMCL	EPA 900	Eurofins
beta particles and photon emitters	PMCL	EPA 900	Eurofins
radium 226 and radium 228	PMCL	GA method	Eurofins
Pathogens			
Cryptosporidium	PMCL	EPA 1623	Eurofins
Giardia lamblia	PMCL	EPA 1623	Eurofins
Legionella	PMCL	IDEXX	Eurofins
Perfluorinated Compounds (25 or 32)			
Perfluorobutanesulfonic Acid (PFBS)	UCMR3	EPA 537/533 (LCMSMS/SPE)	Eurofins
Perfluoroheptanoic Acid (PFHpA)	UCMR3	EPA 537/533 (LCMSMS/SPE)	Eurofins
Perfluorohexanesulfonic Acid (PFHxS)	UCMR3	EPA 537/533 (LCMSMS/SPE)	Eurofins
Perfluoroocnanoic Acid (PFNA)	UCMR3	EPA 537/533 (LCMSMS/SPE)	Eurofins
Perfluorooctanesulfonic Acid (PFOS)	CCL3/CCL4/UCMR3	EPA 537/533 (LCMSMS/SPE)	Eurofins
Perfluorooctanoic Acid (PFOA)	CCL3/CCL4/UCMR3	EPA 537/533 (LCMSMS/SPE)	Eurofins
Perfluorobutanesulfonic Acid (PFBS)		EPA 537/533 (LCMSMS/SPE)	Eurofins
Perfluoroheptanoic Acid (PFHpA)		EPA 537/533 (LCMSMS/SPE)	Eurofins
Perfluorohexanesulfonic Acid (PFHxS)		EPA 537/533 (LCMSMS/SPE)	Eurofins
Perfluoroocnanoic Acid (PFNA)		EPA 537/533 (LCMSMS/SPE)	Eurofins
Perfluorooctanesulfonic Acid (PFOS)		EPA 537/533 (LCMSMS/SPE)	Eurofins
Perfluorooctanoic Acid (PFOA)		EPA 537/533 (LCMSMS/SPE)	Eurofins
Perfluorodecanoic Acid		EPA 537/533 (LCMSMS/SPE)	Eurofins
Perfluorododecanoic Acid		EPA 537/533 (LCMSMS/SPE)	Eurofins
Perfluorohexanoic Acid		EPA 537/533 (LCMSMS/SPE)	Eurofins
Perfluorotetradecanoic Acid		EPA 537/533 (LCMSMS/SPE)	Eurofins
Perfluorotridecanoic Acid		EPA 537/533 (LCMSMS/SPE)	Eurofins
Perfluoroundecanoic Acid		EPA 537/533 (LCMSMS/SPE)	Eurofins
Indicators			
1,4-dioxane		EPA 522 (GC-MS/SPE)	Eurofins
NDMA		EPA 521 (GC-QQQ/SPE)	Eurofins
Perchlorate		EPA 331	Eurofins
VGWP			
Strontium-90	VA GWPS	EPA 905.0	Eurofins

Parameter	Rationale for Monitoring	Method	Laboratory
Tritium	VA GWPS	EPA 906.0	Eurofins
Aldrin	VA GWPS	EPA 8081A (GC)	Eurofins
Dieldrin	VA GWPS	EPA 8081A (GC)	Eurofins
2,4'-DDT		EPA 8081A (GC)	Eurofins
4,4'-DDT	VA GWPS	EPA 8081A (GC)	Eurofins
Mirex	VA GWPS	EPA 8081A (GC)	Eurofins
Phenols	VA GWPS	MWH420/SW9066	Eurofins
CECs (all 96 compounds)			
tris(2-carboxyethyl)phosphine (TCEP)		LCMSMS	Eurofins
DEET		LCMSMS	Eurofins
Ethinyl estradiol		LCMSMS	Eurofins
Cotinine		LCMSMS	Eurofins
Primidone		LCMSMS	Eurofins
Phenytoin (Dilantin)		LCMSMS	Eurofins
Meprobamate		LCMSMS	Eurofins
Atenolol		LCMSMS	Eurofins
Carbemazepine		LCMSMS	Eurofins
Estrone		LCMSMS	Eurofins
Sucralose		LCMSMS	Eurofins
Triclosan		LCMSMS	Eurofins
VOCs			
Bromochloromethane	CCL3/CCL4/UCMR3	EPA 524.2 (GC-MS)	Eurofins
Bromomethane	CCL3/CCL4/UCMR3	EPA 524.2 (GC-MS)	Eurofins
1,1-dichloroethane	UCMR3	EPA 524.2 (GC-MS)	Eurofins
1,2,3-trichloropropane	CCL3/CCL4/UCMR3	EPA 524.2 (GC-MS)	Eurofins
Chloromethane	CCL3/CCL4/UCMR3	EPA 524.2 (GC-MS)	Eurofins
Formaldehyde	CCL3/CCL4	EPA 556 (GC)	Eurofins
Hormone, Natural or Synthetic			
17-β-estradiol	CCL3/CCL4/UCMR3	EPA 539 (LC-ESI-MS-MS/SPE)	Eurofins
16-α-hydroxyestradiol (estriol)	CCL3/CCL4/UCMR3	EPA 539 (LC-ESI-MS-MS/SPE)	Eurofins
17-α-ethynylestradiol	CCL3/CCL4/UCMR3	EPA 539 (LC-ESI-MS-MS/SPE)	Eurofins

Parameter		Rationale for Monitoring	Method	Laboratory
	4-androstene -3,17-dione (Androstenedione)	UCMR3	EPA 539 (LC-ESI-MS-MS/SPE)	Eurofins
	Equilin	CCL3/CCL4/UCMR3	EPA 539 (LC-ESI-MS-MS/SPE)	Eurofins
	Estriol	Chemical of interest	EPA 539 (LC-ESI-MS-MS/SPE)	Eurofins
	Bisphenol A	Chemical of interest	EPA 539 (LCMAMS)	Eurofins
Cyanotoxins				
	Total Microcystin	CCL4/UCMR4	LCMSMS	Eurofins
	Anatoxin-a	CCL3/CCL4	LCMSMS	Eurofins
	Cylindrospermopsin	CCL3/CCL4	LCMSMS	Eurofins
	Microcystin-LR	CCL3/CCL4	LCMSMS	Eurofins
Flame Retardants				
	BDE-100	Chemical of interest	GC-QQQ PBDE	Eurofins
	BDE-153	Chemical of interest	GC-QQQ PBDE	Eurofins
	BDE-154	Chemical of interest	GC-QQQ PBDE	Eurofins
	BDE-183	Chemical of interest	GC-QQQ PBDE	Eurofins
	BDE-209	Chemical of interest	GC-QQQ PBDE	Eurofins
	BDE-28	Chemical of interest	GC-QQQ PBDE	Eurofins
	BDE-47	Chemical of interest	GC-QQQ PBDE	Eurofins
	BDE-99	Chemical of interest	GC-QQQ PBDE	Eurofins
	Musk Ketone	Chemical of interest	GC-QQQ PBDE	Eurofins
	Galaxolide	Chemical of interest	GC-QQQ PBDE	Eurofins
	Chlorpyrifos	CCL4	GC-QQQ PBDE	Eurofins
	cis-Permethrin	UCMR4	GC-QQQ PBDE	Eurofins
	Fenitrothion	Chemical of interest	GC-QQQ PBDE	Eurofins
	Fipronil	Chemical of interest	GC-QQQ PBDE	Eurofins
	Kepone	Chemical of interest	GC-QQQ PBDE	Eurofins
	Total Permethrin	UCMR4	GC-QQQ PBDE	Eurofins
	trans-Permethrin	UCMR4	GC-QQQ PBDE	Eurofins
	Bifenthrin	Chemical of interest	GC-QQQ PBDE	Eurofins

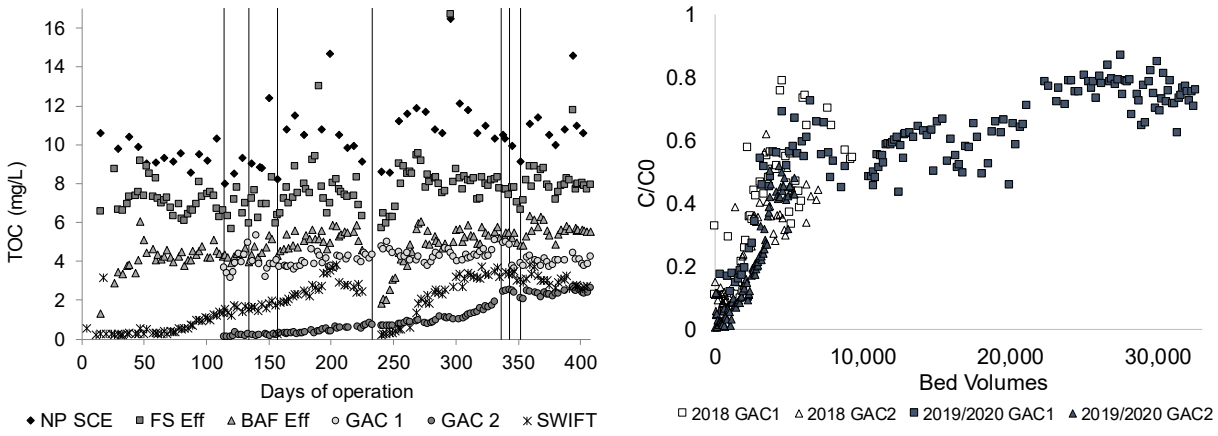

Figure SI-1a. TOC data from Startup 2. Vertical lines represent flow split changes between GAC 1 and GAC 2 (90-10, 80-20, 70-30, 80-20, 70-30, 50-50, 70-30 **SI-1b.** GAC TOC breakthrough from Startup 1 (2018) and 2 (2019-2020).

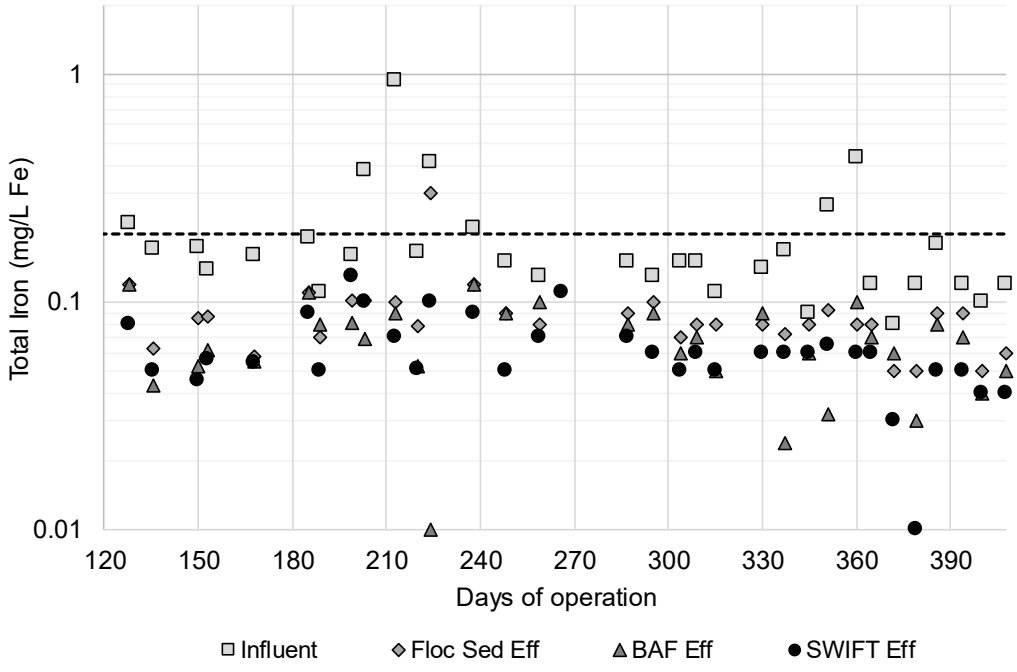

Figure SI-2. Total iron throughout SWIFT process. Dashed line represents method reporting limit = 0.2 mg/L

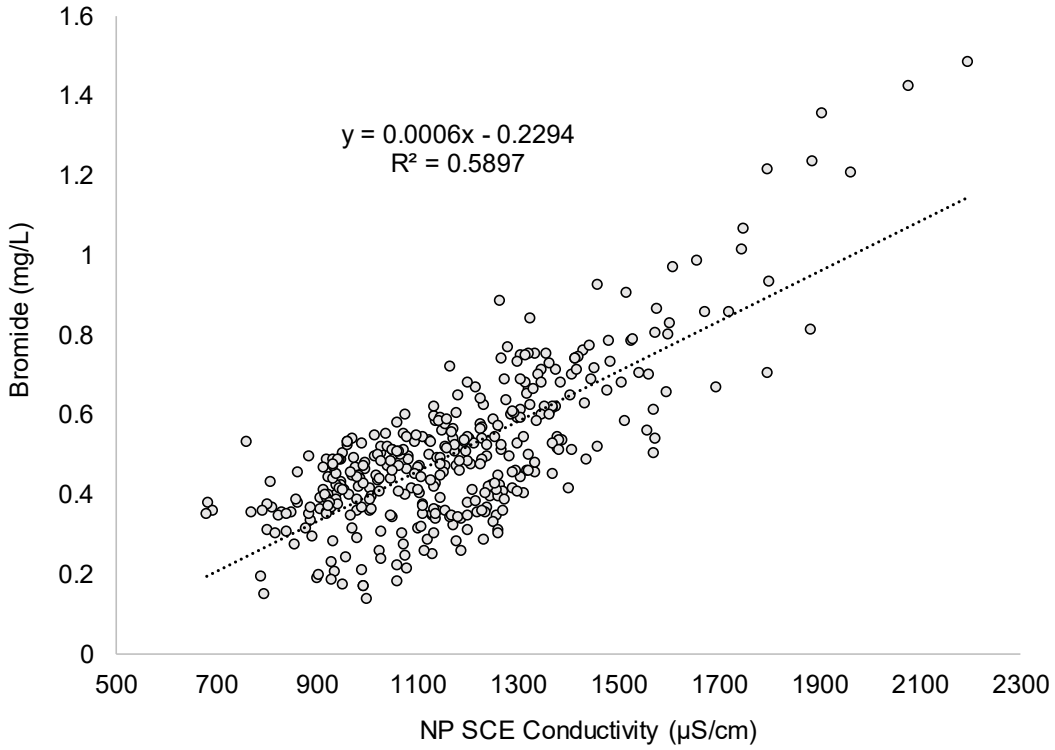

Figure SI-3. Correlation between conductivity and bromide

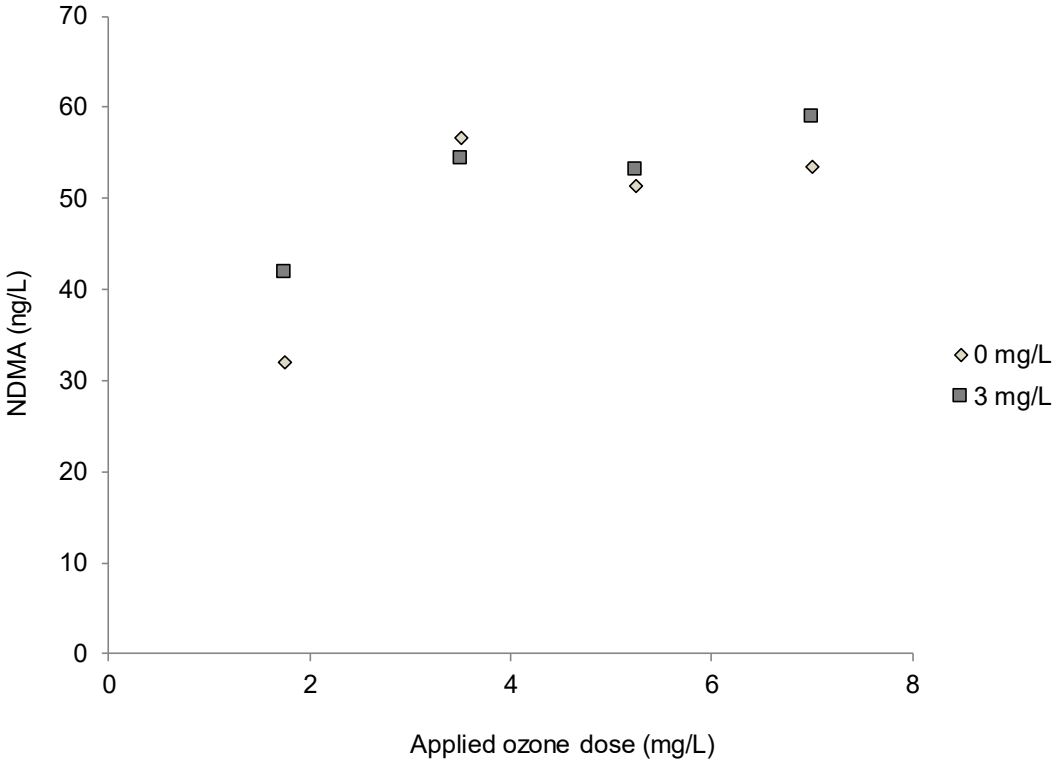

Figure SI-4. NDMA formation during ozonation with 3 mg/L NH_2Cl and without chemical addition

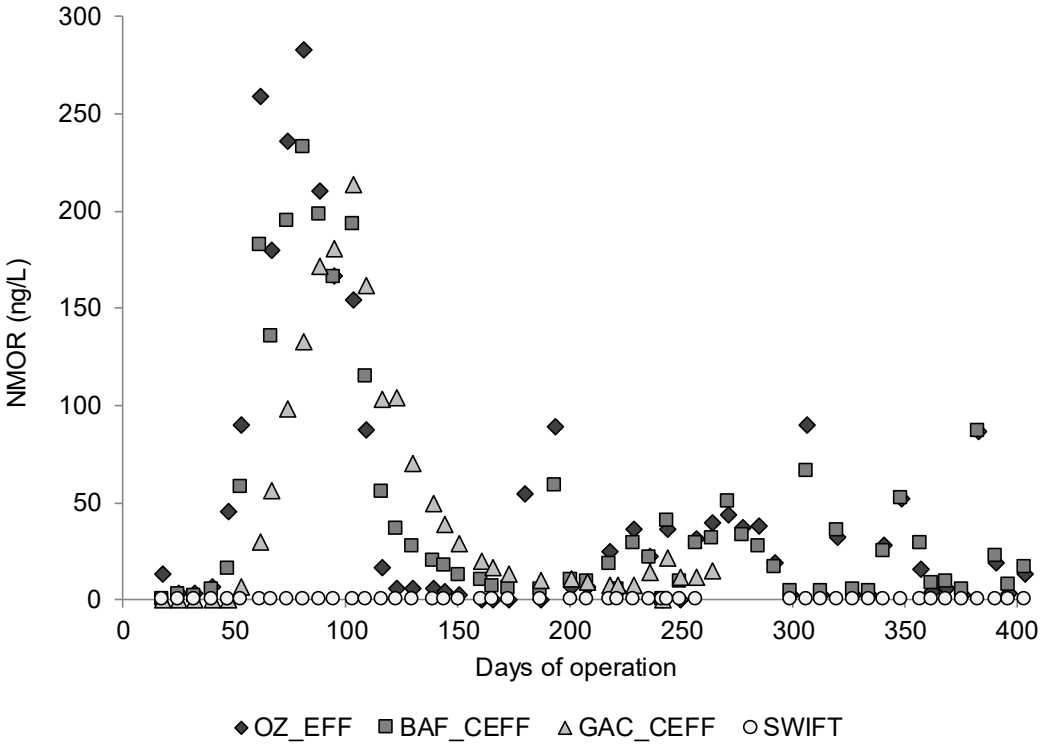

Figure SI-5. NMOR (Startup 2)

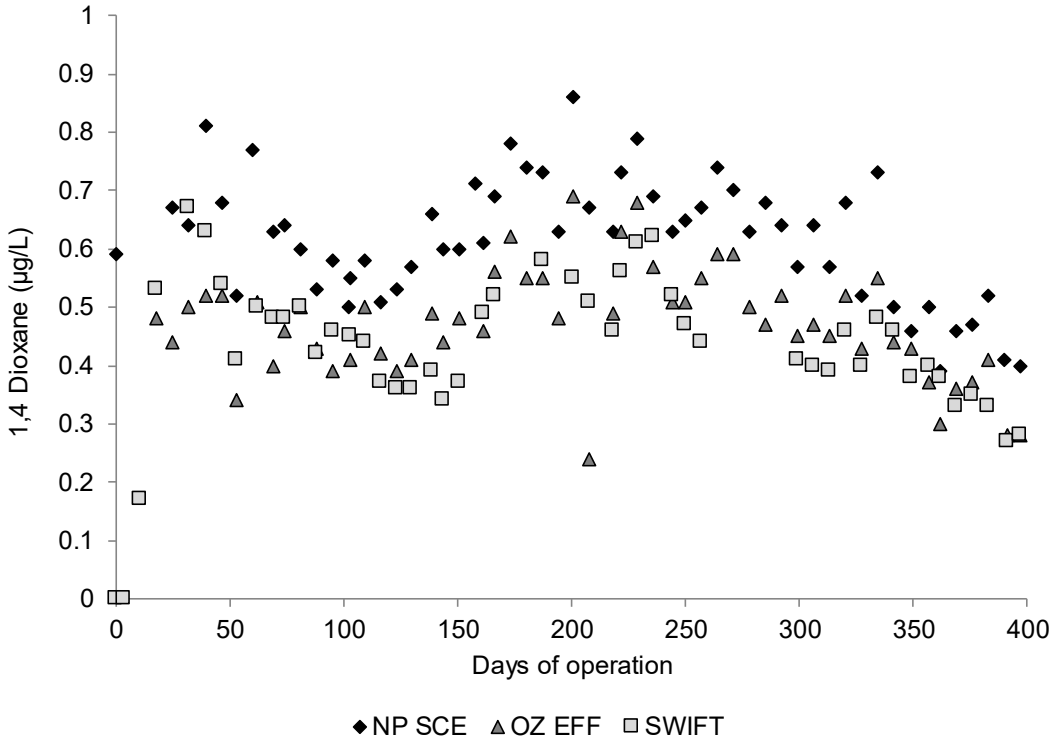

Figure SI-6. 1,4-dioxane throughout SWIFT process (Startup 2)

Table SI-4. Water Quality Indicators

Category	Constituent	Limit	Unit	Notes
Public Health	1,4-dioxane	1	µg/L	CCL4, CA Notification Limit
	NDMA	10	ng/L	CCL4, CA Notification Limit
	17-beta-estradiol	N/A	ng/L	CCL4
	DEET	200	µg/L	MN Health Guidance
	Ethinyl estradiol	N/A	ng/L	CCL4
	Perchlorate	6	µg/L	CA Notification Limit
	PFOA+PFOS	70	ng/L	CCL4, EPA Health Guidance
	TCEP	5	µg/L	MN Health Guidance
Treatment Effectiveness	Cotinine	1	µg/L	Surrogate for low molecular weight partially charged cyclics
	Primidone	10	µg/L	
	Phenytoin	2	µg/L	
	Meprobamate	200	µg/L	High occurrence in WWTP effluent
	Atenlol	4	µg/L	
	Carbamazepine	10	µg/L	Unique structure
	Estrone	320	µg/L	Surrogate for steroids
	Sucralose	150	mg/L	Surrogate for water soluble, uncharged chemicals with moderate molecular weight
	Triclosan	2100	µg/L	Chemical of interest

Chapter 3 Optimizing Ozone Disinfection in Water Reuse: Controlling Bromate Formation and Enhancing Trace Organic Contaminant Oxidation

Samantha Hogard[1,2], Robert Pearce[1,2], Kathleen Yetka[2], Raul Gonzalez[2], Charles Bott[2]

[1]Civil and Environmental Engineering Department, Virginia Polytechnic Institute and State University, Blacksburg, VA, USA

[2]Hampton Roads Sanitation District, PO Box 5911, Virginia Beach, VA 23471-0911

Hogard, S., Pearce, R., Gonzalez, R., Yetka, K., & Bott, C. (2023). Optimizing Ozone Disinfection in Water Reuse: Controlling Bromate Formation and Enhancing Trace Organic Contaminant Oxidation. Environmental Science and Technology. https://doi.org/10.1021/acs.est.3c00802

10 pages

Environmental Science & Technology

pubs.acs.org/est

Article

Optimizing Ozone Disinfection in Water Reuse: Controlling Bromate Formation and Enhancing Trace Organic Contaminant Oxidation

Samantha Hogard,* Robert Pearce, Raul Gonzalez, Kathleen Yetka, and Charles Bott

Cite This: https://doi.org/10.1021/acs.est.3c00802

Read Online

ACCESS | Metrics & More | Article Recommendations | Supporting Information

ABSTRACT: The use of ozone/biofiltration advanced treatment has become more prevalent in recent years, with many utilities seeking an alternative to membrane/RO based treatment for water reuse. Ensuring efficient pathogen reduction while controlling disinfection byproducts and maximizing oxidation of trace organic contaminants remains a major barrier to implementing ozone in reuse applications. Navigating these challenges is imperative in order to allow for the more widespread application of ozonation. Here, we demonstrate the effectiveness of ozone for virus, coliform bacteria, and spore forming bacteria inactivation in unfiltered secondary effluent, all the while controlling the disinfection byproduct bromate. A greater than 6-log reduction of both male specific and somatic coliphages was seen at specific ozone doses as low as 0.75 O_3:TOC. This study compared monochloramine and hydrogen peroxide as chemical bromate control measures in high bromide water (Br^- = 0.35 ± 0.07 mg/L). On average, monochloramine and hydrogen peroxide resulted in an 80% and 36% decrease of bromate formation, respectively. Neither bromate control method had any appreciable impact on virus or coliform bacteria disinfection by ozone; however, the use of hydrogen peroxide would require a non-Ct disinfection framework. Maintaining ozone residual was shown to be critical for achieving disinfection of more resilient microorganisms, such as spore forming bacteria. While extremely effective at controlling bromate, monochloramine was shown to inhibit TrOC oxidation, whereas hydrogen peroxide enhanced TrOC oxidation.

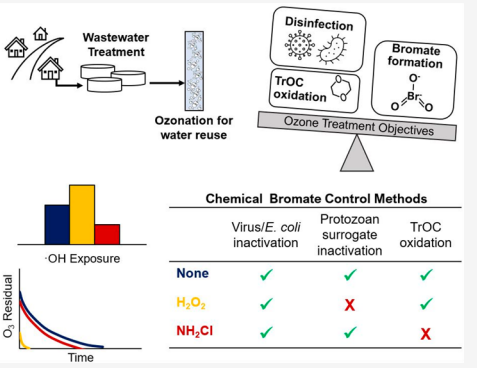

KEYWORDS: *Ozone, Water reuse, Virus, Disinfection, Bromate, 1,4-dioxane*

1. INTRODUCTION

Ensuring pathogen removal and microbial safety of finished water remains the greatest acute health concern in water reuse applications. Full advanced treatment trains commonly employed for water reuse in the United States achieve pathogen removal via membrane filtration and high dose UV.[1,2] In recent years, ozone/biofiltration based treatment has emerged as an alternative that can meet nearly every treatment goal for indirect potable reuse.[3−6] The lack of regulations surrounding pathogen removal in water reuse has in some cases led to the extension of drinking water treatment regulations to these applications.[5] Applying conservative drinking water frameworks presents a challenge when high log-removal values are required. For example, the use of Ct (concentration*time) to quantify ozone inactivation of viruses has been shown to be relatively conservative and difficult to manage in high bromide secondary effluent.[7] Other approaches can be considered and validated to ensure that sufficient pathogen removal is achieved in water reuse. For example, one study showed that parameters such as change in UV254 absorbance can correlate with virus log reduction even when no measurable Ct is achieved.[8]

Ozone is a well-known disinfectant that has been applied in water treatment applications for decades,[9,10] and recent studies demonstrate similar efficacy in water reuse.[11] Ozone reacts relatively fast with microorganisms with reaction rates of 10^5–10^6 M^{-1} s^{-1} and 1.04 × 10^5 M^{-1} s^{-1} reported for enteric viruses and *E. coli*, respectively.[12,13] Ozone is also effective at inactivating chlorine-resistant microorganisms such as *Cryptosporidium parvum* (k = 6.7 × 10^2 M^{-1} s^{-1}).[9] Pilot validation studies performed previously have shown a greater than 6.5 log removal of MS2 in filtered secondary wastewater effluent.[3] Ozone also provides the benefit of efficiently oxidizing trace organic contaminants (TrOCs).[14,15] The primary drawback to ozone application is the formation of disinfection byproducts (DBPs) such as bromate, aldehydes, and nitrosamines such as NDMA.[16−18] This is a challenge in water reuse applications, where the concentration of precursor compounds is elevated. Many DBPs formed during ozonation are biodegradable in downstream biofiltration (e.g., NDMA[19]); however, bromate is not. Therefore, bromate is of particular concern due to the 10

Special Issue: Oxidative Water Treatment: The Track Ahead

Received: January 31, 2023
Revised: June 6, 2023
Accepted: June 7, 2023

	Unit	Mean value +/- st. dev
Temp	°C	20 +/- 0.87
pH		7.1 +/- 0.11
TOC	mg/L	8.4 +/- 0.66
NO_3^-	mg/L-N	2.27 +/- 0.83
NO_2^-	mg/L-N	0.05 +/- 0.04
NH_4^+	mg/L-N	0.2 +/- 0.2
Br^-	mg/L	0.35 +/- 0.07
1,4-dioxane	µg/L	0.46 +/- 0.08
NDMA	ng/L	9.5 +/- 8.07
Alkalinity	mg/L $CaCO_3$	148.6 +/- 16.3

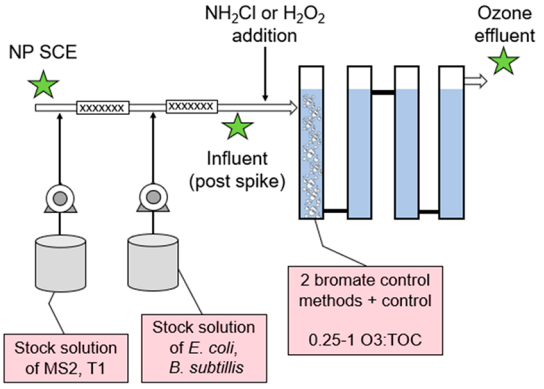

Figure 1. Nansemond SCE water quality and the HRSD ozone pilot testing setup including sampling locations indicated with star symbols.

µg/L maximum contaminant level (MCL) put in place by the United States EPA and the World Health Organization.[20,21] Common bromate control methods used in water treatment include pH suppression and ammonia addition;[22] however, these are often insufficient in wastewater treatment applications where bromide is elevated and hydroxyl radical (*OH) bromate formation pathways dominate.[16] Alternative chemical control measures including chlorine/ammonia-based strategies and the use of hydrogen peroxide have been shown to suppress bromate formation below the MCL.[23,24] Multiple studies have been completed demonstrating the efficacy of preformed monochloramine for bromate control in a high bromide reuse water.[5,7]

Each of these bromate control methods has other impacts on the ozonation process that are not well documented, especially in potable reuse. Preformed monochloramine is a well-known *OH scavenger; in fact, this is hypothesized to be one of the primary mechanisms for bromate control[5,7,25] and could be a detriment to *OH mediated TrOC oxidation.[7] Additionally, monochloramine itself may contribute to further DBP formation.[26,27] Hydrogen peroxide limits bromate formation by accelerating ozone decomposition and minimizing ozone exposure as well as reducing hypobromous acid which forms during bromate formation.[23,28,29] The addition of hydrogen peroxide during ozonation has also been shown to enhance TrOC oxidation in some cases.[29,30] Currently, the requirement to maintain a dissolved ozone residual for Ct credit would preclude a treatment facility from using hydrogen peroxide for bromate control.

As the application of ozone in water reuse becomes more prevalent, it is important to determine the optimal strategy to balance disinfection and TrOC oxidation with bromate formation. The objectives of the study described herein were to (1) investigate the performance of ozone disinfection in water reuse at the pilot scale, (2) compare monochloramine and hydrogen peroxide as chemical bromate control methods in high bromide secondary effluent, and (3) determine the ancillary impacts of these bromate control strategies on disinfection and oxidation of TrOCs during ozonation.

2. MATERIALS AND METHODS

2.1. Ozone Pilot Description. Experiments done as a part of this study were performed on a 3.78 Lpm (1 gpm) ozone pilot located at the Hampton Roads Sanitation District's (HRSD) demonstration scale indirect potable reuse plant and research center in southeast Virginia. Unfiltered secondary clarifier effluent from HRSD's five-stage Bardenpho Nansemond Wastewater Treatment Plant was the feedwater for these experiments. The ozone pilot was operated in fine bubble diffusion with the first column being a counter flow bubble diffusion chamber (detention time = 1.5 min) and the remaining five columns functioning as the contact chamber. The ozone pilot included an oxygen concentrator and ozone generator. The ozone dose was entered manually and controlled automatically by varying the ozone gas concentration and gas flow rate. Ozone feed gas and off-gas concentrations were measured using ozone gas analyzers, and transfer efficiency typically remained >95%. The residence time of the entire ozone pilot was approximately 10 min total. For both the monochloramine and hydrogen peroxide testing conditions, chemicals were added upstream of the ozone contactor. Preformed monochloramine was obtained on site from the chemical feed system at the demonstration scale indirect potable reuse plant. This system includes a GAC contactor and ion exchange unit that are used to dechlorinate and soften tap water which serves as the carrier water prior to sequential addition of sodium hypochlorite and ammonium sulfate. This chemical stock solution was collected on the day of testing to ensure the concentration was >1500 mg/L-Cl_2. A fixed monochloramine dose of 3 mg/L-Cl_2 was used for the testing described herein. Monochloramine was quenched at the end of the ozone contactor before sampling by using sodium bisulfite. Hydrogen peroxide (30%) was diluted 100-fold for use on the pilot scale. A molar ratio of 1:1 H_2O_2:O_3 was used for these experiments. A control test was also completed for each of these chemicals, where ozone was turned off in order to observe the effects of these chemicals alone.

2.2. Microbial Surrogates. Challenge experiments were performed by spiking model viruses including male specific coliphage, MS2 and somatic coliphage, T1. *Escherichia coli* was used as a vegetative bacteria surrogate, and the spore forming bacteria *Bacillus subtillis* and *Clostridium perfringens* were used as surrogates for protozoan pathogens. Pepper mild mottle virus (PMMoV), crAssphage, and the general *Bacteroides* assay (GenBac) were identified as useful molecular indicators, as they are frequently detected at elevated concentrations in the secondary clarifier effluent. PMMoV and the bacteriophage, crAssphage, are commonly used as markers for fecal contamination and can be representative of pathogenic virus

https://doi.org/10.1021/acs.est.3c00802
Environ. Sci. Technol. XXXX, XXX, XXX−XXX

removal in wastewater treatment processes.[31] *E. coli* and total coliform were assayed using the 24-h IDEXX Colilert-18 method. Male-specific and somatic coliphages were quantified using the single agar layer procedure on undiluted or diluted samples.[32] Although MS2 and T1 were used as representative viruses, this culture based analysis also includes background concentrations of indigenous male specific and somatic coliphages. Therefore, results will indicate the log reduction of total male specific and somatic coliphages. *Clostridium perfringens* and aerobic spore forming bacteria (SFB) were quantified by BCS Laboratories in Gainesville, FL using ASTM D5916 and Standard Method 9218, respectively. In addition to these added surrogates, the removal of indigenous viruses and bacterial indicators was also examined by the droplet digital polymerase chain reaction (ddPCR) in this study. The molecular sampling methods and workflow for sample processing are included in the Supporting Information (Section SI-2).

The added culture concentrations were approximately 10^6−10^7 PFU/100 mL of both MS2 and T1 coliphages, 10^5 CFU/100 mL *E. coli*, and 10^5 CFU/100 mL *Bacillus subtilis* spores. This concentration of the coliphage was selected in an effort to limit the organic carbon that was introduced to the feedwater via the added culture. Stock solutions were prepared by adding the viral/bacterial cultures to five liters of phosphate buffered saline. These solutions were then added to the feedwater via Masterflex peristaltic pumps. The addition points were followed by static mixers to ensure sufficient mixing and even distribution of the added cultures. A diagram of the pilot test setup can be found in Figure 1.

2.3. Water Quality Analytical Methods. Field parameters, such as pH, temperature, and UV absorbance, were measured in a timely manner on the day of testing. A Thermo Scientific pH probe was used to periodically check that the pH remained constant in ozone influent samples. Temperature was controlled using a chiller system that recirculated water to the pilot feed tank, and it was verified on every sample using a HANNA Instruments thermometer. UV 254 absorbance was measured on 0.45 μm filtered influent and ozone effluent samples using a Thermo Scientific Genesys 150 UV−vis Spectrophotometer. Dissolved ozone residual was measured according to the Standard Method 4500 Indigo colorimetric method. Samples for water quality parameters, including alkalinity, total organic carbon (TOC), bromate, and bromide, were analyzed by HRSD's Central Environmental Laboratory. TOC was analyzed according to Standard Method 5310 using a Shimadzu TOC 4200. Bromate was analyzed according to EPA method 300.1 with a Dionex 5000 plus ion chromatograph, and bromide was analyzed by EPA method 300 using a Dionex Integrion high-pressure ion chromatograph. NDMA and 1,4-dioxane were analyzed according to EPA methods 521 and 522, respectively, using an Agilent 7010B GC/MS Triple Quadrupole (Santa Clara, CA). A suite of 106 TrOCs was analyzed by Eurofins Eaton Analytical (Monrovia, CA) using liquid chromatography with tandem mass spectrometry (LC-MS-MS).

3. RESULTS AND DISCUSSION

3.1. Ozone and *OH Exposure. The secondary clarifier effluent water quality characteristics are summarized in Figure 1. The temperature of the pilot feed was controlled to 20 ± 0.87 °C, while TOC and nitrite only varied slightly with an average of 8.4 and 0.05 mg/L-N, respectively. As a result, the ozone decay characteristics were similar between testing days when evaluating the control condition with no chemical addition (Table SI-1). For every test, the 0.25 O_3:TOC condition resulted in minimal measurable ozone residual, and therefore, ozone decay could not be characterized. The average first order ozone decay rate in the control condition decreased in magnitude from 3 to 0.62 min^{-1} when increasing the ozone dose 0.5−1 O_3:TOC as expected.[33] The initial ozone demand (IOD) is defined as the applied ozone dose minus the dissolved ozone concentration measured in the effluent of the diffusion column. In the absence of any chemicals added for bromate control, the IOD was between 56 and 68% of the applied ozone dose at 0.75−1 O_3:TOC for both tests 1 and 2, and this proportion increased to ∼80% at 0.5 O_3:TOC. This demonstrates the potential for bulk organic matter alone to impose a significant ozone demand. The addition of 3 mg/L-Cl_2 monochloramine resulted in a minor increase in the ozone decay rate and increased IOD at each applied O_3:TOC ratio. This was primarily attributed to the reaction between ozone and monochloramine ($O_3 + NH_2Cl \rightarrow NO_3^- + Cl^- + H^+$, k = 26 M^{-1} s^{-1}).[34] A previous study performed on the same source water found that monochloramine had little impact on the ozone decay rate and IOD.[7] In general, the impact of monochloramine may vary depending on the concentration of other ozone demand inducing constituents, and it is likely that ozone decay will be governed by the bulk organic concentration and reactivity in wastewater. The addition of hydrogen peroxide dramatically increased the ozone decay rate which is consistent with previous studies in drinking water.[29] Example ozone decay curves for an ozone dose of 0.75 O_3:TOC under all bromate control conditions are shown in Figure 2. In addition, complete ozone residual curves are shown for each test condition in the Supporting Information (Figures SI-1−6). For this work, the maximum instantaneous single point Ct was used to evaluate disinfection results, and a summary of maximum single point Ct, total integrated ozone exposure, and the average decay rate for each testing condition is presented in Table SI-1 and Table SI-2. While there are multiple methods used for calculating ozone exposure, the single point Ct approach was used to represent full-scale operational data. This method is limited in several ways as it underestimates the total ozone exposure, it does not include the ozone exposure that occurs during dissolution, and it can vary widely depending on where the residual is measured. These data can be compared to the total ozone exposure in Tables SI-1 and SI-2 to emphasize the conservative nature of single point Ct. Total ozone exposure is calculated by integrating the ozone residual curve beginning immediately after the ozone diffuser.

The *OH exposure can be calculated using the second order reaction rate constant and measured removal of 1,4-dioxane using eq 1[35] shown in the SI, where the reaction rate of 1,4-dioxane and *OH is 3×10^9 M^{-1} s^{-1}.[10] The total ozone exposure and *OH exposure for test 1 are summarized in Tables SI-1 and 3, respectively. When increasing the ozone dose from 0.25 to 1 O_3:TOC, the average *OH exposure for two tests increased linearly from 0.65 to 3.04×10^{-10} M*s. At an O_3:TOC of 1, the addition of 3 mg/L-Cl_2 NH_2Cl resulted in an average 48% reduction of *OH exposure, while a 1:1 molar ratio of H_2O_2 resulted in a 40% increase.

3.2. Microorganism Inactivation by Ozone. *3.2.1. Coliphage.* Male specific and somatic coliphage inactivation is shown for each treatment condition in Figure 3. These data

https://doi.org/10.1021/acs.est.3c00802
Environ. Sci. Technol. XXXX, XXX, XXX−XXX

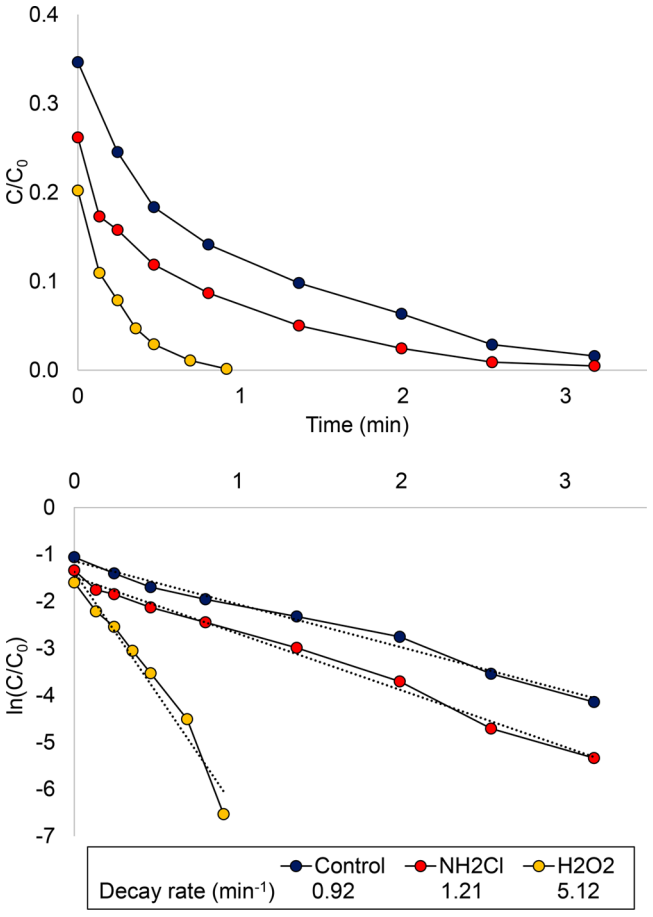

Figure 2. Representative ozone decay characteristics for each bromate control scenario at a specific ozone dose of 0.75 O_3:TOC. The ozone dose for each scenario was 6.93 mg/L (control), 7.7 mg/L (3 mg/L-Cl_2 NH_2Cl), and 6.88 mg/L (1:1 O_3:H_2O_2).

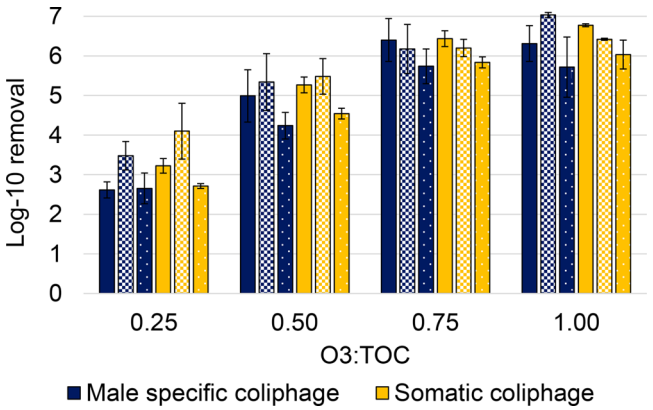

Figure 3. Log-10 reduction of male specific and somatic coliphages by ozone. Solid bars represent the control condition, checkered bars are the hydrogen peroxide condition, and dotted bars are the monochloramine condition. Bars represent average log-removal data for two independent tests with error bars showing the range.

include the indigenous coliphage as well as spiked MS2 and T1 coliphages. Even at the lowest ozone dose of 0.25 O_3:TOC, greater than 2-log reduction of male specific and somatic coliphages was observed for all conditions. Given the relatively fast reaction rate reported for ozone with the male specific coliphage, MS2 ($k = 1.9 \times 10^6$ M^{-1} s^{-1}), and a morphologically similar somatic coliphage T4 (1.3×10^6 M^{-1} s^{-1}), this result is expected.[12] At the higher ozone doses (0.75−1 O_3:TOC), a greater than 6-log reduction of both male specific and somatic coliphages was demonstrated. These elevated ozone doses resulted in nearly nondetect values, producing the maximum LRV possible (>6 log) under these conditions. One study found that a 6.5-log reduction of MS2 is equivalent to a 5 log-reduction of poliovirus, which is required by California's Title 22 water reuse regulations.[36] The observed log-reduction appears to level off after 0.75 O_3:TOC due to the limitation associated with spiking additional coliphages discussed previously. These results are aligned with previous bench-scale ozonation studies performed on filtered wastewater effluent which showed a greater than 5-log reduction of MS2 at ozone doses greater than 0.25 O_3:TOC.[8] The results of the present study highlight the efficacy of ozone for virus disinfection in highly treated wastewater, regardless of tertiary filtration. A recent review on ozone disinfection indicated that somatic coliphages (DNA viruses) may follow more similar inactivation kinetics to mammalian viruses in pure water, whereas MS2 displays the greatest susceptibility to inactivation by ozone.[37] However, the results presented herein suggest that both male specific and somatic coliphages experience similar inactivation in this wastewater matrix for a given ozone dose among all tested conditions.

It is generally believed that molecular ozone is primarily responsible for virus inactivation, whereas *OH is not expected to play a significant role in disinfection.[15] However, the results of this experiment demonstrate that marginally elevated coliphage inactivation was achieved with the addition of hydrogen peroxide when compared with the control condition and the monochloramine condition. This disparity between the bromate control conditions is more apparent at lower ozone doses where minimal measurable ozone exposure is achieved. A control test was completed for both monochloramine and hydrogen peroxide to determine if each oxidant was responsible for virus inactivation independent from ozone. There was negligible removal achieved by hydrogen peroxide and monochloramine alone (<0.5 log removal of male specific and somatic coliphages in all cases).

Given that each bromate control method did not have any impact on the inactivation of coliphage, these data were correlated with three independent variables including change in UV254 absorbance, applied specific ozone dose (O_3:TOC corrected for nitrite), and single point ozone Ct. These correlations are presented in Figure 4a-c. The correlation of male specific and somatic coliphage inactivation with change in UV absorbance and O_3:TOC display relatively high correlation coefficients (R^2 = 0.78 and 0.74, respectively, and $p < 0.05$) suggesting these would be useful parameters for process monitoring and disinfection verification. This is well aligned with previous bench scale studies that have shown that MS2 inactivation correlates well with change in UV254 absorbance, change in fluorescence, and applied ozone dose.[8,38] Further, the correlation of coliphage inactivation with ozone exposure is relatively weak, with the data reaching an asymptote beyond a single point Ct of 0.5 mg/L-min as a result of the coliphage detection limit being nearly reached. This is especially true for scenarios where hydrogen peroxide is used for bromate control and minimal ozone exposure is achieved. In Figure 4c, the EPA model for virus inactivation by ozone at 20 °C is overlaid on the data collected in the present study. This highlights the conservative nature of drinking water frameworks when

https://doi.org/10.1021/acs.est.3c00802
Environ. Sci. Technol. XXXX, XXX, XXX−XXX

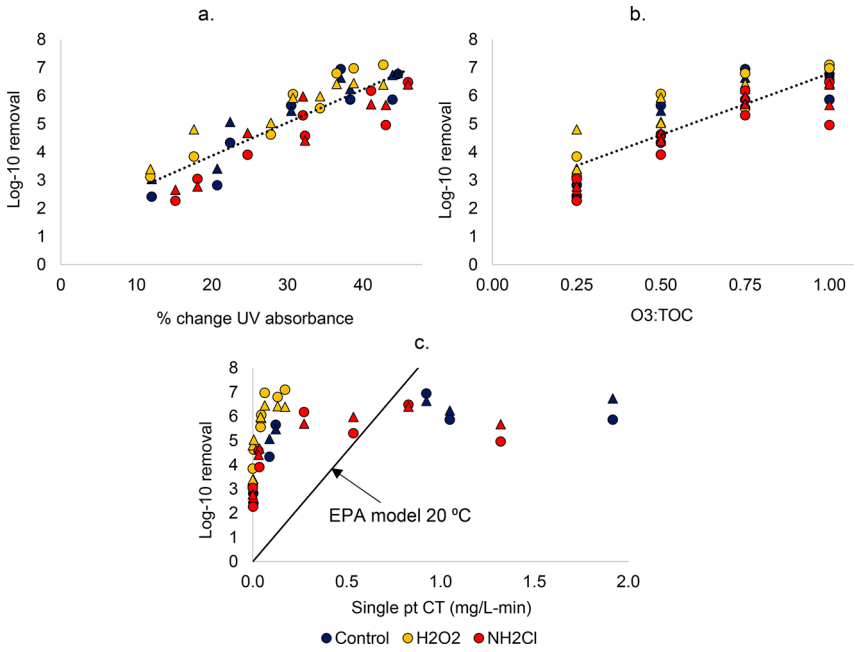

Figure 4. Log reduction of male specific (circles) and somatic (triangles) coliphages correlated with (a) % change in UV absorbance (R^2 = 0.78), (b) O_3:TOC corrected for nitrite (R^2 = 0.74), and (c) single point ozone exposure (C*t) with the US EPA model @ 20 C overlaid.

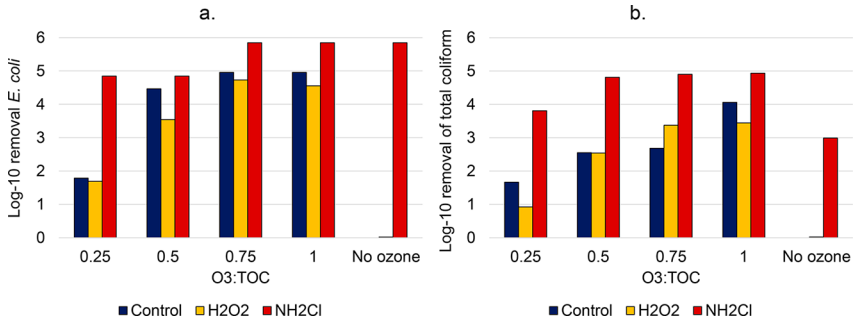

Figure 5. (a) *E. coli* and (b) total coliform removal by ozone for each bromate control condition.

compared with the actual observed coliphage inactivation at lower ozone doses.

3.2.2. Molecular Markers. In addition to the culturable viruses, a group of viral and bacterial indicators was analyzed by molecular methods. As discussed previously, PMMoV, crAssphage, and the general *Bacteroides* assay (GenBac) were identified as useful indicators due to the elevated concentration present in the secondary effluent. These data are presented in Figure SI-7 for each of the treatment conditions tested. In the control condition, there is a clear trend between the applied O_3:TOC ratio and log-removal of each indicator. However, with the introduction of monochloramine and hydrogen peroxide, the trends become less distinct with some indicators having little relationship with applied O_3:TOC at all. The appearance of negative removal of PMMoV is likely explained by the difference in the influent sample volume and variations in recovery during the ddPCR process. These details are outlined in Table SI-4. There are several well-documented shortcomings associated with using molecular methods to demonstrate inactivation by oxidative disinfection methods.[39,40] These analytical methods are inherently conservative in that they cannot distinguish between viable and nonviable viruses, and they only target a relatively small segment of the genome of interest.[39,41] Therefore, molecular results will show inactivation only if the oxidant damages the specific segment of the genome that is targeted by the molecular assay. The addition of monochloramine and hydrogen peroxide may inhibit the attack of molecular ozone on the specific gene segment of interest for some indicators. The present study highlights the difficulty associated with using molecular methods to demonstrate log-reduction of viral and bacterial indicators by ozonation.

3.2.3. Coliform Bacteria. Both *E. coli* and total coliform log-removal are presented in Figure 5. It is apparent from these results that coliform bacteria cannot be effectively used as an indicator of ozone treatment when using monochloramine for bromate control due to the high log reduction achieved by monochloramine alone. Samples were quenched with sodium bisulfite upon collection; therefore, the contact time with monochloramine was equal to the residence time of the ozone contactor (~10 min). The results from the control condition and hydrogen peroxide condition were very similar, suggesting that the majority of inactivation happens rapidly during the initial phase of ozone exposure and decomposition. Negligible log-reduction was observed with the use of hydrogen peroxide alone. This is also well aligned with data from previous studies that estimated a relatively high reaction rate of ozone with *E. coli* of 1.04×10^5 M^{-1} s^{-1}.[13] Other studies have shown similar

https://doi.org/10.1021/acs.est.3c00802
Environ. Sci. Technol. XXXX, XXX, XXX−XXX

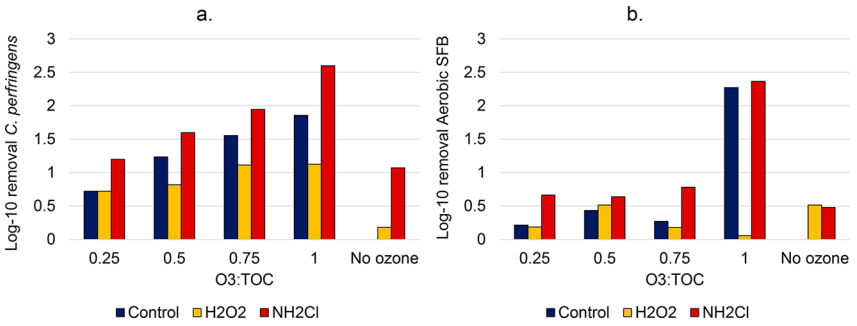

Figure 6. (a) *C. perfringens* and (b) aerobic SFB removal by ozone for each bromate control condition.

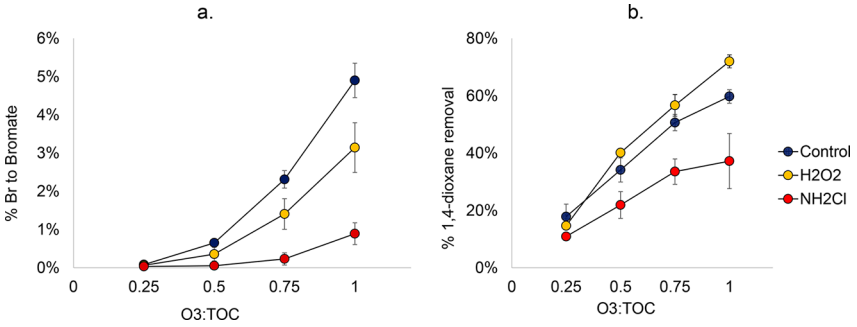

Figure 7. (a) Molar conversion of bromide to bromate. Data points represent average values for three independent tests with error bars showing standard deviation. (b) Percent removal of 1,4-dioxane. Data points represent average values for two independent tests, with error bars showing the range.

results with the addition of hydrogen peroxide or a radical scavenger, such as tertiary butanol, not having a significant impact on total coliform or *E. coli* disinfection by ozone.[8,13]

3.2.4. Spore Forming Bacteria. The removal of spore-forming bacteria by ozone is presented in Figure 6. The average influent concentration of *C. perfringens* was 790 CFU/100 mL. The trend of *C. perfringens* removal with an increasing ozone dose is consistent with each treatment condition. However, the addition of monochloramine alone results in approximately an additional 1 log-reduction of the bacteria. Therefore, the bars for the monochloramine condition are approximately 1 log unit above the others for every ozone dose. It also appears that these bacteria are more susceptible to molecular ozone than *OH due to the suppressed removal when hydrogen peroxide is added. This is in direct contrast with results presented in a previous study, showing enhanced removal of *C. perfringens* during ozonation with the addition of hydrogen peroxide in surface water (TOC = 2−4 mg/L).[42] Another study performed in surface water (DOC = 2.1−5.5 mg/L) found that elevated TOC concentration resulted in enhanced removal of *C. perfringens*, and the authors hypothesized that this could be a result of organics promoting *OH formation.[43] The present study shows that the conclusions of these previous studies are not necessarily valid for ozonation of a wastewater matrix.

Aerobic SFB inactivation was also quantified under each treatment condition. *Bacillus subtilis* spores are commonly used as surrogates for ozone disinfection of heartier microorganisms such as *C. parvum*.[9,44] Both chemicals used for bromate control were apparently responsible for nearly a 0.5 log-reduction of aerobic SFB alone. It is clear from the trend in removal of these bacteria that they are much more resistant to ozonation compared to other pathogens and indicators discussed previously. One study in drinking water reported a Ct-lag of 2.9 mg/L-min,[44] and another study performed in wastewater found a Ct-lag of 9 mg/L-min.[8] In the present study, a >0.7 log reduction of aerobic SFB was not observed until an ozone exposure of approximately 5 mg/L-min was achieved in the control and monochloramine conditions. Negligible log removal was achieved at any ozone dose with the use of hydrogen peroxide due to the lack of measurable ozone residual.

3.3. Bromate and 1,4-Dioxane. The background bromide concentration averaged 0.35 ± 0.07 mg/L throughout the duration of testing. In the control condition, the average molar conversion of bromide to bromate (mol Br^-/mol BrO_3^-) increased from <0.1% to ~5% when increasing O_3:TOC from 0.25 to 1. This can be seen in Figure 7a. At each O_3:TOC, the addition of hydrogen peroxide and monochloramine resulted in 36 ± 8% and 80 ± 14% suppression in bromide conversion, respectively, when compared with the control condition. Understanding the relative contributions of molecular ozone and *OH is imperative in order to sufficiently limit bromate formation in wastewater ozonation. It has been hypothesized that bromate formation in treated wastewater is dominated by the "indirect" reaction with *OH as opposed to "direct" reactions with molecular ozone.[16] The primary mechanism of bromate control by monochloramine is elucidated by Figure 7b that displays the difference in 1,4-dioxane oxidation. As mentioned previously, this compound is primarily oxidized by *OH (k_{*OH} = 3 × 10^9 M^{-1} s^{-1}, k_{O3} = <1 $M^{-1}s^{-1}$),[10] and by using this compound as a surrogate to calculate *OH exposure, we can conclude that the addition of monochloramine results in up to 60% lower hydroxyl radical exposure. Monochloramine has also been shown to react to form intermediate compounds that act as reservoirs of bromine and prevent bromate formation.[45] Additionally, a recent study showed the rapid reaction rate

https://doi.org/10.1021/acs.est.3c00802
Environ. Sci. Technol. XXXX, XXX, XXX−XXX

between monochloramine and the bromine radical during bromate formation which provides another important mechanism for limiting bromate formation.[46] Hydrogen peroxide primarily limits bromate formation by both reacting relatively rapidly with ozone ($k_{pH=7.1} = 1.92 \times 10^2$ M^{-1} s^{-1})[10,47] resulting in minimal measurable ozone exposure, as well as reducing hypobromous acid to bromide.[29,48] The significant impact of hydrogen peroxide on ozone decay is shown by the example ozone decay curve shown in Figure 2. Additionally, hydrogen peroxide moderately enhances *OH exposure, as shown by the increased removal of 1,4-dioxane in Figure 7b. These data support the hypothesis that *OH bromate formation pathways dominate during wastewater ozonation seeing as the reduction in *OH exposure by monochloramine was far more effective in controlling bromate compared with the elimination of molecular ozone exposure coupled with enhanced *OH exposure by hydrogen peroxide. Ultimately, these results may vary for wastewater matrices with variable organics composition and reactivity. The impact of hydrogen peroxide and monochloramine on NDMA formation was also investigated; however, these data were not conclusive and are presented in Figure SI-8 and Section SI-3.3.

3.5. Trace Organic Contaminants. As a part of this study, a full suite of 106 TrOCs was monitored at each treatment condition in a separate test conducted on a single day. Duplicate influent samples were collected, and values were averaged for redundancy. Of the 106 TrOCs, only 50 were detected in both influent samples. Additionally, out of the 50 compounds detected in both influent samples, ten were removed below the detection limit in every ozone treatment condition. This is due to the very high reaction rate of ozone with these compounds. These raw data are summarized in the Supporting Information (Table SI-5).

The compounds, which are more resistant to ozonation or have a higher affinity for reacting with *OH, reveal more information about the relative ozone and *OH exposure. The removal of these compounds is summarized in Table 1.

Table 1. Trace Organic Contaminant Removal by Ozone[a]

	rate k ($M^{-1}s^{-1}$)[b]		Control		H_2O_2		NH_2Cl	
O3:TOC	O_3	*OH	0.25	0.75	0.25	0.75	0.25	0.75
Sucralose	<0.1[53]	1.5-1.6 * 10^9 [53]	2%	37%	13%	48%	6%	24%
Iohexol	N/A	5.7 * 10^8 [54]	16%	56%	24%	68%	16%	44%
Primidone	<10 [55]	6.7 * 10^9 [56]	35%	77%	30%	85%	21%	50%
Meprobamate	<1 [55]	3.7*10^9 [55]	27%	63%	23%	62%	-2%	35%
Sulfamethoxazole	5.7*10^5 [57]	5.5*10^9 [57]	82%	99%	78%	99%	80%	99%*

[a]% removal values denoted with an asterisk (*) were calculated using the detection limit as the raw value was below the method detection limit. Gradient color scale represents the relative removal of each compound. [b]Reaction rate sources[53−57]

Sucralose, iohexol, primidone, and meprobamate can be used as indicator compounds that have well-defined, relatively high reaction rates with *OH. Low-moderate removal is observed for each of these compounds with ozone alone, and removal is enhanced marginally with the addition of hydrogen peroxide. The addition of monochloramine for bromate control results in decreased removal of almost every compound for both 0.25 and 0.75 O_3:TOC when compared with the control condition. As discussed previously, any of these compounds can be utilized to effectively measure *OH exposure, and for the purposes of this study, 1,4-dioxane was used as a probe compound. The resulting hydroxyl radical exposure is shown in Table SI-3. The addition of 1 mol H_2O_2/mol O_3 resulted in approximately 23% greater *OH exposure on average at 0.5 O_3:TOC, and this increased to 40% greater *OH exposure at a specific ozone dose of 1 O_3:TOC. This is supported by previous lab scale experiments that show the benefit of hydrogen peroxide is greater at higher applied ozone doses.[49] These results are also aligned with those of previous lab-scale studies showing that the addition of just 0.5 mol H_2O_2/mol O_3 can enhance *OH production by as much as 30−40% in a source water with similar DOC concentrations (8.6−12.2 mg/L).[30] In contrast, monochloramine resulted in a 40−48% decrease in *OH exposure for every ozone dose tested. Sulfamethoxazole is a compound that reacts rapidly with both molecular ozone and *OH. Regardless of the complete elimination of a dissolved ozone residual with the addition of hydrogen peroxide, a similar removal of this compound is observed for every treatment scenario. It is clear from the results presented that utilizing hydrogen peroxide provides a benefit with regard to enhancing *OH exposure, while monochloramine will diminish the oxidative capacity of ozonation.

4. ENGINEERING IMPLICATIONS

Ozone provides a robust barrier for pathogen inactivation and TrOC oxidation when applied in water reuse applications. This study elucidates several important mechanisms related to disinfection, TrOC oxidation, and DBP formation, which occur during the ozonation of treated wastewater. When ozone is applied in these treatment scenarios, it is critical to optimize the relative ozone and *OH exposure in order to balance treatment goals with DBP formation. In this study, two chemical bromate control strategies were evaluated, including hydrogen peroxide and monochloramine, for the ozonation of a high bromide secondary clarifier effluent. The results of this study show that three primary considerations must be made before selecting a bromate control method including (1) ozone disinfection objectives, (2) ambient bromide concentration, and (3) TrOC oxidation objectives. If the treatment goal is to achieve protozoa inactivation with ozone, considering these surrogate results, hydrogen peroxide cannot be used for bromate control, as this eliminates ozone exposure necessary for the inactivation of these microorganisms. If virus/*E. coli* inactivation is the goal, either monochloramine or hydrogen peroxide can be used for bromate control as a greater than 6-log reduction of male specific and somatic coliphages and a 4-log reduction of *E. coli* was observed at ozone doses of 0.75−1 O_3:TOC for every bromate control condition. The inactivation of model viruses correlated well with operational parameters other than ozone exposure, which supports the move away from Ct based disinfection frameworks for virus inactivation in water reuse. While monochloramine presents a significant benefit with regard to bromate control, it also quenches *OH thus preventing complete oxidation of ozone-resistant TrOCs. If protozoa disinfection and ozone resistant TrOC oxidation are both treatment goals to be addressed with ozone, then it may be necessary to implement alternate treatment technologies or remove point sources of bromide to the source water.

This study provides a continuous flow pilot-scale validation of ozone disinfection for water reuse in high bromide source water. Continuous flow pilot scale studies allow for more confident extrapolation to full-scale applications to aid in the process design and control. Further, this study provides

https://doi.org/10.1021/acs.est.3c00802
Environ. Sci. Technol. XXXX, XXX, XXX−XXX

guidance to utilities that will implement ozonation for water reuse and wastewater disinfection applications. The guidance provided regarding alternative ozone monitoring frameworks will ultimately allow for lower overall ozone doses to achieve virus disinfection, representing capital and operational cost savings. Recent trends have suggested the use of ozone is on the rise as it is a more efficient alternative to other advanced oxidation processes.[50] In fact, the California State Waterboard has created guidelines for direct potable reuse that require ozone/biofiltration as a pretreatment step for reverse osmosis.[51] Additionally, many utilities in Europe have planned to implement ozone to treat TrOCs in wastewater.[52] This study shows that even when applied at relatively low doses, TrOC oxidation and significant disinfection can be achieved in wastewater ozonation. Future research should include the development of kinetic models that can more accurately determine the mechanisms responsible for pathogen inactivation, bromate control, and TrOC oxidation in various water matrices. Additionally, further studies should be completed to validate the alternative (non-Ct) ozone disinfection frameworks under a range of water quality parameters (e.g., pH, temperature, and TOC concentrations).

■ ASSOCIATED CONTENT

Supporting Information

The Supporting Information is available free of charge at https://pubs.acs.org/doi/10.1021/acs.est.3c00802.

Experimental methods, additional tables, figures, and text (PDF)

■ AUTHOR INFORMATION

Corresponding Author

Samantha Hogard − *Civil and Environmental Engineering Department, Virginia Polytechnic Institute and State University, Blacksburg, Virginia 24060, United States; Hampton Roads Sanitation District, Virginia Beach, Virginia 23471, United States;* orcid.org/0000-0001-9364-7257; Email: shogard@vt.edu

Authors

Robert Pearce − *Civil and Environmental Engineering Department, Virginia Polytechnic Institute and State University, Blacksburg, Virginia 24060, United States; Hampton Roads Sanitation District, Virginia Beach, Virginia 23471, United States*

Raul Gonzalez − *Hampton Roads Sanitation District, Virginia Beach, Virginia 23471, United States;* orcid.org/0000-0002-8115-7709

Kathleen Yetka − *Hampton Roads Sanitation District, Virginia Beach, Virginia 23471, United States*

Charles Bott − *Hampton Roads Sanitation District, Virginia Beach, Virginia 23471, United States*

Complete contact information is available at: https://pubs.acs.org/10.1021/acs.est.3c00802

Notes

The authors declare no competing financial interest.

■ ACKNOWLEDGMENTS

Funding for this project was provided by the Hampton Roads Sanitation District. The authors would like to thank the staff of the HRSD Pathogen Laboratory and Central Environmental Laboratory for their hard work performing analyses to support this project. Specifically, the efforts of Hannah Thompson, Hila Stephens, and Errin Carter are very appreciated.

■ REFERENCES

(1) Pecson, B. M.; Trussell, R. S.; Pisarenko, A. N.; Trussell, R. R. Achieving reliability in potable reuse: The four rs. *J. Am. Water Works Assoc.* **2015**, *107*, 48−58.

(2) Gerrity, D.; Pecson, B.; Shane Trussell, R.; Rhodes Trussell, R. Potable reuse treatment trains throughout the world. *J. Water Supply Res. Technol. - AQUA* **2013**, *62*, 321−338.

(3) Gerrity, D.; Gamage, S.; Holady, J. C.; Mawhinney, D. B.; Quiñones, O.; Trenholm, R. A.; Snyder, S. A. Pilot-scale evaluation of ozone and biological activated carbon for trace organic contaminant mitigation and disinfection. *Water Res.* **2011**, *45*, 2155−2165.

(4) Sundaram, V.; Pagilla, K.; Guarin, T.; Li, L.; Marfil-Vega, R.; Bukhari, Z. Extended field investigations of ozone-biofiltration advanced water treatment for potable reuse. *Water Res.* **2020**, *172*, 115513.

(5) Hogard, S.; Salazar-Benites, G.; Pearce, R.; Nading, T.; Schimmoller, L.; Wilson, C.; Heisig-Mitchell, J.; Bott, C. Demonstration-scale evaluation of ozone−biofiltration−granular activated carbon advanced water treatment for managed aquifer recharge. *Water Environ. Res.* **2021**, *93*, 1157.

(6) Hooper, J.; Funk, D.; Bell, K.; Noibi, M.; Vickstrom, K.; Schulz, C.; Machek, E.; Huang, C. H. Pilot testing of direct and indirect potable water reuse using multi-stage ozone-biofiltration without reverse osmosis. *Water Res.* **2020**, *169*, No. 115178.

(7) Pearce, R.; Hogard, S.; Buehlmann, P.; Salazar-benites, G.; Wilson, C.; Bott, C. Evaluation of preformed monochloramine for bromate control in ozonation for potable reuse. *Water Res.* **2022**, *211*, No. 118049.

(8) Gamage, S.; Gerrity, D.; Pisarenko, A. N.; Wert, E. C.; Snyder, S. A. Evaluation of Process Control Alternatives for the Inactivation of Escherichia coli, MS2 Bacteriophage, and Bacillus subtilis Spores during Wastewater Ozonation. *Ozone Sci. Eng.* **2013**, *35*, 501−513.

(9) von Gunten, U. Ozonation of drinking water: Part II. Disinfection and by-product formation in presence of bromide, iodide or chlorine. *Water Res.* **2003**, *37*, 1469−1487.

(10) von Sonntag, C.; von Gunten, U. *Chemistry of Ozone in Water and Wastewater Treatment: From Basic Principles to Applications. Chemistry of Ozone in Water and Wastewater Treatment: From Basic Principles to Applications* **2012**, DOI: 10.2166/9781780400839.

(11) Gerrity, D.; Owens-Bennett, E.; Venezia, T.; Stanford, B. D.; Plumlee, M. H.; Debroux, J.; Trussell, R. S. Applicability of Ozone and Biological Activated Carbon for Potable Reuse. *Ozone Sci. Eng.* **2014**, *36*, 123−137.

(12) Wolf, C.; von Gunten, U.; Kohn, T. Kinetics of Inactivation of Waterborne Enteric Viruses by Ozone. *Environ. Sci. Technol.* **2018**, *52*, 2170−2177.

(13) Hunt, N. K.; Marinas, B. Kinetics of Escherichia coli inactivation with ozone. *Water Res.* **1997**, *31*, 1355−1362.

(14) Gerrity, D.; Snyder, S. Review of ozone for water reuse applications: Toxicity, regulations, and trace organic contaminant oxidation. *Ozone Sci. Eng.* **2011**, *33*, 253−266.

(15) von Gunten, U. Ozonation of drinking water: Part I. Oxidation kinetics and product formation. *Water Res.* **2003**, *37*, 1443−1467.

(16) Soltermann, F.; Abegglen, C.; Tschui, M.; Stahel, S.; von Gunten, U. Options and limitations for bromate control during ozonation of wastewater. *Water Res.* **2017**, *116*, 76−85.

(17) Schechter, D. S.; Singer, P. C. Formation Of Aldehydes During Ozonation. *Ozone Sci. Eng.* **1995**, *17*, 53−69.

(18) Marti, E. J.; Pisarenko, A. N.; Peller, J. R.; Dickenson, E. R. V. N-nitrosodimethylamine (NDMA) formation from the ozonation of model compounds. *Water Res.* **2015**, *72*, 262−270.

(19) Vaidya, R.; Wilson, C.; Salazar-Benites, G.; Pruden, A.; Bott, C. Factors affecting removal of NDMA in an ozone-biofiltration process for water reuse. *Chemosphere* **2021**, *264*, No. 128333.

(20) US EPA. *Stage 1 Disinfectants and Disinfection Byproduct Rule*; 1998.
(21) World Health Organization. *Bromate in Drinking Water*; World Health Organization: 2003.
(22) Pinkernell, U.; von Gunten, U. Bromate minimization during ozonation: Mechanistic considerations. *Environ. Sci. Technol.* **2001**, *35*, 2525−2531.
(23) Lee, Y.; Gerrity, D.; Lee, M.; Gamage, S.; Pisarenko, A.; Trenholm, R. A.; Canonica, S.; Snyder, S. A.; Von Gunten, U. Organic Contaminant Abatement in Reclaimed Water by UV/H2O2 and a Combined Process Consisting of O3/H2O2 Followed by UV/H2O2: Prediction of Abatement Efficiency, Energy Consumption, and Byproduct Formation. *Environ. Sci. Technol.* **2016**, *50*, 3809−3819.
(24) Wert, E. C.; Neemann, J. J.; Johnson, D.; Rexing, D.; Zegers, R. Pilot-scale and full-scale evaluation of the chlorine-ammonia process for bromate control during ozonation. *Ozone Sci. Eng.* **2007**, *29*, 363−372.
(25) Buffle, M. O.; Galli, S.; von Gunten, U. Enhanced bromate control during ozonation: The chlorine-ammonia process. *Environ. Sci. Technol.* **2004**, *38*, 5187−5195.
(26) Jones, D. B.; Saglam, A.; Triger, A.; Song, H.; Karan, T. I-THM Formation and Speciation : Preformed Monochloramine versus Prechlorination Followed by Ammonia Addition. *Environ. Sci. Technol.* **2011**, *45*, 10429−10437.
(27) Sharma, V. K.; Zboril, R.; Donald, T. J. M. C. Formation and toxicity of brominated disinfection byproducts during chlorination and chloramination of water : A review. *J. Environ. Sci. Heal.* **2014**, *49*, 212−228.
(28) von Gunten, U.; Oliveras, Y. Advanced oxidation of bromide-containing waters: Bromate formation mechanisms. *Environ. Sci. Technol.* **1998**, *32*, 63−70.
(29) Acero, J.; von Gunten, U. Characterization of Oxidation Processes: Ozonation and the AOP O3/H2O2. *J. Am. Water Works Assoc.* **2001**, *93*, 90−100.
(30) Hübner, U.; Zucker, I.; Jekel, M. Options and limitations of hydrogen peroxide addition to enhance radical formation during ozonation of secondary effluents. *J. Water Reuse Desalin* **2015**, *5*, 8−16.
(31) Tandukar, S.; Sherchan, S. P.; Haramoto, E. Applicability of crAssphage, pepper mild mottle virus, and tobacco mosaic virus as indicators of reduction of enteric viruses during wastewater treatment. *Sci. Rep.* **2020**, *10*, 3616.
(32) US EPA. *Method 1643: Male-specific (F+) and Somatic Coliphage in Recreational Waters and Wastewater by Ultrafiltration (UF) and Single Agar Layer (SAL) Procedure*; Office of Water, US EPA: 2018; pp 1−40.
(33) Buffle, M. O.; Schumacher, J.; Meylan, S.; Jekel, M.; Von Gunten, U. Ozonation and advanced oxidation of wastewater: Effect of O3 dose, pH, DOM and HO.-scavengers on ozone decomposition and HO. generation. *Ozone Sci. Eng.* **2006**, *28*, 247−259.
(34) Haag, W. R.; Hoigné, J. Ozonation of water containing chlorine or chloramines. Reaction products and kinetics. *Water Res.* **1983**, *17*, 1397−1402.
(35) Hübner, U.; Keller, S.; Jekel, M. Evaluation of the prediction of trace organic compound removal during ozonation of secondary effluents using tracer substances and second order rate kinetics. *Water Res.* **2013**, *47*, 6467−6474.
(36) Ishida, C.; Salveson, A.; Robinson, K.; Bowman, R.; Snyder, S. Ozone disinfection with the HiPOX reactor: Streamlining an 'old technology' for wastewater reuse. *Water Sci. Technol.* **2008**, *58*, 1765−1773.
(37) Morrison, C. M.; Hogard, S.; Pearce, R.; Gerrity, D.; von Gunten, U.; Wert, E. C. Ozone disinfection of waterborne pathogens and their surrogates: A critical review. *Water Res.* **2022**, *214*, No. 118206.
(38) Gerrity, D.; Gamage, S.; Jones, D.; Korshin, G. V.; Lee, Y.; Pisarenko, A.; Trenholm, R. A.; von Gunten, U.; Wert, E. C.; Snyder, S. A. Development of surrogate correlation models to predict trace organic contaminant oxidation and microbial inactivation during ozonation. *Water Res.* **2012**, *46*, 6257−6272.
(39) Young, S.; Torrey, J.; Bachmann, V.; Kohn, T. Relationship Between Inactivation and Genome Damage of Human Enteroviruses Upon Treatment by UV254, Free Chlorine, and Ozone. *Food Environ. Virol.* **2020**, *12*, 20−27.
(40) Pecson, B. M.; Ackermann, M.; Kohn, T. Framework for using quantitative PCR as a nonculture based method to estimate virus infectivity. *Environ. Sci. Technol.* **2011**, *45*, 2257−2263.
(41) Sobsey, M.; Battigelli, D.; Shin, G.-A.; Newland, S. RT-PCR amplification detects inactivated viruses in water and wastewater. *Water Sci. Technol.* **1998**, *38*, 91−94.
(42) Lanao, M.; Ormad, M. P.; Ibarz, C.; Miguel, N.; Ovelleiro, J. L. Bactericidal effectiveness of O3, O3/H 2O2 and O3/TiO2 on Clostridium perfringens. *Ozone Sci. Eng.* **2008**, *30*, 431−438.
(43) Hijnen, W. A. M.; Baars, E.; Bosklopper, T. G. J.; Van Der Veer, A. J.; Meijers, R. T.; Medema, G. J. Influence of DOC on the inactivation efficiency of ozonation assessed with Clostridium perfringens and a lab-scale continuous flow system. *Ozone Sci. Eng.* **2004**, *26*, 465−473.
(44) Driedger, A. M.; Staub, E.; Pinkernell, U.; Marinas, B.; Koster, W.; von Gunten, U. INACTIVATION OF BACILLUS SUBTILIS SPORES AND FORMATION OF BROMATE DURING OZONATION. *Water Res.* **2001**, *35*, 2950−2960.
(45) Buffle, M.-O.; Galli, S.; von Gunten, U. Enhanced Bromate Control during Ozonation: The Chlorine-Ammonia Process. *Environ. Sci. Technol.* **2004**, *38*, 5187−5195.
(46) Lim, S.; Barrios, B.; Minakata, D.; Von Gunten, U. Reactivity of Bromine Radical with Dissolved Organic Matter Moieties and Monochloramine: Effect on Bromate Formation during Ozonation. *Environ. Sci. Technol.* **2023**, DOI: 10.1021/acs.est.2c07694.
(47) Sein, M. M.; Golloch, A.; Schmidt, T. C.; Von Sonntag, C. No marked kinetic isotope effect in the peroxone (H2O 2/D2O2 + O3) reaction: Mechanistic consequences. *ChemPhysChem* **2007**, *8*, 2065−2067.
(48) von Gunten, U.; Oliveras, Y. Kinetics of the reaction between hydrogen peroxide and hypobromous acid: Implication on water treatment and natural systems. *Water Res.* **1997**, *31*, 900−906.
(49) Pocostales, J. P.; Sein, M. M.; Knolle, W.; Von Sonntag, C.; Schmidt, T. C. Degradation of ozone-refractory organic phosphates in wastewater by ozone and ozone/hydrogen peroxide (peroxone): The role of ozone consumption by dissolved organic matter. *Environ. Sci. Technol.* **2010**, *44*, 8248−8253.
(50) Rosenfeldt, E. J.; Linden, K. G.; Canonica, S.; von Gunten, U. Comparison of the efficiency of {radical dot}OH radical formation during ozonation and the advanced oxidation processes O3/H2O2 and UV/H2O2. *Water Res.* **2006**, *40*, 3695−3704.
(51) California Division of Drinking Water. *DPR Framework 2nd edition Addendum − Early Draft of Anticipated Criteria for Direct Potable Reuse*; 2021; Vol. 3, pp 1−40.
(52) Pistocchi, A.; Alygizakis, N. A.; Brack, W.; Boxall, A.; Cousins, I. T.; Drewes, J. E.; Finckh, S.; Gallé, T.; Launay, M. A.; McLachlan, M. S.; Petrovic, M.; Schulze, T.; Slobodnik, J.; Ternes, T.; Van Wezel, A.; Verlicchi, P.; Whalley, C. European scale assessment of the potential of ozonation and activated carbon treatment to reduce micropollutant emissions with wastewater. *Sci. Total Environ.* **2022**, *848*, 157124.
(53) Bourgin, M.; Borowska, E.; Helbing, J.; Hollender, J.; Kaiser, H. P.; Kienle, C.; McArdell, C. S.; Simon, E.; von Gunten, U. Effect of operational and water quality parameters on conventional ozonation and the advanced oxidation process O3/H2O2: Kinetics of micropollutant abatement, transformation product and bromate formation in a surface water. *Water Res.* **2017**, *122*, 234−245.
(54) Hu, C. Y.; Hou, Y. Z.; Lin, Y. L.; Deng, Y. G.; Hua, S. J.; Du, Y. F.; Chen, C. W.; Wu, C. H. Kinetics and model development of iohexol degradation during UV/H 2 O 2 and UV/S 2 O 82− oxidation. *Chemosphere* **2019**, *229*, 602−610.
(55) Lee, Y.; von Gunten, U. Quantitative structure-activity relationships (QSARs) for the transformation of organic micro-

https://doi.org/10.1021/acs.est.3c00802
Environ. Sci. Technol. XXXX, XXX, XXX−XXX

pollutants during oxidative water treatment. *Water Res.* **2012**, *46*, 6177−6195.
(56) Real, F. J.; Javier Benitez, F.; Acero, J. L.; Sagasti, J. J. P.; Casas, F. Kinetics of the chemical oxidation of the pharmaceuticals primidone, ketoprofen, and diatrizoate in ultrapure and natural waters. *Ind. Eng. Chem. Res.* **2009**, *48*, 3380−3388.
(57) Huber, M. M.; Göbel, A.; Joss, A.; Hermann, N.; Löffler, D.; McArdell, C. S.; Ried, A.; Siegrist, H.; Ternes, T. A.; Von Gunten, U. Oxidation of pharmaceuticals during ozonation of municipal wastewater effluents: A pilot study. *Environ. Sci. Technol.* **2005**, *39*, 4290−4299.

https://doi.org/10.1021/acs.est.3c00802
Environ. Sci. Technol. XXXX, XXX, XXX−XXX

Chapter 3 Supplementary Information
Optimizing ozone disinfection in water reuse: controlling bromate formation and enhancing organics oxidation

Samantha Hogard*[1,2], Robert Pearce[1,2], Raul Gonzalez[2], Kathleen Yetka[2], Charles Bott[2]

[1]Civil and Environmental Engineering Department, Virginia Polytechnic Institute and State University, Blacksburg, VA, USA 24060

[2]Hampton Roads Sanitation District, PO Box 5911, Virginia Beach, VA USA 23471

Keywords: Ozone, Water reuse, Disinfection, Bromate, 1,4-dioxane

Summary: 13 pages, 8 figures, 5 tables
*Corresponding author: shogard@vt.edu

SI- 2 Materials and Methods

Molecular methods

The *E. coli* culture was generated by HRSD's Central Environmental Lab several days prior to testing. E. coli K12 (ATCC 29425) was grown according to the propagation of bacteria stock cultures in EPA method 1642. Large volumes of high titer MS2 male specific and T1 somatic coliphage and bacterial spores were obtained from GAP EnviroMicrobial Services Ltd (London, ON). Due to the high titer spikes, range-finding was conducted to determine appropriate dilution levels. Sample volumes (1-10 L) were concentrated using dead-end ultrafiltration according to the methods previously described in a previous publication.[1] Elution from the ultrafilter was done using the FluidPrep High Volume Tris Elution Fluid (SKU HC08018-T; InnovaPrep, Drexel, MO, USA). The final elution volumes ranged between approximately 100-200 mL. Beef extract (BD-BBL Reference 212303) was added to each eluate at a concentration of 1.5 g/100 mL, then stirred for 10 minutes. The eluate was then centrifuged at 10,000 G for 10 minutes at 4°C. The supernatants were acidified to a pH of 3.5 with 20% HCl, then filtered through mixed cellulose ester filters (AAWP04700; Millipore, Billerica, MA, USA). Immediately after concentration, the filters and centrifuged pellets were stored in a -80°C freezer until total nucleic extraction using the KingFisher Apex System (Waltham, MA, USA) was completed. Details of nucleic acid extraction and inhibition controls have been described in a previous publication.[2]

Droplet digital PCR (ddPCR) was used to enumerate pepper mild mottle virus (PMMoV), general *Bacteroides* (GenBac), and crAssphage. Assay primers and probes used include hepatitis G Armored RNA and Salmon Sperm DNA assays. DNA (ddPCR) and RNA (RT-ddPCR) molecular assays were analyzed on a Bio-Rad QX200 (Bio-Rad, Hercules, CA, USA) according to protocols in Worley-Morse et al. (2019). Filter and associated pellet concentrations were summed.

SI- 3 Results and Discussion

3.1 Ozone and *OH Exposure

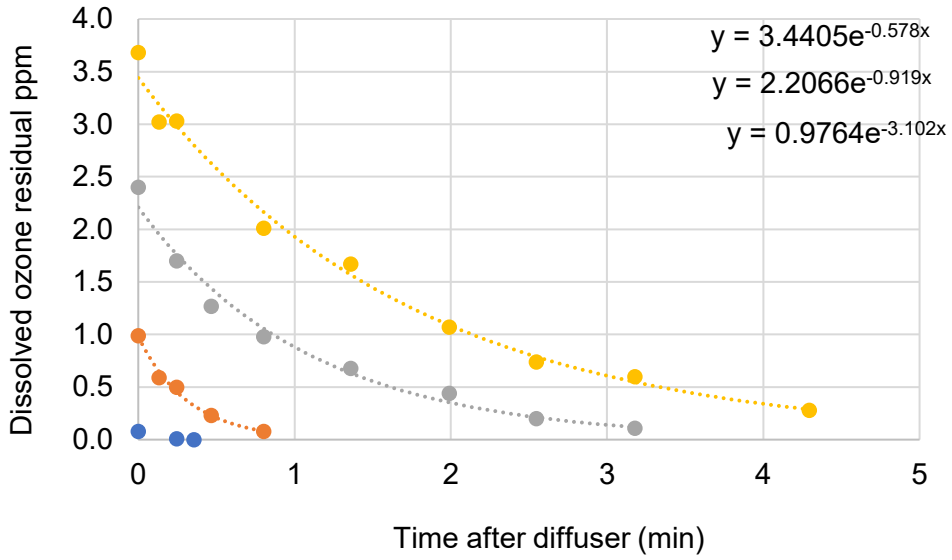

Figure SI-1 Ozone decay curves- Control test 1 (yellow = 1:1 O3:TOC, grey = 0.75 O3:TOC, orange = 0.5 O3:TOC, blue = 0.25 O3:TOC)

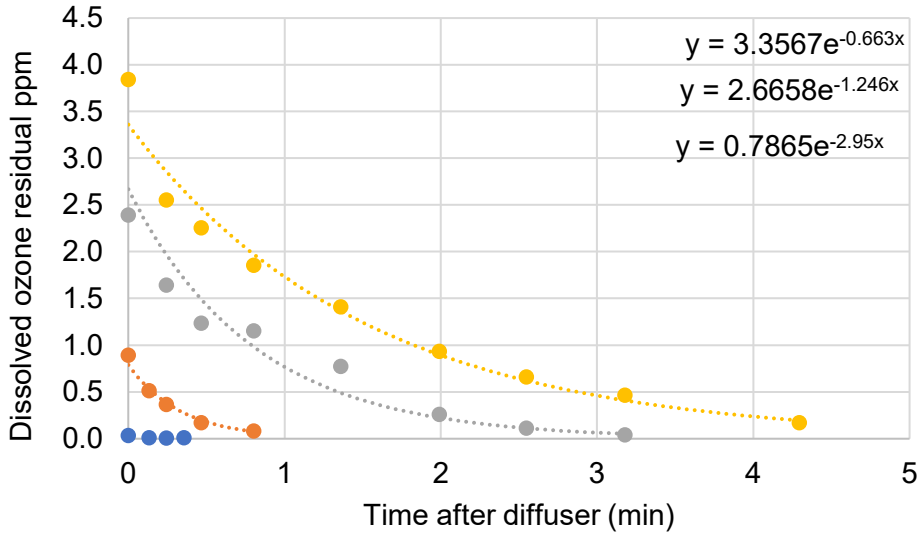

Figure SI-2 Ozone decay curves- Control test 2 (yellow = 1:1 O3:TOC, grey = 0.75 O3:TOC, orange = 0.5 O3:TOC, blue = 0.25 O3:TOC)

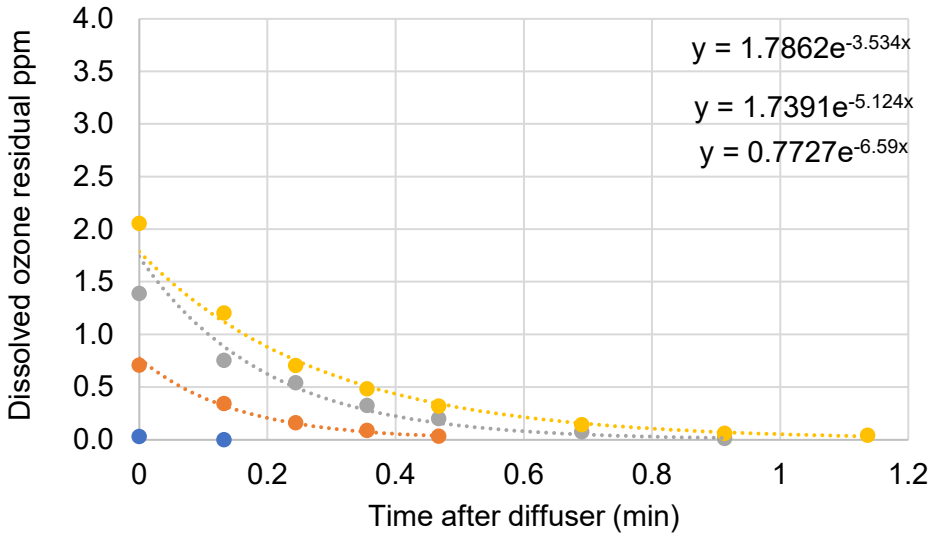

Figure SI-3 Ozone decay curves- Hydrogen peroxide test 1 (yellow = 1:1 O3:TOC, grey = 0.75 O3:TOC, orange = 0.5 O3:TOC, blue = 0.25 O3:TOC)

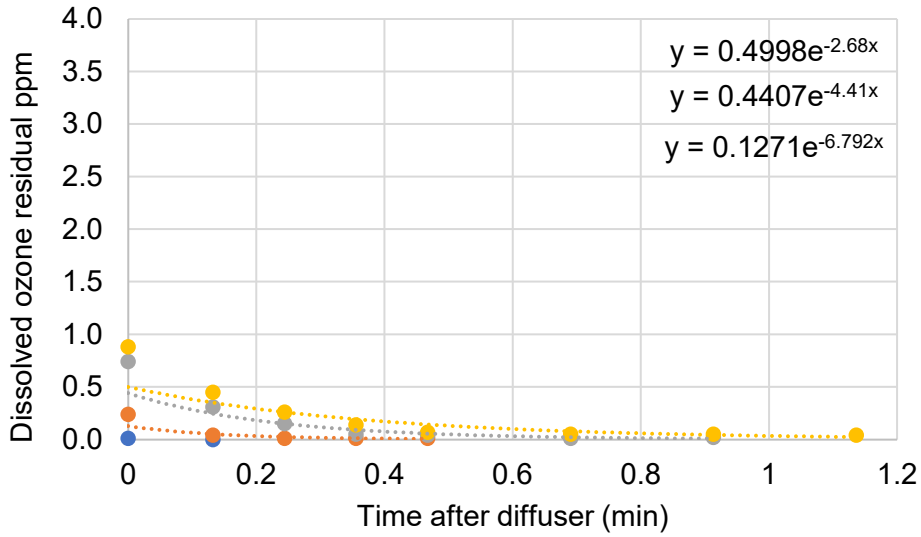

Figure SI-4 Ozone decay curves- Hydrogen peroxide test 2 (yellow = 1:1 O3:TOC, grey = 0.75 O3:TOC, orange = 0.5 O3:TOC, blue = 0.25 O3:TOC)

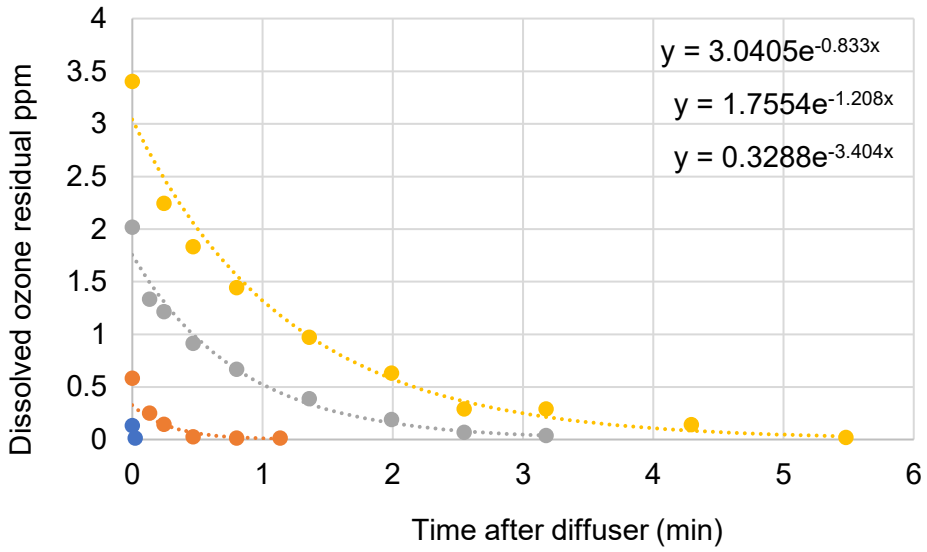

Figure SI-5 Ozone decay curves- Monochloramine test 1 (yellow = 1:1 O3:TOC, grey = 0.75 O3:TOC, orange = 0.5 O3:TOC, blue = 0.25 O3:TOC)

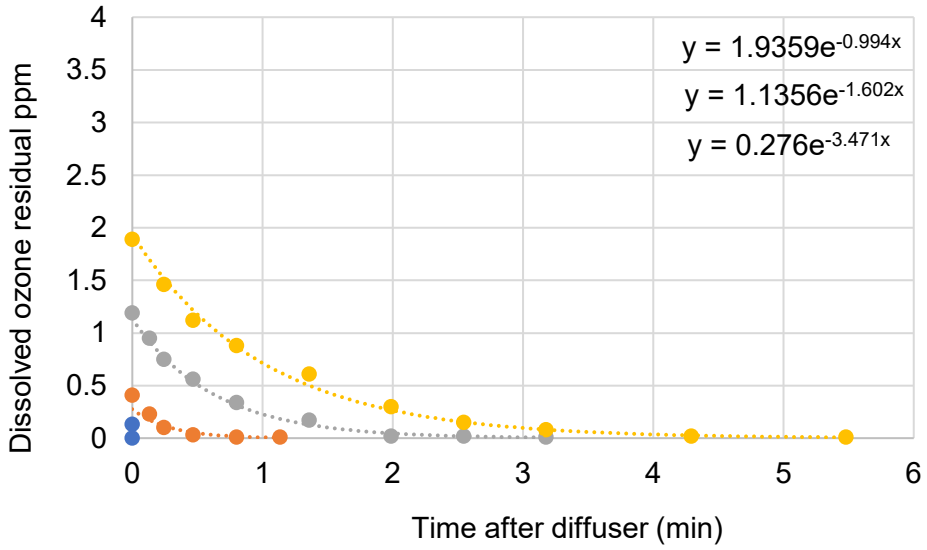

Figure SI-6 Ozone decay curves- Monochloramine test 2 (yellow = 1:1 O3:TOC, grey = 0.75 O3:TOC, orange = 0.5 O3:TOC, blue = 0.25 O3:TOC)

For the purpose of these experiments, hydroxyl radical exposure can be calculated using the equation below using the second order reaction rate constant of the ozone-resistant compound 1,4-dioxane.[3]

Equation 1. $\int * OH = \frac{-\ln(C/C_0)}{k\ (1,4d,*OH)}$

Table SI-1 Ozone decay characteristics for test 1

O3:TOC	Applied ozone dose (mg/L)	C_0	IOD % of applied ozone dose	k (min^{-1})	Max single pt. CT (mg/L-min)	Total integrated ozone exposure (mg/L-min)
Control test 1						
0.25	2.39	-	-	-	0.002	0.003
0.5	4.66	0.976	79%	3.1	0.12	0.33
0.75	6.93	2.21	68%	0.92	0.92	2.47
1	9.08	3.44	62%	0.58	2.27	5.49
Hydrogen peroxide test 1						
0.25	2.49	-	-	-	0	0
0.5	4.68	0.77	84%	6.59	0.04	0.21
0.75	6.88	1.74	75%	5.12	0.13	0.50
1	9.07	1.79	80%	3.53	0.17	0.94
Monochloramine test 1						
0.25	2.81	-	-	-	0.002	0.003
0.5	5.26	0.33	94%	3.40	0.035	0.11
0.75	7.70	1.76	77%	1.21	0.53	1.45
1	10.14	3.04	70%	0.83	1.32	3.55

Table SI-2 Ozone decay characteristics for test 2

O3:TOC	Applied ozone dose (mg/L)	C_0	IOD % of applied ozone dose	k (min^{-1})	Max single pt. CT (mg/L-min)	Total integrated ozone exposure (mg/L-min)
Control test 2						
0.25	2.08	-	-	-	0.003	0.006
0.5	4.05	0.79	80%	2.95	0.08	0.28
0.75	6.02	2.67	56%	1.25	1.05	2.29
1	8.00	3.36	58%	0.66	1.92	4.80
Hydrogen peroxide test 2						
0.25	2.29	-	-	-	0	0
0.5	4.52	0.13	97%	6.79	0.005	0.05
0.75	6.76	0.44	93%	4.41	0.04	0.19
1	8.99	0.50	94%	2.68	0.06	0.29
Monochloramine test 2						
0.25	2.45	-	-	-	0	0
0.5	4.73	0.28	94%	3.47	0.03	0.09
0.75	7.06	1.14	84%	1.60	0.27	0.77
1	9.49	1.94	80%	0.99	0.83	2.03

Table SI-3 *OH exposure (M*s) calculated using 1,4-dioxane removal

		Control	H2O2	NH2Cl	% change H2O2	% change NH2Cl
Test 1 - ln(C/C0)/k	0.25	7.09E-11	3.61E-11	3.64E-11	-49%	-49%
	0.5	1.39E-10	1.48E-10	6.31E-11	7%	-55%
	0.75	2.10E-10	2.58E-10	1.59E-10	22%	-24%
	1	2.85E-10	4.54E-10	1.08E-10	59%	-62%
Replicate - ln(C/C0)/k	0.25	5.99E-11	7.02E-11	4.03E-11	17%	-33%
	0.5	1.39E-10	1.95E-10	1.03E-10	40%	-26%
	0.75	2.62E-10	3.01E-10	1.15E-10	15%	-56%
	1	3.23E-10	3.97E-10	2.11E-10	23%	-35%
average OH exposure	0.25	6.54E-11	5.31E-11	3.84E-11	-19%	-41%
	0.5	1.39E-10	1.72E-10	8.30E-11	23%	-40%
	0.75	2.36E-10	2.79E-10	1.37E-10	18%	-42%
	1	3.04E-10	4.25E-10	1.59E-10	40%	-48%

3.2.2 Molecular Markers

a.

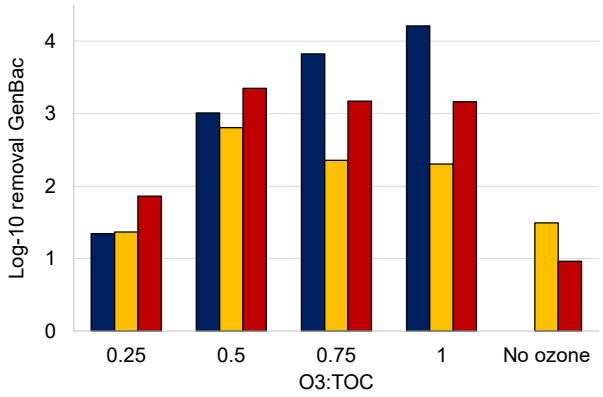

b.

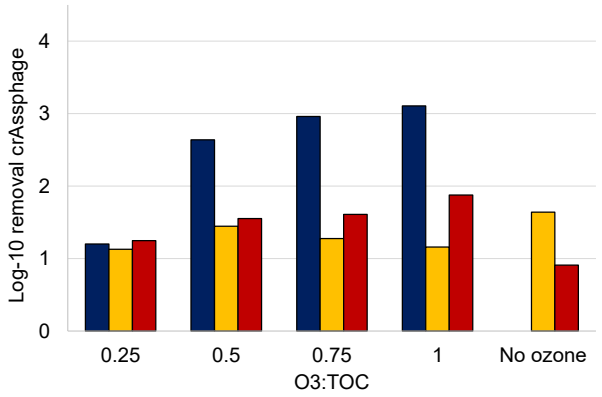

c.

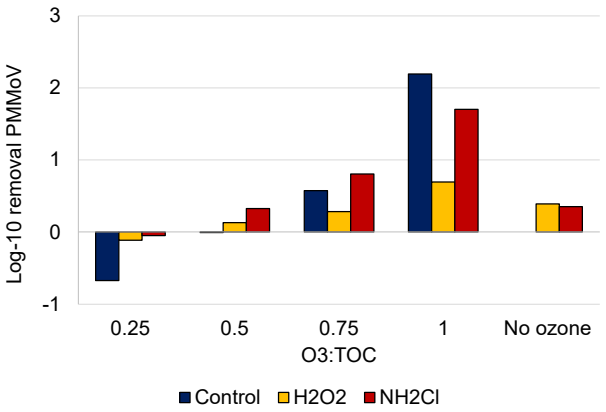

Figure SI-7. Molecular marker removal by ozone for each bromate control method a. GenBac b. crAssphage and c. PMMoV

Table SI-4 Molecular sample volume and internal standard recovery

Sample ID	Sample Volume (L)	Sketa % recovery	HepG % recovery
Control			
Influent 1 (Ctrl)	1	105.55%	21.23%
Influent 2(Ctrl)	1	95.91%	23.49%
Influent 1 pellet (Ctrl)	N/A	48.59%	0.28%
Influent 2 pellet (Ctrl)	N/A	30.94%	0.05%
Ozone 1	10	183.80%	10.68%
Ozone 2	10	70.43%	2.57%
Ozone 3	10	77.34%	0.92%
Ozone 4	10	58.33%	0.72%
Ozone 1- pellet	N/A	0.35%	0.00%
Ozone 2- pellet	N/A	0.20%	0.00%
Ozone 3- pellet	N/A	0.66%	0.00%
Ozone 4- pellet	N/A	0.56%	0.59%
H_2O_2			
Influent 1 (H2O2)	1	96.15%	75.00%
Influent 2(H2O2)	1	89.10%	55.00%

Influent 1 pellet (H2O2)	N/A	75.00%	21.67%
Influent 2 pellet (H2O2)	N/A	63.14%	37.50%
Ozone 5	10	75.64%	11.67%
Ozone 6	10	74.36%	54.17%
Ozone 7	10	75.64%	21.67%
Ozone 8	10	78.85%	11.67%
Ozone 5- pellet	N/A	0.35%	0.00%
Ozone 6- pellet	N/A	4.04%	0.00%
Ozone 7- pellet	N/A	0.96%	0.00%
Ozone 8- pellet	N/A	5.26%	5.00%
NH_2Cl			
Influent 1 (NH2Cl)	1	83.98%	13.32%
Influent 2 (NH2Cl)	1	60.94%	9.75%
Influent 1 pellet (NH2Cl)	N/A	20.70%	2.02%
Influent 2 pellet (NH2Cl)	N/A	28.38%	3.65%
Ozone 9	10	46.89%	3.69%
Ozone 10	10	15.65%	0.62%
Ozone 11	10	30.50%	0.00%
Ozone 12	10	31.38%	0.00%
Ozone 9- pellet	N/A	2.63%	0.00%
Ozone 10- pellet	N/A	2.27%	0.00%
Ozone 11- pellet	N/A	1.32%	0.02%
Ozone 12- pellet	N/A	0.94%	0.00%

3.3 NDMA

The formation of NDMA increased with increasing O3:TOC ratio for every condition, with the exception of a minor decrease at the highest ozone dose (Figure 8c). The plateau of NDMA formed around 0.5 O3:TOC is likely a result of the NDMA formation potential being reached at this ozone dose.[4] The addition of monochloramine resulted in a minor increase in NDMA formation at 0.75-1 O3:TOC. This may be a result of monochloramine scavenging *OH and thus preventing

the direct oxidation of NDMA by *OH ($k = 4.5*10^8$ $M^{-1}s^{-1}$).[4–6] This would however depend on the precursors present and how rapidly they form NDMA upon ozonation considering that *OH exposure is greatest during the initial phase of ozonation.[7] Monochloramine may also contribute to NDMA formation directly by reactions with monochloramine-reactive precursors[8,9], however some of these precursors can be oxidized by ozone.[10] This complex interplay between precursors and oxidants prevents the authors from determining a certain cause of this elevated NDMA formation. Previous ozone pilot testing data collected on the same source water showed no difference in NDMA formation with the addition of monochloramine[11] while monitoring data collected post ozonation at the 1-MGD scale on the same source water showed that monochloramine increased NDMA formation only at lower ozone doses.[12] The elevated NDMA formation in this case may simply be due to variations in NDMA precursor concentrations on a given day. In this study, the addition of hydrogen peroxide resulted in a decrease in NDMA formation for every ozone dose tested, most likely as a result of the limited ozone exposure. It may also be a result of *OH directly oxidizing NDMA resulting in overall lower concentration. This highlights another potential benefit of using hydrogen peroxide for bromate control. NDMA formation is however completely dependent on the water matrix and the precursors that are present, therefore conclusions presented herein may not be relevant for every source water.

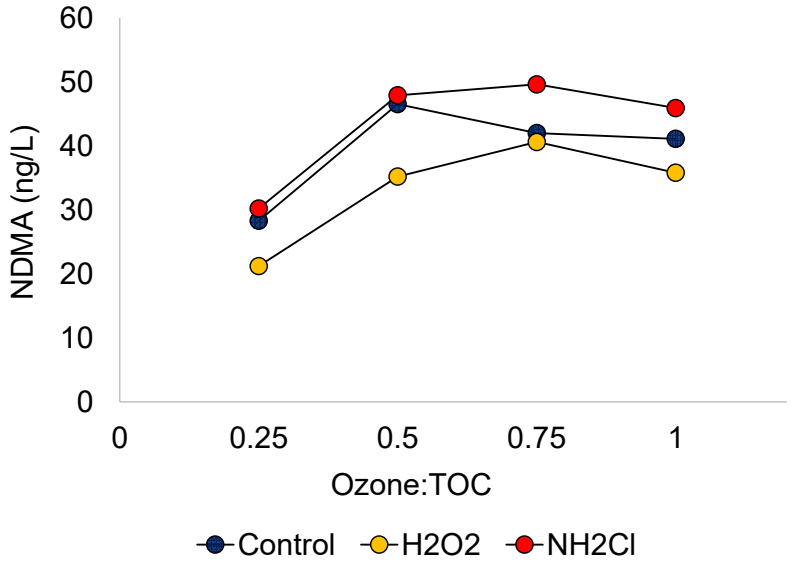

Figure SI-8 NDMA formation by ozone for each bromate control condition

3.4 Trace Organic Contaminants

Table SI- 5 TrOC Concentration

MDL (ng/L)	CEC	Concentration (ng/L)						
		Influent avg	Low	High	Low-H2O2	High-H2O2	Low NH2Cl	High NH2Cl
400	4-nonylphenol - semi quantitative	565	ND	ND	ND	ND	ND	ND
25	4-tert-Octylphenol	64	44	ND	42	ND	28	28
5	Diclofenac	590	7.1	ND	18	ND	9.1	ND
5	Gemfibrozil	64	12	ND	15	ND	10	ND

20	Acesulfame-K	64.5	35	ND	47	ND	ND	ND
100	Sucralose	63500	62000	40000	55000	33000	60000	48000
20	Iohexol	25000	21000	11000	19000	8000	21000	14000
10	Butalbital	49	ND	ND	10	ND	ND	ND
5	Methadone	180	92	ND	83	ND	100	ND
10	TCEP	105	110	100	100	90	100	100
10	Hydrocodone	17	ND	ND	ND	ND	ND	ND
5	Primidone	115	75	27	80	17	91	58
5	Sulfamerazine	75	ND	ND	5.1	ND	ND	ND
5	Propranolol	235	17	ND	27	ND	18	ND
200	TCPP	770	760	1100	ND	380	740	940
100	TDCPP	350	410	480	ND	180	300	390
5	Lidocaine	975	110	ND	180	ND	60	ND
5	Thiabendazole	15	9.3	ND	7.2	ND	13	ND
5	Albuterol	18.5	ND	ND	ND	ND	ND	ND
5	Atrazine	5.3	ND	ND	ND	ND	ND	ND
5	Ketoprofen	5.5	ND	ND	ND	ND	ND	ND
20	Amoxicillin (semi-quantitative)	1150	ND	ND	44	ND	ND	ND
5	Atenolol	445	210	ND	230	19	270	ND
5	Carbamazepine	240	7.6	ND	16	ND	ND	ND
5	Bromacil	11	ND	ND	ND	ND	ND	ND
5	Diuron	37	23	ND	13	ND	32	9.2
5	Linuron	13.5	9.4	ND	ND	ND	10	ND
20	Isoproturon	56.5	44	ND	59	ND	64	26
5	Bezafibrate	9.9	ND	ND	ND	ND	ND	ND
5	Diltiazem	475	14	ND	32	ND	8.3	ND
10	Cotinine	34.5	34	33	38	28	38	36
5	Metolachlor	20.5	13	ND	ND	ND	13	6.3
20	Lopressor	975	460	ND	570	31	600	ND
5	Cimetidine	195	5.7	ND	6.8	ND	6.4	ND
10	Fluoxetine	230	200	ND	140	ND	170	21
20	Dilantin	45.5	31	ND	32	ND	46	20
5	Meprobamate	60	44	22	46	23	61	39
10	Caffeine	160	43	ND	14	21	37	90
10	Theophylline (semi-quantitative)	60	22	ND	43	12	17	39
5	1,7-Dimethylxanthine	31	9.3	ND	16	5.4	5.7	15
5	Dehydronifedipine	16	8.5	9.1	5.9	6.7	9.5	9

5	Sulfadiazine	37.5	ND	ND	ND	ND	ND	ND
5	Sulfamethoxazole	715	130	7.7	160	5.4	140	ND
5	Trimethoprim	285	10	ND	26	ND	8.4	ND
5	Ketorolac	22.5	ND	ND	ND	ND	ND	ND
10	Codeine	41.5	ND	ND	ND	ND	ND	ND
5	Carisoprodol	11.15	8.3	ND	7.1	ND	12	7.3
50	Theobromine	215	120	ND	110	ND	84	81
10	Venlafaxine	575	350	ND	440	ND	460	ND
10	1H-Benzotriazole	520	380	84	370	50	420	130

References

1. Vaidya, R., Buehlmann, P. H., Salazar-Benites, G., Schimmoller, L., Nading, T., Wilson, C. A., Bott, C., Gonzalez, R. & Novak, J. T. Pilot Plant Performance Comparing Carbon-Based and Membrane-Based Potable Reuse Schemes. *Environ. Eng. Sci.* **36**, 1369–1378 (2019).

2. Worley-Morse, T., Mann, M., Khunjar, W., Olabode, L. & Gonzalez, R. Evaluating the fate of bacterial indicators, viral indicators, and viruses in water resource recovery facilities. *Water Environ. Res.* **91**, 830–842 (2019).

3. Hübner, U., Keller, S. & Jekel, M. Evaluation of the prediction of trace organic compound removal during ozonation of secondary effluents using tracer substances and second order rate kinetics. *Water Res.* **47**, 6467–6474 (2013).

4. Marti, E. J., Pisarenko, A. N., Peller, J. R. & Dickenson, E. R. V. N-nitrosodimethylamine (NDMA) formation from the ozonation of model compounds. *Water Res.* **72**, 262–270 (2015).

5. Liao, X., Shen, L., Jiang, Z., Gao, M., Qiu, Y., Qi, H. & Chen, C. NDMA formation during ozonation of metformin: Roles of ozone and hydroxyl radicals. *Sci. Total Environ.* **796**, (2021).

6. Lee, C., Yoon, J. & Von Gunten, U. Oxidative degradation of N-nitrosodimethylamine by conventional ozonation and the advanced oxidation process ozone/hydrogen peroxide. *Water Res.* **41**, 581–590 (2007).

7. Elovitz, M. S. & von Gunten, U. Hydroxyl radical/ozone ratios during ozonation processes. I. The R(ct) concept. *Ozone Sci. Eng.* **21**, 239–260 (1999).

8. Sgroi, M., Vagliasindi, F. G. A., Snyder, S. A. & Roccaro, P. N-Nitrosodimethylamine (NDMA) and its precursors in water and wastewater: A review on formation and removal. *Chemosphere* **191**, 685–703 (2018).

9. Mitch, W. A. & Schreiber, I. M. Degradation of tertiary alkylamines during chlorination/chloramination: implications for formation of aldehydes, nitriles, halonitroalkanes, and nitrosamines. *Environ. Sci. Technol.* **42**, 4811–4817 (2008).

10. Lee, C., Schmidt, C., Yoon, J. & von Gunten, U. Oxidation of N-nitrosodimethylamine (NDMA) precursors with ozone and chlorine dioxide: Kinetics and effect on NDMA formation potential. *Environ. Sci. Technol.* **41**, 2056–2063 (2007).

11. Pearce, R., Hogard, S., Buehlmann, P., Salazar-benites, G., Wilson, C. & Bott, C. Evaluation of preformed monochloramine for bromate control in ozonation for potable reuse. *Water Res.* **211**, 118049 (2022).

12. Hogard, S., Salazar-Benites, G., Pearce, R., Nading, T., Schimmoller, L., Wilson, C., Heisig-Mitchell, J. & Bott, C. Demonstration-scale evaluation of ozone–biofiltration–granular activated carbon advanced water treatment for managed aquifer recharge. *Water Environ. Res.* 1–16 (2021) doi:10.1002/wer.1525.

Chapter 4 Virus inactivation in low ozone exposure water reuse applications

Samantha Hogard[1,2], Robert Pearce[1,2], Kathleen Yetka[2], Raul Gonzalez[2], Charles Bott[2]

[1]Civil and Environmental Engineering Department, Virginia Polytechnic Institute and State University, Blacksburg, VA, USA

[2]Hampton Roads Sanitation District, PO Box 5911, Virginia Beach, VA 23471-0911

Under review in Water Research

Abstract

The use of ozone in wastewater and water reuse applications has risen in recent years as it has emerged as a cost-effective treatment barrier for trace organic contaminants and pathogens. In drinking water applications, an ozone exposure (Ct) based framework has been historically used to validate ozone disinfection. However, significant viral inactivation can be achieved with little to no measurable ozone exposure. Additionally, ozone exposure can vary depending on multiple water quality variables as well as the calculation/ozone measurement method used. In this study, we evaluated alternative ozone monitoring frameworks as well as the impact of water quality variables on ozone decay kinetics and virus/coliform inactivation. Here we show that both change in UV_{254} absorbance and applied O_3:TOC frameworks are resilient to changes in water quality. Both temperature and pH significantly impact the ozone decay rate and resulting ozone exposure, however, due to the increased reaction rate of ozone with viruses at elevated temperature and pH, there was only a minor impact in overall disinfection performance for a given O_3:TOC. These frameworks were also considered for variable source water with TOC (5-11 mg/L) and TSS (1.2-5.8 mg/L). Change in UV_{254} absorbance or applied ozone dose (mg/L) were the strongest indicators of disinfection performance for source waters of variable TOC, however site-specific testing may be needed to apply this framework. Challenge testing with influent nitrite also indicated the importance of accounting for this value in the applied ozone dose. Multi-point ozone dissolution was investigated as an alternative ozone application method that may present a benefit with respect to overall disinfection performance especially if nitrite was present.

Developing alternative monitoring frameworks and ozone application methods is imperative in water reuse applications where elevated ozone exposure may lead to harmful byproduct formation.

1. Introduction

Ozone has been applied for water and wastewater disinfection for decades, and more recently for water reuse applications. Ozone is very efficient at inactivating viruses, coliform bacteria, and protozoa with relatively high reaction rates on the order of 10^5-10^6, 10^5, and 10^2-10^4 $M^{-1}*s^{-1}$ respectively (Hunt & Marinas, 1997; Rennecker et al., 1999; von Gunten, 2003; Wolf et al., 2018). More recent studies have shown similar efficacy during wastewater ozonation even in the presence of other ozone demanding constituents (Burns et al., 2007; Gerrity et al., 2012; Hogard et al., 2023; Wolf et al., 2019). Current drinking water treatment guidelines in the United States use ozone exposure (dissolved ozone concentration*time, i.e. Ct) to quantify disinfection performance (US EPA, 1991). While maintaining ozone Ct is important for the inactivation of microorganisms that are resistant to disinfection, it has been shown that significant virus and bacteria inactivation can be achieved with low to no measurable Ct (Gamage et al., 2013; Gerrity et al., 2012; Hogard et al., 2023; Wolf et al., 2018). Therefore, the use of this framework for viral inactivation can result in unnecessarily high applied ozone doses for disinfection and thus the formation of disinfection byproducts (DBPs) such as bromate. This is especially true in wastewater where the concentration of DBP precursors is elevated.

A recent review compiled decades of ozone disinfection research and highlighted how conservative the Ct framework is for viruses specifically (Morrison et al., 2022). This review also underscored the difficulty associated with comparing data across ozonation studies due to the complexity of ozone systems, and inconsistencies in experimental descriptions, data reporting, and Ct calculation methods. The EPA's Surface Water Treatment Rule (SWTR) and Long Term 2 Enhanced SWTR (LT2ESWTR) define several ways to calculate ozone Ct for various reactor

configurations (US EPA, 1991; US EPA, 2006). Ozone is typically added via fine bubble diffusion (FBD) or sidestream injection (SSI). In FBD, 1-log virus credit is given for the diffusion zone if a dissolved ozone residual of >0.1 mg/L is maintained at the effluent of the dissolution zone. In the reaction chambers, Ct can be calculated using the contact time at which 10% of the water has passed through (t_{10}), or a baffle factor can be multiplied by the hydraulic detention time. Greater Ct credit can be achieved using extended calculation methods with multiple dissolved ozone residual monitoring points (Rakness et al., 2005). In bench or pilot-scale experimental conditions, greater resolution on the ozone decay curve allows for more accurate calculation of ozone exposure.

In wastewater ozonation applications, it is normally more challenging to maintain a measurable ozone residual due to rapid ozone decay primarily as a result of elevated dissolved organic matter (DOM) concentrations (M. O. Buffle et al., 2006). Higher temperatures, variable pH, and residual nitrite in wastewater can also contribute to increased ozone decay and demand. Additionally, it is often desirable to limit ozone exposure to limit DBP formation. For instance, hydrogen peroxide can be used to accelerate the ozone decay rate thereby limiting formation of the DBP bromate (Hübner et al., 2015). Higher temperatures also result in accelerated ozone decay rates and thus lower Ct for a given applied ozone dose. The impact of temperature on the reaction rate of enteric viruses with ozone was determined by a previous study (Wolf et al., 2018). It was shown that increasing temperature by 10 ºC results in 1.2-1.4x increase in reaction rate constant for MS2, resulting in an activation energy of 22 kJ/mol (Wolf et al., 2018). The resulting overall impact of these two conflicting principles on ozone disinfection performance in wastewater has not been determined. Another variable that significantly influences ozone decay kinetics is pH. In drinking water, lower pH results in stabilized ozone decay as a result of lower hydroxide ion (OH^-) concentrations which act as important initiators in ozone decomposition chain reactions (Staehelin

& Holgné, 1982). In wastewater, pH also governs ozone decay but this can also be a result of the deprotonation of organic compounds at higher pH resulting in greater reactivity (M.-O. Buffle et al., 2006). There have been several studies aimed at investigating the impact of pH on ozone disinfection with conflicting results reported for different organisms (Cho et al., 2002; Jamil et al., 2017). The study performed by Wolf et al. (2018) determined that increasing pH results in a 1.4-2x greater MS2 reaction rate constant with ozone. Therefore, similar to other variables discussed, the overall impact of pH on ozone disinfection is not well known. The source water pH also influences the rate of reaction of ozone and H_2O_2. In ambient source water pH, H_2O_2 alone has been shown to have negligible impact on virus inactivation by ozone (Gamage et al., 2013; Hogard et al., 2023), however this might vary at different pH values. Using ozone post wastewater treatment also introduces the risk of having residual nitrite as a result of incomplete nitrification/denitrification. Nitrite reacts rapidly and thus stoichiometrically with ozone with a demand of 3.43 mg/L O_3/mg/L-N. Therefore, residual NO_2 may necessitate higher ozone doses to meet Ct requirements, but the actual impact on disinfection is unknown. Finally, the ozone application method (e.g. single vs. multiple diffusion zones) can impact the ozone exposure and how it is measured. However, the difference in ozone disinfection performance for various methods of ozone application is not well documented.

Ozone exposure is sensitive to many water quality constituents, design parameters, and the calculation method selected. In order to more accurately validate ozone disinfection, it is important to evaluate frameworks that do not rely on ozone exposure. This topic has been the subject of several previous studies over a narrow range of water quality conditions (Gamage et al., 2013; Gerrity et al., 2012; Wolf et al., 2019). The objective of this study was to investigate the impact of water quality parameters such as temperature, pH, total organic carbon (TOC), total suspended solids (TSS), and nitrite concentration on ozone disinfection in order to determine the most suitable alternative monitoring framework that can be used across a range of low ozone exposure

conditions. Applied specific ozone dose (O_3:TOC), and the change in UV_{254} absorbance will be considered for validation of ozone disinfection at pilot scale.

2. Materials and Methods

2.1 Ozone Pilot Testing Description

The ozone pilot setup used for the purpose of this study is described in detail elsewhere (Hogard et al., 2023; Pearce et al., 2022). Briefly, the continuous flow pilot operates with a flow rate of 3.78 Lpm (1 gal/min). The source water for the majority of experiments described herein was unfiltered secondary clarifier effluent (SCE) from HRSD's Nansemond Treatment Plant located in Suffolk, Virginia (Plant A). Experiments described in section 3.3 used source water from tertiary denitrification filter effluent (DNE) from HRSD's York River Treatment Plant (Plant B). For these tests, water was collected in a tanker truck and delivered to the pilot location. Additionally, these source waters were ozonated with and without upstream coagulation/flocculation/sedimentation (floc/sed) as shown in Figure 1. The floc/sed pilot consisted a 1 minute rapid mix basin, followed by tapered three-stage flocculation. Aluminum chlorohydrate coagulant and a cationic flocculation-aid polymer were added at doses of 15 mg/L and 1 mg/L as product respectively to the rapid mix basin. Finally, the sedimentation basin utilized plate settlers with a loading rate of 0.15 m/h. Experiments in sections 3.1-3.4 were performed in FBD configuration with the first column being the counter-flow diffusion zone, and the remaining columns serving as the reaction chamber. Additional testing (Section 3.5) was performed with the ozone dose split between multiple diffusion zones, using the "optional" ozone gas lines as shown in Figure 1. The source water temperature was controlled using a recirculating chiller unit and a heater on the pilot feed tank. All chemicals were added continuously via Masterflex peristaltic pumps upstream of ozonation. In order to modify the source water pH, 1% H_2SO_4 and 1% NaOH were added at flow rates of approximately 1-10 mL/min. Additionally, diluted reagent grade H_2O_2 was used for experiments examining the impact of H_2O_2 on ozone disinfection at various pH levels. To simulate

nitrite spikes, 1.5% $NaNO_2$ was added upstream of ozone at various doses. A summary of the variables evaluated in this study are shown in Table 1.

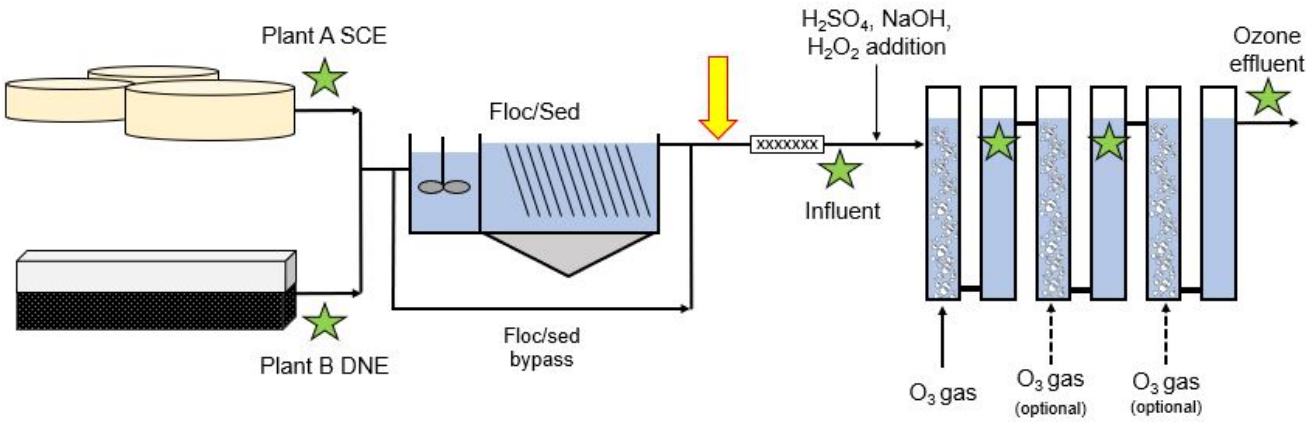

Figure 1. Ozone pilot diagram. Yellow arrow indicates location of coliphage and *E. coli* addition and green stars indicate sampling locations.

Table 1. Summary of variables evaluated

Parameter	Value	Units
Temperature	12-30	ºC
pH	5.5-8.4	
TOC	5-11	mg/L
TSS	1.2-5.8	mg/L
NO_2	0.6-1	mg/L-N

2.2 Analytical Methods

Field parameters such as pH, temperature, and UV_{254} absorbance were measured in grab samples throughout the duration of testing. A Thermo Scientific pH probe was used to verify pH on ozone influent samples. Temperature was verified on grab samples using a HANNA Instruments thermometer. UV_{254} 254 absorbance was measured on 0.45 micron filtered influent and ozone effluent samples using a Thermo Scientific Genesys 150 UV-Vis Spectrophotometer. Dissolved ozone residual was measured according to Standard Method 4500 Indigo colorimetric method. When reported, the total integrated ozone exposure was calculated by adding the area under the dissolved ozone concentration vs time curve. This includes both the ozone exposure in

the bubble column diffusion zone and the contact chamber (after ozone degas). “Credited” ozone exposure is calculated by subtracting the ozone exposure in the bubble column from the total ozone exposure. Single point Ct values were found by multiplying the ozone exposure by the residence time. Samples for water quality parameters including alkalinity, TOC, and total suspended solids (TSS) were analyzed by HRSD’s Central Environmental Laboratory. TOC was analyzed according to Standard Method 5310 using a Shimadzu TOC 4200. TSS was analyzed according to EPA Method 160.2.

2.3 Culture Information

Male specific coliphage, MS2 (single stranded RNA virus), and somatic coliphage, T1UV (double stranded DNA virus), were used as viral surrogates and *E. coli* was used as a bacterial surrogate. The MS2 and T1UV coliphage stock were purchased from GAP EnviroMicrobial Services Ltd (London, ON) and the *E. coli* stock was prepared at the HRSD Central Environmental Laboratory. Detailed information on the cultures used is provided in a previous publication (Hogard et al., 2023). The stock solution of each culture was diluted with phosphate buffer solution to the desired concentration and then added continuously to the influent water via Masterflex peristaltic pump. Each addition point was followed by an in-line static mixer. Throughout each test, duplicate influent grab samples were collected to ensure consistent feed was maintained during the experiment. The target influent coliphage and *E. coli* concentrations were approximately 10^6-10^7 PFU/100 mL, and 10^5-10^6 CFU/100 mL respectively. Male-specific and somatic coliphages were quantified using the single agar layer procedure on undiluted or diluted samples according to EPA method 1643 (US EPA, 2018). *E. coli* and total coliform were assayed using the 24-hour IDEXX Colilert-18 method.

2.4 Statistical Analysis

All statistical analysis and quantitative figures were produced using R software (R Core Team, 2021).

3. Results and Discussion

3.1 Temperature

While wastewater temperatures vary depending on geographic region, historical secondary effluent temperatures at Plant A range from 13.8-29.4 ºC (average 22.1 ± 4.2 ºC), therefore water temperatures of 12-30 ºC were investigated. As expected, temperature was shown to have a significant impact on ozone decay rate (Figure 2). The observed ozone decay rate at a specific ozone dose of 1.0 O_3:TOC increased from 0.6 to 5.2 min^{-1}, resulting in greater than seven-fold decrease in the integrated ozone exposure when temperature increased from 12 to 30 ºC. This has a significant impact on ozone process monitoring when using a Ct based framework, where varying temperatures would require different Ct values and as a result, different applied ozone doses. Additionally, higher temperatures result in lower ozone gas solubility in water and thus lower transfer efficiency (transfer efficiency was not measured in this study). As shown in Figure 2, at an applied O_3:TOC of 1, the initial C/C_0 value decreases from >0.3 for 12 ºC to <0.1 at 30 ºC. Figure 3 provides the resulting correlations (with 95% confidence intervals shaded) of virus log-removal values (LRV) with change in (a) UV_{254} absorbance and (b) O_3:TOC. Figure 3b shows that for a given specific ozone dose, marginally worse disinfection performance was achieved at warmer temperatures. This result is more apparent at lower ozone doses (0.25-0.5 O_3:TOC) where the maximum disinfection has not yet been achieved. At 0.75-1 O_3:TOC, the regression lines for each temperature condition begin to converge and the spread in data is less pronounced. A previous study showed that increasing temperature by 10 ºC increased the rate of reaction of ozone with MS2 by a factor of 1.2-1.4 depending on pH (Wolf et al., 2018). This result is conservatively reflected in the assumptions of the EPA Ct model where the required ozone exposure for a certain LRV doubles for a 10 ºC decrease in temperature. This somewhat weak relationship with temperature, combined with the rapid ozone decay and potentially lower transferred ozone dose at high temperatures, results in lower disinfection performance for a given

ozone dose. However, it is notable that the minor decreased disinfection efficacy is not proportional to the decrease in measured ozone exposure. Figure 3a shows that as a result of lower ozone exposure, there is also less change in UV_{254} absorbance at higher temperatures. The R^2 for these relationships are 0.69, 0.69, 0.43 for 12, 20, and 30 ºC respectively ($p<0.05$). The R^2 for the entire data set combined is 0.6, indicating that there is a strong correlation for these data across all temperatures tested. Therefore, the change in UV_{254} absorbance is a more suitable surrogate measure of ozone disinfection performance across a wide range of temperatures.

Table 2 Average ozone decay characteristics for temperature ranging 12-30 ºC

Temp (C)	O3:TOC	Average Decay Rate k (min^{-1})	Int. Ozone Exposure (mg/L-min)
12	0.25	-*	0.06
	0.5	3.24	0.51
	0.75	1.04	2.58
	1	0.62	6.26
20	0.25	-*	0.04
	0.5	7.57	0.33
	0.75	2.29	1.38
	1	1.15	3.34
30	0.25	-*	0.05
	0.5	-*	0.13
	0.75	10.23	0.37
	1	5.24	0.88

*Ozone decay rate could not be calculated

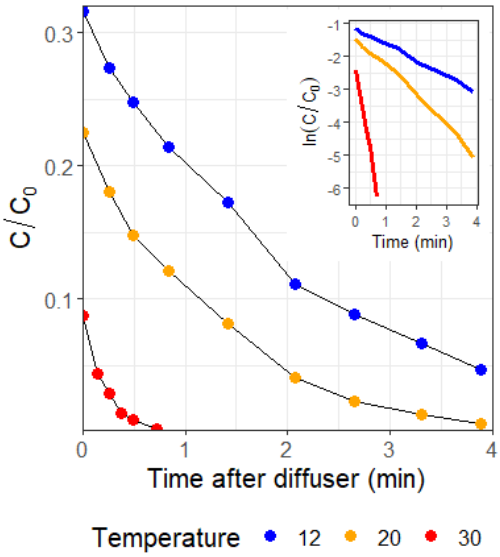

Figure 2. Example ozone decay curves at 1:1 O3:TOC

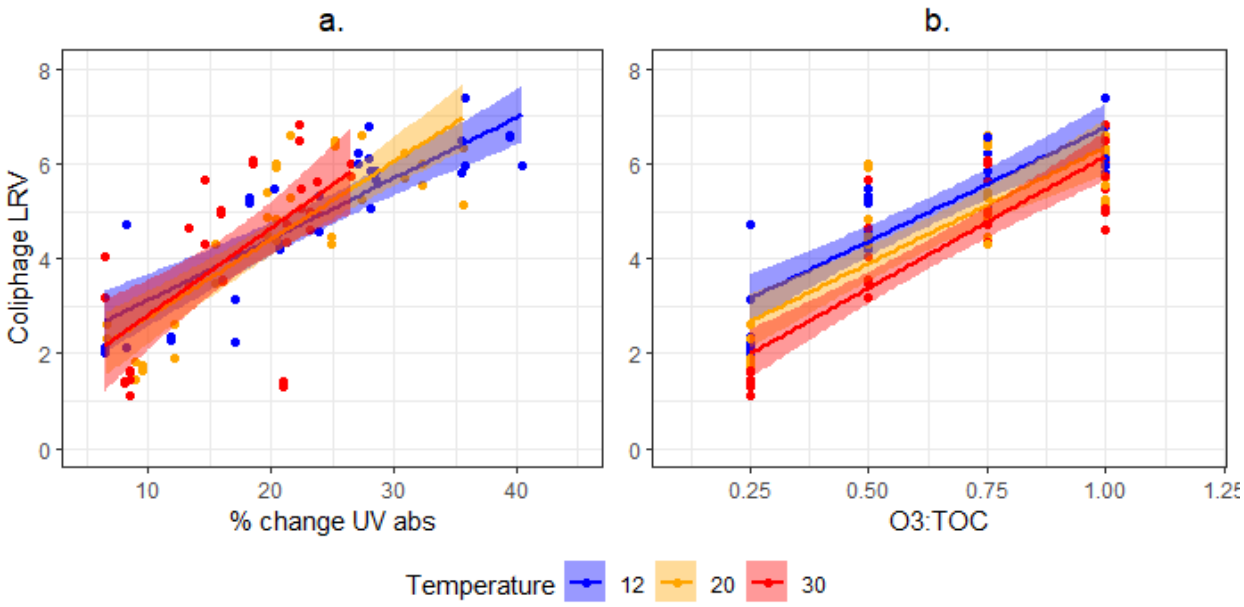

Figure 3. Male specific and somatic coliphage LRV correlated with (a) % change in UV absorbance and (b) O3:TOC

3.2 pH

Based on the results presented for ozone disinfection under various temperatures, an O_3:TOC of 0.6 was selected for evaluation of a range of pH conditions. The variation in ozone decay as a result of changing pH is shown in Figure 4a. Ozone decay accelerates at elevated pH due to the increased reactivity of deprotonated forms of DOM which control ozone decay in wastewater (Buffle et al., 2006). For an O_3:TOC of 0.6, increasing pH from 6-8.4 resulted in an 82% decrease in ozone exposure. The total ozone exposure is calculated for each condition and presented in the SI. A previous study also determined the rate of reaction of ozone with viruses increased 1.4-2 fold when pH increased from 6.5-8.5 (Wolf et al., 2018). The pH not only influences the ozone decay rate, but also determines the surface charge properties (isoelectric point) of viruses (Michen & Graule, 2010). This plays a significant role when considering physical removal of viruses, but this is not expected to affect virus inactivation by ozone. Similar to the trend seen with temperature, increasing pH appeared to marginally reduce coliphage disinfection efficacy for a given applied ozone dose (Figure 4b). A similar trend was observed for *E. coli* as shown in the Supplementary Information (Figure SI-1). This is likely a similar phenomenon described

previously where the decrease in ozone exposure plays a more significant role than the increase in reaction rate. However, the decrease in ozone exposure was not proportional to the minor decrease in disinfection performance. When comparing pH of 6 to pH of 8 for the same ozone dose, the total integrated ozone exposure decreased by >90% whereas the inactivation predicted by least squares regression line for the data in Figure 4b only decreased by 18%. This minor decrease in disinfection performance is better represented by the change in UV_{254} absorbance as shown by Figure 11 in Section 3.7. As a result, the impact of pH on ozone disinfection efficacy overall is not significant in the range that is likely observed in wastewater treatment effluent. It is notable that pH is not considered in the existing EPA Ct guidelines despite the impact it has on ozone exposure. These results show a more suitable framework for ozone disinfection across a range of pH values is the change in UV_{254} absorbance.

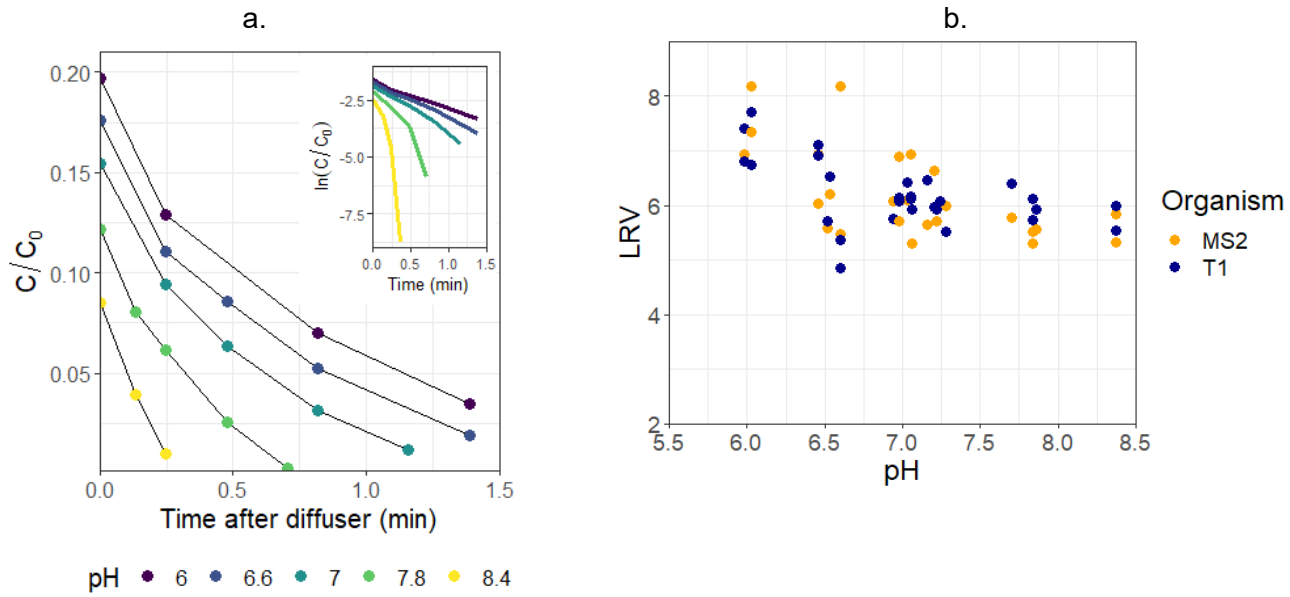

Figure 4. (a) Example ozone decay curves at 0.6 O3:TOC and (b) log removal of coliphage at various pH

The pH also determines the reaction rate of hydrogen peroxide with ozone. As mentioned previously, H_2O_2 is often used as a chemical bromate control strategy. Ozone reacts with the

deprotonated form of H_2O_2 (hydroperoxide ion HO_2^-, pK_a = 11.6) at a rate that is proportional to $k*10^{(pH-pK)}$ (von Sonntag & von Gunten, 2012). Therefore, one unit increase in pH results in a 10x faster reaction rate with ozone. Combined with increased ozone decay at higher pH, there is essentially no measurable ozone exposure at the highest pH value with the addition of 1:1 molar ratio of H_2O_2. Inactivation data presented in Figure 4b and SI-1 include samples taken with and without the addition of H_2O_2. A Wilcoxon signed-rank test was performed comparing the samples taken at various pH levels with and without H_2O_2, and there was no significant difference observed between the two groups ($p>0.05$, fail to reject H_0 that groups are not different).

3.3 TOC and TSS

A range of TOC and TSS conditions were investigated by using two different source waters and evaluating direct ozonation compared with ozonation post coag/floc/sed. Plant A has secondary clarifier average effluent TOC = 9.1 mg/L and TSS = 5.8 mg/L. Plant B has tertiary denitrification filters with average effluent TOC = 7.0 mg/L and TSS = 1.2 mg/L. In these experiments, floc/sed provided approximately 26-39% TOC removal. For Plant A, floc/sed reduced the TSS concentration from 5.75 to 1.9 mg/L, whereas for Plant B the TSS increased post floc/sed from 1.2 to 1.6 mg/L. This is likely due to the addition of chemicals to the already extremely low TSS water. The resulting ozone disinfection performance for Plant A and Plant B is presented in Figure 5 and Figure 6 respectively. It should be noted that samples were collected with and without the addition of 1:1 molar ratio of H_2O_2 and since there was no apparent difference with the introduction of H_2O_2, these data are presented together without distinction on Figure 5. In Figure 5a, it appears that log-inactivation values achieved at a given O_3:TOC are higher for higher TOC. However, this is a result of the applied doses being proportionally higher for the higher TOC water. This highlights a critical consideration for using the O_3:TOC framework for virus removal in various water matrices and the necessity for site-specific testing. When the coliphage inactivation is correlated with change in UV_{254} absorbance or the applied ozone dose (ppm) there is less

discrepancy between the low and high TOC water. In general, the correlation of coliphage inactivation with each variable is stronger for Plant B (Figure 6). This is likely a result of fewer data points from a single test compared to two data sets for Plant A. This variability in the Plant A data set is inherent to this type of experiment where the water matrix and thus ozone reactivity can change from day to day. Despite the spread in data for Plant A, there is still a clear positive linear relationship with all three parameters evaluated. In Figure 6a the disparity between low and high TOC water disinfection for a given O_3:TOC is less apparent until 0.75-1 O_3:TOC suggesting this may not be a concern in lower TOC waters except at higher ozone doses. Further, the relationship between coliphage inactivation and change in UV_{254} absorbance or applied ozone dose show no obvious difference for low and high TOC water. The inactivation of *E.coli* followed a similar trend with O3:TOC for each plant and is shown in Figure SI-2.

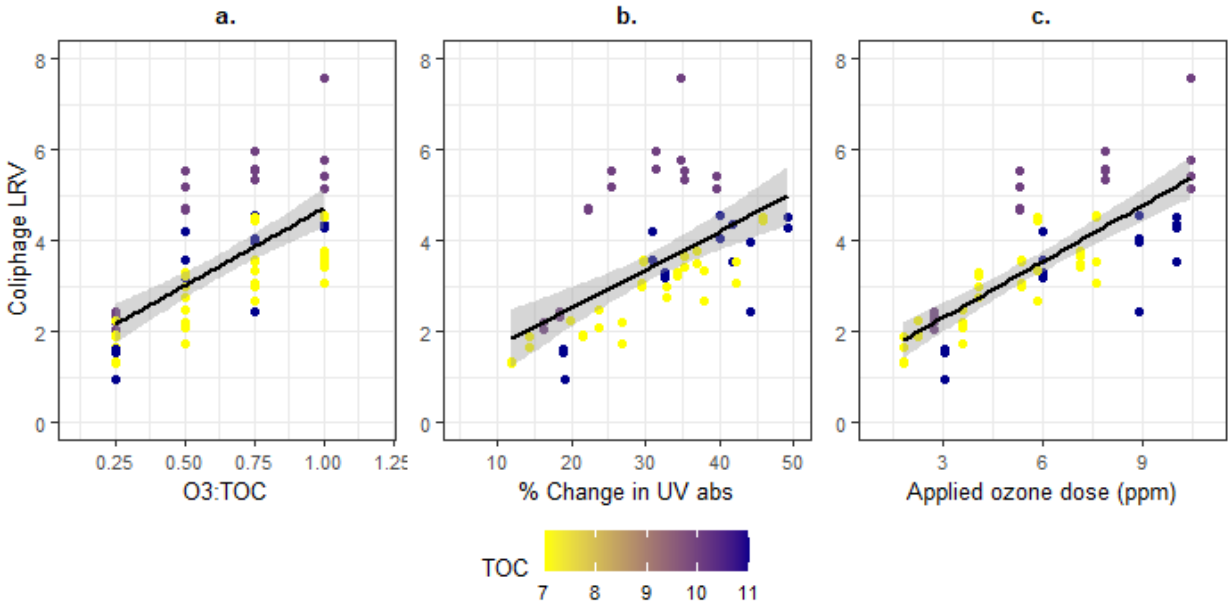

Figure 5. Log coliphage removal correlated with (a) O3:TOC, (b) % change in UV abs, and (c) applied ozone dose for Plant A

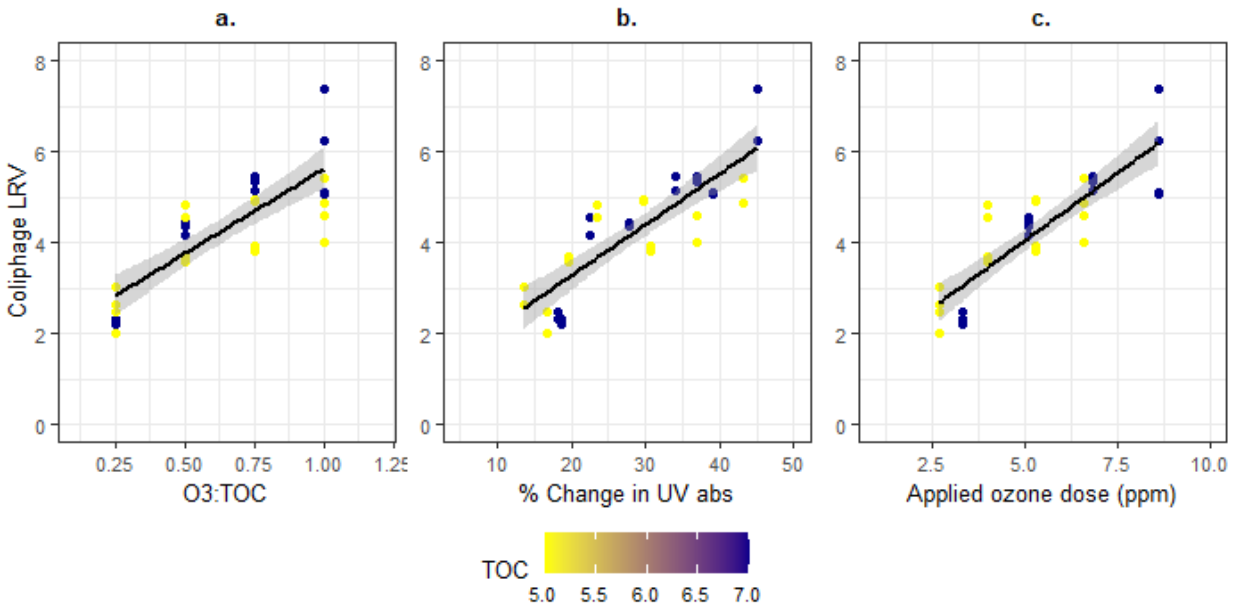

Figure 6. Log coliphage removal correlated with (a) O3:TOC, (b) % change in UV abs, and (c) applied ozone dose for Plant B

Previous studies have evaluated the impact of TOC and suspended solids concentrations on ozone disinfection (Haas et al., 1996; Hijnen et al., 2004; Lazarova et al., 2014). It has been hypothesized that pathogens may be shielded from ozone inactivation by suspended particles in the water column resulting in lower disinfection performance for “poor” quality water. However, this study showed there is not a significant difference in ozone disinfection performance for the water quality conditions evaluated. Further, there was not a notable improvement in ozone disinfection after upstream floc/sed and TOC removal for either source water. Although it should be noted that both source waters tested in this study are highly treated wastewater from advanced BNR facilities with relatively low TOC and suspended solids concentrations prior to any advanced treatment. Particle shielding may present a greater impact on ozone disinfection when there is inefficient solids removal in upstream wastewater treatment processes or in the case of non-nitrifying high-rate activated sludge or trickling filter processes.

3.4 Nitrite

Thus far, several parameters have been evaluated that influence ozone decay characteristics including source water temperature, pH, and TOC concentration. While residual NO_2 does not necessarily impact ozone decay, it does exert a stoichiometric ozone demand of 3.43 mg/L of ozone per mg-N/L. Therefore, if not accounted for in the applied ozone dose, NO_2 will result in a significant reduction in ozone exposure as shown in Figure 7. Since NO_2 acts as a sink for ozone rather than an initiator or propagator for ozone decomposition, residual NO_2 did in fact significantly hinder ozone disinfection performance. It can be seen in Table 3 that while spiking 1 mg/L-N of NO_2, the total ozone exposure measured was reduced from ~1 mg/L-min to 0.2 mg/L-min. This resulted in suppressed disinfection performance for each microorganism evaluated. However, there was still 3.1-3.4 log removal of MS2 and T1 achieved respectively presumably as a result of the ozone exposure achieved in the diffusion zone. Similar results were seen with regard to *E.coli* inactivation and are summarized in Table SI-1. These data show that in the event of short term upstream NO_2 spikes, some disinfection will still be achieved by ozonation. However, if online NO_2 monitoring is possible, this value should always be accounted for in the applied ozone dose control system. As shown in Figure 7 and Table 3, when the ozone dose is corrected for the NO_2 concentration, the same ozone exposure is achieved, and disinfection performance is maintained. It is also notable that the change in UV_{254} absorbance for the control sample (38%) and the sample taken after ozone dose was corrected for NO_2 concentration (40%) were roughly equivalent, whereas the sample taken during NO_2 spiking without correcting the dose was suppressed (24% change in UV_{254} absorbance). Therefore either O_3:TOC corrected for NO_2 or change in UV_{254} absorbance would be suitable for monitoring or control (and validation). Considering the significant ozone demand imposed by residual NO_2, this may present a significant operational cost if NO_2 cannot be well controlled upstream. A similar impact may be observed for other ozone

demanding compounds that react rapidly such as reduced metal species (Fe^{2+}, Mn^{2+}) (von Sonntag & von Gunten, 2012).

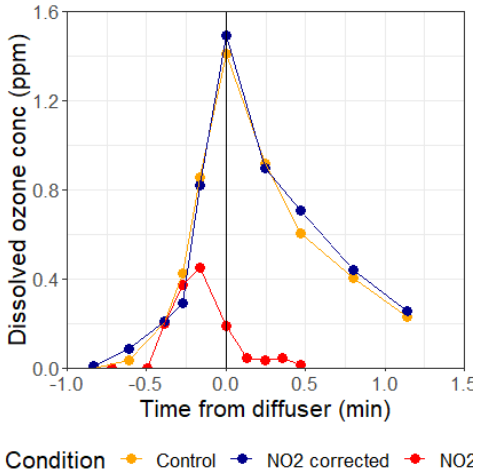

Figure 7. Example ozone decay curve during NO_2 spiking

Table 3. Ozone disinfection performance during NO_2 spike events

	Ozone dose (mg/L)	Ozone exposure (mg/L-min)	LRV	
			MS2	T1
Control	5.8	1.05	6.6	6.0
NO_2 spike (~1 mg/L)	5.8	0.17	3.1	3.4
Corrected for NO2	9	1.09	5.7	5.9

3.5 Ozone application method

Experiments were performed to evaluate the impact of spreading out the applied ozone dose to three diffusion zones. A similar concept has been explored previously in the context of bromate control (Merle et al., 2017; Morrison et al., 2023). Minimizing the localized ozone residual while applying the same overall ozone dose has been shown to provide a benefit with respect to decreasing bromate formation and maintaining trace organic contaminant oxidation (Merle et al., 2017). For the one diffusion zone condition (0.6 O_3:TOC), samples were collected both directly after the bubble column (ozone residual was quenched with sodium thiosulfate) and at the end of the contactor. This showed that most of the disinfection occurs in the diffusion zone itself, and there is minimal additional disinfection occurring in the subsequent contact zones. The SWTR awards only one-log virus removal if the residual leaving the diffusion zone is >0.1 mg/L. These data suggest that most if not all virus and coliform disinfection occurs in this zone. Samples were

also collected while using two diffusion zones (0.3 O_3:TOC at each diffuser) and three diffusion zones (0.2 O_3:TOC at each diffuser). Similar ozone exposure was achieved for each scenario as shown in Figure 8a. Slightly greater exposure was achieved for three diffusion zone case potentially as a result of the preoxidation that occurs in the prior diffusion zones. For these experiments, no significant difference in coliphage or coliform bacteria inactivation was observed when comparing the use of one, two or three diffusion zones at a typical O_3:TOC of 0.6 (Figure SI-3). Each microorganism displayed a similar trend shown for T1 phage in Figure 8b. Previous studies explored a similar concept in the context of multi-point wastewater chlorination and found a benefit with respect to disinfection performance and DBP formation (Li, Yang, et al., 2017; Li, Zhang, et al., 2017). This was hypothesized to be a result of multiple contact points with the disinfectant preventing the microorganism cell wall from repairing itself (Li, Zhang, et al., 2017). A similar result was not observed here as the maximum possible disinfection performance was nearly achieved (effluent concentration ~1-10 PFU/100 mL) for both model viruses when using one, two, or three diffusion zones. When considering *E. coli* inactivation, there were still 10^2-10^3 CFU/100 mL detected in the effluent samples and there was no difference observed in the log-removal values when comparing one, two, and three diffusion zones.

In this study, the use of multiple diffusion zones presented the greatest benefit for disinfection performance in the event of elevated ozone demand in the form of residual NO_2 in the source water. Testing was performed comparing the disinfection performance during NO_2 spike events while using one vs three diffusion zones. With approximately 1 mg/L-N NO_2 in the influent, virus inactivation was reduced from >6-log removal to 1.4 and 2-log for MS2 and T1 respectively. However, when the same applied ozone dose is split between three diffusion zones, disinfection performance for MS2 and T1 increases to 2.5 and 3.6-log respectively. This is likely a result of the nitrite being oxidized primarily in the first and second diffusion zones, allowing for greater

disinfection capacity in the third zone. This strategy can be useful to achieve similar disinfection with lower ozone doses in the event of uncontrolled/unmanaged NO_2 input.

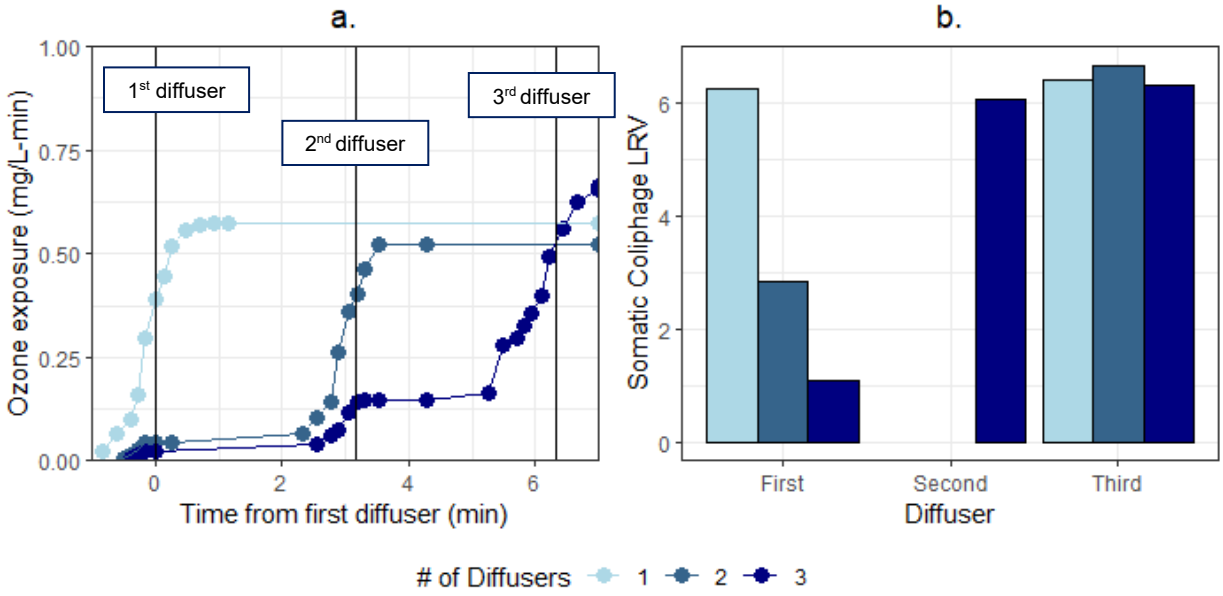

Figure 8. (a) Cumulative ozone exposure for multiple diffusers and (b) Somatic coliphage log-inactivation. “Third diffuser” samples were taken in the reactor effluent.

3.6 Ozone Exposure Calculations

The method used to calculate the ozone exposure can significantly influence the resulting value. Methods utilized in full-scale applications can generally be defined in one of three ways, (1) single point Ct, (2) multiple point Ct values summed, or (3) determination of the ozone decay rate and modeling the decay curve to estimate the total ozone exposure. Single point estimates can be calculated in various ways including multiplying the reactor effluent concentration by the residence time and a baffle factor (effluent method) or by using the geometric or arithmetic mean of the diffusion zone effluent and the reaction zone effluent. Multiple Ct values can be summed throughout the contactor, however this necessitates multiple dissolved ozone probes which represents significant maintenance cost. An even more accurate estimate of Ct can be made using the “extended CSTR” method whereby three ozone residual monitoring points are used to

estimate the first order ozone decay rate and thus the area under the decay curve. These methods are outlined in the SWTR, LT2ESWTR, and other publications (Morrison et al., 2022; Rakness et al., 2005; USEPA, 2006). Typically, in drinking water applications, even the most conservative method for calculating Ct is suitable for claiming giardia and virus log-removal credit, as these frameworks require a lower Ct value when compared to the much greater Ct values required for Cryptosporidium credit (Rakness et al., 2005). However, in wastewater and water reuse ozonation, the ozone demand is typically much greater, and the ozone decay rate is much higher than those typically reported in drinking water. Therefore, efforts should be made to not only limit ozone exposure, but also accurately characterize the total ozone exposure so as to not overdose ozone. As shown in Figure 9a, a single point Ct value can change significantly depending on where it is measured. This point can be optimized by considering the decay curve, determining the decay rate, and finding the optimal point for process monitoring. Assuming first order decay, the maximum single point Ct occurs at the time 1/k downstream of the dissolution zone, where k is the first order ozone decay rate (derived in Text SI-1). However, even when monitoring at the point of greatest Ct, this still greatly underestimates the actual ozone exposure in the downstream contactor by at least a factor of 2.7 (as demonstrated in section SI-1, Figure 9c, and Figure SI-4 in greater detail). Additionally, as shown in Figure 9b, this does not include the exposure occurring in the dissolution zone (orange) which accounted for nearly all of the ozone exposure at the lowest doses and approximately 40% at an ozone dose of 1:1 O_3:TOC (shown in Figure 9b). Further, the exposure in the dissolution zone is partially or totally uncredited depending on the organism of interest. The results of this study showed that at a reasonable O_3:TOC dose of 0.6, the majority of disinfection occurs in this zone.

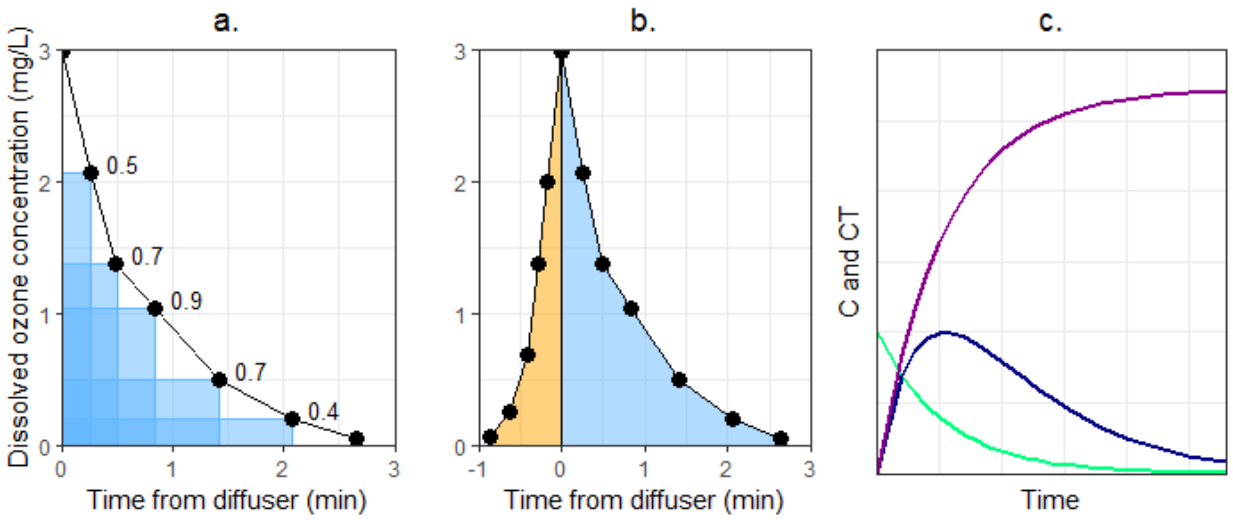

Figure 9. (a) Single point Ct calculation with Ct labeled for each time point (b) Integrated ozone exposure in the bubble diffusion chamber (orange) and contact zone (blue) (c) First order ozone decay curve (green), single point Ct (blue) and integrated ozone exposure (purple)

The discussion of ozone exposure measurement is confounded completely by the addition of H_2O_2, where similar levels of virus inactivation were achieved despite a greater than 5-fold reduction in ozone exposure at pH 7. Other variables that have a disproportionate impact on ozone exposure compared to actual disinfection performance are temperature, pH, and potentially TOC as described previously. This is demonstrated in Figure 10 where the LRV is plotted as a function of the total ozone exposure (diffusion column + reactive chambers) and the credited ozone exposure (reactive chambers only) for each of these variables. In each scenario, the LRV reaches an asymptote at or before 0.5 mg/L-min as a result of the maximum disinfection being achieved at this point. These plots demonstrate just how conservative Ct frameworks are, especially when only considering the “credited” ozone exposure.

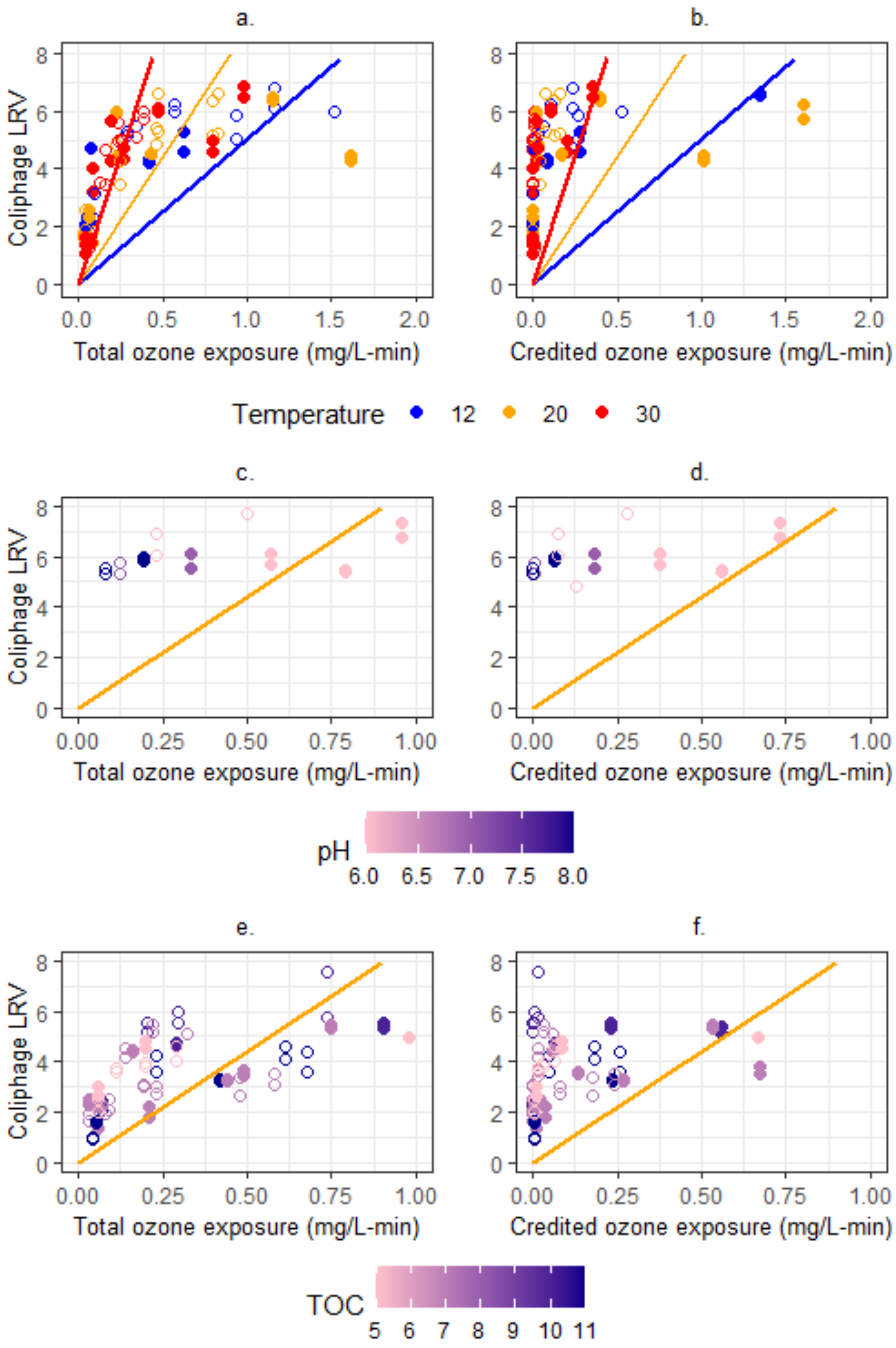

Figure 10. Coliphage LRV as a function of total and credited ozone exposure at a range of (a-b) temperature conditions, (c-d) pH values, and (e-f) TOC concentrations. Open symbols represent samples taken with the addition of H_2O_2. Lines represent the EPA Ct models at 12 (blue), 20 (orange), and 30 ºC (red).

3.7 Applying Alternative Frameworks

When evaluating ozone disinfection on the basis of specific ozone dose (O_3:TOC), several variables need to be considered including temperature, pH, and TOC. If this framework is being used, site-specific ozone dose-response testing should be performed to include the range of conditions that may be observed at the project location. Experiments can be performed to develop correlations for the expected boundary conditions, which can then be interpolated between. When using the specific ozone dose framework, it is also important to account for the NO_2 concentration which would require online monitoring upstream of the ozone process. Another notable drawback to using O_3:TOC corrected for NO_2, is the time delay associated with discrete sampling by both the online TOC and NO_2 analyzers. If the % change in UV_{254} absorbance is used instead, there is a benefit to continuous online optical sensors that respond rapidly to changes in water quality. Measuring the UV_{254} absorbance continuously before and after ozonation also provides a valuable feedback component that ensures disinfection goals are met consistently. Additionally, when using % change in UV_{254} absorbance, a single correlation can likely be considered for the range of variables. For example, in Figure 11, the data from temperature, pH, and NO_2 spike testing described previously were combined. This includes data for temperature of 12-30 C, pH of 6-8.4, NO_2 0-1 mg-N/L, and TOC 8-11 mg/L. A linear trend is demonstrated for the data collected across this wide range of water quality variables. Therefore, if this framework is used, a narrower range of variables can be tested to develop the validating equations. Regardless of the selected framework, a more conservative prediction interval should be selected to ensure protection against system failures. It should also be noted that both the specific ozone dose, and change in UV_{254} absorbance can be used to simultaneously validate trace organic contaminant oxidation (Gerrity et al., 2012; Lee et al., 2013).

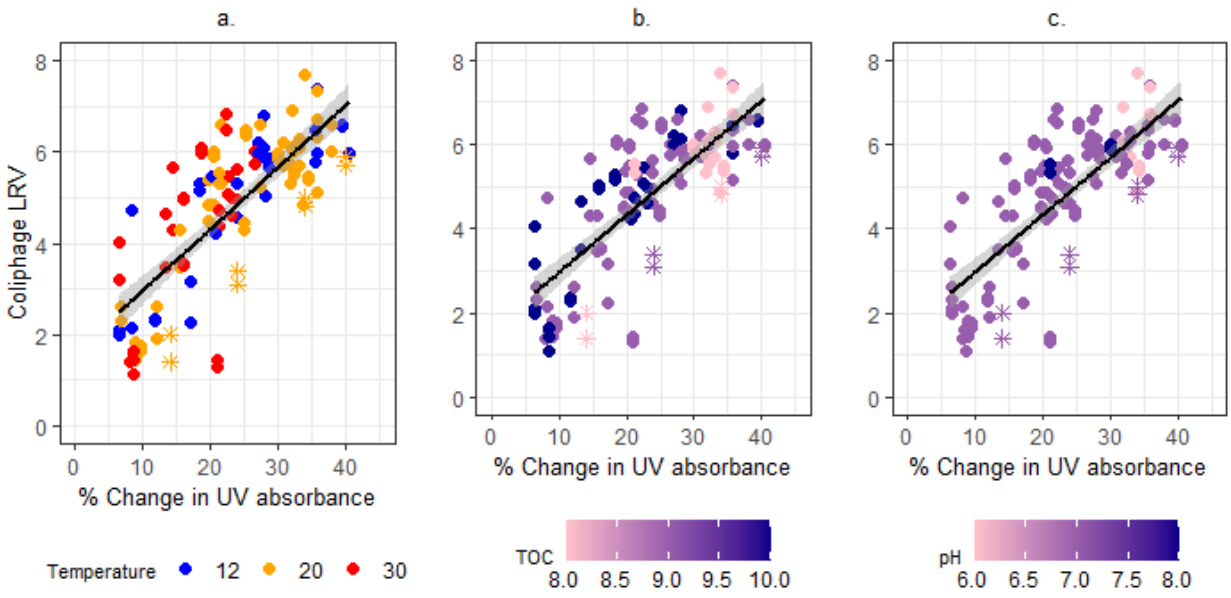

Figure 11. Change in UV absorbance and resulting coliphage LRV. Starred symbols represent samples taken while spiking NO_2.

4. Conclusion

There is a clear need for public health protection from pathogens in potable and nonpotable reuse applications, and ozone can be a very important disinfection barrier. The recent attention to microbial risk assessment methods in potable reuse highlights this clearly, and the development of LRV targets for indirect and direct potable reuse reflect this approach to safeguard public health. This work suggests that a tiered approach could be applied to validate ozone disinfection whereby a certain amount of virus credit can be claimed depending on the level of site-specific testing that is performed. Additionally, safety factors can be implemented to limit negative impacts of potential system failures and excursions from specifications. The level of conservatism applied should be carefully considered such that the alternative monitoring framework does not become more conservative than the existing Ct based framework.

The data presented herein demonstrated the following:

- Ozone pilot testing revealed the significant impact of temperature and pH on ozone decay in wastewater reuse. Both increasing temperature and pH were shown to have a minor deleterious impact on ozone inactivation of male specific and somatic coliphage. However, this impact is not nearly proportional to the observed reduction in ozone exposure.
- Both source waters evaluated (SCE and denitrification filter effluent) showed similar coliphage inactivation trends as a function of change in UV_{254} absorbance and applied ozone dose (mg/L) despite a range of water quality conditions. Upstream TOC and TSS removal by floc/sed did not have any significant impact on disinfection performance. Though it should be noted that TOC and TSS concentrations of the source waters examined were relatively low.
- Nitrite consumes ozone rapidly and as a result, impedes disinfection performance significantly. O_3:TOC corrected for nitrite or change in UV_{254} absorbance were shown to be suitable monitoring frameworks in the event of nitrite spikes.
- There was no difference in disinfection performance observed when comparing one, two or three ozone dissolution zones. Using multiple diffusion zones was shown to be a benefit in the event of nitrite spiking.
- The method used to calculate ozone Ct can also create large discrepancies in reported ozone exposure for a given ozone dose. Additionally, the uncredited region of the bubble column was shown to be where most ozone disinfection occurred.
- Both change in UV_{254} absorbance or applied O_3:TOC corrected for NO_2 were shown to be reliable frameworks for monitoring ozone disinfection across a range of water quality conditions, though site-specific testing may be necessary.

Acknowledgements

Funding for this project was provided by the Hampton Roads Sanitation District. This work is also in-kind contribution to the WRF project 5129. The authors would like to thank the WRF 5129 project team for valuable input throughout the project. Additionally, the authors express their gratitude to Hannah Thompson, Errin Carter, Hila Stephens, and Tina Marie Haskell of HRSD pathogen laboratory.

References

Buffle, M.-O., Schumacher, J., Meylan, S., Jekel, M., & von Gunten, U. (2006). Ozonation and Advanced Oxidation of Wastewater: Effect of O3 Dose, pH, DOM and HO Scavengers on Ozone Decomposition and HO Generation. *Ozone: Science and Engineering*, *28*(4), 247–259.

Buffle, M. O., Schumacher, J., Meylan, S., Jekel, M., & Von Gunten, U. (2006). Ozonation and advanced oxidation of wastewater: Effect of O3 dose, pH, DOM and HO.-scavengers on ozone decomposition and HO . generation. *Ozone: Science and Engineering*, *28*(4), 247–259. https://doi.org/10.1080/01919510600718825

Burns, N., Hunter, G., Jackman, A., Hulsey, B., Coughenour, J., & Walz, T. (2007). The return of ozone and the hydroxyl radical to wastewater disinfection. *Ozone: Science and Engineering*, *29*(4), 303–306. https://doi.org/10.1080/01919510701463206

Cho, M., Chung, H., & Yoon, J. (2002). *Effect of pH and Importance of Ozone initiated Radical Reactions In Inactivating Bacillus subtilis Spore*. *9512*. https://doi.org/10.1080/01919510208901605

Gamage, S., Gerrity, D., Pisarenko, A. N., Wert, E. C., & Snyder, S. A. (2013). Evaluation of Process Control Alternatives for the Inactivation of Escherichia coli, MS2 Bacteriophage, and Bacillus subtilis Spores during Wastewater Ozonation. *Ozone: Science and Engineering*, *35*(6), 501–513. https://doi.org/10.1080/01919512.2013.833852

Gerrity, D., Gamage, S., Jones, D., Korshin, G. V., Lee, Y., Pisarenko, A., Trenholm, R. A., von Gunten, U., Wert, E. C., & Snyder, S. A. (2012). Development of surrogate correlation models to predict trace organic contaminant oxidation and microbial inactivation during ozonation. *Water Research*, *46*(19), 6257–6272. https://doi.org/10.1016/j.watres.2012.08.037

Haas, C. N., Joffe, J., Anmangandla, U., Jacangelo, J. G., & Heath, M. (1996). Water quality and disinfection kinetics. *Journal / American Water Works Association*, *88*(3), 95–103. https://doi.org/10.1002/j.1551-8833.1996.tb06522.x

Hijnen, W. A. M., Baars, E., Bosklopper, T. G. J., Van Der Veer, A. J., Meijers, R. T., & Medema, G. J. (2004). Influence of DOC on the inactivation efficiency of ozonation assessed with Clostridium perfringens and a lab-scale continuous flow system. *Ozone: Science and Engineering*, *26*(5), 465–473. https://doi.org/10.1080/01919510490507784

Hogard, S., Pearce, R., Gonzalez, R., Yetka, K., & Bott, C. (2023). *Optimizing Ozone Disinfection in Water Reuse : Controlling Bromate Formation and Enhancing Trace Organic Contaminant Oxidation*. https://doi.org/10.1021/acs.est.3c00802

Hübner, U., Zucker, I., & Jekel, M. (2015). Options and limitations of hydrogen peroxide addition to enhance radical formation during ozonation of secondary effluents. *Journal of Water Reuse and Desalination*, *5*(1), 8–16. https://doi.org/10.2166/wrd.2014.036

Hunt, N. K., & Marinas, B. (1997). Kinetics of Escherichia coli inactivation with ozone. *Water Research*, *31*(6), 1355–1362.

Jamil, A., Farooq, S., & Hashmi, I. (2017). Ozone Disinfection Efficiency for Indicator Microorganisms at Different pH Values and Temperatures. *Ozone: Science and Engineering*, *39*(6), 407–416. https://doi.org/10.1080/01919512.2017.1322489

Lazarova, V., Liechti, P. A., Savoye, P., & Hausler, R. (2014). Ozone disinfection: Main parameters for process design in wastewater treatment and reuse. *Journal of Water Reuse and Desalination*, *3*(4), 337–345. https://doi.org/10.2166/wrd.2013.007

Lee, Y., Gerrity, D., Lee, M., Bogeat, A. E., Salhi, E., Gamage, S., Trenholm, R. A., Wert, E. C., Snyder, S. A., & Von Gunten, U. (2013). Prediction of micropollutant elimination during ozonation of municipal wastewater effluents: Use of kinetic and water specific information. *Environmental Science and Technology*, *47*(11), 5872–5881. https://doi.org/10.1021/es400781r

Li, Y., Yang, M., Zhang, X., Jiang, J., Liu, J., Yau, C. F., Graham, N. J. D., & Li, X. (2017). Two-step chlorination: A new approach to disinfection of a primary sewage effluent. *Water Research*, *108*, 339–347. https://doi.org/10.1016/j.watres.2016.11.019

Li, Y., Zhang, X., Yang, M., Liu, J., Li, W., Graham, N. J. D., Li, X., & Yang, B. (2017). Three-step effluent chlorination increases disinfection efficiency and reduces DBP formation and toxicity. *Chemosphere*, *168*, 1302–1308. https://doi.org/10.1016/j.chemosphere.2016.11.137

Merle, T., Pronk, W., & Von Gunten, U. (2017). MEMBRO3X, a novel combination of a membrane contactor with advanced oxidation (O3/H2O2) for simultaneous micropollutant abatement and bromate minimization. *Environmental Science and Technology Letters*, *4*(5), 180–185. https://doi.org/10.1021/acs.estlett.7b00061

Michen, B., & Graule, T. (2010). *Isoelectric points of viruses*. *109*, 388–397. https://doi.org/10.1111/j.1365-2672.2010.04663.x

Morrison, C. M., Hogard, S., Pearce, R., Gerrity, D., von Gunten, U., & Wert, E. C. (2022). Ozone disinfection of waterborne pathogens and their surrogates: A critical review. *Water Research*, *214*(November 2021), 118206. https://doi.org/10.1016/j.watres.2022.118206

Morrison, C. M., Hogard, S., Pearce, R., Mohan, A., Pisarenko, A. N., Dickenson, E. R. V., von Gunten, U., & Wert, E. C. (2023). Critical Review on Bromate Formation during Ozonation and Control Options for Its Minimization. *Environmental Science and Technology*. https://doi.org/10.1021/acs.est.3c00538

Pearce, R., Hogard, S., Buehlmann, P., Salazar-benites, G., Wilson, C., & Bott, C. (2022). Evaluation of preformed monochloramine for bromate control in ozonation for potable reuse. *Water Research*, *211*, 118049. https://doi.org/10.1016/j.watres.2022.118049

R Core Team. (2021). *R: A language and environment for statistical computing*. https://www.r-project.org/.

Rakness, K. L., Najm, I., Elovitz, M., Rexing, D., & Via, S. (2005). Cryptosporidium log-inactivation with ozone using effluent CT10, geometric mean CT10, extended integrated CT10 and extended CSTR calculations. *Ozone: Science and Engineering*, *27*(5), 335–350. https://doi.org/10.1080/01919510500250267

Rennecker, J. L., Mariñas, B. J., Owens, J. H., & Rice, E. W. (1999). Inactivation of Cryptosporidium parvum oocysts with ozone. *Water Research*, *33*(11), 2481–2488. https://doi.org/10.1016/S0043-1354(99)00116-5

Staehelin, J., & Holgné, J. (1982). Decomposition of Ozone in Water: Rate of Initiation by Hydroxide Ions and Hydrogen Peroxide. *Environmental Science and Technology*, *16*(10), 676–681. https://doi.org/10.1021/es00104a009

Guidance Manual for Compliance with the Filtration and Disinfection Requirements for Public Water Systems Using Surface Water Sources, American Water Works Association, Denver, CO 580 (1991). https://www.epa.gov/sites/production/files/2015-10/documents/guidance_manual_for_compliance_with_the_filtration_and_disinfection_requirements.pdf

Long Term 2 Enhanced Surface Water Treatment Rule, 47640 (2006).

US EPA. (2018). Method 1643: Male-specific (F+) and Somatic Coliphage in Recreational Waters and Wastewater by Ultrafiltration (UF) and Single Agar Layer (SAL) Procedure. *Office of Water*, *April*, 1–40. www.epa.gov

von Gunten, U. (2003). Ozonation of drinking water: Part II. Disinfection and by-product formation in presence of bromide, iodide or chlorine. *Water Research*, *37*(7), 1469–1487. https://doi.org/10.1016/s0043-1354(02)00458-x

von Sonntag, C., & von Gunten, U. (2012). Chemistry of Ozone in Water and Wastewater Treatment: From Basic Principles to Applications. In *Chemistry of Ozone in Water and Wastewater Treatment: From Basic Principles to Applications*. https://doi.org/10.2166/9781780400839

Wolf, C., Pavese, A., von Gunten, U., & Kohn, T. (2019). Proxies to monitor the inactivation of viruses by ozone in surface water and wastewater effluent. *Water Research*, *166*, 115088. https://doi.org/10.1016/j.watres.2019.115088

Wolf, C., von Gunten, U., & Kohn, T. (2018). Kinetics of Inactivation of Waterborne Enteric Viruses by Ozone. *Environmental Science and Technology*, *52*(4), 2170–2177. https://doi.org/10.1021/acs.est.7b05111

Chapter 4 Supplementary Information

Virus inactivation in low ozone exposure water reuse applications

Samantha Hogard[1,2], Robert Pearce[1,2], Kathleen Yetka[2], Raul Gonzalez[2], Charles Bott[2]

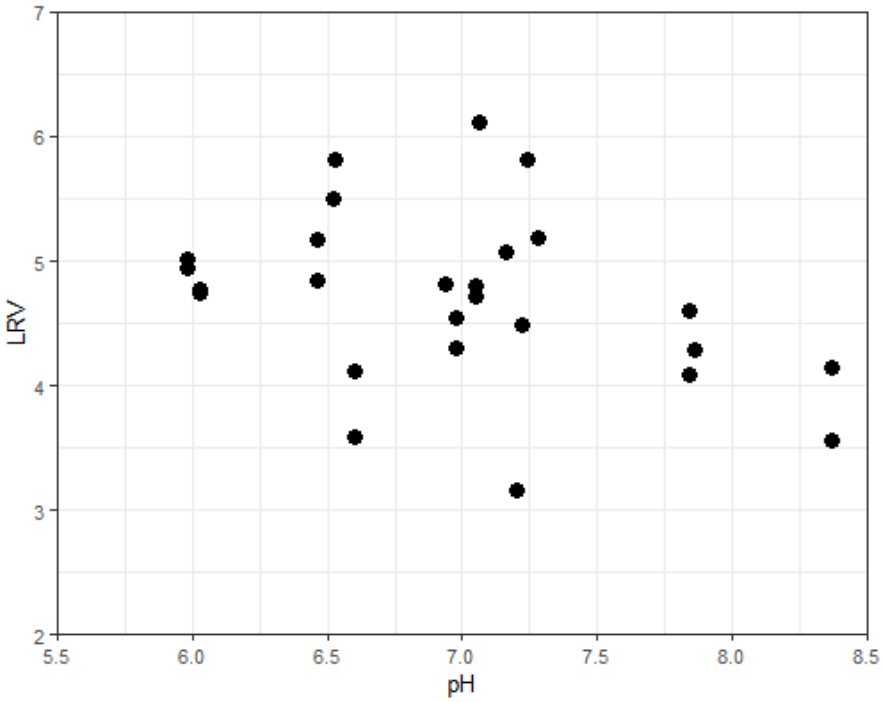

Figure SI-1 Inactivation of *E. coli* correlated with pH

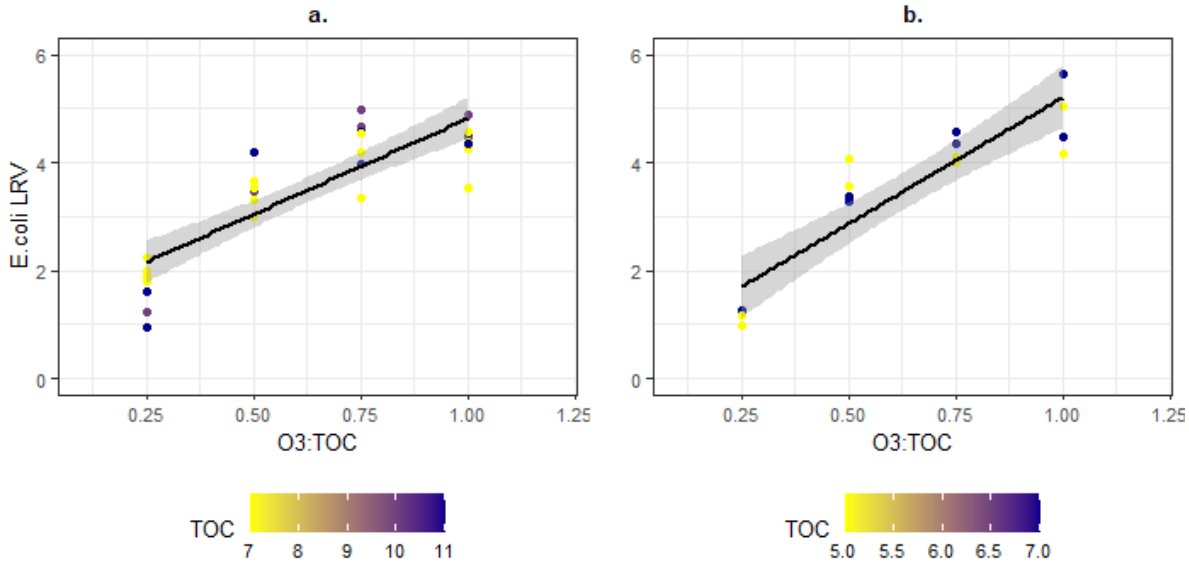

Figure SI-2 Inactivation of *E. coli* for (a) Plant A and (b) Plant B

Table SI-1 Ozone disinfection performance during NO_2 spike events

	Ozone dose (mg/L)	Ozone exposure (mg/L-min)	LRV *E.coli*
Control	5.8	1.05	5.2
NO_2 spike (~1 mg/L)	5.8	0.17	1.2
Corrected for NO2	9	1.09	4.8

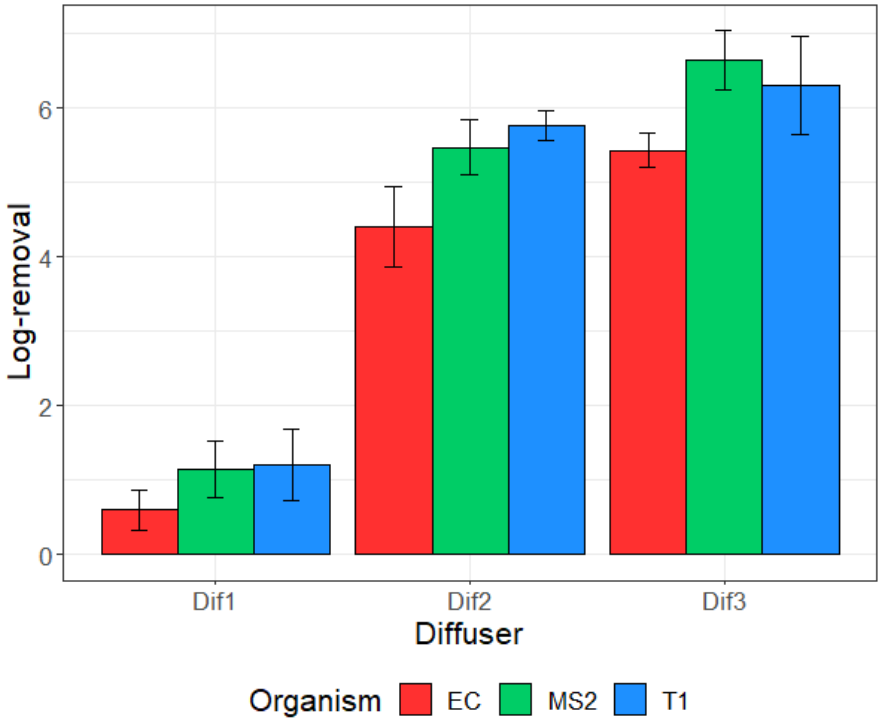

Figure SI-3 Inactivation of *E. coli,* MS2, and T1 phage when using 1, 2, and 3 diffusion zones

SI-1 Maximum Ozone CT Calculation

$C = C_0 e^{-kt}$

$CT = C_o e^{-kt} * Baffle\ Factor * t$

$$\frac{d(CT)}{dt} = BF * C_o \left(\left(e^{-kt} * -k\right) + \left(1 * e^{-kt}\right)\right)$$

$$\frac{d(CT)}{dt} = BF * C_o (e^{-kt}(-kt + 1))$$

Find the zeros:

$0 = BF * C_o (e^{-kt}(-kt + 1))$

$0 = e^{-kt}(-kt + 1)$

$0 = -kt + 1$

$\boldsymbol{t = 1/k}$

$0 = e^{-kt}$

$\ln 0 = -kt$

$t \neq 0$

Maximum Single point CT at t=1/k

$$CT = C_o e^{-k*1/k} * \frac{1}{k} = \frac{C_o}{e * k}$$

Integrated CT

$$\int_0^\infty C_o e^{-k*t} dt = \frac{C_o}{k}$$

$$\frac{Integrated\ C * t}{Maximum\ single\ point\ C * t} = \frac{C_0/_k}{\frac{C_0}{e * k}} = e$$

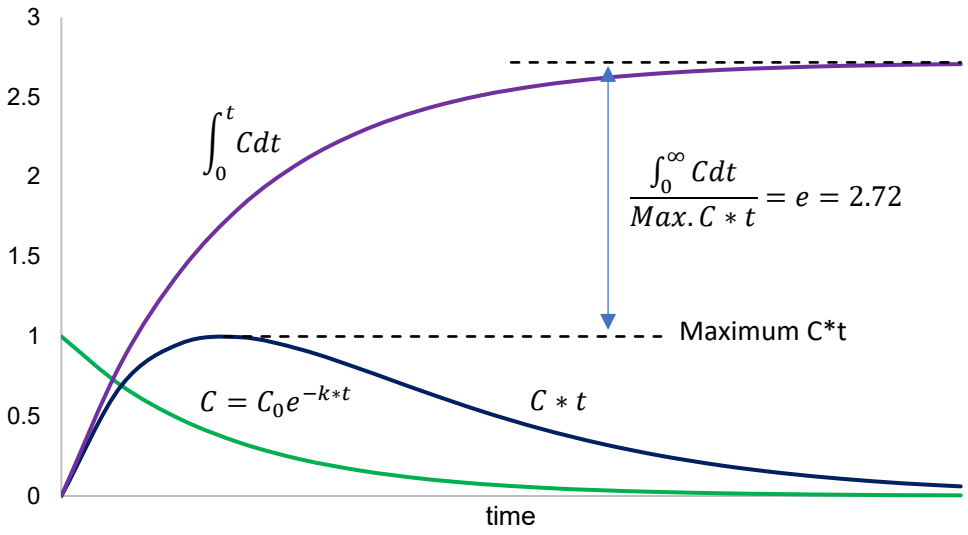

Figure SI-4 First order ozone decay, single point ozone exposure, and integrated ozone exposure comparison

Chapter 5 Demonstrating pathogen reduction in coagulation/flocculation/sedimentation, ozone, and biofiltration indirect potable water reuse treatment trains

Samantha Hogard[1,2], Kathleen Yetka[2], Robert Pearce[1,2], Hannah Thompson[2], Kyle Curtis[2], Raul Gonzalez[2], Charles Bott[2]

[1]Civil and Environmental Engineering Department, Virginia Polytechnic Institute and State University, Blacksburg, VA, USA

[2]Hampton Roads Sanitation District, PO Box 5911, Virginia Beach, VA 23471-0911

Target journal: Water Research

Abstract

Exposure to pathogens remains the greatest acute health concern related to potable and nonpotable water reuse applications. As the implementation of water reuse becomes broader, carbon-based advanced water treatment (AWT) trains have become more commonplace and thus require more extensive validation for pathogen reduction in water reuse applications. Here, we implement high volume sample concentration for both molecular- and culture-based analyses to evaluate pathogen and surrogate removal through a 1-MGD scale coagulation, flocculation, sedimentation, ozonation, and biofiltration treatment train. *Cryptosporidium* and *Giardia* reduction was quantified across the wastewater treatment plant and the AWT process. Considering the low influent concentrations, only 2 and 4 total LRV could be demonstrated for *Cryptosporidium* and *Giardia*, respectively. Both aerobic spore forming bacteria and *Clostridium perfringens* were shown to be representative surrogates for protozoa reduction through coag/floc/sed and ozonation. Adenovirus, rotavirus, norovirus GI, and norovirus GII concentration and reduction were quantified using ddPCR across the AWT process. Average enteric virus LRV through coag/floc/sed, ozonation, and biofiltration was shown to be 1.5, 0.3, and 2 LRV, respectively. Both molecular and culture-based nonpathogenic viral surrogates were shown to be representative of enteric virus reduction by physical removal treatment processes. Due to the low concentration of indigenous pathogens and surrogates, challenge tests were performed on the pilot scale to evaluate pathogen inactivation and removal by ozone and biofiltration. Two methods were

successfully employed to more accurately characterize ozone inactivation with molecular methods including capsid integrity PCR and correlating molecular and culture-based results. Further, challenge testing performed on the biofiltration pilot showed that granular media filtration alone is not a significant barrier for virus/*E.coli* reduction, and upstream coagulation is required for efficient virus/bacteria removal. These full-scale monitoring data and pilot challenge testing data provide validation of the pathogen LRV credit claimed in ozone-biofiltration based AWT which is necessary to protect public health in reuse scenarios.

1. Introduction

The application of water reuse around the world has accelerated in recent years due to widespread water shortages as a result of overuse and drought conditions (EPA, 2017; Gerrity et al., 2013). There are many constituents of concern when recycling treated wastewater; however, the primary acute health risk associated with potable and nonpotable water reuse is the potential exposure to pathogens. Pathogens present in treated wastewater include viruses, bacteria, and protozoa. Due to the level of risk involved with pathogen exposure, water reuse treatment trains are required to achieve high levels of log-reduction values (LRV) using multiple treatment barriers. For example, California indirect potable reuse (IPR) guidelines, require 12-10-10 LRV of enteric viruses, *Giardia*, and *Cryptosporidium,* respectively (California CR Title 22). Additionally, for each of these pathogens, no more than 6 LRV can be claimed for a single treatment process and at least three processes must be credited with at least 1 LRV, thus ensuring a multi-barrier approach. These guidelines were created using risk assessment models assuming an annual acceptable risk to be 1/10,000 infections per person per year (Gerrity et al., 2023). Additionally, the wastewater influent pathogen concentrations were conservatively estimated to be 10^5 MPN/L viruses, 10^5 cysts/L of *Giardia*, and 10^4 oocysts/L of *Cryptosporidium*. The proposed direct potable reuse (DPR) guidelines include additional redundancy in the event of process failure resulting in LRVs of 20/14/15 for viruses, *Cryptosporidium*, and *Giardia* (California DDW, 2021).

Accurate pathogen concentration characterization in raw wastewater is crucial for the reliability of risk models specific to each project location. Among the most prevalent pathogenic bacteria that transmit via fecal-oral route and detected in raw wastewater are *Escherichia coli, Salmonella sp.*, and *Campylobacter jejuni* (Haas et al., 2014). Enteric coliform bacteria are often used as representative bacterial indicators due to their high concentrations and established methods of detection in wastewater. Common enteric viruses shed in human feces and found in wastewater include enteroviruses, adenoviruses, rotaviruses, and caliciviruses (Haas et al., 2014). There are established methods for culturing adenoviruses and enteroviruses (Rodriguez et al., 2013; US EPA, 2014), but many cannot yet be cultured or the methods are not yet universally achievable (e.g. norovirus). Consequently, molecular methods such as quantitative PCR and digital PCR have become indispensable for the sensitive quantification of viral loads in environmental waters, overcoming the limitations of culture-based methods (Girones et al., 2010). To improve these PCR-based methods, strategies to more precisely assess viral infectivity and inactivation include capsid integrity PCR and analysis of larger genome segments have been developed (Canh et al., 2021; Pecson et al., 2011; Rockey et al., 2020; Young et al., 2020). Given the challenges in viral concentration and culturing, surrogates like the pepper mild mottle virus (PMMoV) and coliphages (coliform bacteriophages) are often used due to their higher prevalence (Haas et al., 2014; Kitajima et al., 2014; Papp et al., 2020; Symonds et al., 2018; Tandukar et al., 2020). For protozoan pathogens such as *Giardia lamblia* and *Cryptosporidium sp.* detection commonly relies on concentration, immunomagnetic separation, and identification by microscopy (US EPA, 2005). Spore forming bacteria (SFB) are often used as indigenous surrogates to track removal of these protozoan pathogens (Hijnen & Medema, 2010).

In addition to quantifying pathogen and indicator removal across wastewater treatment, it is also important to validate treatment processes selected for advanced water treatment. This study included an assessment of pathogen removal in non-RO treatment processes including

coagulation/flocculation/sedimentation (coag/floc/sed), ozonation, and biofiltration. These treatment technologies are commonly employed in drinking water treatment and more recently in water reuse applications. In the US EPA Surface Water Treatment Rule (SWTR), conventional filtration (coag/floc/sed + filtration) is awarded 2, 2, and 2.5 LRV of viruses, *Cryptosporidium*, and *Giardia,* respectively, if filter effluent turbidity limits are met (<0.15 NTU 95% of the time) (Long Term 2 Enhanced Surface Water Treatment Rule, 2006). Additional credit can be achieved for meeting lower filter effluent turbidity limits. If direct filtration is employed without a sedimentation basin, then 1 and 0.5 less virus and *Giardia* LRV is achieved, respectively. The SWTR framework for achieving pathogen removal credit with ozone is based on the ozone exposure (concentration*time, Ct) achieved. Several studies have investigated using alternative monitoring frameworks for validating ozone disinfection in water reuse where it is comparatively more difficult to maintain a measurable ozone Ct (Gamage et al., 2013; Hogard et al., 2023). These crediting frameworks and technologies that were created for drinking water treatment have not been extensively validated for water reuse.

There have been multiple studies aimed at characterizing the concentration of pathogens and their surrogates in wastewater and drinking water treatment (Hijnen & Medema, 2010; Rose et al., 2004). Recently, greater attention has been directed toward validating pathogen removal by treatment processes used for water reuse applications. This study employed both full-scale monitoring as well as pilot-scale challenge tests to (1) evaluate pathogen and surrogate removal across wastewater treatment processes, as well as coag/floc/sed, ozonation, and biofiltration advanced water treatment using culture and molecular-based analytical methods, (2) assess the usefulness of culture vs molecular methods for demonstrating inactivation during ozonation, and (3) identify the most useful pathogen indicator microorganisms for long term monitoring purposes.

2. Materials and Methods

2.1 Summary of Advanced Water Treatment Pathogen LRV

The Hampton Roads Sanitation District (HRSD) has recently implemented ozone/biofiltration based advanced water treatment (AWT) for indirect potable reuse via managed aquifer recharge in southeast Virginia. This project is known as the Sustainable Water Initiative for Tomorrow (SWIFT), and the treatment train includes coag/floc/sed, ozonation, biofiltration, granular activated carbon (GAC) adsorption, and ultraviolet (UV) disinfection. Upstream of the advanced water treatment process, is a five-stage Bardenpho wastewater treatment plant that achieves secondary effluent with N < 4 mg/L and P < 1.0 mg/L. The 3.8 MLD (1-MGD) SWIFT Research Center (SWIFT RC) demonstration facility has been in operation, recharging the Potomac Aquifer since 2018 (Hogard et al., 2021). Disinfection credit is currently achieved at the SWIFT RC as follows:

- Two-log removal of viruses and 2.5-log *Giardia* removal is granted per the *Surface Water Treatment Rule (SWTR) Guidance Manual*, 1991 edition, section 5.5.2, for a well operated conventional filtration treatment plant.
- Three-log *Cryptosporidium* removal is granted per the *Long Term 2 Enhanced SWTR (LT2ESWTR) Toolbox Guidance Manual* section 1.4.1 if the combined filter effluent (CFE) is less than 0.3 NTU 95% of the time and never greater than 1.0 NTU. An additional 0.5-log credit is granted in section 7.2.1 for achieving individual filter effluent (IFE) of 0.15 NTU 95% of the time and having no two consecutive measurements 15 minutes apart greater than 0.3 NTU. And an additional 0.5-log credit is granted in section 7.2.1 for achieving CFE of 0.15 NTU 95% of the time (US EPA, 2010).
- Ozone was operated to achieve at least 3-log reduction of viruses and 1.5-log reduction of *Giardia*. This is granted by controlling the ozone residual setpoint to achieve the desired

LRV by interpolation of Table C-13 in EPA Disinfection Profiling and Benchmarking Guidance Manual (Hogard et al., 2021).

- The design ultraviolet (UV) dose of 186 mJ/cm2 provides 4-log removal of viruses according to Table 1.4 of the *Ultraviolet Disinfection Guidance Manual for the Final LT2ESWTR* (US EPA, 2006). Extrapolation of this table estimates that 6-log *Cryptosporidium* and *Giardia* would be easily achieved at the design dose of 186 mJ/cm^2. Validation of UV disinfection was not performed in this study, because a previously validated reactor was used in the demonstration facility.

These values will likely change for future full-scale SWIFT installations that may include a slightly different treatment train. The possible LRV values for conventional and direct filtration are summarized in Table 1.

Table 1. Pathogen log-removal values for carbon-based treatment

Conventional Filtration					
	Coag/floc/sed + BAF	Ozone	UV	SAT	Total
Enteric virus	2	-	4	6	12
Cryptosporidium	4	-	4	6	14
Giardia	2.5	-	4	6	12.5
Direct Filtration					
	Coag/floc + BAF	Ozone	UV	SAT	Total
Enteric virus	1	1	4	6	12
Cryptosporidium	3.5	-	4	6	13.5
Giardia	2	-	4	6	12

2.2 Virus and Bacteria Analytical Methods

Quarterly sampling was performed at the 3.8 MLD SWIFT RC from 2018-2023 for each sample location shown in Figure 1. The wastewater plant raw water influent (RWI) is not shown on this diagram. The SWIFT sample location is post UV prior to final chemical addition. Sample volumes (50 mL aliquots and 1-1000 L concentrated) varied throughout the duration of this study. See

supplementary Table SI-1 for the range of sample volumes per location. They are reflected in the varying detection limits (within a location) shown in subsequent figures. Bacterial and viral pathogens and indicators were quantified by HRSD's water quality laboratory. Culture-based *E. coli* and total coliform were assayed using the 18-hour IDEXX Colilert-18 method. In general, the workflow for processing culture and molecular samples is shown in Figure 2. Samples were concentrated using dead-end ultrafiltration (DEUF) according to the methods described in a previous publication (Vaidya et al., 2019) and depicted in Figure 2. Coliphage samples were eluted from the DEUF filters using 200 mL elution solution, then male-specific and somatic coliphages were quantified using the single agar layer procedure (US EPA, 2018). For molecular processing, elution from the ultrafilter was done with FluidPrep High Volume Tris Elution Fluid (SKU HC08018-T; InnovaPrep, Drexel, MO, USA). The final elution volumes ranged between approximately 20-200 mL. Beef extract (BD-BBL Reference 212303) was added to each eluate at a concentration of 1.5 g/100 mL, then stirred for 10 minutes. The eluate was then centrifuged at 10,000 G for 10 minutes at 4°C. The supernatants were acidified to a pH of 3.5 with 20% HCl, then filtered through 0.8 um pore size mixed cellulose ester filters (AAWP04700; Millipore, Billerica, MA, USA). Immediately after concentration, the filters and centrifuged pellets were stored in a -80°C freezer until total nucleic extraction using a NucliSENS easyMag (bioMerieux, Inc., Durham, NC, USA). Details of nucleic acid extraction and inhibition controls have been described in a previous publication (Worley-Morse et al., 2019).

Droplet digital PCR (ddPCR) was used to enumerate adenovirus, rotavirus, norovirus GI and GII, pepper mild mottle virus (PMMoV), crAssphage, general Bacteroides (GenBac), 16S RNA, and *E. coli*. Assay primers and probes used include hepatitis G Armored RNA and Salmon Sperm DNA assays. DNA (ddPCR) and RNA (RT-ddPCR) molecular assays were analyzed on a Bio-Rad QX200 (Bio-Rad, Hercules, CA, USA) according to protocols in Worley-Morse et al. (2019) and Gonzalez et al., 2020. Filter and associated pellet concentrations were summed.

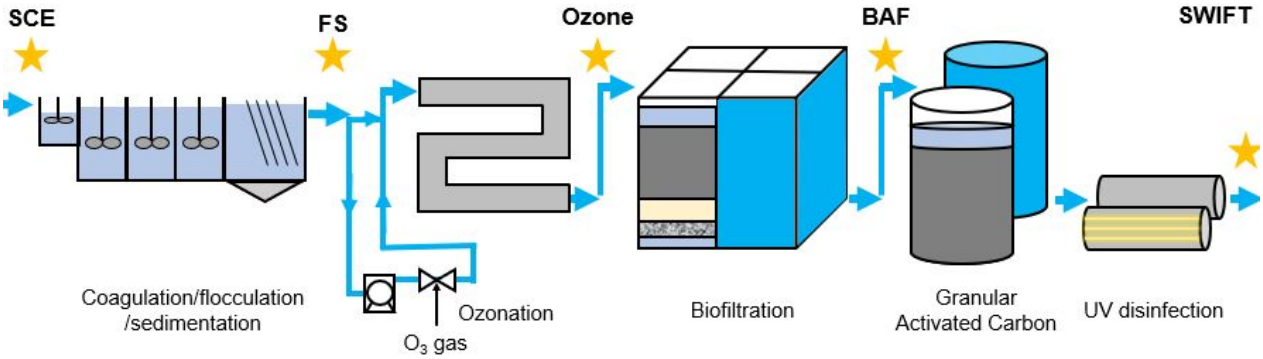

Figure 1. Process Flow Diagram with yellow stars indicating sample locations

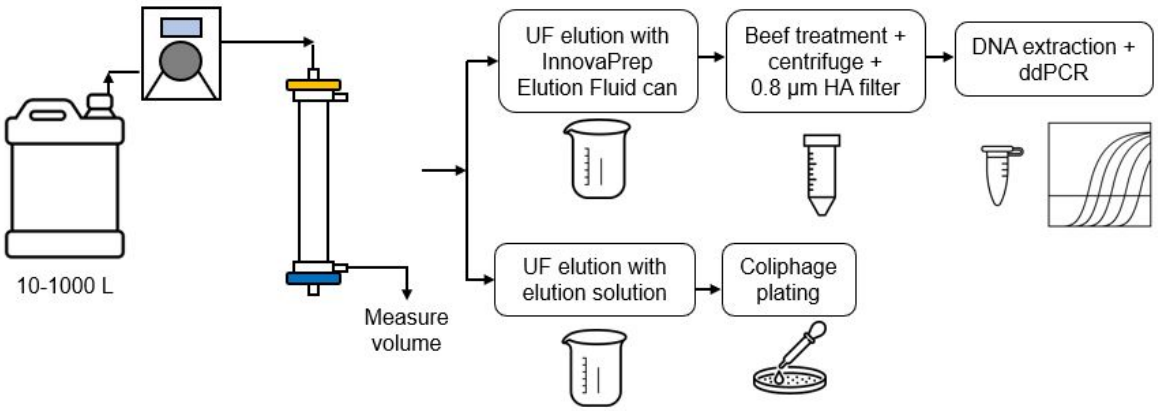

Figure 2. Coliphage and ddPCR workflow

2.2.1 Capsid Integrity ddPCR

Twenty sets of paired samples were collected on RWI, SCE, and pilot ozone effluent over the course of four days to capture a representative snapshot of ozone disinfection performance. RWI and SCE samples were aliquoted into microcentrifuge vials, two 1 mL replicates per sample, without further concentration. One of the replicates was placed in the -80°C freezer until nucleic acid extraction and the other was placed in the 4°C refrigerator until propidium monoazide (PMA) treatment which occurred within an hour of being received at the lab. To concentrate ozone samples, two 100 mL replicates were filtered using the InnovaPrep Concentrating Pipette (InnovaPrep, Drexel, MO, USA) with a 0.05 um hollow fiber filter (SKU CC08020-10; InnovaPrep), resulting in a final eluate volume of 1 mL after elution with InnovaPrep Tris Elution Fluid (SKU HC08001; InnovaPrep). For each sample, one of the eluates was placed in the -80°C freezer until

nucleic extraction and the second was placed in the 4°C refrigerator until PMA treatment within the hour.

One replicate of each sample was put through the PMA pre-treatment workflow. Triton X-100 (BP151-100, Fisher Scientific, Hampton, NH, USA) was added to the final eluate to a concentration of 0.5%. PMAxx (Cat: 40069, Biotium, Fremont, CA, USA) stock was diluted to a concentration of 10 mM and the samples were spiked to a final concentration of 100 µM. Samples were vortexed intermittently while incubated at room temperature for 15 minutes. All eluates were then placed in the PMA-Lite LED Photolysis Device (Cat: E90006, Biotium) where they remained under LED for 15 minutes of exposure time. Post-exposure, eluates were placed in the -80°C freezer until nucleic acid extraction with the non-exposed replicates.

2.3 Protozoan Analytical Methods

For regulatory quarterly monitoring samples, *Cryptosporidium* and *Giardia* were quantified in RWI, SCE, and SWIFT water with 1-10L samples. This analysis was performed by Eurofins Eaton Analytical, LLC according to EPA method 1623. Additional samples were collected using various concentration methods for *Cryptosporidium*, *Giardia*, and spore forming bacteria and were sent to Biological Consulting Services in Gainesville, FL. For secondary effluent samples, direct centrifugation and analysis of a 1 L sample was tested first. Subsequently larger volumes of water were concentrated using dead end ultrafiltration. BAF samples were also concentrated using high-volume dead-end ultrafiltration. Total aerobic spore forming bacteria were quantified using Standard Method 9218 and *C. perfringens* were quantified using method ASTM D5916.

2.4 Pilot Challenge Testing

Ozone pilot challenge testing was performed using the pilot setup and methods described previously (Hogard et al., 2023). Biofilter pilot challenge testing was performed on two identical filter columns filled with 1.5m (5ft) of pre-exhausted and biologically acclimated F816 GAC filter media (collected from the SRC biofilters) on top of 0.3m (1ft) of sand. In direct filtration operation, the filter was preceded by ozone, rapid mix, and two short flocculation tanks. Alum and

flocculation-aid polymer were added to rapid mix at concentrations of 1 mg/L-Al and 5 mg/L, respectively. These chemical doses were selected after extensive pilot testing showed sufficient charge neutralization and turbidity reduction in this range. Alum was selected for this application specifically due to enhanced orthophosphate removal observed when compared with other coagulants. In conventional filtration, the process flow mirrored that of the demonstration facility shown in Figure 1. Aluminum chlorohydrate (ACH) and coagulant-aid polymer were added to rapid mix at concentrations or 30 and 1 mg/L as product, respectively. Higher coagulant doses were used for coagulation here to facilitate TOC reduction in floc/sed. Both coliphage and *E.coli* were spiked in the filter influent using methods described in Hogard et al. (2023).

2.5 Data analysis

All statistical analyses were performed in R (R Core Team, 2021). The box in the boxplots represents the interquartile range (IQR), with the median denoted with the middle line. Lines represent the 25^{th} and 75^{th} percentile values +/- 1.5 the IQR. All points beyond these lines are considered outliers. If values were below detection limit, the detection limit was plotted and used to calculate these parameters. Dot plots are overlain the boxplots to show data distribution. Throughout the results and discussion, LRV was calculated between paired samples as $\log_{10}(C_0/C)$. Average LRV was then calculated for each treatment step. Using only paired samples for these calculations can result in LRV being overestimated or underestimated due to fluctuations in pathogen concentration. Therefore, additional methods for estimating LRV that consider the entire distribution of data were evaluated in Section 3.6 including (1) calculating the LRV for paired samples and fitting these values to a log-normal distribution, and (2) randomly sampling from the distributions of influent and effluent samples using a Monte Carlo simulation to create a lognormal distribution of possible LRV values as described in Bartolo & Kenny, (2020).

3. Results and Discussion

3.1 Coliform Bacteria

It should be noted that the only regulatory samples collected at the AWT process were total coliform (TC) and *E. coli* collected daily on SWIFT water. The facility is permitted to meet TC <1 CFU/100 mL for every sample collected on SWIFT water. Weekly samples were collected on the SCE sample point. The average SCE *E.coli* concentration was 5300 +/- 15470 CFU/100 mL. With these data alone, greater than 3 LRV of *E. coli* is demonstrated across the entire treatment process. Due to low influent concentrations, these data are limited as to what LRV can be calculated.

Full-scale testing was performed to evaluate the fate of *E. coli* in early treatment processes as shown in Figure 3. Paired samples comparing SCE to FS effluent show an average of 1.4 LRV by coagulation, flocculation, and sedimentation. This was during normal operating conditions with a floc-aid polymer dose of 1 mg/L and an ACH dose of 30 mg/L as product. Samples were also collected from the first and third flocculation basins to determine if the added chemicals were having any biocidal effect prior to sedimentation. Compared to the SCE concentration, 0.1 LRV was shown across the first flocculation basin and 0.5 LRV was seen across the third flocculation basin. This sampling event indicates there may be minimal inactivation resulting from the aluminum coagulant. This has been shown in previous studies to a minor extent (Matsui et al., 2003). This apparent reduction in the flocculation tanks may also be a result of sampling from the top of the flocculation basin when heavier flocs have already begun to settle. Another 1.4 LRV of *E. coli* was observed across ozonation in full-scale sampling. The low-level detections post ozone are believed to be a result of sample line contamination considering that >5 LRV of *E. coli* has been demonstrated on the pilot scale (Hogard et al., 2023).

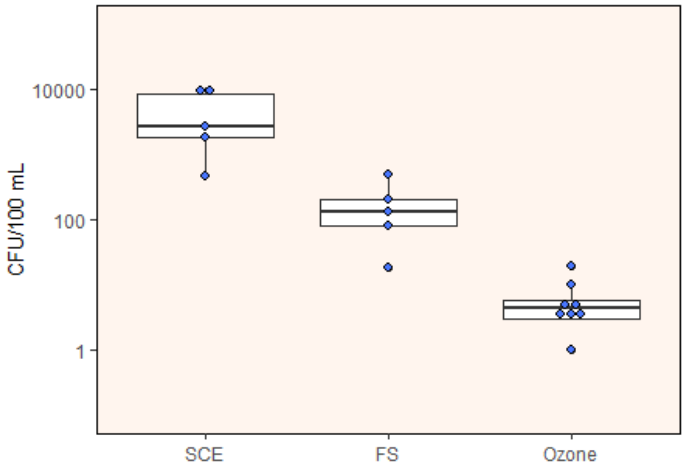

Figure 3. *E. coli* removal by coag/floc/sed and ozone

3.2 Protozoa and Spore Forming Bacteria

Average RWI concentration of *Cryptosporidium* and *Giardia* were 29.3 oocysts/L and $1.16*10^3$ cysts/L, respectively (Figure 4). These values are consistent with a recent study that found wastewater protozoa influent concentrations consistently lower than those used for risk models described previously (Teel et al., 2022). Across the wastewater treatment process, these values are reduced to an average *Cryptosporidium* and *Giardia* concentration of 0.44 oocysts/L and 8.83 cysts/L, respectively. When examining RWI/SCE samples, the average LRV demonstrated by the wastewater treatment process for *Cryptosporidium* and *Giardia* was approximately 1.5 and 2, respectively. These LRV values are also consistent with the study by Teel et al., (2022). Historical samples have been collected on SWIFT water quarterly that show no detections of either protozoan parasite in a 10 L sample volume. Additional sampling was performed using various concentration methods prior to analysis as summarized in Table 2. High volume ultrafiltration did not yield any greater quantification of *Cryptosporidium* or *Giardia* in the SCE compared to monitoring data. Further, high volume sampling on the BAF effluent also resulted in no detectable protozoa concentrations. With the low starting concentrations, it is only possible to demonstrate 1-2 LRV across the SWIFT treatment process by direct protozoa measurement.

Considering the low influent concentration of these pathogenic protozoa of interest, SFB have been used in water treatment applications as surrogate microorganisms that show similar trends for removal (Hijnen & Medema, 2010). As shown in Figure 5, the SCE concentrations of both aerobic SFB and C. perfringens are considerably higher when compared to Cryptosporidium and Giardia. When comparing paired samples, an average of approximately 1.6 LRV of both aerobic SFB and C. perfringens is demonstrated across coag/floc/sed suggesting that either of these organisms can be used for monitoring purposes. These results align with a study performed at a full-scale water treatment plant where 1-2 LRV of sulfite reducing clostridia was achieved by coagulation/flocculation (Hijnen & Medema, 2010). A review performed to evaluate microorganism reduction through water treatment processes found very similar results (average 1.4 LRV) when comparing multiple studies (Hijnen & Medema, 2010). The same study found slightly higher removal of Cryptosporidium and Giardia by coag/floc/sed (depending on operating conditions). Therefore, these bacterial surrogates can be considered a conservative indicator of physical removal by coag/floc/sed. Additionally, several studies have shown that bacterial spores can be used as an effective surrogate for Cryptosporidium inactivation by ozone (Hijnen et al., 2002). As shown in Figure 5, an average of >2 LRV was achieved for both microorganisms. Considering that these bacteria show similar inactivation trends as protozoan pathogens (Hijnen et al., 2007), these are a useful surrogate to indicate ozone disinfection performance. After ozone <1 LRV of C. perfringens can be demonstrated by biofiltration as most values in BAF effluent were nondetect. The concentration of aerobic SFB increased post biofiltration indicating that these microorganisms may populate and accumulate in the BAF making them an ineffective surrogate for BAF pathogen removal performance.

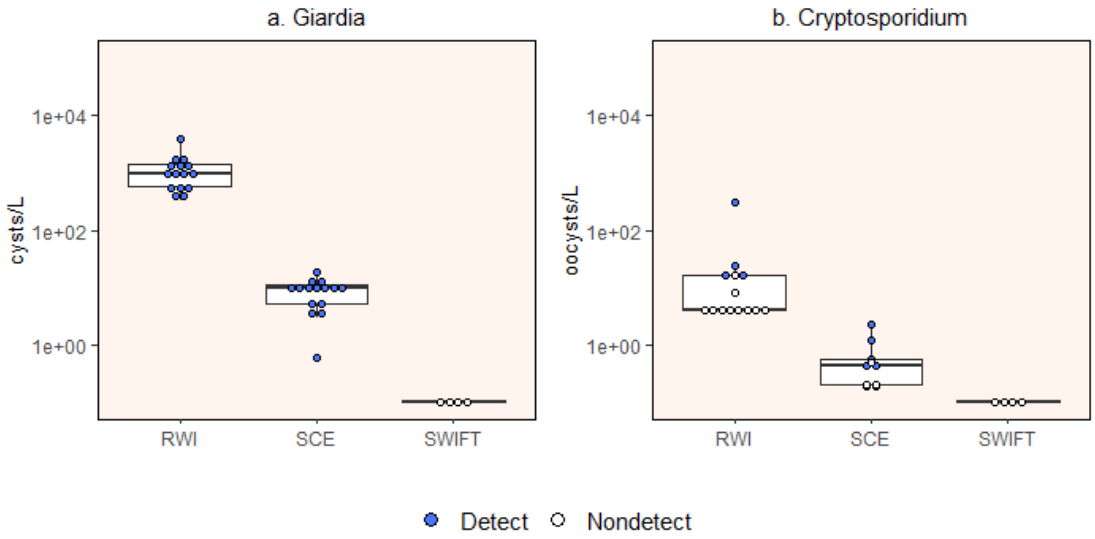

Figure 4. Protozoa monitoring data (a) *Giardia* and (b) *Cryptosporidium*

Table 2. *Crypto/Giardia* Monitoring Data

SCE			BAF Effluent		
[tqzr j% uwthjxxji%Q.	Hw~uyt% -tth~xyx465%Q.%	Lrfwirf -h~xyx465%Q.%	[tqzr j% uwthjxxji%Q.%	Hw~uyt% -tth~xyx465%Q.%	Lrfwirf -h~xyx465%Q.%
6%hjsywkzlj.	A65	A75	756%JH.%	A53:	A53:
66%ZK.%	A53>	A53>	6><%ZK.%	A53;	A53;
6=8%ZK.%	A5399	73;7	=;=%ZK.%	A536	A536

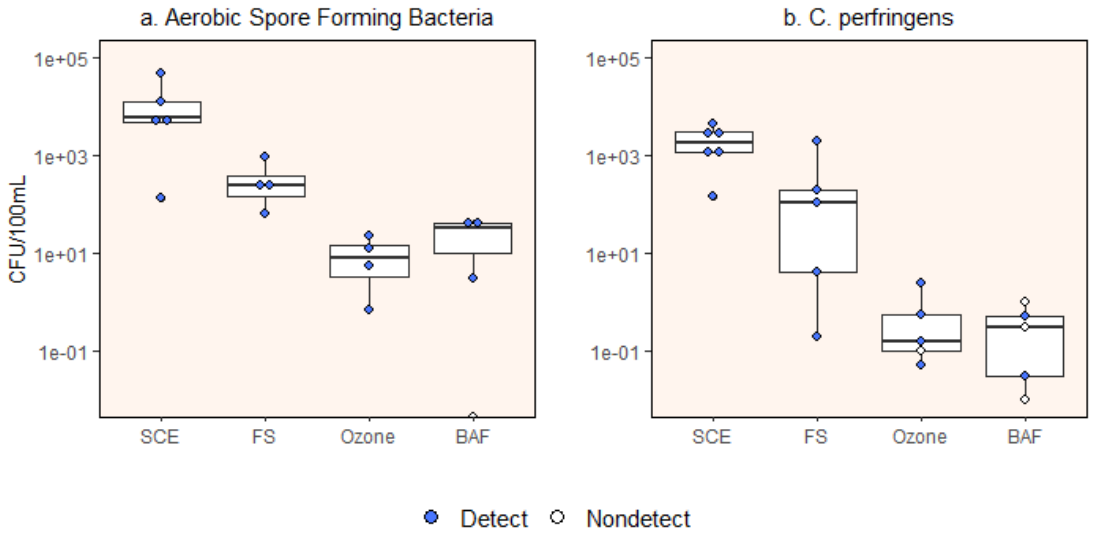

Figure 5. Spore forming bacteria monitoring data (a) aerobic spore forming bacteria and (b) *Clostridium perfringens*

3.3 Viruses and Coliphage

The molecular monitoring data for enteric viruses and surrogate viruses are presented in Figure 6 and 7, respectively. All enteric viruses shown were measured at average concentrations in the order of 10^4-10^5 gc/100 mL in the RWI. While each of these viruses span several orders of magnitude in concentration, no consistent seasonal trend was noted by visual examination alone. There are many factors that influence the concentration of viruses in wastewater including, the rate of infection in the region, season, socioeconomic status, and water use (Gerba et al., 2017). One study that monitored 11 viruses at two wastewater plants showed the plant virus, PMMoV, was the most prevalent virus in raw and treated wastewater (Kitajima et al., 2014). In this study, the only virus measured with a greater average concentration was crAssphage, a nonpathogenic virus which resides in the human gut at relatively high concentration (Dutilh et al., 2014). This virus is now recognized as ubiquitous in wastewater and well correlated with other human specific molecular and cultural human fecal indicators (Stachler et al., 2018). An average of 2 LRV was observed for all enteric viruses across the wastewater treatment process. The documented removal by wastewater treatment processes is variable between plant sites due to a wide range of treatment technologies employed (Rose et al., 2004; Scott et al., 2003; Worley-Morse et al.,

2019). PMMoV is a highly conservative surrogate in this study showing <1 LRV on average across the wastewater plant, whereas crAssphage showed an average ~3 LRV. Both male specific and somatic coliphage removal across the wastewater treatment process was greater than 2 LRV (Figure 8).

Relatively similar LRV values are observed across coag/floc/sed for the enteric viruses, surrogates, and coliphage (1-2 LRV) suggesting that the removal of these surrogate microorganisms can be used to deduce enteric virus reduction in full-scale applications. Ultimately, the LRV value achieved through coag/floc/sed will depend on multiple operating parameters including the selected coagulant, dose, and solids removal technology employed (e.g. lamella plates, dissolved air flotation) (Hijnen & Medema, 2010). It is notable, and expected, that there was insignificant removal of molecular targets observed across ozonation considering that ddPCR does not indicate viability intrinsically (Girones et al., 2010). Greater than 2 LRV of somatic coliphage can be observed through ozonation since this is a culture-based indicator. Additional experiments were performed at the pilot-scale and are described in subsequent sections to evaluate ozone LRV. An additional 1.7-3.3 LRV was demonstrated by BAF by means of filtering a larger volume of water and effectively lowering the detection limit post BAF. Given the challenges described regarding molecular methods, it is difficult to ascertain whether these LRV should be attributed to physical removal by BAF or inactivation by ozone prior to filtration. It should be noted that the only viral surrogate that is consistently detected beyond BAF is PMMoV indicating that it is highly stable and resistant to treatment when compared with enteric viruses (Kitajima et al., 2018; Shirasaki et al., 2020). Therefore, this plant virus can be regarded as a molecular “tracer” through the treatment process rather than an indicator of treatment efficacy.

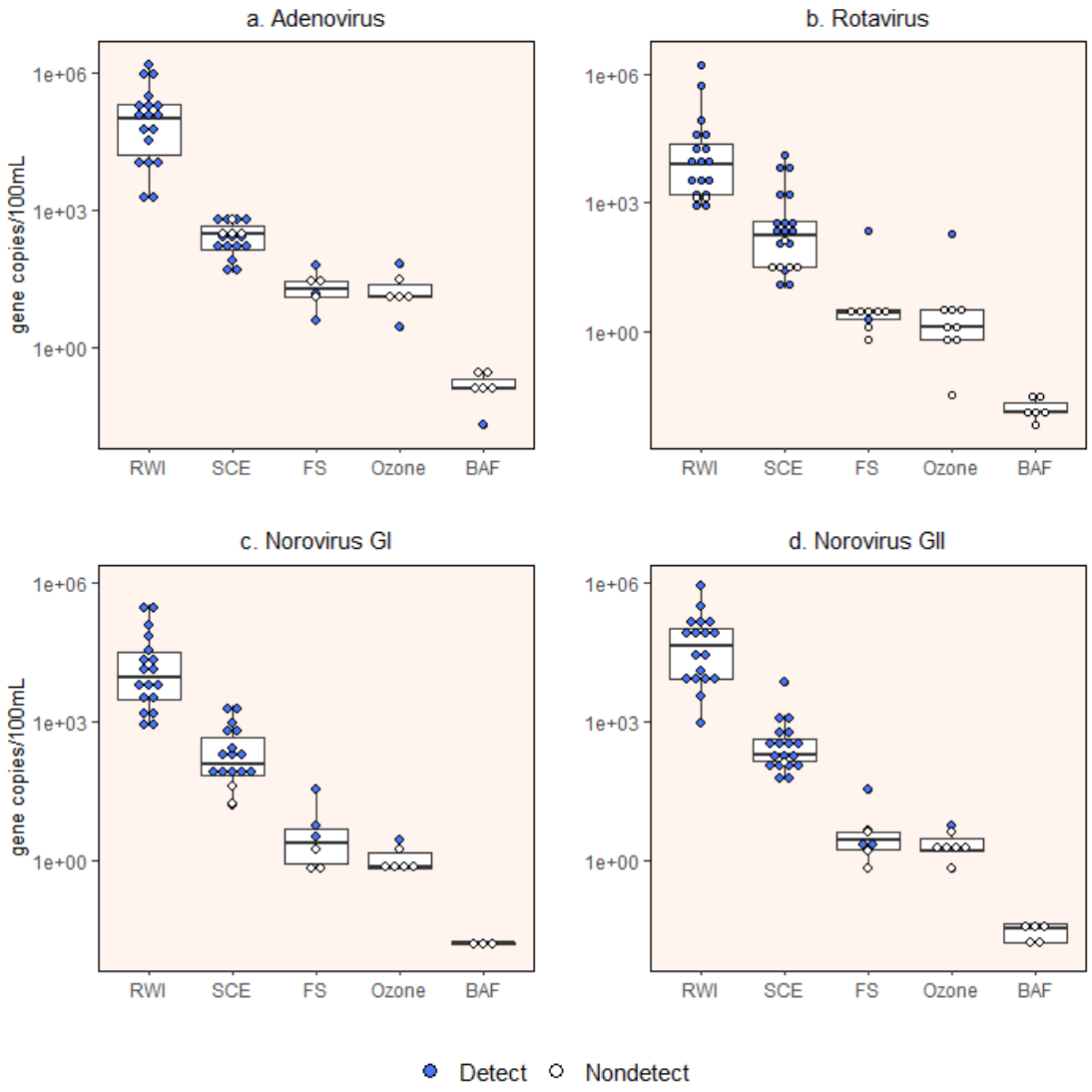

Figure 6. Enteric virus monitoring data (a) Adenovirus, (b) Rotavirus, (c) Norovirus GI, and (d) Norovirus GII

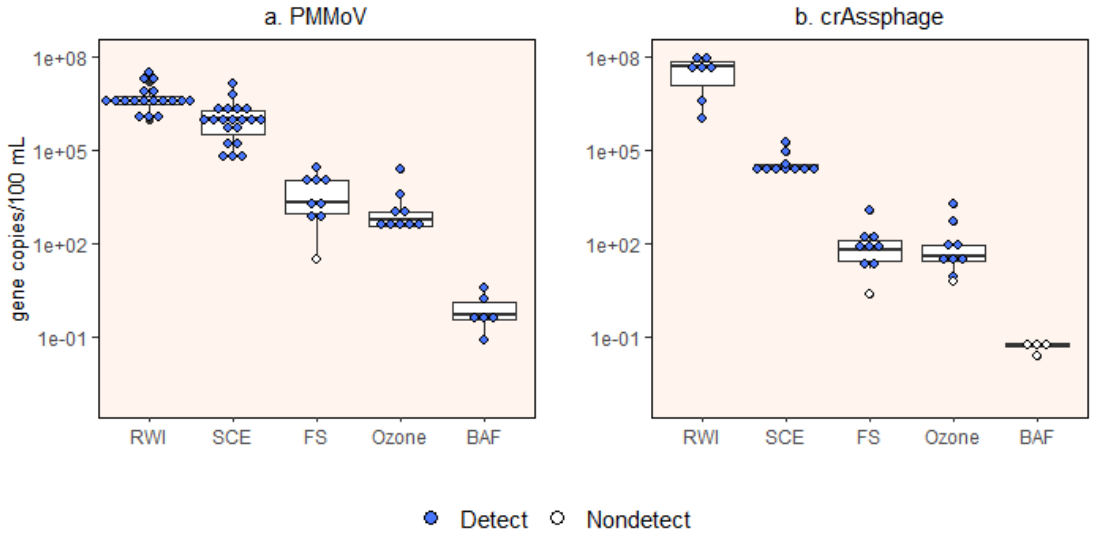

Figure 7. Viral molecular surrogate removal (a) PMMoV and (b) crAssphage

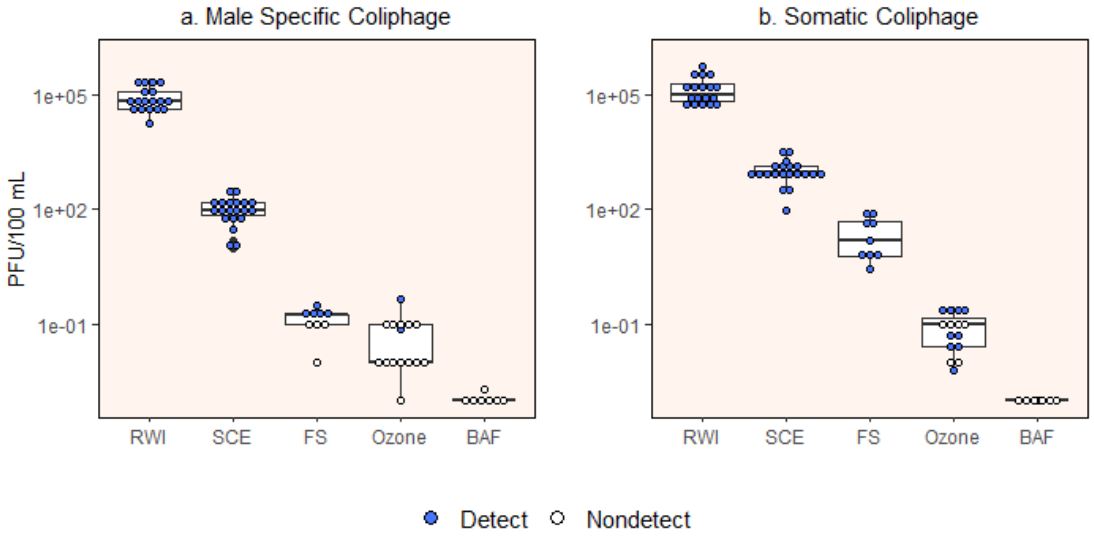

Figure 8. (a) Male specific and (b) somatic coliphage removal

Table 3. Average Virus LRV

		RWI-SCE	SCE-FS	FS-Ozone	Ozone-BAF	Total
Enteric viruses	Adenovirus	2.47	1.01	0.08	1.88	5.4
	NoVI	1.87	1.77	0.43	2.05	6.1
	NoVII	2.08	2.01	0.22	2.03	6.3
	Rotavirus	1.60	1.15	0.31	2.26	5.3
Viral surrogates	crassphage	2.90	2.77	0.00	3.31	9.0
	PMMoV	0.77	2.15	0.38	3.27	6.6
Coliphage	Male specific coliphage	2.91	2.79	0.41	1.67	7.8
	Somatic coliphage	2.14	1.69	2.38	1.80	8.0

3.4 Bacteria and Bacterial Surrogates

Although there are no established bacteria LRV requirements for potable reuse, the removal of pathogenic bacteria and bacterial surrogates was assessed across the wastewater treatment plant and the AWT process. The bacterial surrogate monitoring data are summarized in Figure 9 for GenBac, 16S rRNA, and *E. coli*. Due to the known ubiquity of these bacterial surrogates, they are detected at relatively higher concentration when compared to the viruses discussed previously. Figure 9 shows that each of these surrogates were extremely persistent throughout the treatment process with several log physical reduction observed by the wastewater treatment process and by coag/floc/sed. Here again, there was no appreciable reduction observed by ozonation and limited additional LRV shown through BAF. Given the persistence of these molecular markers through the treatment process, they can also be treated as extremely conservative treatment surrogates.

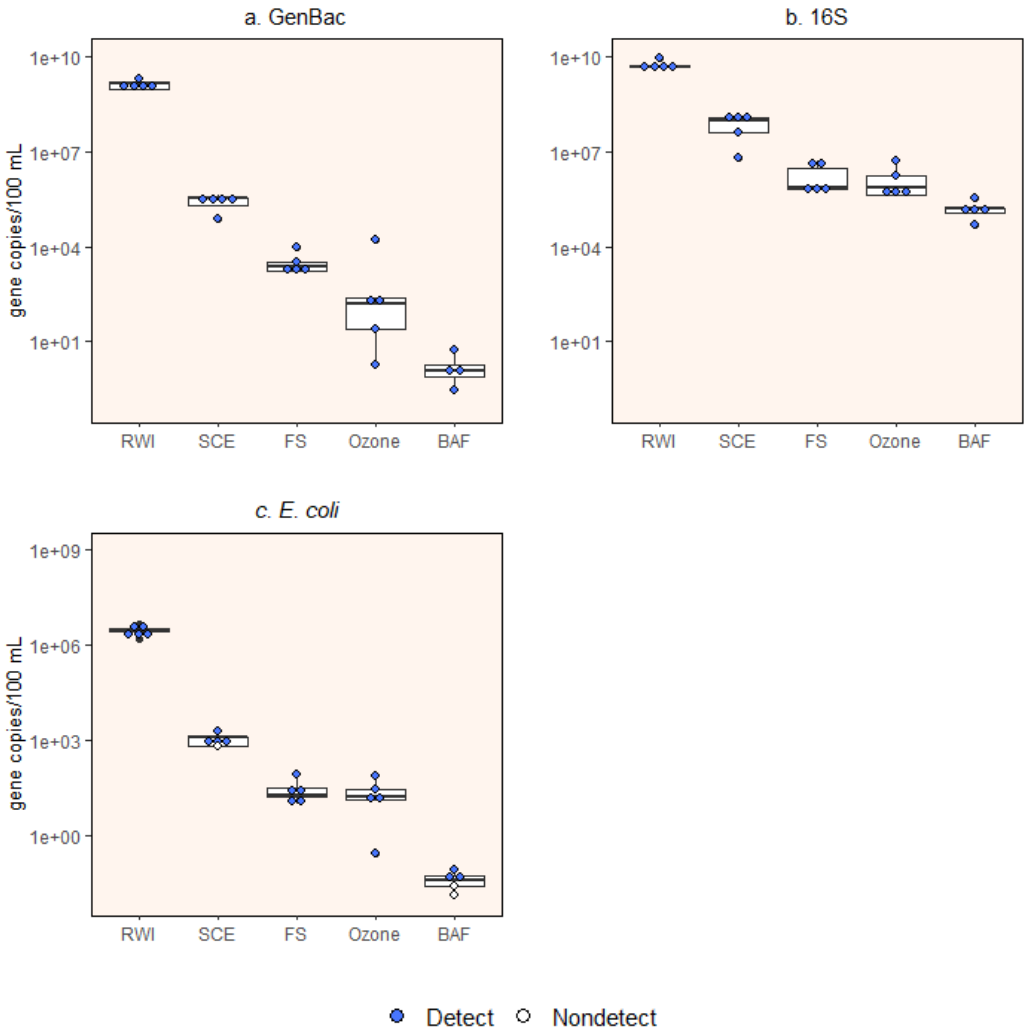

Figure 9. Bacterial molecular indicator removal

3.5 Treatment processes

3.5.1 Ozone

As discussed, there are several limitations associated with using the aforementioned methods to quantify inactivation by ozonation. In order to delineate uncompromised viruses versus compromised and extracellular nucleic acids using ddPCR, capsid integrity PCR was evaluated on the RWI, SCE, and ozone effluent sample points. This testing was conducted on the pilot to allow for the bypass of coag/floc/sed and manipulation of the ozone dose. As a result, the concentrations of the surrogate viruses were elevated and log reductions were observed, even in the control samples. Results are summarized for the control and PMA dosed samples in Figure

10 for both crAssphage and PMMoV. Capsid integrity (%) was calculated for each sample by dividing the PMA sample result by the control result. The average was then calculated for each sample location. CrAssphage capsid integrity ranged from 75% in the RWI to 25% and 65% for SCE and ozone samples, respectively. Considering that capsid integrity decreases across the wastewater plant, this suggests that the treatment process may preferentially remove intact viruses, or the viruses are being inactivated as shown by PMA-PCR. When comparing the mean control values at each sample location there is nearly 3 LRV of crAssphage observed across the wastewater process compared with >3.5 LRV when considering the PMA values. When calculating LRV across ozonation, approximately 2 LRV was achieved when considering the control and PMA values alike. PMMoV capsid integrity remained relatively constant from RWI (95%) to SCE (91%) and decreased to approximately 48% post ozonation suggesting capsid destruction may be the mode of ozone inactivation of PMMoV. The average LRV calculated across the wastewater plant for the control samples and the PMA samples was approximately 0.9 LRV. The LRV shown post ozone was 1-log for the control samples and increased to 1.4 LRV for the PMA samples. In this study, the LRV calculated for samples with and without PMA treatment is not significantly different.. Also, note PMA concentrations were lower than non-PMA controls for every sample location suggesting this method can be used to distinguish intact viruses vs compromised viral capsids in wastewater treatment and water reuse. For full-scale monitoring the use of PCR with intercalating dyes such as PMA can play an important role in determining the true LRV across oxidative inactivation processes. However, it should be noted that this method is still extremely conservative given that capsid integrity does not equate to viability but rather indicates an intact viral capsid (Leifels et al., 2021).

In addition to the capsid integrity analysis, samples were collected during pilot challenge tests while spiking MS2 and *E. coli* for a range of ozone doses (0.25-1 O3:TOC). These samples were analyzed by both conventional culture-based methods as well as ddPCR in order to establish a

relationship between loss of culturability and decrease in ddPCR signal. Figure 11 summarizes these LRV data for each sample. The regression equations for these data are shown below where y = inactivation measured by culture, and x = inactivation measured by molecular methods.

E. coli: y = 0.5x + 3

MS2: y = 0.8x + 2

If there was a perfect 1:1 correlation between the two methods, they would follow the dotted line shown in Figure 11. However, the LRV measured by culture-based methods plotted on the y-axis more accurately depict the inactivation achieved whereas the molecular results plotted on the x-axis are inherently conservative. The slope of the MS2 line shown in Figure 11 is approximately equal to 0.8 indicating that the rate of removal measured by ddPCR is nearly proportional to the inactivation measured by culture just shifted up by 2 units. Using the resulting regression equations, molecular LRV results can be effectively translated to LRV inactivation.

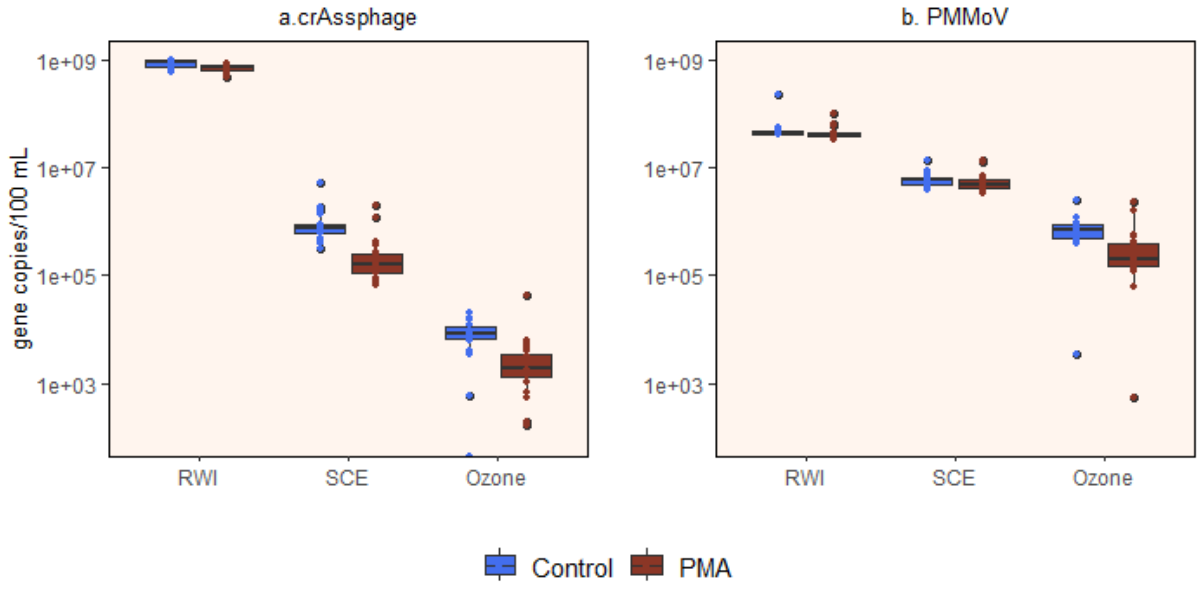

Figure 10. Capsid integrity PCR results for (a) crAssphage and (b) PMMoV

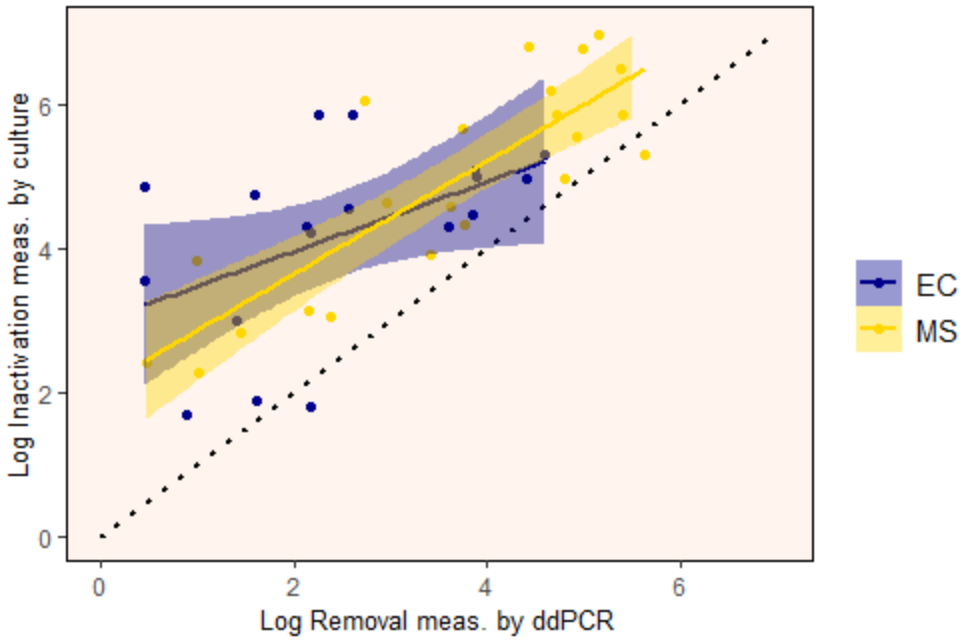

Figure 11. Correlation between ddPCR signal and culturability after ozonation.

3.5.2 BAF

Pilot scale challenge tests were performed to evaluate the removal of viruses and *E.coli* by biofiltration. In conventional filtration, BAF was preceded by coag/floc/sed and ozonation. Filter influent turbidity was relatively low (<0.5 NTU) in this case. Here, we show negligible virus and *E.coli* LRV across the filter (calculated as $\log\frac{BAF\ influent}{BAF\ effluent}$) throughout the filter run time of over 48 hours. These results are also aligned with those of Hijnen et al., (2010) where negligible removal of viruses or *E. coli* was observed in a pilot-scale exhausted GAC filter of similar contact time. The same study showed significant LRV of both *Cryptosporidium* oocysts and *Giardia* cysts that was attributed to attachment in the GAC media. It should be noted that the removal of added cultures may not exactly match that of indigenous viruses and bacteria that were coagulated upstream (and potentially particle-associated). The significant reduction by upstream coag/floc/sed and ozonation make it impossible to quantify the removal of these previously coagulated indigenous microorganisms.

In direct filtration, BAF was preceded by ozonation followed by a rapid mix tank where chemicals were added, and two short flocculation basins. In this case, biofilter influent turbidity was 1-2 NTU. Previous jar testing on this source water showed the chemical doses used effectively reduce zeta potential to nearly neutral values. Significant (>4 LRV) coliphage and *E. coli* removal was achieved consistently during the first 20 hours of the filter run. The inflection point of the turbidity line around this time indicates the point where chemical feed was intentionally stopped to simulate turbidity breakthrough. At that time, both male specific and somatic coliphage concentrations spiked in the filter effluent and there was <1 LRV observed across the filter. This reinforces the importance of coagulant and cationic polymer for particle destabilization prior to BAF for both turbidity reduction and virus/*E.coli* removal in direct filtration applications. This is consistent with previous fundamental studies showing that disrupting chemical feed ahead of filtration resulted in rapid decline in performance (Trussell et al., 1980). In this case, turbidity was a suitable process monitoring tool to ensure pathogen reduction targets are being met. The primary drawback to direct filtration is the elimination of the particle removal barrier of sedimentation which results in a treatment process that is more susceptible to failures.

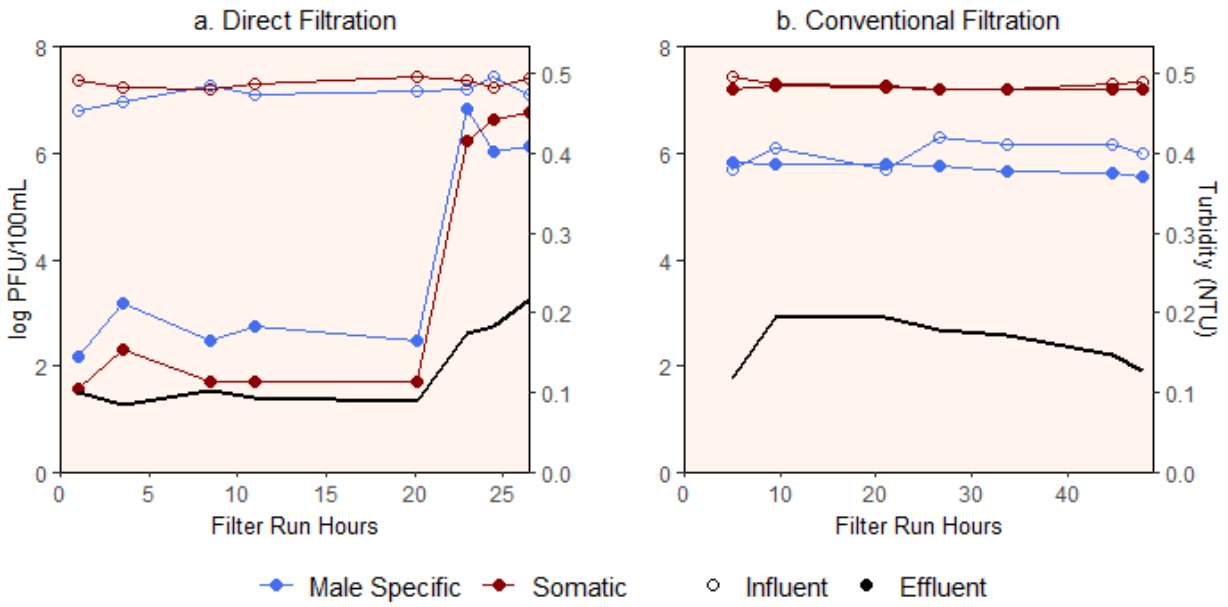

Figure 12. Coliphage and E. coli removal by pilot BAF in (a) direct filtration and (b) conventional filtration operation. Black lines show filter effluent turbidity.

3.6 Determining LRV in potable reuse

Validating pathogen removal in water reuse treatment processes remains a topic of active and evolving research as new methods emerge. The most appropriate method for crediting LRV for many advanced treatment processes is still being developed. One of the methods used in this study was adapted from Bartolo & Kenny, (2020) which was focused on determining LRV through wastewater treatment using monitoring data for indigenous pathogens and surrogates. These methods were described previously in Section 2.5. The results from both the pairwise subtraction method and the Monte Carlo method for the selected pathogens and surrogates is presented in the Supplementary Information (Table SI-1) and summarized for viruses only in Figure 13. The 5th percentile, median, and 95th percentile of the resulting distribution is included for each pathogen and surrogate. In most cases, the two approaches yielded similar results especially when calculating LRV between RWI-SCE and SCE-FS where ample monitoring data above detection are available for most constituents of interest. However, it should be noted that calculating LRV with paired data on a given day, can result in over or underestimation of the

apparent LRV. While using the Monte Carlo method to randomly pair influent and effluent samples eliminates this issue, it can result in a distribution of LRVs that are likely not possible (e.g. negative LRV). Therefore, the method used should be selected carefully depending on the quantity and quality of data available for each sample location. The results for *Cryptosporidium* and *Giardia* reduction across the wastewater process for the pairwise subtraction method (5th percentile 0.9 and 1.7 LRV, respectively) are relatively similar to those reported in a recent study in Nevada (0.5 and 2 LRV for *Cryptosporidium* and *Giardia* respectively) (Teel et al., 2022). For viruses, the resulting LRV for each method strongly depended on the availability of data above the detection limit. This is illustrated clearly in Figure 13, where relatively representative LRV values are calculated for RWI-SCE and SCE-FS, whereas the LRV values for FS-O3 and O3-BAF are much lower than expected as a result of pathogen/surrogate concentrations that are low or below detection limit. Again, this demonstrates the necessity of using high quality and representative monitoring data to establish LRV credits for each treatment process. In the case of ozone and biofiltration, the credited LRV can be ascertained from site-specific challenge testing when the capacity for full-scale monitoring is limited.

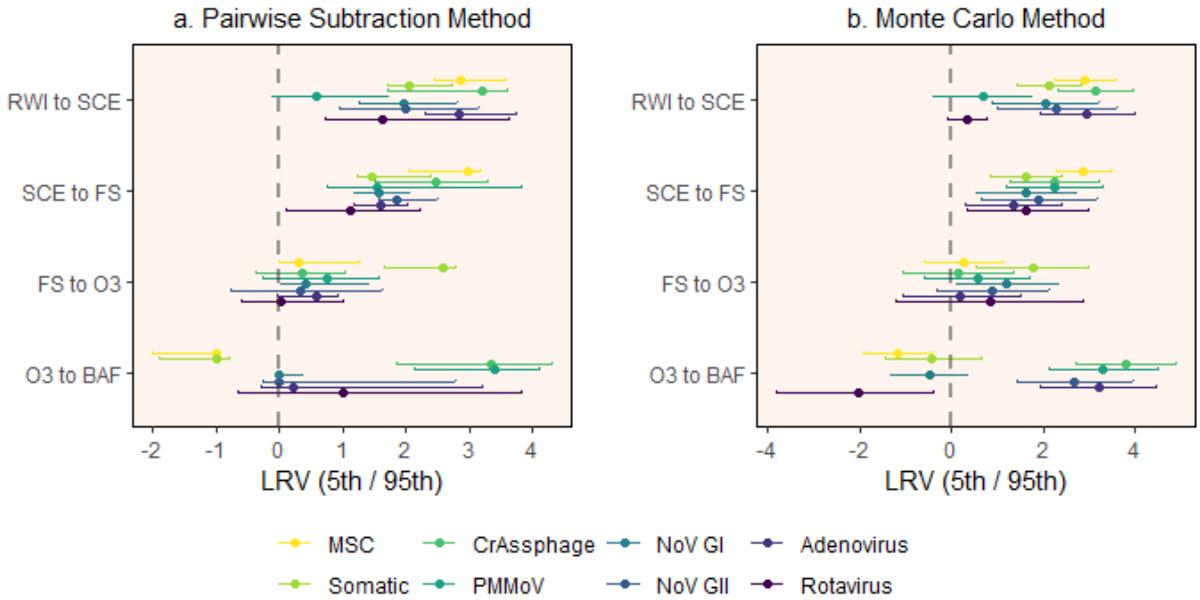

Figure 13. Virus LRV distributions calculated using pairwise subtraction method and Monte Carlo

method. Points indicate the median LRV, upper and lower bars denote the 95th and 5th percentile values.

4. Conclusion

This study provides full-scale validation of LRVs claimed in a carbon-based water reuse treatment train. Direct quantification of pathogens proved to be difficult as a result of low concentrations in raw wastewater, therefore large volume sampling was employed in an effort to determine LRV of pathogens and surrogates by both culture-based and molecular methods. Potential surrogate microorganisms were identified for full-scale monitoring purposes. The results of this study can be summarized as follows:

- The upstream wastewater plant was shown to be a significant barrier for protozoa, virus, and viral/bacterial surrogate reduction prior to AWT.
- Both aerobic spore forming bacteria and *C. perfringens* were identified as suitable conservative surrogate microorganisms for protozoa reduction by coag/floc/sed and inactivation by ozone.
- 1-2 LRV of enteric viruses was demonstrated by molecular methods across both coag/floc/sed and biofiltration. This was generally consistent with the LRV of the viral surrogates and coliphage shown across each of these processes. Therefore, direct measurement of enteric viruses by molecular methods, or examination of viral surrogates can be used to monitor physical removal of viruses and bacteria.
- Molecular methods were shown to greatly underestimate the viral inactivation provided by ozonation. Both capsid integrity PCR and relating molecular to culture-based results were presented as alternative approaches to surmise inactivation from molecular data.
- Challenge testing performed on the biofiltration pilot showed that in a conventional filtration treatment train, biofiltration alone would not provide a significant barrier against virus or bacteria removal. However, in the case of direct filtration with chemical addition and short

flocculation time ahead of the filter, significant virus and *E.coli* reduction were demonstrated.

References

Bartolo, M., & Kenny, J. (2020). *Additional Pathogen Monitoring at the North City Water Reclamation Plant - Draft Test Protocol Prepared by Trussell Technologies, Inc. for the San Diego Public Utilities*.

DPR Framework 2nd edition Addendum – Early Draft of Anticipated Criteria for Direct Potable Reuse, 3 1 (2021).

Canh, V. D., Torii, S., Yasui, M., Kyuwa, S., & Katayama, H. (2021). Capsid integrity RT-qPCR for the selective detection of intact SARS-CoV-2 in wastewater. *Science of The Total Environment*, *791*, 148342. https://doi.org/10.1016/j.scitotenv.2021.148342

Dutilh, B. E., Cassman, N., McNair, K., Sanchez, S. E., Silva, G. G. Z., Boling, L., Barr, J. J., Speth, D. R., Seguritan, V., Aziz, R. K., Felts, B., Dinsdale, E. A., Mokili, J. L., & Edwards, R. A. (2014). A highly abundant bacteriophage discovered in the unknown sequences of human faecal metagenomes. *Nature Communications*, *5*, 1–11. https://doi.org/10.1038/ncomms5498

EPA. (2017). *Potable Reuse Compendium*. 203. https://www.epa.gov/sites/production/files/2018-01/documents/potablereusecompendium_3.pdf

Gamage, S., Gerrity, D., Pisarenko, A. N., Wert, E. C., & Snyder, S. A. (2013). Evaluation of Process Control Alternatives for the Inactivation of Escherichia coli, MS2 Bacteriophage, and Bacillus subtilis Spores during Wastewater Ozonation. *Ozone: Science and Engineering*, *35*(6), 501–513. https://doi.org/10.1080/01919512.2013.833852

Gerba, C. P., Betancourt, W. Q., & Kitajima, M. (2017). How much reduction of virus is needed for recycled water: A continuous changing need for assessment? *Water Research*, *108*, 25–31. https://doi.org/10.1016/j.watres.2016.11.020

Gerrity, D., Crank, K., Steinle-Darling, E., & Pecson, B. M. (2023). Establishing pathogen log reduction value targets for direct potable reuse in the United States. *AWWA Water Science*, *5*(5), 1–16. https://doi.org/10.1002/aws2.1353

Gerrity, D., Pecson, B., Shane Trussell, R., & Rhodes Trussell, R. (2013). Potable reuse treatment trains throughout the world. *Journal of Water Supply: Research and Technology - AQUA*, *62*(6), 321–338. https://doi.org/10.2166/aqua.2013.041

Girones, R., Ferrús, M. A., Alonso, J. L., Rodriguez-Manzano, J., Calgua, B., de Abreu Corrêa, A., Hundesa, A., Carratala, A., & Bofill-Mas, S. (2010). Molecular detection of pathogens in water - The pros and cons of molecular techniques. In *Water Research* (Vol. 44, Issue 15, pp. 4325–4339). https://doi.org/10.1016/j.watres.2010.06.030

Haas, C. N., Rose, J. B., & Gerba, C. P. (2014). Quantitative microbial risk assessment. In *Routledge Handbook of Water and Health*. John Wiley & Sons, Ltd. https://doi.org/10.4324/9781315693606

Hijnen, W. A. M., Dullemont, Y. J., Schijven, J. F., Hanzens-Brouwer, A. J., Rosielle, M., & Medema, G. (2007). Removal and fate of Cryptosporidium parvum, Clostridium perfringens and small-sized centric diatoms (Stephanodiscus hantzschii) in slow sand filters. *Water Research*, *41*(10), 2151–2162. https://doi.org/10.1016/j.watres.2007.01.056

Hijnen, W. A. M., & Medema, G. J. (2010). *Elimination of Micro-organisms by Drinking Water Treatment Processes - A Review*. IWA Publishing.

Hijnen, W. A. M., Suylen, G. M. H., Bahlman, J. A., Hanzens-Brouwer, A. J., & Medema, G. J. (2010). GAC adsorption filters as barriers for viruses, bacteria and protozoan (oo)cysts in water treatment | Elsevier Enhanced Reader. *Water Research*, 1224–1234. https://reader.elsevier.com/reader/sd/pii/S004313540900671X?token=669D63C9CD1FEF907666C71DA5831A0BFA11C0FEAAFF175ACCEF795242FEC2FAB6E89FA7B9BF38A0DAD0236A41E74786&originRegion=eu-west-1&originCreation=20211101102427

Hijnen, W. A. M., Van der Veer, A. J., Van Beveren, J., & Medema, G. J. (2002). Spores of sulphite-reducing clostridia (SSRC) as surrogate for verification of the inactivation capacity of full-scale ozonation for Cryptosporidium. *Water Science and Technology: Water Supply*, *2*(1), 163–170. https://doi.org/10.2166/ws.2002.0021

Hogard, S., Pearce, R., Gonzalez, R., Yetka, K., & Bott, C. (2023). *Optimizing Ozone Disinfection in Water Reuse : Controlling Bromate Formation and Enhancing Trace Organic Contaminant Oxidation*. https://doi.org/10.1021/acs.est.3c00802

Hogard, S., Salazar-Benites, G., Pearce, R., Nading, T., Schimmoller, L., Wilson, C., Heisig-Mitchell, J., & Bott, C. (2021). Demonstration-scale evaluation of ozone–biofiltration–granular activated carbon advanced water treatment for managed aquifer recharge. *Water Environment Research*, 1–16. https://doi.org/10.1002/wer.1525

Kitajima, M., Iker, B., Pepper, I., & Gerba, C. P. (2014). Relative abundance and treatment reduction of viruses during wastewater treatment processes- Indentification of potential viral indicators. *Science of the Total Environment*, *488*, 290–296.

Kitajima, M., Sassi, H. P., & Torrey, J. R. (2018). Pepper mild mottle virus as a water quality indicator. *Npj Clean Water*, *1*(1). https://doi.org/10.1038/s41545-018-0019-5

Leifels, M., Cheng, D., Sozzi, E., Shoults, D. C., Wuertz, S., Mongkolsuk, S., & Sirikanchana, K. (2021). *Capsid integrity quantitative PCR to determine virus infectivity in environmental and food applications e A systematic review*. *11*.

Matsui, Y., MATSUSHITA, T., SAKUMA, S., GOJO, T., MAMIYA, T., SUZUOKI, H., & Inoue, T. (2003). *Virus Inactivation in Aluminum and Polyaluminum Coagulation*. 5175–5180.

Papp, K., Moser, D., & Gerrity, D. (2020). Viral Surrogates in Potable Reuse Applications: Evaluation of a Membrane Bioreactor and Full Advanced Treatment. *Journal of Environmental Engineering*, *146*(2), 1–11. https://doi.org/10.1061/(asce)ee.1943-7870.0001617

Pecson, B. M., Ackermann, M., & Kohn, T. (2011). Framework for using quantitative PCR as a nonculture based method to estimate virus infectivity. *Environmental Science and Technology*, *45*(6), 2257–2263. https://doi.org/10.1021/es103488e

R Core Team. (2021). *R: A language and environment for statistical computing*. https://www.r-project.org/.

Rockey, N., Young, S., Kohn, T., Pecson, B., Wobus, C. E., Raskin, L., & Wigginton, K. R. (2020). UV Disinfection of Human Norovirus: Evaluating Infectivity Using a Genome-Wide PCR-Based Approach. *Environmental Science and Technology*, *54*(5), 2851–2858. https://doi.org/10.1021/acs.est.9b05747

Rodriguez, R. A., Polston, P. M., Wu, M. J., Wu, J., & Sobsey, M. D. (2013). *An improved infectivity assay combining cell culture with real-time PCR for rapid quantification of human adenoviruses 41 and semi-quantification of human adenovirus in sewage*. *7*, 3–11.

Rose, J. B., Dickson, L., Farrah, S., & Carnahan, R. (2004). Removal of Pathogenic and Indicator Microorganisms by a Full-Scale Water Reclamation Facility. *Water Research*, *30*(11), 2785–2797.

Scott, T. M., McLaughlin, M. R., Harwood, V. J., Chivukula, V., Levine, A., Gennaccaro, A., Lukasik, J., Farrah, S. R., & Rose, J. B. (2003). Reduction of pathogens, indicator bacteria, and alternative indicators by wastewater treatment and reclamation processes. *Water Science and Technology: Water Supply*, *3*(4), 247–252. https://doi.org/10.2166/ws.2003.0069

Shirasaki, N., Matsushita, T., Matsui, Y., & Koriki, S. (2020). Suitability of pepper mild mottle virus as a human enteric virus surrogate for assessing the efficacy of thermal or free-chlorine disinfection processes by using infectivity assays and enhanced viability PCR. *Water Research*, *186*, 116409. https://doi.org/10.1016/j.watres.2020.116409

Stachler, E., Akyon, B., Carvalho, N. A. De, Ference, C., & Bibby, K. (2018). *Correlation of crAssphage qPCR Markers with Culturable and Molecular Indicators of Human Fecal Pollution in an Impacted Urban Watershed*. https://doi.org/10.1021/acs.est.8b00638

Symonds, E. M., Nguyen, K. H., Harwood, V. J., & Breitbart, M. (2018). *Pepper mild mottle virus : A plant pathogen with a greater purpose in (waste) water treatment development and public health management*. *144*.

Tandukar, S., Sherchan, S. P., & Haramoto, E. (2020). Applicability of crAssphage, pepper mild mottle virus, and tobacco mosaic virus as indicators of reduction of enteric viruses during wastewater treatment. *Scientific Reports*, *10*(1), 1–8. https://doi.org/10.1038/s41598-020-60547-9

Teel, L., Olivieri, A., Danielson, R., Delić, B., Pecson, B., Crook, J., & Pagilla, K. (2022). Protozoa reduction through secondary wastewater treatment in two water reclamation facilities. *Science of the Total Environment*, *807*. https://doi.org/10.1016/j.scitotenv.2021.151053

Trussell, R. R., Trussell, A. R., Lang, J. S., & Tate, C. H. (1980). *Recent developments in filtration system design*. *C*. https://doi.org/10.1002/j.1551-8833.1980.tb04617.x

US EPA. (2005). *Method 1623: Cryptosporidium and Giardia in Water by Filtration/IMS/FA*. *December*.

Long Term 2 Enhanced Surface Water Treatment Rule, 47640 (2006).

US EPA. (2006). *Ultraviolet disinfection guidance manual for the final long term 2 enhanced surface water treatment rule*. *November*.

US EPA. (2010). *Long Term 2 Enhanced Surface Water Treatment Rule Toolbox Guidance Manual*. http://water.epa.gov/lawsregs/rulesregs/sdwa/lt2/basicinformation.cfm

US EPA. (2014). *Method 1615: Measurement of Enterovirus and Norovirus Occurence in Water by Culture and RT-qPCR*.

US EPA. (2018). Method 1643: Male-specific (F+) and Somatic Coliphage in Recreational Waters and Wastewater by Ultrafiltration (UF) and Single Agar Layer (SAL) Procedure. *Office of Water*, *April*, 1–40. www.epa.gov

Vaidya, R., Buehlmann, P. H., Salazar-Benites, G., Schimmoller, L., Nading, T., Wilson, C. A., Bott, C., Gonzalez, R., & Novak, J. T. (2019). Pilot Plant Performance Comparing Carbon-Based and Membrane-Based Potable Reuse Schemes. *Environmental Engineering*

Science, *36*(11), 1369–1378. https://doi.org/10.1089/ees.2018.0559

Worley-Morse, T., Mann, M., Khunjar, W., Olabode, L., & Gonzalez, R. (2019). Evaluating the fate of bacterial indicators, viral indicators, and viruses in water resource recovery facilities. *Water Environment Research*, *91*(9), 830–842. https://doi.org/10.1002/wer.1096

Young, S., Torrey, J., Bachmann, V., & Kohn, T. (2020). Relationship Between Inactivation and Genome Damage of Human Enteroviruses Upon Treatment by UV254, Free Chlorine, and Ozone. *Food and Environmental Virology*, *12*(1), 20–27. https://doi.org/10.1007/s12560-019-09411-2

Chapter 5 Supplementary Information

Demonstrating pathogen reduction in flocculation/sedimentation, ozone, and biofiltration indirect potable water reuse treatment trains

Table SI-1 LRV Estimated using pairwise subtraction and lognormal Monte Carlo method

Cryptosporidium						
	Pairwise Subtraction			**LogNormal MC Method**		
Process Step	**5th Percentile**	**Median**	**95th Percentile**	**5th Percentile**	**Median**	**95th Percentile**
RWI -> SCE	0.885	1.602	2.508	0.339	1.589	2.831
SCE -> SWIFT	0.000	0.322	1.174	-0.249	0.463	1.172

Giardia						
	Pairwise Subtraction			**LogNormal MC Method**		
Process Step	**5th Percentile**	**Median**	**95th Percentile**	**5th Percentile**	**Median**	**95th Percentile**
RWI -> SCE	1.718	2.019	2.945	1.491	2.087	2.661
SCE -> SWIFT	1.276	1.994	2.195	1.573	1.914	2.264

MSC						
	Pairwise Subtraction			**LogNormal MC Method**		
Process Step	**5th Percentile**	**Median**	**95th Percentile**	**5th Percentile**	**Median**	**95th Percentile**
RWI -> SCE	2.443	2.859	3.567	2.241	2.9	3.543
SCE -> FS	2.044	2.969	3.182	2.297	2.879	3.471
FS -> O3	0.000	0.301	1.245	-0.578	0.273	1.113
O3 -> BAF	-2.000	-1.000	-1.000	-1.89	-1.15	-0.376

Somatic Coliphage						
	Pairwise Subtraction			**LogNormal MC Method**		
Process Step	**5th Percentile**	**Median**	**95th Percentile**	**5th Percentile**	**Median**	**95th Percentile**
RWI -> SCE	1.717	2.037	2.723	1.446	2.131	2.819
SCE -> FS	1.237	1.451	2.386	0.865	1.633	2.392
FS -> O3	1.638	2.581	2.786	0.534	1.780	2.967

O3 -> BAF	-1.910	-1.000	-0.789	-1.450	-0.416	0.662

CrAssphage						
	Pairwise Subtraction			**LogNormal MC Method**		
Process Step	**5th Percentile**	**Median**	**95th Percentile**	**5th Percentile**	**Median**	**95th Percentile**
RWI -> SCE	1.702	3.210	3.597	2.335	3.132	3.935
SCE -> FS	1.500	2.457	3.275	1.274	2.247	3.222
FS -> O3	-0.367	0.354	1.033	-1.033	0.148	1.341
O3 -> BAF	1.854	3.346	4.299	2.697	3.774	4.877

Adenovirus						
	Pairwise Subtraction			**LogNormal MC Method**		
Process Step	**5th Percentile**	**Median**	**95th Percentile**	**5th Percentile**	**Median**	**95th Percentile**
RWI -> SCE	2.303	2.835	3.724	1.92	2.956	3.984
SCE -> FS	1.163	1.584	2.022	0.292	1.346	2.382
FS -> O3	-0.040	0.574	0.921	-1.063	0.205	1.492
O3 -> BAF	-0.298	0.213	3.213	1.927	3.199	4.453

NoV GI						
	Pairwise Subtraction			**LogNormal MC Method**		
Process Step	**5th Percentile**	**Median**	**95th Percentile**	**5th Percentile**	**Median**	**95th Percentile**
RWI -> SCE	1.264	1.97	2.805	0.867	2.037	3.227
SCE -> FS	1.181	1.576	2.033	0.525	1.609	2.688
FS -> O3	0.010	0.404	1.388	0.117	1.214	2.307
O3 -> BAF	0.000	0.000	0.359	-1.312	-0.484	0.357

NoV GII						
	Pairwise Subtraction			**LogNormal MC Method**		
Process Step	**5th Percentile**	**Median**	**95th Percentile**	**5th Percentile**	**Median**	**95th Percentile**
RWI -> SCE	0.944	1.998	3.15	1.002	2.298	3.617
SCE -> FS	1.553	1.854	2.487	0.635	1.899	3.177
FS -> O3	-0.777	0.325	1.617	-0.328	0.896	2.106
O3 -> BAF	-0.259	0.000	2.791	1.422	2.686	3.957

PMMoV						
	Pairwise Subtraction			**LogNormal MC Method**		
Process Step	**5th Percentile**	**Median**	**95th Percentile**	**5th Percentile**	**Median**	**95th Percentile**
RWI -> SCE	-0.120	0.587	1.718	-0.396	0.687	1.752
SCE -> FS	0.760	1.549	3.809	1.177	2.228	3.271
FS -> O3	-0.261	0.739	1.577	-0.598	0.572	1.705

O3 -> BAF	2.137	3.403	4.095	2.142	3.304	4.498

Rotavirus						
	Pairwise Subtraction			**LogNormal MC Method**		
Process Step	**5th Percentile**	**Median**	**95th Percentile**	**5th Percentile**	**Median**	**95th Percentile**
RWI -> SCE	0.713	1.629	3.609	-0.093	0.338	0.758
SCE -> FS	0.087	1.119	2.220	0.327	1.619	2.970
FS -> O3	-0.600	0.004	1.008	-1.211	0.838	2.864
O3 -> BAF	-0.670	1.000	3.826	-3.786	-2.010	-0.384

Chapter 6 Conclusion and Engineering Significance

These studies demonstrate pathogen and microbial surrogate reduction in both full-scale and pilot-scale floc/sed-ozone-biofiltration advanced water treatment facility. This work shows that both culture and molecular-based methods are important tools for monitoring pathogen reduction in water reuse applications. Surrogate microorganisms for tracking virus (coliphage, PMMoV, crAssphage) and protozoa (aerobic spore forming bacteria, *C. perfringens*) reduction are proposed herein for monitoring purposes. Additionally, the suggested workflow for processing large volume samples is presented as guidance to utilities that seek to do the same. The noted limitations of full-scale monitoring also serve as important lessons learned in this field. Overall, these monitoring data will inform pathogen crediting for water reuse projects in the future including full-scale SWIFT application.

One of the major barriers to ozone implementation in water reuse is the formation of DBPs. This holistic study compared the use of NH_2Cl, and H_2O_2 for bromate control in a relatively high bromide water while examining the impact on disinfection and trace organics oxidation. Neither of these bromate control methods were shown to have a significant impact on virus or coliform inactivation, however there was negligible inactivation of spore forming bacteria when H_2O_2 was used as it eliminated measurable ozone exposure. Additionally, NH_2Cl was shown to suppress the oxidation of ozone resistant organic contaminants, while H_2O_2 marginally improved oxidation. Utilities that seek to use ozone disinfection in their water reuse treatment train can regard this study as a framework to determine the most effective strategy to control bromate formation while also achieving the desired treatment goals (oxidation, disinfection).

Finally, both changing water quality parameters and the use of H_2O_2 for bromate control warrants the creation of an alternative framework for ozone process control. In this study, the applied specific ozone dose and the change in UV_{254} absorbance were evaluated as ozone monitoring frameworks across a range of water quality characteristics. Both increasing temperature and pH

were shown to significantly impact ozone decay kinetics (and thus Ct) and marginally impede virus inactivation. The frameworks tested were shown to be useful across a range of water quality characteristics including temperature, pH, TOC, and TSS. The implementation of a non-Ct framework will allow for overall lower applied ozone doses and thus lower chemical costs. The capability for consistent and reliable ozone process monitoring will eliminate another implementation barrier.

The efforts described in this dissertation will allow for more widespread application and regulatory confidence in the carbon-based technology for water reuse. Additionally, ozone-biofiltration has been proposed as a polishing step in the RO treatment train, and this study shows how it can beneficially supplement that process for further pathogen reduction. Further demonstrating these processes opens the door for water reuse implementation in regions where the use of RO is not feasible or cost effective.

Appendix A. License Agreement for Chapter 2 Demonstration-scale evaluation of ozone–biofiltration–granular activated carbon advanced water treatment for managed aquifer recharge

6 pages

JOHN WILEY AND SONS LICENSE
TERMS AND CONDITIONS

Dec 18, 2023

This Agreement between Ms. Samantha Hogard ("You") and John Wiley and Sons ("John Wiley and Sons") consists of your license details and the terms and conditions provided by John Wiley and Sons and Copyright Clearance Center.

License Number	5692001245314
License date	Dec 18, 2023
Licensed Content Publisher	John Wiley and Sons
Licensed Content Publication	WATER ENVIRONMENT RESEARCH
Licensed Content Title	Demonstration-scale evaluation of ozone–biofiltration–granular activated carbon advanced water treatment for managed aquifer recharge
Licensed Content Author	Charles Bott, Jamie Heisig-Mitchell, Christopher Wilson, et al
Licensed Content Date	Feb 17, 2021
Licensed Content Volume	93
Licensed Content Issue	8
Licensed Content Pages	16

Type of use	Dissertation/Thesis
Requestor type	Author of this Wiley article
Format	Electronic
Portion	Full article
Will you be translating?	No
Title of new work	Validating Pathogen Reduction in Ozone-Biofiltration Water Reuse Applications
Institution name	Virginia Tech
Expected presentation date	Jan 2024
Requestor Location	Ms. Samantha Hogard 6909 Armstead Rd Suffolk, VA 23435 United States Attn: Ms. Samantha Hogard
Publisher Tax ID	EU826007151
Total	0.00 USD

Terms and Conditions

TERMS AND CONDITIONS

This copyrighted material is owned by or exclusively licensed to John Wiley & Sons, Inc. or one of its group companies (each a"Wiley Company") or handled on behalf of a society with which a Wiley Company has exclusive publishing rights in relation to a particular work (collectively "WILEY"). By clicking "accept" in connection with completing this licensing transaction, you agree that the following terms and conditions apply to this transaction (along with the billing and payment terms and conditions established by the

Copyright Clearance Center Inc., ("CCC's Billing and Payment terms and conditions"), at the time that you opened your RightsLink account (these are available at any time at http://myaccount.copyright.com).

Terms and Conditions

- The materials you have requested permission to reproduce or reuse (the "Wiley Materials") are protected by copyright.

- You are hereby granted a personal, non-exclusive, non-sub licensable (on a stand-alone basis), non-transferable, worldwide, limited license to reproduce the Wiley Materials for the purpose specified in the licensing process. This license, **and any CONTENT (PDF or image file) purchased as part of your order,** is for a one-time use only and limited to any maximum distribution number specified in the license. The first instance of republication or reuse granted by this license must be completed within two years of the date of the grant of this license (although copies prepared before the end date may be distributed thereafter). The Wiley Materials shall not be used in any other manner or for any other purpose, beyond what is granted in the license. Permission is granted subject to an appropriate acknowledgement given to the author, title of the material/book/journal and the publisher. You shall also duplicate the copyright notice that appears in the Wiley publication in your use of the Wiley Material. Permission is also granted on the understanding that nowhere in the text is a previously published source acknowledged for all or part of this Wiley Material. Any third party content is expressly excluded from this permission.

- With respect to the Wiley Materials, all rights are reserved. Except as expressly granted by the terms of the license, no part of the Wiley Materials may be copied, modified, adapted (except for minor reformatting required by the new Publication), translated, reproduced, transferred or distributed, in any form or by any means, and no derivative works may be made based on the Wiley Materials without the prior permission of the respective copyright owner.**For STM Signatory Publishers clearing permission under the terms of the STM Permissions Guidelines only, the terms of the license are extended to include subsequent editions and for editions in other languages, provided such editions are for the work as a whole in situ and does not involve the separate exploitation of the permitted figures or extracts,** You may not alter, remove or suppress in any manner any copyright, trademark or other notices displayed by the Wiley Materials. You may not license, rent, sell, loan, lease, pledge, offer as security, transfer or assign the Wiley Materials on a stand-alone basis, or any of the rights granted to you hereunder to any other person.

- The Wiley Materials and all of the intellectual property rights therein shall at all times remain the exclusive property of John Wiley & Sons Inc, the Wiley Companies, or their respective licensors, and your interest therein is only that of having possession of and the right to reproduce the Wiley Materials pursuant to Section 2 herein during the continuance of this Agreement. You agree that you own no right, title or interest in or to the Wiley Materials or any of the intellectual property rights therein. You shall have no rights hereunder other than the license as provided for above in Section 2. No right, license or interest to any trademark, trade name, service mark or other branding ("Marks") of WILEY or its licensors is granted hereunder, and you agree that you shall not assert any such right, license or

interest with respect thereto

- NEITHER WILEY NOR ITS LICENSORS MAKES ANY WARRANTY OR REPRESENTATION OF ANY KIND TO YOU OR ANY THIRD PARTY, EXPRESS, IMPLIED OR STATUTORY, WITH RESPECT TO THE MATERIALS OR THE ACCURACY OF ANY INFORMATION CONTAINED IN THE MATERIALS, INCLUDING, WITHOUT LIMITATION, ANY IMPLIED WARRANTY OF MERCHANTABILITY, ACCURACY, SATISFACTORY QUALITY, FITNESS FOR A PARTICULAR PURPOSE, USABILITY, INTEGRATION OR NON-INFRINGEMENT AND ALL SUCH WARRANTIES ARE HEREBY EXCLUDED BY WILEY AND ITS LICENSORS AND WAIVED BY YOU.

- WILEY shall have the right to terminate this Agreement immediately upon breach of this Agreement by you.

- You shall indemnify, defend and hold harmless WILEY, its Licensors and their respective directors, officers, agents and employees, from and against any actual or threatened claims, demands, causes of action or proceedings arising from any breach of this Agreement by you.

- IN NO EVENT SHALL WILEY OR ITS LICENSORS BE LIABLE TO YOU OR ANY OTHER PARTY OR ANY OTHER PERSON OR ENTITY FOR ANY SPECIAL, CONSEQUENTIAL, INCIDENTAL, INDIRECT, EXEMPLARY OR PUNITIVE DAMAGES, HOWEVER CAUSED, ARISING OUT OF OR IN CONNECTION WITH THE DOWNLOADING, PROVISIONING, VIEWING OR USE OF THE MATERIALS REGARDLESS OF THE FORM OF ACTION, WHETHER FOR BREACH OF CONTRACT, BREACH OF WARRANTY, TORT, NEGLIGENCE, INFRINGEMENT OR OTHERWISE (INCLUDING, WITHOUT LIMITATION, DAMAGES BASED ON LOSS OF PROFITS, DATA, FILES, USE, BUSINESS OPPORTUNITY OR CLAIMS OF THIRD PARTIES), AND WHETHER OR NOT THE PARTY HAS BEEN ADVISED OF THE POSSIBILITY OF SUCH DAMAGES. THIS LIMITATION SHALL APPLY NOTWITHSTANDING ANY FAILURE OF ESSENTIAL PURPOSE OF ANY LIMITED REMEDY PROVIDED HEREIN.

- Should any provision of this Agreement be held by a court of competent jurisdiction to be illegal, invalid, or unenforceable, that provision shall be deemed amended to achieve as nearly as possible the same economic effect as the original provision, and the legality, validity and enforceability of the remaining provisions of this Agreement shall not be affected or impaired thereby.

- The failure of either party to enforce any term or condition of this Agreement shall not constitute a waiver of either party's right to enforce each and every term and condition of this Agreement. No breach under this agreement shall be deemed waived or excused by either party unless such waiver or consent is in writing signed by the party granting such waiver or consent. The waiver by or consent of a party to a breach of any provision of this Agreement shall not operate or be construed as a waiver of or consent to any other or subsequent breach by such other party.

- This Agreement may not be assigned (including by operation of law or otherwise) by you without WILEY's prior written consent.

- Any fee required for this permission shall be non-refundable after thirty (30) days from receipt by the CCC.

- These terms and conditions together with CCC's Billing and Payment terms and conditions (which are incorporated herein) form the entire agreement between you and WILEY concerning this licensing transaction and (in the absence of fraud) supersedes all prior agreements and representations of the parties, oral or written. This Agreement may not be amended except in writing signed by both parties. This Agreement shall be binding upon and inure to the benefit of the parties' successors, legal representatives, and authorized assigns.

- In the event of any conflict between your obligations established by these terms and conditions and those established by CCC's Billing and Payment terms and conditions, these terms and conditions shall prevail.

- WILEY expressly reserves all rights not specifically granted in the combination of (i) the license details provided by you and accepted in the course of this licensing transaction, (ii) these terms and conditions and (iii) CCC's Billing and Payment terms and conditions.

- This Agreement will be void if the Type of Use, Format, Circulation, or Requestor Type was misrepresented during the licensing process.

- This Agreement shall be governed by and construed in accordance with the laws of the State of New York, USA, without regards to such state's conflict of law rules. Any legal action, suit or proceeding arising out of or relating to these Terms and Conditions or the breach thereof shall be instituted in a court of competent jurisdiction in New York County in the State of New York in the United States of America and each party hereby consents and submits to the personal jurisdiction of such court, waives any objection to venue in such court and consents to service of process by registered or certified mail, return receipt requested, at the last known address of such party.

WILEY OPEN ACCESS TERMS AND CONDITIONS

Wiley Publishes Open Access Articles in fully Open Access Journals and in Subscription journals offering Online Open. Although most of the fully Open Access journals publish open access articles under the terms of the Creative Commons Attribution (CC BY) License only, the subscription journals and a few of the Open Access Journals offer a choice of Creative Commons Licenses. The license type is clearly identified on the article.

The Creative Commons Attribution License

The Creative Commons Attribution License (CC-BY) allows users to copy, distribute and transmit an article, adapt the article and make commercial use of the article. The CC-BY license permits commercial and non-

Creative Commons Attribution Non-Commercial License

The Creative Commons Attribution Non-Commercial (CC-BY-NC)License permits use, distribution and reproduction in any medium, provided the original work is properly cited and is not used for commercial purposes.(see below)

Creative Commons Attribution-Non-Commercial-NoDerivs License

The Creative Commons Attribution Non-Commercial-NoDerivs License (CC-BY-NC-ND) permits use, distribution and reproduction in any medium, provided the original work is properly cited, is not used for commercial purposes and no modifications or adaptations are made. (see below)

Use by commercial "for-profit" organizations

Use of Wiley Open Access articles for commercial, promotional, or marketing purposes requires further explicit permission from Wiley and will be subject to a fee.

Further details can be found on Wiley Online Library
http://olabout.wiley.com/WileyCDA/Section/id-410895.html

Other Terms and Conditions:

v1.10 Last updated September 2015

Questions? customercare@copyright.com.

Appendix B. Ozone disinfection of waterborne pathogens and their surrogates: A critical review

Morrison, C. M., Hogard, S., Pearce, R., Gerrity, D., von Gunten, U., & Wert, E. C. (2022). Ozone disinfection of waterborne pathogens and their surrogates: A critical review. Water Research, 214(November 2021), 118206. https://doi.org/10.1016/j.watres.2022.118206

13 pages

Water Research 214 (2022) 118206

Contents lists available at ScienceDirect

Water Research

journal homepage: www.elsevier.com/locate/watres

Ozone disinfection of waterborne pathogens and their surrogates: A critical review

Christina M. Morrison [a,*], Samantha Hogard [b,c], Robert Pearce [b,c], Daniel Gerrity [a], Urs von Gunten [d,e], Eric C. Wert [a]

[a] Southern Nevada Water Authority (SNWA), P.O. Box 99954, Las Vegas, NV 89193-9954, USA
[b] Civil and Environmental Engineering Department, Virginia Polytechnic Institute and State University, Blacksburg, VA, USA
[c] Hampton Roads Sanitation District, P.O. Box 5911, Virginia Beach, VA 23471-0911
[d] Eawag, Swiss Federal Institute of Aquatic Science and Technology, Ueberlandstrasse 133, CH-8600 Dubendorf, Switzerland
[e] School of Architecture, Civil and Environmental Engineering (ENAC), Ecole Polytechnique Fédérale de Lausanne (EPFL), 1015 Lausanne, Switzerland

ARTICLE INFO

Key Words:
Ozone
Disinfection
Cryptosporidium
Giardia
Virus
Pathogen

ABSTRACT

Viruses, *Giardia* cysts, and *Cryptosporidium parvum* oocysts are all major causes of waterborne diseases that can be uniquely challenging in terms of inactivation/removal during water and wastewater treatment and water reuse. Ozone is a strong disinfectant that has been both studied and utilized in water treatment for more than a century. Despite the wealth of data examining ozone disinfection, direct comparison of results from different studies is challenging due to the complexity of aqueous ozone chemistry and the variety of the applied approaches. In this systematic review, an analysis of the available ozone disinfection data for viruses, *Giardia* cysts, and *C. parvum* oocysts, along with their corresponding surrogates, was performed. It was based on studies implementing procedures which produce reliable and comparable datasets. Datasets were compiled and compared with the current USEPA Ct models for ozone. Additionally, the use of non-pathogenic surrogate organisms for prediction of pathogen inactivation during ozone disinfection was evaluated. Based on second-order inactivation rate constants, it was determined that the inactivation efficiency of ozone decreases in the following order: Viruses >> *Giardia* cysts > *C. parvum* oocysts. The USEPA Ct models were found to be accurate to conservative in predicting inactivation of *C. parvum oocysts and viruses, respectively,* however they overestimate inactivation of *Giardia* cysts at ozone Ct values greater than ~1 mg min L^{-1}. Common surrogates of these pathogens, such as MS2 bacteriophage and *Bacillus subtilis* spores, were found to exhibit different inactivation kinetics to mammalian viruses and *C. parvum* oocysts, respectively. The compilation of data highlights the need for further studies on disinfection kinetics and inactivation mechanisms by ozone to better fit inactivation models as well as for proper selection of surrogate organisms.

1. Introduction

Ozone has been widely applied as a disinfectant for water treatment for more than a century (Rakness, 2015; von Gunten, 2003a; von Sonntag and von Gunten, 2012) and more recently in wastewater and water reuse applications (Burns et al., 2007; Gerrity et al., 2012; von Gunten, 2018). In the United States, a shift to alternative disinfectants (i.e., non-chlorine), including ozonation, was driven by regulations implemented by the United States Environmental Protection Agency (USEPA). These required drinking water utilities to optimize inactivation of protozoan pathogens and viruses relative to the potential formation of disinfection byproducts (DBPs) primarily related to chlorine disinfection (USEPA, 2006, 1999, 1991). Moreover, ozone treatment provides auxiliary benefits including transformation of bulk organic matter and oxidation of trace organics and taste and odor compounds (Camel and Bermond, 1998; Lee et al., 2013; Lee and von Gunten, 2016; von Gunten, 2003b; von Sonntag and von Gunten, 2012).

Viruses, *Giardia* cysts, and *Cryptosporidium parvum* oocysts are all major causes of waterborne diseases that can be uniquely challenging in terms of inactivation/removal during water and wastewater treatment and water reuse (Betancourt, 2019; Efstratiou et al., 2017; Leclerc et al., 2002; Soller et al., 2017). Ozone is acknowledged as an effective

* Corresponding author.
E-mail address: christina.morrison@snwa.com (C.M. Morrison).

https://doi.org/10.1016/j.watres.2022.118206
Received 16 November 2021; Received in revised form 14 February 2022; Accepted 15 February 2022
Available online 18 February 2022

disinfectant for bacteria, encysted protozoans, as well as viruses (von Sonntag and von Gunten, 2012). However, direct comparison of results from ozone disinfection studies is challenging due to the complexity of aqueous ozone chemistry in addition to the variety of different approaches utilized to conduct such studies. The goal of this review is to systematically analyze available ozone disinfection literature by reviewing studies that implemented procedures producing reliable and comparable datasets. Specifically, the review aims to evaluate: (a) bench-scale inactivation kinetics of the three regulated pathogen groups (viruses, *Giardia*, and *Cryptosporidium*) and their potential surrogates in buffered ultrapure water or surface water, (b) mechanisms of inactivation, and (c) current research needs as indicated by data gaps in the ultimate findings of this review.

2. Background

In the United States, the shift to alternative drinking water disinfectants was driven by USEPA treatment regulations. Over time, these regulations specified the required abatement of viruses, *Giardia* cysts, and *C. parvum* oocysts and defined maximum contaminant levels (MCLs) for DBPs. This rigorous approach is unique to the USA and only partially applied in other countries, where ozone is commonly applied as a disinfectant for drinking water treatment (von Sonntag and von Gunten, 2012). Amendments to the Surface Water Treatment Rule (SWTR) required drinking water treatment plants to achieve removal and/or inactivation of at least 4 $\log_{10}$ for virus and 3 $\log_{10}$ for *Giardia* cysts. The SWTR also introduced the "Ct" concept to establish predicted pathogen inactivation levels based on the concentration of the applied disinfectant (C) and the contact time (t), which in the case of full-scale systems is the retention time at which 10% of the volume has passed through the reactor basin, which must be determined via tracer studies (See SI S.1). In response to major outbreaks of cryptosporidiosis traced back to contaminated water resources (Hrudey et al., 2003; Mac Kenzie et al., 1994), the Interim Enhanced Surface Water Treatment Rule, and eventually the Long Term 2 Enhanced Surface Water Treatment Rule (LT2ESWTR) were introduced, extending removal requirements and Ct models to *C. parvum* oocysts and requiring at least 2 $\log_{10}$ abatement (USEPA, 2006, 1998).

Despite its properties as a strong oxidant and disinfectant, there are several ozone characteristics that make the study of its disinfection efficiency difficult. Ozone is unstable in water and decomposes rapidly, thereby making it difficult to accurately measure and characterize its exposure (von Sonntag and von Gunten, 2012). Furthermore, ozone decomposition leads to the formation of hydroxyl radicals, another powerful oxidant that can contribute to disinfection and/or oxidation (Hoigné and Bader, 1975; Staehelin and Hoigne, 1985; von Gunten, 2003b). Water quality characteristics such as pH, temperature, dissolved organic matter (DOM) concentration/composition, among others, are major drivers of ozone decay and hydroxyl radical formation during ozonation (Elovitz et al., 2000; Staehelin and Hoigne, 1985). Hydroxyl radicals provide a significant benefit during ozonation by enhancing the oxidation of organic constituents (Huber et al., 2003; von Gunten, 2003b), however the impact of hydroxyl radicals on disinfection is not well established. In general, it is assumed that hydroxyl radical exposure can be neglected for disinfection of drinking water because of the typically high efficiency of direct ozone reactions and its diffusion limitation (von Gunten, 2003a).

There are several kinetic models that can be utilized to model the inactivation of a particular organism and the proper model heavily depends on the disinfectant utilized, the target organism, and the method of application (Gyürek and Finch, 1998). The USEPA assumes a second-order (or pseudo first-order in certain cases) rate law (Equation 1) to model the inactivation of viruses, *Giardia* cysts, and *C. parvum* oocysts in water:

$$\frac{dN}{dt} = -kNC \tag{1}$$

where N is the number of viable organisms at time t, C is the concentration of disinfectant at time t, and k is the second-order inactivation rate constant. Integrating the rate equation with the assumption that the disinfectant concentration remains constant over time provides a model in which the disinfectant exposure, or Ct (concentration x contact time, discussed further below), can be used to predict the log-reduction of pathogens:

$$\int_{N_0}^{N} \frac{dN}{N} = -kC \int_{0}^{t} dt \tag{2a}$$

$$\ln\left(\frac{N}{N_0}\right) = -kCt \tag{2b}$$

or

$$log_{10}\left(\frac{N}{N_0}\right) = -\frac{k}{\ln(10)}Ct \tag{2c}$$

There are more complex models that account for non-linear disinfection kinetics (i.e., shouldering and tailing behaviors, see Gyürek and Finch, 1998), however, the necessity to fit anywhere from 1 - 3 empirical constants, with a lack of description as to what these constants physically represent makes such models difficult to apply to full-scale disinfection processes. Therefore, the second-order disinfection model has been regularly utilized to estimate disinfection efficacy despite sometimes obvious and often unexplainable deviations from a linear relationship, particularly when evaluating ozone disinfection. Some of these problems are related to the instability of ozone in water, which complicates the application of the disinfection kinetic models used to describe and predict inactivation of different microorganisms. One case in point is the formation of hydroxyl radicals, which need to be scavenged (e.g., by the addition of tertiary butanol (*t*-BuOH) or DMSO) when trying to isolate the contribution from ozone, specifically (Wolf et al., 2018). Kinetic studies carried out in absence of such a hydroxyl radical scavenger are fundamentally problematic to determine second-order inactivation rate constants. Furthermore, pH and temperature are two factors which need to be carefully monitored, because of their effect on ozone stability and inactivation kinetics (von Sonntag and von Gunten, 2012).

The rapid decay of ozone makes the determination of the Ct value (i.e., ozone exposure) in real reactors more complicated than simply multiplying the final residual concentration and contact time (i.e., the "effluent" method), which underestimates the true ozone exposure due to ozone instability in solution. Ozone decay can be taken into consideration for Ct determination through the following:

$$C(t) = C_0 e^{-k't} \tag{3}$$

where C(t) is the concentration of ozone at time (t), C_0 is the initial ozone concentration, and k' is the first-order ozone decay rate constant. Accounting for time dependence of C in (1) by substituting (3) into (2a) and integrating results in:

$$ln\frac{N}{N_0} = -k\frac{C_0}{k'}\left(1 - e^{-k't}\right) \tag{4}$$

which is equivalent to the area under the ozone decay curve (if ozone exhibits first order decay). The "integral method" requires the collection of a time series of ozone residual measurements throughout the reaction time for accurate calculation of the decay rate constant. Other methods for estimating the area under the ozone decay curve can be utilized to estimate ozone exposure, particularly when ozone does not display first-order decay (von Gunten and Hoigne, 1994).

Alternative methods of Ct calculation encountered in bench-scale ozone disinfection studies include calculating the geometric mean of the initial and final ozone residual and multiplying by the elapsed time, which is a simple and relatively accurate method if ozone displays first-order decay as described above and can also be used at full scale with respect to different reaction chambers (Rakness et al., 2005). Other methods include estimating C as the arithmetic mean of the initial and final ozone residual, as well as simply substituting the final residual. The variety in Ct calculations among studies adds an additional layer of complexity for comparison of data, more so if the Ct calculation method is not specified.

The inactivation rate constants (*k*) utilized to predict microorganism inactivation are typically derived from bench-scale studies evaluating log inactivation vs. Ct. There are several methods for evaluating ozone disinfection at bench-scale, with specific implications associated with each method. Bench-scale studies include (but are not limited to) true batch, semi-batch, and quench-flow reactor systems. True batch tests are conducted by applying a pre-determined dose of aqueous ozone to a closed batch reactor with constant agitation. The aqueous ozone stock solution is produced by bubbling gaseous ozone/oxygen gas mixture through ultrapure water in a chilled reactor to obtain an aqueous ozone concentration in equilibrium to the gas phase concentration according to Henry's law (Hoigne and Bader, 1994; Rakness, 2015; von Sonntag and von Gunten, 2012). Due to the instability of ozone in aqueous solutions, proper determination of ozone exposure during a batch test should include a time series of ozone residual measurements (Hoigne and Bader, 1994; von Sonntag and von Gunten, 2012). Additionally, the added stock solution produces a diluting effect on the test solution which must be accounted for.

One limitation to batch systems is the inability to accurately characterize the initial phase of ozone decay, low-exposure scenarios, and examining fast reacting compounds or microorganisms (Buffle et al., 2006; Hoigne and Bader, 1994). These problems have been addressed using continuous quench-flow systems or reaction systems in which the ozone exposure was controlled by addition of an ozone-reactive compound (e.g., cinnamic acid) (Buffle et al., 2006; Criquet et al., 2015; Czekalski et al., 2016; Torii et al., 2020; Wolf et al., 2018). In quench-flow systems, a mixed sample/ozone solution is pumped with a fixed velocity/flow regime through a thin reaction tube, the length of which can be altered to allow for different contact times. This system is ideal for evaluating fast reacting compounds, however, proper implementation can be challenging, and special consideration should be given to mixing and flow characteristics through the reaction tube. Careful calibration with known ozone reactions is required (Buffle et al., 2006; Criquet et al., 2015).

Semi-batch tests are conducted by applying ozone gas directly to the test solution, allowing the system to reach steady state (i.e., the dissolved ozone in solution remains constant with time), and directly applying organism to the constant gas/ozone mixture (Rakness, 2015). Ozone exposure can be estimated based on the steady state aqueous ozone residual and contact time. A benefit to this approach is the reduction in effort necessary to account for ozone decay within the system. Additionally, there is no need to account for a dilution effect that occurs when dosing with an aqueous stock solution. However, such systems require greater expertise for proper implementation; improper design and implementation can produce misleading results. For instance, if the solution is not fully saturated, the determined kinetics are a mixture of both ozone mass transfer and inactivation. Additionally, for many inactivation processes, the steady-state concentrations in the reactor are very high and require extremely low residence times to achieve realistic ozone exposures, which is often not feasible. Therefore, the preferred method for evaluating inactivation kinetics of microorganisms by ozone is through the use of true-batch systems (for slower inactivating/more resistant microbes such as *C. parvum* oocysts), and modified batch systems (i.e., addition of cinnamic acid) or quench-flow systems (for faster inactivating/less resistant microbes, such as viruses).

There are many parameters that can influence the efficacy of ozone treatment, including pH, temperature, alkalinity, and other intrinsic properties of the water matrix. These parameters generally affect ozone demand/decay or oxidant scavenging kinetics. When pH decreases, ozone becomes more stable (Staehelin and Hoigne, 1985). The role of pH with respect to inactivation of microorganisms is unclear. pH can influence the surface properties of microorganisms (Harden and Harris, 1952; Hsu and Huang, 2002; Michen and Graule, 2010; Righetti and Caravaggio, 1976), however, the extent to which this influences reactivity with ozone is not well understood. Temperature also plays an important role in the stability of ozone in aqueous solutions. Increasing temperature increases the first-order ozone decay rate which therefore reduces the stability of ozone in solution. However, increased temperature also increases the rate of ozone inactivation for microorganisms (Finch and Li, 1999; Li et al., 2001; Roy et al., 1982). Therefore, temperature changes will affect inactivation kinetics in a complex interplay between ozone stability and susceptibility of microorganisms.

Other water quality parameters, such as dissolved organic matter (DOM), are more complex with respect to ozone stability and hence disinfection efficacy (von Gunten, 2003b; von Sonntag and von Gunten, 2012). Therefore, disinfection studies in DOM-containing matrices can be difficult to conduct and interpret. In addition, interaction of microorganisms with organic matter (e.g., coating of membranes) may alter the susceptibility of microorganisms to ozone. In DOM-heavy matrices such as wastewater, it may be difficult to establish an ozone Ct with low ozone doses due to rapid ozone demand/decay. However, these low Ct or 'sub-residual' dosing scenarios can still achieve inactivation of some microorganisms (Gerrity et al., 2012), potentially necessitating alternative crediting frameworks. This is also the case when ozone is supplemented with hydrogen peroxide to preferentially drive the formation of hydroxyl radicals (i.e., advanced oxidation process), drastically reducing (or eliminating) ozone Ct (Acero and von Gunten, 2001). At the bench scale, many of these issues can be avoided by using quench-flow reactors to understand disinfection kinetics in the early reaction phase.

An empirical approach avoiding complications with ozone chemistry relies on non-Ct based frameworks for obtaining disinfection credit in such cases. For example, Gamage et al. (2013) and Gerrity et al. (2012) evaluated the correlation of non-Ct based parameters such as O_3:DOC ratio, ΔUV_{254} absorbance, and ΔTF (total fluorescence) with inactivation of *B. subtilis* spores, *Escherichia coli*, and MS2 during wastewater ozonation. Another study evaluated ΔUV_{254} absorbance and oxidation of carbamazepine as surrogate parameters to evaluate disinfection of viruses in surface water and wastewater (Wolf et al., 2019). Despite the potential value of these emerging non-Ct frameworks, this review focuses on characterizing ozone disinfection efficacy based on the more traditional Ct framework.

3. Methods

3.1. Literature review

Literature was compiled with the goal of analyzing ozone disinfection efficacy for three pathogen groups regulated in water treatment (i.e., viruses, *Giardia* cysts, and *C. parvum* oocysts), and their potential surrogates. Web of Science core collection was searched during September 2020 using search criteria containing a combination of the following key words: Ozon* AND water AND (inactivation OR kinetics OR disinfection) AND (virus OR protozoa OR pathogen OR bacteria OR microb* OR adenovirus OR enterovirus OR calicivirus OR MS2 OR B. subtilis OR giardia OR cryptosporidium). Articles which were peer-reviewed, written in English, and published after the year 1980 were considered for inclusion within the review. Search results were subjected to an initial screening of the titles and abstracts. Articles were included for full-text review if the title and/or abstract indicated (a) ozone was among the disinfectants being analyzed, (b) disinfection in water was evaluated (i.e., excluding ozone as a surface disinfectant or in

the gas phase), and (c) microbial inactivation was analyzed (i.e., excluding proxies for microbial disinfection). The "Materials & Methods" sections of selected articles were evaluated via random assignment between three reviewers. The evaluated articles were organized by (a) whether disinfection kinetics or mechanisms were evaluated, (b) scale of research (i.e., bench-, pilot-, or full-scale), (c) reactor set-up (i.e., batch vs. semi-batch vs. quench-flow vs. miscellaneous), and water matrix (i.e., buffered ultra-purified water vs. surface water vs. wastewater; pH ranges of 5-8; use of hydroxyl radical scavengers). The publications which evaluated disinfection kinetics in buffered ultra-purified water or surface water in batch or quench-flow reactors at bench-scale were selected for further analyses. Due to the aforementioned complexities of ozone in DOM heavy matrices, studies evaluating wastewater were excluded. Articles which evaluated inactivation mechanisms of ozone for the different pathogen groups were also selected for further review. Articles that did not fall into either of these categories were omitted from the review. The reviewing process and the applied selection criteria are summarized in Figure S1. Additionally, while the core literature search was performed in September 2020, there were no additional relevant publications identified in a subsequent search spanning September 2020 through January 2022.

3.2. Data analysis

To explore the state-of-the-art of bench-scale inactivation of viruses, *Giardia* cysts, and *C. parvum* oocysts by ozone, analyses of $\log_{10}$ inactivation as a function of ozone Ct/exposure, as well as reported inactivation rate constants, were conducted. Articles which measured the disinfection kinetics in bench-scale settings (i.e., not inactivation mechanisms) were subject to additional screening which examined (a) the ability of ozone Ct/exposure data to be extracted or calculated directly from the article, (b) the method of ozone Ct/exposure calculation utilized/allowed for with the provided data (i.e., if Ct was not calculated within the manuscript, Ct was calculated to the best of our ability using the provided residual data), (c) proper implementation of the batch reactor or quench-flow reactor set-up, (d) utilization of methods which either directly examine or infer microbe viability (i.e., exclusion of molecular methods), and (e) basic water quality parameters such as temperature and pH.

The analyses consisted of the determination and comparison of ozone Ct/exposure values and corresponding survival ratios (provided as $\log_{10}(N/N_0)$) and second-order inactivation rate constants (k). If applicable, ozone Ct data and second-order inactivation rate constants were extracted directly from the article. If ozone Ct data were provided/calculated using the integral Ct method, this value was prioritized, otherwise priority was given in the following order: geometric mean Ct > arithmetic mean Ct (select studies which only provided Ct information in such form) > final residual ("effluent") Ct. If not provided in a study, second-order inactivation rate constants were calculated in R using least squares linear regression. Datasets with at least five data points were selected for determination of second-order inactivation rate constants. If the resultant inactivation slope (i.e., k) could not be determined statistically different ($p < 0.05$) from 0, the dataset was excluded. If the regression model had a non-significant ($p > 0.05$) y-intercept, the model was fitted through the origin. Otherwise, the y-intercept model was accepted under the assumption that a positive y-intercept provides a more conservative estimate of inactivation based on the resulting reduced slope, and a negative y-intercept indicates the presence of a lag-phase. Data which contained a significant lag-phase (i.e., a phase in which no inactivation occurs despite of ozone Ct/exposure) were fitted to the delayed Chick Watson model (Rennecker et al., 1999), with the Ct_{lag} value provided:

$$ln\frac{N}{N_0} = \begin{cases} 0; if\ Ct \le Ct_{lag} \\ -k(Ct - Ct_{lag}); if\ Ct > Ct_{lag} \end{cases} \quad (5)$$

The USEPA Ct models for ozone disinfection of viruses, *Giardia* cysts, and *C. parvum* oocysts, described in the SWTR and LT2ESWTR were utilized for comparison of the extracted inactivation data:

$$LRV_{virus} = 2.1744 \times 1.0726^{Temp} \times CT \quad (6)$$

$$LRV_{Giardia} = 1.0380 \times 1.0741^{Temp} \times CT \quad (7)$$

$$LRV_{Cryptosporidium} = 0.0397 \times 1.09757^{Temp} \times CT \quad (8)$$

Extracted data were grouped based on organism and temperature, regardless of pH.

4. Results and discussion

4.1. Literature review and data analysis

The aforementioned search criteria yielded 1,399 articles, which were subsequently reviewed through several iterations (Figure S1). This ultimately resulted in 28 articles from which inactivation vs. ozone Ct/exposure data and/or second-order inactivation rate constants were extracted, as well as 10 articles that evaluated ozone inactivation mechanisms for specific pathogen groups. Datasets from each organism were separated into three temperature ranges: 1-9 °C, 10-19 °C, and 20-25 °C. The pH examined in the different datasets ranged from 5 – 8. Due to the overall lack of data, datasets with and without hydroxyl radical scavengers were ultimately grouped together, which could introduce an additional source of variation within datasets, even though the contribution of hydroxyl radical to inactivation is likely minimal.

4.2. Inactivation of viruses

While viruses encompass a variety of morphologies that may influence their resistance to disinfectants (Sigstam et al., 2013), to remain consistent with USEPA categorization, all mammalian virus data were compiled together regardless of viral species. For analyses of mammalian virus surrogates, bacteriophage data were analyzed separately. Six studies met inclusion criteria for the development of $\log_{10}$ inactivation plots and/or inactivation rate constant compilation (Helmer and Finch, 1993; Lim et al., 2010; Sigmon et al., 2015; Torii et al., 2020; Wolf et al., 2018; Young et al., 2020). Six mammalian viruses were evaluated, including coxsackieviruses B3 and B5 (laboratory and environmental strains), poliovirus 1, echovirus 11, human adenovirus 2, and murine norovirus. Bacteriophages MS2, fr, Qβ, GA, φX174, T4, T1, and PRD1 were evaluated. All inactivation data were collected using cell culture most probable number (MPN) or plaque assays respective to each virus type. Experiments were conducted in either batch or quench-flow reactors.

Fig. 1a-d provide an overview of the compiled $\log_{10}$ inactivation of viruses as a function of ozone Ct (i.e., exposure) for three temperature ranges. Overall, viruses are highly reactive with ozone, indicating that efficient inactivation occurs even at very low ozone Ct/exposure. The USEPA models shown as dashed line in Fig. 1a-d provide a conservative estimate of virus inactivation, underestimating inactivation in most cases. The USEPA model was developed using data from Roy et al. (1982), who evaluated poliovirus inactivation using a CSTR. Because of the reactor setup, this study did not pass our article selection process and was therefore not analyzed. Torii et al. (2020) discussed the shortcomings in how the data from this study was utilized for USEPA models, including the use of the average hydraulic residence time as a substitution for the contact time, which would lead to an overestimation of ozone Ct/exposure. Hydraulic considerations, combined with incomplete mixing, and the additional safety factor of 3 applied by the USEPA, may account for the overly conservative nature of the model.

The data points which cluster directly at or below the USEPA models for temperatures ranging from 20 – 25 °C (Fig. 1c) belong to a single study examining murine norovirus inactivation. These data imply that

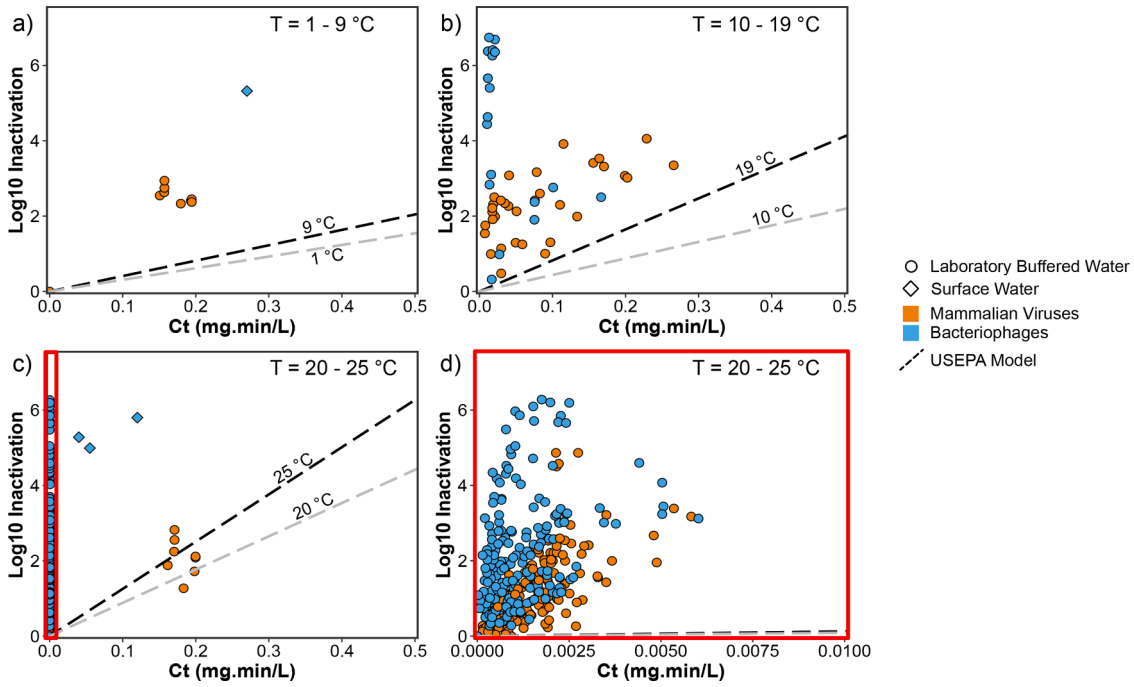

Fig. 1. Virus inactivation by ozone at pH 5-8: $\log_{10}$ inactivation as a function of ozone Ct for viruses at (a) 1-9 °C, (b) 10-19 °C, (c) 20-25 °C (d) 20-25 °C (magnified to highlight low Ct range).

murine noroviruses may be relatively less susceptible to ozone inactivation than other mammalian viruses. However, the ozone Ct/exposure values determined from this study may be inaccurate. Specifically, the study suggests that with ozone decay constants upwards of 5 min^{-1} and an applied ozone dose of 1 mg L^{-1}, there was still measurable ozone residual at the end of the experimental contact times (greater than two minutes). With these parameters a residual ozone concentration of 4.5×10^{-5} mg/L can be calculated, which is far below the detection for ozone in aqueous solution (Eq. 3) (Bader and Hoigné, 1981). This may indicate potential interferences in the ozone residual measurements, or other issues with the experimental set up, which would lead to less reliable ozone decay data. Nevertheless, as the only representative of the virus family *Caliciviridae,* which contains notable human pathogen human norovirus, it was necessary to include the data in this review.

Interestingly, mammalian viruses appear slightly more resistant to ozone than most bacteriophages at all temperature ranges. Figures S2a,b (SI) indicate that bacteriophage MS2 and closely related ssRNA phages (fr, GA, Qβ) (blue symbols in Figure S2) are the least resistant to ozone, while the DNA phages T4, PRD1, and φX174 are more resistant (red symbols in Figure S2). Bacteriophages, particularly MS2, are often utilized as surrogates for enteric, mammalian virus inactivation during water/wastewater treatment due to the ease of culturing and enumeration as compared to mammalian viruses (Amarasiri et al., 2017). The results from our assessment indicate that MS2 may provide a slight overestimation of viral pathogen inactivation by ozone. Bacteriophage T4 or φX174 may be more suitable for conservatively predicting virus inactivation by ozone, however further research is necessary.

The apparent differences in resistance towards ozone between bacteriophages and mammalian viruses are reflected within the compiled second-order inactivation rate constants (*k*), particularly at lower temperatures (Table 1). Inactivation rate constants for bacteriophages are 1-2 orders of magnitude higher than for mammalian viruses at temperatures from 1-19 °C, though this is based on a low number of data points (n=4 for mammalian viruses, n=5 for bacteriophages). This pattern of the range persists at 20-25 °C, however, the median values between the two datasets are comparable (2.3-4.7 x 10^3 mg^{-1} min^{-1} L).

When broken down by individual datasets (Table 2), the majority of the second-order rate constants for both bacteriophages and mammalian viruses fall in the range of 10^3 – 10^4 mg^{-1} min^{-1} L for 20-25 °C. Second-order rate constants outside of this range correspond to bacteriophages MS2 and Qβ on the higher end (1.2 – 3.1 x 10^4 mg^{-1} min^{-1} L) and the mammalian coxsackievirus B5 and murine norovirus at the lower end (0.33 – 6.1 x 10^2 mg^{-1} min^{-1} L). As previously described, the second-order rate constants associated with murine norovirus should be treated with caution. Disregarding murine norovirus, the higher and lower range of second-order inactivation rate constants are all associated with replicate datasets. MS2, Qβ, and coxsackievirus B5 all have additional measured second-order inactivation rate constants which fall within 10^3 – 10^4 mg^{-1} min^{-1} L. Many of the second-order inactivation rate constants were determined in studies utilizing either traditional batch systems, or highly sophisticated systems which allow for the evaluation of very low Ct ranges (<0.01 mg min L^{-1}) (Torii et al., 2020; Wolf et al., 2018; Young et al., 2020). The differences between these reactor systems may influence the variability experienced within the datasets. However, it should be noted that second-order rate constants for the reactions between ozone and specific chemical species have been

Table 1
Range of second-order inactivation rate constants, *k,* (base e, $mg^{-1}min^{-1}L$, $M^{-1}s^{-1}$ provided in parenthesis) of mammalian viruses and bacteriophages by ozone in buffered ultra-purified water.

	Mammalian Viruses				Bacteriophages			
T (°C)	n	Median	Min	Max	n	Median	Min	Max
1 - 9	2	-	2.1 x 10^1 (1.7 x 10^4)	2.9 x 10^1 (2.3 x 10^4)	2	-	1.7 x 10^3 (1.3 x 10^6)	2.4 x 10^3 (1.9 x 10^6)
10 - 19	2	-	1.5 x 10^1 (1.2 x 10^4)	3.4 x 10^1 (2.7 x 10^4)	4	1.4 x 10^3 (1.1 x 10^6)	8.5 x 10^2 (6.8 x 10^5)	3.7 x 10^3 (3.0 x 10^6)
20 - 25	18	2.1 x 10^3 (1.7 x 10^6)	3.3 x 10^1 (2.6 x 10^4)	4.4 x 10^3 (3.6 x 10^6)	11	4.7 x 10^3 (3.8 x 10^6)	1.5 x 10^3 (1.2 x 10^6)	3.1 x 10^4 (2.5 x 10^7)

Table 2
Second-order inactivation rate constants (k, base e) by ozone for specific viral group datasets in ultra-purified buffered waters. CA = *trans*-cinnamic acid, *t*-BuOH = *tert*-butanol.

Organism	Genome	Viral Family	Temp., °C	pH	k, mg^{-1} min^{-1} L	k, $M^{-1}s^{-1}$	Notes	Reference
MS2	ssRNA	*Fiersviridae*	2	6.5	1.7×10^3	1.3×10^6	*t*-BuOH, batch (w/ CA)	Wolf et al. (2018)
MS2	ssRNA	*Fiersviridae*	2	8.5	2.4×10^3	1.9×10^6	*t*-BuOH, batch (w/ CA)	Wolf et al. (2018)
Murine Norovirus	ssRNA	*Caliciviridae*	5	7	2.1×10^1	1.7×10^4	Batch, see discussion in main text	Lim et al. (2010)
Murine Norovirus	ssRNA	*Caliciviridae*	5	5.6	2.9×10^1	2.3×10^4	Batch, see discussion in main text	Lim et al. (2010)
MS2	ssRNA	*Fiersviridae*	12	6.5	2.0×10^3	1.6×10^6	*t*-BuOH, batch (w/ CA)	Wolf et al. (2018)
MS2	ssRNA	*Fiersviridae*	12	8.5	3.7×10^3	3.0×10^6	*t*-BuOH, batch (w/ CA)	Wolf et al. (2018)
MS2	ssRNA	*Fiersviridae*	16	7.5	8.5×10^2	6.8×10^5	Batch	Sigmon et al. (2015)
PRD1	dsDNA	*Tectoviridae*	16	7.5	6.3×10^1	5.1×10^4	Batch	Sigmon et al. (2015)
Coxsackievirus B5	ssRNA	*Picornaviridae*	16	7.5	1.5×10^1	1.2×10^4	Batch	Sigmon et al. (2015)
Human Adenovirus	dsDNA	*Adenoviridae*	16	7.5	3.4×10^1	2.7×10^4	Batch	Sigmon et al. (2015)
GA	ssRNA	*Fiersviridae*	22	7	9.4×10^3	7.5×10^6	Quench Flow	Torii et al. (2020)
MS2	ssRNA	*Fiersviridae*	22	7	1.6×10^4	1.2×10^7	Quench Flow	Torii et al. (2020)
MS2	ssRNA	*Fiersviridae*	22	6.5	1.3×10^4	1.0×10^7	*t*-BuOH, Quench Flow	Wolf et al. (2018)
MS2	ssRNA	*Fiersviridae*	22	8.5	4.7×10^3	3.8×10^6	*t*-BuOH, batch (w/ CA)	Wolf et al. (2018)
MS2	ssRNA	*Fiersviridae*	22	6.5	2.4×10^3	1.9×10^6	*t*-BuOH, batch (w/ CA)	Wolf et al. (2018)
fr	ssRNA	*Fiersviridae*	22	7	1.2×10^4	9.7×10^6	Quench Flow	Torii et al. (2020)
phiX174	ssDNA	*Microviridae*	22	7	3.9×10^3	3.1×10^6	Quench Flow	Torii et al. (2020)
phiX174	ssDNA	*Microviridae*	22	6.5	1.5×10^3	1.2×10^6	*t*-BuOH, batch (w/ CA)	Wolf et al. (2018)
Qβ	ssRNA	*Fiersviridae*	22	7	3.1×10^4	2.5×10^7	Quench Flow	Torii et al. (2020)
Qβ	ssRNA	*Fiersviridae*	22	6.5	4.1×10^3	3.3×10^6	*t*-BuOH, batch (w/ CA)	Wolf et al. (2018)
T4	dsDNA	*Myoviridae*	22	6.5	1.6×10^3	1.3×10^6	*t*-BuOH, batch (w/ CA)	Wolf et al. (2018)
Coxsackievirus B3	ssRNA	*Picornaviridae*	22	7	3.5×10^3	2.8×10^6	Quench Flow	Torii et al. (2020)
Coxsackievirus B3	ssRNA	*Picornaviridae*	22	7	2.3×10^3	1.8×10^6	Environmental culture, Quench flow	Torii et al. (2020)
Coxsackievirus B3	ssRNA	*Picornaviridae*	22	7	1.4×10^3	1.1×10^6	Environmental culture, Quench flow	Torii et al. (2020)
Coxsackievirus B3	ssRNA	*Picornaviridae*	22	7	1.2×10^3	9.6×10^5	Environmental culture, Quench flow	Torii et al. (2020)
Coxsackievirus B5	ssRNA	*Picornaviridae*	22	7	4.4×10^3	3.6×10^6	Quench Flow	Torii et al. (2020)
Coxsackievirus B5	ssRNA	*Picornaviridae*	22	6.5	3.1×10^3	2.5×10^6	Environmental culture, *t*-BuOH, batch (w/ CA)	Wolf et al. (2018)
Coxsackievirus B5	ssRNA	*Picornaviridae*	22	7	2.4×10^3	1.9×10^6	Environmental culture, Quench flow	Torii et al. (2020)
Coxsackievirus B5	ssRNA	*Picornaviridae*	22	6.5	2.3×10^3	1.8×10^6	*t*-BuOH, batch (w/ CA)	Young et al. (2020)
Coxsackievirus B5	ssRNA	*Picornaviridae*	22	7	2.3×10^3	1.8×10^6	Environmental culture, Quench flow	Torii et al. (2020)
Coxsackievirus B5	ssRNA	*Picornaviridae*	22	7	1.8×10^3	1.4×10^6	Environmental culture, Quench flow	Torii et al. (2020)
Coxsackievirus B5	ssRNA	*Picornaviridae*	22	6.5	6.1×10^2	4.9×10^5	Environmental culture, *t*-BuOH, batch (w/ CA)	Wolf et al. (2018)
Coxsackievirus B5	ssRNA	*Picornaviridae*	22	6.5	5.5×10^2	4.4×10^5	*t*-BuOH, batch (w/ CA)	Wolf et al. (2018)
Echovirus 11	ssRNA	*Picornaviridae*	22	6.5	2.4×10^3	1.9×10^6	*t*-BuOH, batch (w/ CA)	Wolf et al. (2018)
Echovirus 11	ssRNA	*Picornaviridae*	22	6.5	2.0×10^3	1.6×10^6	*t*-BuOH, batch (w/ CA)	Young et al. (2020)
Human Adenovirus	dsDNA	*Adenoviridae*	22	6.5	1.1×10^3	9.0×10^5	*t*-BuOH, batch (w/ CA)	Wolf et al. (2018)
Murine Norovirus	ssRNA	*Caliciviridae*	20	5.6	4.0×10^1	3.2×10^4	Batch, see discussion in main text	Lim et al. (2010)
Murine Norovirus	ssRNA	*Caliciviridae*	20	7	3.3×10^1	2.6×10^4	Batch, see discussion in main text	Lim et al. (2010)
Poliovirus 1	ssRNA	*Picornaviridae*	22	7	3.7×10^3	2.9×10^6	Quench Flow	Torii et al. (2020)

shown to vary up to a factor of 5 for different studies (von Sonntag and von Gunten, 2012). Therefore, the variability determined within the virus dataset (up to 8-fold within the same viral species) is not too outstanding.

The slight differences in susceptibility between viral groups may be explained through inactivation mechanisms. Due to the differences in capsid morphology, genome composition, and replication mechanisms for different virus groups (e.g., enteroviruses, caliciviruses, coliphages, etc.), it is impossible to assign a singular ozone inactivation mechanism for viruses as a generalized group at this stage of the knowledge. Studies evaluating ozone inactivation mechanisms for the viral genus *Enterovirus* (family *Pircornaviridae*) are the most abundant. Roy et al. (1981) found RNA damage to account for the majority of inactivation for poliovirus 1. Torrey et al. (2019) came to a similar conclusion for echovirus 11, which was additionally confirmed by Young et al. (2020) for coxsackievirus B5. Results from this study also indicate that multiple genome hits are likely required for inactivation of echovirus 11 and coxsackievirus B5. Despite this, capsid damage cannot be fully ignored as a potential contributor to ozone inactivation, as current methodologies limit the ability to fully differentiate between the two. It is possible that differences in capsid composition/morphology may be an important factor for the differences in inactivation kinetics between genetically similar isolates of the same viruses determined in (Torii et al., 2021). Ozone inactivation mechanisms for viruses relevant to public health outside of *Picornaviridae*, such as human adenoviruses and *Caliciviruses*, have yet to be determined.

In contrast, Kim et al. (1980) was able to confirm capsid damage during ozone treatment of bacteriophage f2, though due to the analytical limitations of the time, it cannot be concluded that this is the primary inactivation mechanisms of ozone over genome damage. Bacteriophage f2, along with bacteriophage fr, are no longer considered distinct virus species, and have since been merged into the viral species MS2 (van Regenmortel et al., 2000). Therefore, it is appropriate to interpret these results as descriptive of MS2. MS2 belongs to the viral family *Fiersviridae* (formerly *Leviviridae*), which includes other closely related ssRNA bacteriophages in this review such as Qβ and GA (Callanan et al., 2020; Stockdale et al., 2020). Further research utilizing updated methods for MS2 and closely related bacteriophages could potentially explain their increased susceptibility to ozone disinfection compared to *Enteroviruses*. DNA bacteriophages φX174, T4, and PRD1, which behaved more similar to the mammalian viruses, are all taxonomically distinct from MS2 and other members of *Fiersviridae* up to the order of virus realm (ICTV, 2020). Therefore, it is inappropriate to assume that ozone inactivation mechanisms for these particular bacteriophages would be similar without further investigations. In general, more research is needed to explore the inactivation mechanisms and kinetics of DNA phages as well as mammalian DNA viruses (such as human adenoviruses). Based on similar inactivation mechanisms and kinetics a better surrogate than MS2 could be selected to assess viral inactivation during ozonation.

4.3. Inactivation of Giardia spp.

Seven studies investigating inactivation of *Giardia spp.* met the specific analysis criteria for extracting $\log_{10}$ inactivation vs. ozone Ct/

exposure data (Finch et al., 1993b; Haas and Kaymak, 2003; Labatiuk et al., 1994, 1992a, 1992b, 1991; Li et al., 2004). Of these seven studies, only two second-order inactivation rate constants are available for review (Haas and Kaymak, 2003; Labatiuk et al., 1992a). The majority of studies evaluated *Giardia muris*, a surrogate for the human pathogen *Giardia lamblia. G. muris* is advantageous in the laboratory setting as it is non-pathogenic to humans and maintains reproducible patterns of infection in mouse models (Belosevic and Faubert, 1983). There is conflicting evidence of the relative resistance of *G. muris* compared to *G. lamblia*, with some studies indicating higher resistance to ozone (Wickramanayake et al., 1985), while others finding no statistical differences (Finch et al., 1993b). Three different methods (*in vivo* mouse and gerbil models and *in vitro* excystation) were utilized to quantify *Giardia* survival ratios in the selected studies, which could lead to variability in study conclusions (Labatiuk et al., 1991). However, due to the overall lack of available data, studies using either of these methods were included for evaluation.

Compiled $\log_{10}$ inactivation vs. ozone Ct/exposure data at different temperature ranges are provided in Fig. 2a-c. All three temperature ranges indicate significant inactivation of *G. muris* cysts in the lower Ct ranges (< 1 mg min L^{-1}) with a tailing effect for higher ozone exposures. This effect is apparent regardless of the experimental matrix. Because of the tailing effect, the USEPA models (dashed lines in Fig. 2) overestimate inactivation of *Giardia* cysts for an ozone Ct $>$ ~1-2 mg min L^{-1} for most temperatures.

The USEPA model was developed from a single study that did not pass through the systematic review protocol due to its use of a semi-batch reactor set up (Wickramanayake et al., 1985; USEPA, 1991). Additionally, this study was performed at a single temperature (5 °C), which was used for extrapolation of inactivation models to higher temperatures. Based on the limited dataset used to develop the model, it is expected that it does not accurately predict *Giardia* cyst inactivation for the data analyzed in this review. This tailing effect highlights one of the weaknesses of utilizing a linear kinetic model for predicting inactivation.

The two available second-order inactivation rate constants for *G. muris* cysts are provided in Table 3. The values differ by over a factor of 10, and seemingly indicate higher efficiency at lower temperatures.

Table 3
Second-order inactivation rate constants, *k* (base e, $mg^{-1}min^{-1}L$, $M^{-1}s^{-1}$ provided in parenthesis) of *Giardia muris* cysts by ozone in buffered ultra-purified water.

	Giardia muris cysts	
T (°C)	n	Median
1 - 9	0	-
10 - 19	1	3.7×10^1 (3.0×10^4)
20 - 25	1	1.0×10^0 (8.3×10^2)

However, it should be noted that the second-order inactivation rate constant for T=10-19 °C (Haas and Kaymak, 2003) was determined at very low Ct values (all < 1 mg min L^{-1}), and therefore is reflective of the initial rapid inactivation phase evident prior to tailing. The data used to calculate second- order rate constants for T=20-25 °C (from Labatiuk et al., 1992a), examined higher Ct values, and therefore exhibited considerable tailing, which resulted in a poor model fit ($R^2 = 0.374$). Omitting data points influenced by tailing increased the second-order rate constant to 3.73 mg^{-1} min^{-1} L but remains almost exactly one order of magnitude lower than the second-order rate constants determined by Haas and Kaymak (2003). The compiled data indicate that a linear kinetic model may be inappropriate for estimating inactivation of *Giardia* cysts by ozone at higher Ct/exposure.

Studies examining the mechanism of *Giardia* cyst inactivation have reported that ozone produces severe degradation of the inner membranous layer of the cyst wall, irregular vacuole formation, and detachment of the trophozoite within the cyst (Li et al., 2004). These changes in cyst morphology were consistent with cyst inactivation. However, it remains unclear if the observed tailing effect is related to the inactivation mechanism by ozone. Labatiuk et al. (1992b) determined that *Giardia* cysts are rapidly inactivated within the first two minutes of ozonation, with little inactivation occurring thereafter, even in the presence of considerable ozone residual. Additionally, it was observed that ozone decreased in efficiency with lower concentrations of *Giardia* cysts, which would be the scenario encountered after the rapid initial inactivation (Haas and Kaymak, 2003). Regardless of the potential cause of the tailing effect, it is evident that at least 1 $\log_{10}$ inactivation of *Giardia* cysts can be obtained by an ozone exposure of ~1 mg min L^{-1}.

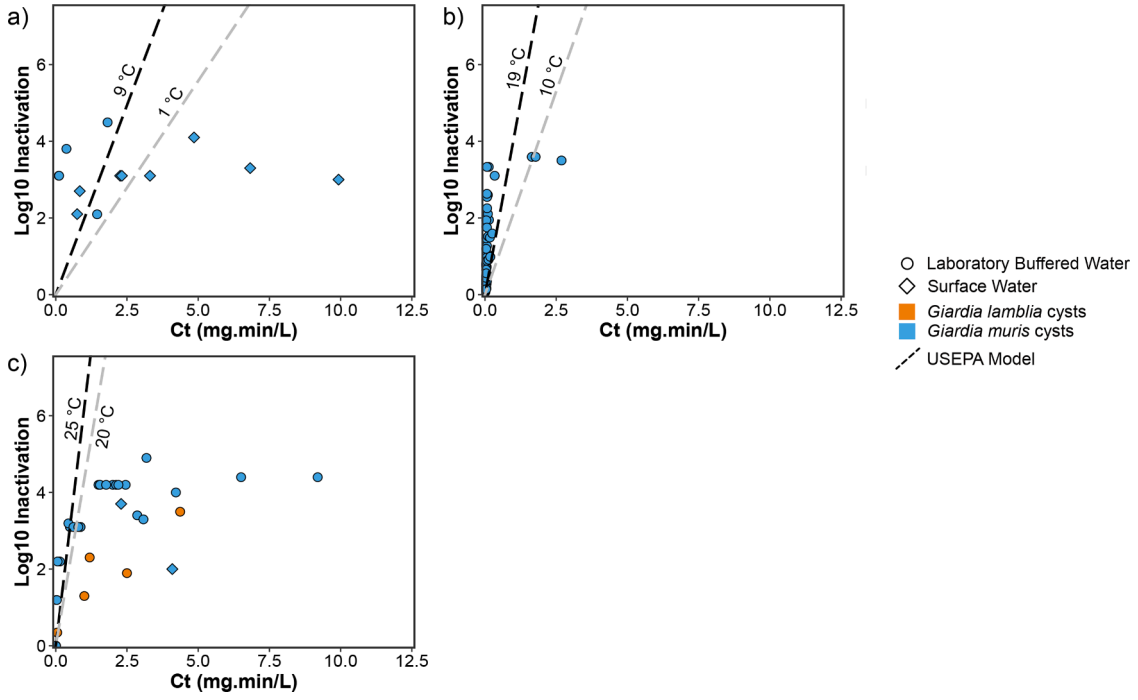

Fig. 2. *Giardia spp.* cyst inactivation by ozone at pH 5-8: $\log_{10}$ inactivation as a function of ozone Ct for *Giardia spp.* cysts at (a) 1-9 °C, (b) 10-19 C, (c) 20-25 °C.

4.4. Inactivation of Cryptosporidium parvum oocysts and surrogates

Eight studies met the criteria for inclusion for log_{10} inactivation vs. ozone Ct/exposure analysis of *C. parvum* oocysts (Cho and Yoon, 2007; Craik et al., 2003; Finch et al., 1993a; Finch and Li, 1999; Gyurek et al., 1999; Lewin et al., 2001; Li et al., 2001; Wohlsen et al., 2007), with six of the studies reporting second-order inactivation rate constants (Cho and Yoon, 2007; Craik et al., 2003; Finch et al., 1993a; Gyurek et al., 1999; Lewin et al., 2001; Li et al., 2001). The evaluated studies utilized either *in vivo* mouse models or *in vitro* excystation to quantify inactivation of *C. parvum* oocysts. In studies where both *in vivo* and *in vitro* methods were utilized, *in vivo* data were preferentially selected for analysis due to evidence of *in vitro* methods underestimating inactivation (Bukhari et al., 2000; Finch et al., 1993a). While the studies specifically utilized *C. parvum*, the stocks were largely obtained from different sources or batches. In addition to *C. parvum* oocysts, data evaluating disinfection of *Bacillus subtilis* spores from nine studies were also evaluated to assess its potential as a surrogate for *C. parvum* oocysts (Cho et al., 2006, 2003a, 2003b, 2002; Choi et al., 2007; Craik et al., 2002; Dow et al., 2006; Driedger et al., 2001).

C. parvum oocyst inactivation data for three temperature ranges are provided in Fig. 3a-c. *C. parvum* oocysts exhibit greater resistance to ozone than both viruses and *Giardia*. The data do not provide evidence of a lag-phase or tailing at low or high ozone Cts, respectively. The USEPA models (dashed lines) are closely aligned with the inactivation data from the compiled studies, providing the most accurate prediction of inactivation of the three selected pathogen group models. The model over-predicts *C. parvum* oocyst inactivation for 8% of the 135 total data points. Even though this is a good agreement, it is unclear if these deviations from the model are due to natural variability of the organism (thus indicating the model is not conservative to oocyst inactivation) or due to variability in experimental methods.

The USEPA model for *C. parvum* oocysts was developed from the data of four studies (Li et al., 2001; Oppenheimer et al., 2000; Owens et al., 2000; Rennecker et al., 1999). Only one of the four studies was included in our analysis (Li et al., 2001), as the remainder of the studies either utilized semi-batch systems, evaluated inactivation at pilot-scale, or were not published in a peer-reviewed article (i.e., only project report); all of which were selective constraints of the literature review process in this article. The *C. parvum* oocyst inactivation models developed by USEPA utilized a less stringent safety factor due to concerns related to bromate formation. Therefore, it is expected that the model would provide a less conservative prediction of inactivation in comparison to the virus model.

The inactivation efficiency of *B. subtilis* during ozonation was also examined (Fig. 3d-f, blue symbols). In contrast to *C. parvum* oocysts, there is an apparent shouldering, or inactivation lag-phase, at each temperature. This lag-phase appears to change with temperature, but with no clear pattern (i.e., the lag-phase in the 10 -19 °C range appears larger than both 5 – 9 °C and 20 – 25 °C), despite a clear temperature relationship determined in Driedger et al. (2001). This could be due to the grouping of data regardless of pH, which has been previously demonstrated to influence the lag-phase (Cho et al., 2003b, 2003a, 2002; Dow et al., 2006). It is also possible that additional water quality parameters may be influencing the lag. Dow et al. (2006) evaluated parameters influencing the lag-phase of *B. subtilis* inactivation and did

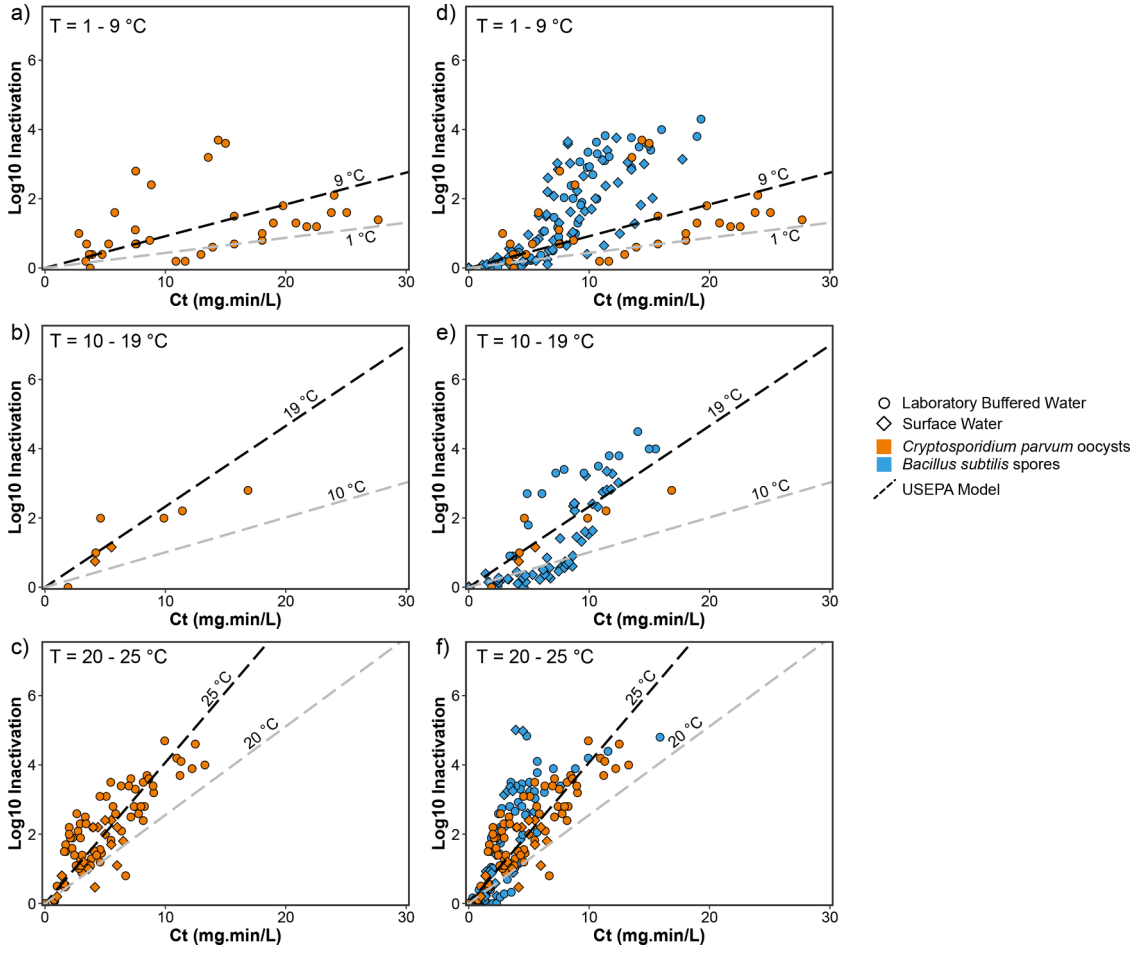

Fig. 3. *C. parvum* oocyst inactivation by ozone at pH 5-8: log_{10} inactivation as a function of ozone Ct for *C. parvum* oocysts at (a) 1-9 °C, (b) 10-19 °C, (c) 20-25 °C, *C. parvum* oocysts and *B. subtillis* spores at (d) 1-9 C, (e) 10-19 °C, and (f) 20-25 °C.

not find any significant influence of bulk DOC concentration or turbidity, however, differences in DOM composition were not considered. It is currently unclear which water quality parameter, if any, may be influencing the extent of the lag-phase.

Table 4 provides second-order inactivation rate constants for both *C. parvum* oocysts and *B. subtilis* spores, respectively, using either the second-order linear model or delayed Chick-Watson model. Overall, second-order inactivation rate constants for *C. parvum* oocysts are much lower than for viruses or *Giardia* cysts, indicating that it is much more resistant to ozone. In addition to second-order rate constants in buffered solutions, values in various synthetic or natural surface waters are also provided for each organism. Based on limited data for both *C. parvum* oocysts and *B. subtilis* spores, it is not clear that natural or synthetic surface water significantly influences the inactivation rate. The median second-order inactivation rate constants for both organisms in natural/synthetic surface water fall within the ranges determined in buffered solutions, albeit this is based on very limited data in the case of *C. parvum* oocysts.

To evaluate *B. subtilis* spores as a surrogate for *C. parvum* oocyst inactivation, the ozone Ct/exposure for 2 $\log_{10}$ inactivation were calculated using the respective inactivation models for direct comparison. For the temperature range of 20 – 25 °C, a Ct/exposure of 4.8 – 8.8 mg min L^{-1} would be necessary for 2 $\log_{10}$ inactivation of *C. parvum* oocysts. However, for *B. subtilis*, a Ct ranging from 0.4 to 12.6 mg min L^{-1} is required. The wide variety of factors influencing *B. subtilis* spore inactivation exclude it as a surrogate for *C. parvum oocyst* inactivation, in agreement with Driedger et al. (2001).

The consistent lag-phase for *B. subtilis* spores, but not *C. parvum* oocysts, may provide potential evidence of different ozone inactivation mechanisms. Shouldering can be indicative of a multiple-hit inactivation mechanism, in which multiple areas of an organism must be damaged by the disinfectant prior to its inactivation (Kimball, 1953). The shouldering phase dissipates once the necessary number of targets are destroyed within the organism, usually leading to an exponential phase of inactivation. This contrasts with a single-hit mechanism, in which the destruction of one target results in the inactivation of the organism (i.e., exponential disinfection begins immediately upon application). It has been found that the inner-membrane of the *B. subtilis* spore is likely the site of lethal damage, with ozone damage to the spore coat likely necessary prior to destruction of the inner-membrane (Young and Setlow, 2004). However, it cannot be ruled out that the damage to the inner membrane is limited by ozone diffusion through the spore coat. Regardless, the ultimate effect remains the same in which the spore coat provides an initial resistance to disinfection, resulting in a perceived lag-phase and thus supports the use of a delayed Chick-Watson model.

The mechanism of ozone inactivation for *C. parvum* oocysts has not been evaluated previously, to the best of our knowledge. The oocyst wall is likely composed of an outer glycocalyx layer followed by a lipid hydrocarbon layer, a layer of cysteine-rich proteins, and ultimately a structural polysaccharide layer, underneath which exists the sporozoite (Jenkins et al., 2010). The *C. parvum* sporozoite cannot survive without its oocyst, and it is unable to complete its life cycle until it reaches the gut of a host, excysts, and attaches to intestinal lining (Smith et al., 2005). Encysting is a lifecycle requirement for *C. parvum*. This is in contrast with *B. subtilis* which can freely exist as a vegetative bacterial cell without its spore; spore formation is a survival mechanism for low-nutrient environmental conditions (Sella et al., 2014). These differences in life cycles and the ensuing differences in cell structures likely influence the discrepancy in ozone inactivation kinetics between the two distinct organisms. Interestingly, studies have determined that *in-vitro* excystation predicts less inactivation of *C. parvum oocysts* when compared to *in-vivo* mouse models for similar ozone exposures (Bukhari et al., 2000; Finch et al., 1993a), i.e., some sporozoites successfully excyst when provided gut-mimicking conditions, however, they may lack the capability of completing their life cycle once excysted. This could indicate damage to the sporozoite by ozone, however, further research would be necessary to verify this. In contrast to previous studies, the results from this review did not indicate a large discrepancy between *in-vivo* and *in-vitro* methods (Figure S3, SI).

4.5. Limitations of previous studies and research needs

In this review, there were several limitations associated with the comparison of inactivation data from different sources. First and foremost, a large portion of disinfection studies were excluded during the review process due to the use of non-batch or non-quench-flow reactor designs. In particular, many of the excluded bench-scale studies utilized semi-batch reactors. This drastically reduced the number of studies for data extraction (69 of 210 articles omitted for this reason). Semi-batch reactors were excluded from examination due to the inherent difficulty in proper application of such systems (Finch et al., 2001). Moreover, as a reviewer, it can be difficult to assess proper implementation of semi-batch systems due to the limited information provided within manuscripts. A more unified approach to studying ozone disinfection kinetics would help to increase the availability of comparable data produced in future studies.

In studies utilizing similar approaches, there were still many systematic differences that made comparison difficult, such as differences in reactor volumes utilized (5 mL to 5 L) and ozone residual measurement methods (direct absorbance at 260 nm vs. indigo trisulfonate at 600 nm), the use of hydroxyl radical scavengers (Table S1). Additionally, the purity level of the microbial stocks can influence results and skew interpretation due to the interactions between the organic matter present in microbial growth media and ozone (Mesquita et al., 2010;

Table 4
Second-order inactivation rate constants, *k* (base e, $mg^{-1}min^{-1}L$, $M^{-1}s^{-1}$ provided in parenthesis) and Ct_{lag} (mg min L^{-1}) values (when applicable) of *C. parvum* oocysts and *B. subtilis* spores by ozone in buffered ultra-purified water (or similarly low DOC matrix) and natural or synthetic surface water.

		***C. parvum* oocysts**				***B. subtilis* spores**						
			***k*, mg^{-1} min^{-1} L ($M^{-1}s^{-1}$)**				***k*, mg^{-1} min^{-1} L ($M^{-1}s^{-1}$)**			**Ct_{lag}, mg min L^{-1}**		
	***T* (°C)**	**n**	**Median**	**Min**	**Max**	**n**	**Median**	**Min**	**Max**	**Median**	**Min**	**Max**
Laboratory Buffer	*1 - 9*	1	1.1×10^{-1} (9.0×10^{1})	-	-	2	-	6.9×10^{-1} (5.5×10^{2})	1.2×10^{0} (9.6×10^{2})	-	3.4	5.1
	10 - 19	0	-	-	-	1	(9.3×10^{-1}) (7.4×10^{2})	-	-	2.6	-	-
	20 - 25	4	7.2×10^{-1} (5.7×10^{2})	5.3×10^{-1} (2.4×10^{2})	9.6×10^{-1} (7.7×10^{2})	21	1.7×10^{0} (1.3×10^{3})	4.3×10^{-1} (3.4×10^{2})	5.2×10^{0} (4.2×10^{3})	1.2	0.3	2.0
Natural/synthetic surface water	*1 - 9*	0	-	-	-	4	1.2×10^{0} (9.8×10^{2})	9.7×10^{-1} (7.8×10^{2})	2.0×10^{0} (1.6×10^{3})	5.2	4.6	10
	10 - 19	0	-	-	-	2	-	1.6×10^{0} (1.3×10^{3})	2.8×10^{0} (2.2×10^{3})		2.7	6.1
	20 - 25	1	9.0×10^{-1} (7.2×10^{2})	-	-	11	2.9×10^{0} (2.3×10^{3})	1.3×10^{0} (1.1×10^{3})	6.3×10^{0} (5.1×10^{3})	1.4	0.6	2.9

Wolf et al., 2018). Furthermore, the method in which ozone Ct is determined can influence data interpretation. Of the 1,038 data points collected for $\log_{10}$ inactivation vs. ozone Ct, 72 data points had sufficient information to estimate ozone Ct using the four methods encountered in this review (integral, geometric mean, final residual, and arithmetic mean). Assuming integration of the ozone residual curve provides the most accurate estimation of ozone exposure, comparison of this value with the alternative approaches determined that the geometric mean Ct method provided the closest estimate of Ct/exposure based on residual sum of squares. Fig. 4 demonstrates the ability of the geometric mean Ct method to accurately estimate the ozone exposure, which is to be expected as long as ozone exhibits first-order decay in a specific matrix and there is a final residual ozone concentration > 0 (Gyürek and Finch, 1998). In contrast, as shown in Fig. 4, the arithmetic mean overestimates and the final residual ("effluent") method underestimates the ozone exposure. While arithmetic mean deviates less from the integral method when compared to the "effluent" method, it requires the same input values as the geometric mean (i.e., C_0, C, and t). Therefore, there is no practical reason to utilize the arithmetic over the geometric mean. Figure S4 (SI) provides a conceptual overview of the different ozone Ct estimation methods.

It should be mentioned that while we have demonstrated only slight deviations in the different Ct estimation methods, these quick estimation methods begin to deviate considerably with increasing ozone decay rates, such as those seen during wastewater treatment. Therefore, it is not recommended to employ these estimation methods under such conditions. If an ozone decay curve cannot be collected for whatever reason, a more accurate estimation consists of estimating the first order ozone decay rate constant with the initial and final ozone residual concentration measurements and time elapsed between the two:

$$k' = -\frac{ln\left(\frac{C}{C_0}\right)}{t} \tag{10}$$

The calculated value for k' can then be substituted into (4). However, this method also requires an assumption of first-order ozone decay. Integration of an ozone residual time series is recommended as best practice.

Studies were also eliminated if they did not provide sufficient information to confidently compare either $\log_{10}$ inactivation and Ct or second-order inactivation rate constants, either through lack of ozone decay data, missing pertinent water quality data (i.e., temperature, pH, etc.), lack of sufficient reactor set-up description, improper microbiological data reporting, among others. It is recommended that ozone disinfection studies should provide the water quality and system characteristics previously described in Hoigné (1994) and Hoigné and Bader (1994) as necessary for general ozone related studies. Such characteristics include water temperature, pH, DOC concentration, alkalinity, among others. Additionally, disinfection studies should provide organism strain/identifier, cultivation and purification techniques, initial spike concentrations, and particularly the method used to handle data which fall below limits of detection (i.e., avoiding substitution with detection limit).

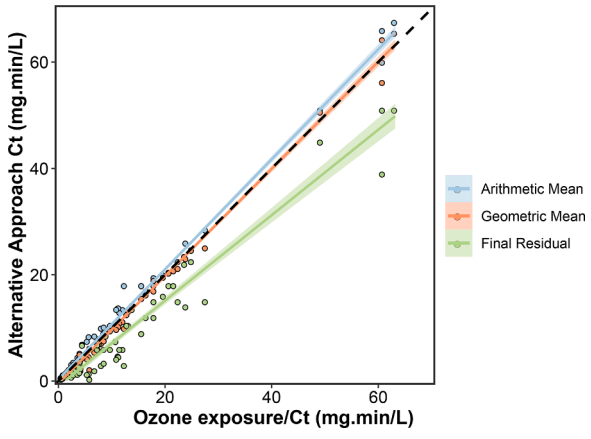

Fig. 4. Comparison of Ct calculation methods (at ozone decay rates < 0.5 min^{-1}) based on 72 data points from the literature search which provided enough information to calculate Ct with the four different approaches (integration of residual curve, i.e., "true" ozone exposure, geometric mean, arithmetic mean, and final residual). Orange symbols indicate the geometric mean Ct calculation. Green symbols indicate the final residual (effluent) Ct calculation. Blue symbols indicate arithmetic mean Ct calculation. Linear regression lines with 95% confidence intervals are also provided. The dashed line represents a scenario in which the alternative Ct approach perfectly predicts the ozone exposure determined via integration of the ozone residual curve.

While the evaluation of virus inactivation via ozone has progressed through time with increasingly sophisticated techniques, studies on *Giardia* cysts and *C. parvum* oocysts have stalled, with the most recent publications meeting our selection criteria published more than 14 years ago. After several outbreaks of cryptosporidiosis initially spurred interest in this topic (Fox and Lytle, 1996), support for such research waned and is still currently lacking. This is likely in large part due to limitations in cultivating and assessing viability of each organism, which require *in vivo* animal models. However, particularly in the case of *Giardia* which deviated the furthest from the USEPA models based on data within this review, new data would be of great benefit, particularly in discerning the cause of the apparent tailing effect.

Similarly, ozone inactivation kinetics evaluated at varying temperature ranges were sparse, with the majority of studies included within this review evaluating inactivation at 20-25 °C. Furthermore, very few studies evaluated inactivation at varying temperatures within the same study. As described previously, systematic differences between studies make direct comparisons of data difficult. Therefore, it is difficult to provide confident assertations regarding the effect of temperature on disinfection efficacy based on these studies alone. Once again, this was strikingly evident for *Giardia* cysts in which *k* values for the 10-19 °C range appear significantly larger than the 20-25 °C, which is contrary to what might be expected.

There is a lack of mechanistic explanations for the different inactivation kinetics exhibited by the different organisms, largely due to the lack of studies evaluating inactivation mechanisms of ozone in general, particularly for encysted protozoans. Ozone inactivation mechanisms are summarized in Fig. 5. However, there have been advances in the study of viral inactivation mechanisms. Torrey et al. (2019) and Young et al. (2020) provide novel methodologies for estimating viral inactivation mechanisms, particularly relating to genome destruction. These methods could be applied to other virus species, and potentially validate the differences in inactivation mechanisms between MS2 and closely related bacteriophages and other ssRNA mammalian viruses, as well as provide justification for potentially better surrogate candidates such as φX174 or T4.

It is important to recognize that while the reported kinetics of surrogate bacteriophages and mammalian viruses appear to deviate from one another, when compared to Ct requirements for *Giardia* cysts and *C. parvum* oocysts, those apparent differences become negligible (Fig. 6). Specifically, drinking water systems designed for 2 $\log_{10}$ inactivation of *C. parvum* oocysts will require a significant ozone Ct/exposure (i.e., much greater than 1 mg min L^{-1}), which would ensure considerable inactivation of mammalian viruses and bacteriophages ($\gg 2$ $\log_{10}$ at 20 °C). However, in situations where little to no ozone exposure is achieved, such as in sub-residual water reuse applications or with ozone AOP (i.e., supplemented with H_2O_2), these differences could become relevant, and thus further exploration into alternate virus surrogates is warranted, particularly with the increasing interest in ozone for water reuse applications and the significant virus inactivation requirements in such systems.

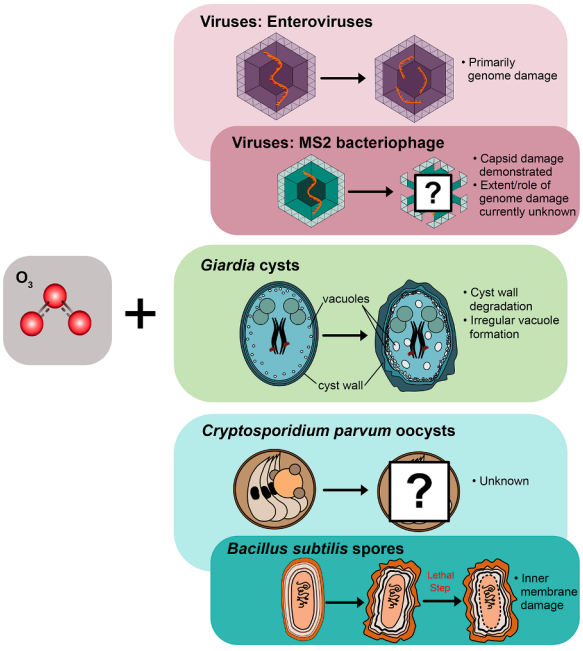

Fig. 5. Summary of ozone inactivation mechanisms for each pathogen group and associated surrogates.

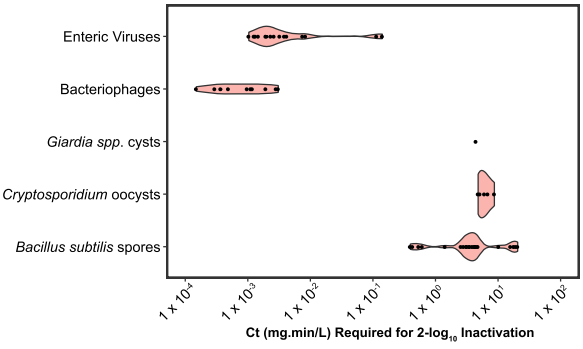

Fig. 6. Ct required for 2 $\log_{10}$ inactivation of different organisms with ozone as determined by compiled inactivation rate constants at 20-25 °C. For data see Tables 1-3. Shaded area around points provides insight into the distribution of Ct values.

5. Conclusions

Based on a critical review of ozone disinfection the following conclusions can be drawn:

- Ozone is an effective disinfectant against chlorine resistant pathogens such as *C. parvum* oocysts, can effectively inactivate other pathogens such as *Giardia* cysts, and performs rapidly against viruses.
- USEPA models which were developed more recently using multiple datasets (*C. parvum* oocysts) were more accurate than earlier models developed using a single dataset (viruses and *Giardia* cysts). Comparison of the data compiled in this review suggests the need for improvements in USEPA models for viruses and *Giardia* cysts.
- Further research on the applicability of non-pathogenic surrogates such as MS2 and *B. subtilis* spores is necessary. The data compiled in this review indicate that these organisms do not accurately reflect the behavior of the pathogens they represent. Studies directly evaluating pathogenic organisms are costly and time consuming, therefore further investigation of appropriate surrogates may help advance the knowledge, and ultimately the prediction, of ozone disinfection.
- Greater emphasis should be placed on minimizing differences in ozone disinfection study approaches and development of standard protocols. This would allow for better comparability between studies and allow for greater consensus on ozone inactivation of pathogens.

Declaration of Competing Interest

The authors declare that they have no known competing financial interests or personal relationships that could have appeared to influence the work reported in this paper.

Acknowledgments

This review was funded by The Water Research Foundation Project Number 5035: Impact of Bromate Control Measures on Ozone Oxidation/Disinfection and Downstream Treatment Processes in Potable Reuse. We would also like to sincerely thank two anonymous reviewers for their thoughtful comments and suggestions which helped improve the quality of this review article.

Supplementary materials

Supplementary material associated with this article can be found, in the online version, at doi:10.1016/j.watres.2022.118206.

References

Acero, J.L., von Gunten, U., 2001. Characterization of oxidation processes: ozonation and the AOP O3/H2O2. J. Am. Water Work. Assoc. 93, 90–100. https://doi.org/10.1002/j.1551-8833.2001.tb09311.x.

Amarasiri, M., Kitajima, M., Nguyen, T.H., Okabe, S., Sano, D., 2017. Bacteriophage removal efficiency as a validation and operational monitoring tool for virus reduction in wastewater reclamation. Review. Water Res. 121, 258–269. https://doi.org/10.1016/j.watres.2017.05.035.

Bader, H., Hoigné, J., 1981. Determination of ozone in water by the indigo method. Water Res 15, 449–456. https://doi.org/10.1016/0043-1354(81)90054-3.

Belosevic, M., Faubert, G.M., 1983. Giardia muris : correlation between oral dosage , course of infection , and trophozoite distribution in the mouse small intestine. Expermental Parisitology 56, 93–100.

Betancourt, W., 2019. Part three: specfic exreted pathoges: environmental and epidemology aspects - cryptospororidum spp. Glob. Water Pathog. Proj. 7, 1–49.

Buffle, M.O., Schumacher, J., Salhi, E., Jekel, M., von Gunten, U., 2006. Measurement of the initial phase of ozone decomposition in water and wastewater by means of a continuous quench-flow system: Application to disinfection and pharmaceutical oxidation. Water Res 40, 1884–1894. https://doi.org/10.1016/j.watres.2006.02.026.

Bukhari, Z., Marshall, M.M., Korich, D.G., Fricker, C.R., Smith, H.V., Rosen, J., Clancy, J. L., 2000. Comparison of Cryptosporidium parvum viability and infectivity assays following ozone treatment of oocysts. Appl. Environ. Microbiol. 66, 2972–2980. https://doi.org/10.1128/AEM.66.7.2972-2980.2000.

Burns, N., Hunter, G., Jackman, A., Hulsey, B., Coughenour, J., Walz, T., 2007. The return of ozone and the hydroxyl radical to wastewater disinfection. Ozone Sci. Eng. 29, 303–306. https://doi.org/10.1080/01919510701463206.

Callanan, J., Stockdale, S.R., Shkoporov, A., Draper, L.A., Ross, R.P., Hill, C., 2020. Expansion of known ssRNA phage genomes: from tens to over a thousand. Sci. Adv. 6 https://doi.org/10.1126/sciadv.aay5981.

Camel, V., Bermond, A., 1998. The use of ozone and associated oxidation processes in drinking water treatment. Water Res 32, 3208–3222. https://doi.org/10.1016/S0043-1354(98)00130-4.

Cho, M., Chung, H., Yoon, J., 2003a. Quantitative evaluation of the synergistic sequential inactivation of Bacillus subtilis spores with ozone followed by chlorine. Environ. Sci. Technol. 37, 2134–2138. https://doi.org/10.1021/es026135h.

Cho, M., Chung, H., Yoon, J., 2003b. Disinfection of water containing natural organic matter by using ozone-initiated radical reactions. Appl. Environ. Microbiol. 69, 2284–2291. https://doi.org/10.1128/AEM.69.4.2284-2291.2003.

Cho, M., Chung, H., Yoon, J., 2002. Effect of pH and importance of ozone initiated radical reactions in inactivating Bacillus subtilis spore. Ozone Sci. Eng. 24, 145–150. https://doi.org/10.1080/01919510208901605.

Cho, M., Kim, J.H., Yoon, J., 2006. Investigating synergism during sequential inactivation of Bacillus subtilis spores with several disinfectants. Water Res 40, 2911–2920. https://doi.org/10.1016/j.watres.2006.05.042.

Cho, M., Yoon, J., 2007. Quantitative evaluation and application of Cryptosporidium parvum inactivation with ozone treatment. Water Sci. Technol. 55, 241–250. https://doi.org/10.2166/wst.2007.008.

Choi, Y., Cho, M., Lee, Y., Choi, J., Yoon, J., 2007. Inactivation of Bacillus subtilis spores during ozonation in water treatment plant: Influence of pre-treatment and consequences for positioning of the ozonation step. Chemosphere 69, 675–681. https://doi.org/10.1016/j.chemosphere.2007.05.045.

Craik, S.A., Smith, D.W., Belosevic, M., Chandrakanth, M., 2002. Use of Bacillus subtilis spores as model microorganisms for ozonation of Cryptosporidium parvum in drinking water treatment. J. Environ. Eng. Sci. 1, 173–186. https://doi.org/10.1139/S02-012.

Craik, S.A., Smith, D.W., Chandrakanth, M., Belosevic, M., 2003. Effect of turbulent gas-liquid contact in a static mixer on Cryptosporidium parvum oocyst inactivation by ozone. Water Res 37, 3622–3631. https://doi.org/10.1016/S0043-1354(03)00285-9.

Criquet, J., Rodriguez, E.M., Allard, S., Wellauer, S., Salhi, E., Joll, C.A., von Gunten, U., 2015. Reaction of bromine and chlorine with phenolic compounds and natural organic matter extracts - electrophilic aromatic substitution and oxidation. Water Res 85, 476–486. https://doi.org/10.1016/j.watres.2015.08.051.

Czekalski, N., Imminger, S., Salhi, E., Veljkovic, M., Kleffel, K., Drissner, D., Hammes, F., Bürgmann, H., von Gunten, U., 2016. Inactivation of antibiotic resistant bacteria and resistance genes by ozone: from laboratory experiments to full-scale wastewater treatment. Environ. Sci. Technol. 50, 11862–11871. https://doi.org/10.1021/acs.est.6b02640.

Dow, S.M., Barbeau, B., von Gunten, U., Chandrakanth, M., Amy, G., Hernandez, M., 2006. The impact of selected water quality parameters on the inactivation of Bacillus subtilis spores by monochloramine and ozone. Water Res 40, 373–382. https://doi.org/10.1016/j.watres.2005.10.018.

Driedger, A., Staub, E., Pinkernell, U., Mariñas, B., Köster, W., von Gunten, U., 2001. Inactivation of bacillus subtilis spores and formation of bromate during ozonation. Water Res 35, 2950–2960. https://doi.org/10.1016/S0043-1354(00)00577-7.

Efstratiou, A., Ongerth, J.E., Karanis, P., 2017. Waterborne transmission of protozoan parasites: review of worldwide outbreaks - an update 2011–2016. Water Res 114, 14–22. https://doi.org/10.1016/j.watres.2017.01.036.

Elovitz, M.S., von Gunten, U., Kaiser, H.P., 2000. Hydroxyl radical/ozone ratios during ozonation processes. II. The effect of temperature, pH, alkalinity, and DOM properties. Ozone Sci. Eng. 22, 123–150. https://doi.org/10.1080/01919510008547216.

Finch, G.R., Black, E.K., Gyurek, L., Belosevic, M., 1993a. Ozone inactivation of Cryptosporidium parvum in demand-free phosphate buffer determined by in vitro excystation and animal infectivity. Appl. Environ. Microbiol. 59, 4203–4210. https://doi.org/10.1128/aem.59.12.4203-4210.1993.

Finch, G.R., Black, E.K., Labatiuk, C.W., Gyurek, L., Belosevic, M., 1993b. Comparison of Giardia lamblia and Giardia muris cyst inactivation by ozone. Appl. Environ. Microbiol. 59, 3674–3680. https://doi.org/10.1128/aem.59.11.3674-3680.1993.

Finch, G.R., Haas, C.N., Oppenheimer, J.A., Gordon, G., Trussell, R.R., 2001. Design criteria for inactivation of Cryptosporidium by ozone in drinking water. Ozone Sci. Eng. 23, 259–284. https://doi.org/10.1080/01919510108962010.

Finch, G.R., Li, H., 1999. Inactivation of cryptosporidium at 1°C using ozone or chlorine dioxide. Ozone Sci. Eng. 21, 477–486. https://doi.org/10.1080/01919512.1999.10382886.

Fox, K.R., Lytle, D.A., 1996. Milwaukee's crypto outbreak: investigation and recommendations. J. Am. Water Works Assoc. 88, 87–94.

Gamage, S., Gerrity, D., Pisarenko, A.N., Wert, E.C., Snyder, S.A., 2013. Evaluation of process control alternatives for the inactivation of escherichia coli, ms2 bacteriophage, and bacillus subtilis spores during wastewater ozonation. Ozone Sci. Eng. 35, 501–513. https://doi.org/10.1080/01919512.2013.833852.

Gerrity, D., Gamage, S., Jones, D., Korshin, G.V, Lee, Y., Pisarenko, A., Trenholm, R.A., von Gunten, U., Wert, E.C., Snyder, S.A., 2012. Development of surrogate correlation models to predict trace organic contaminant oxidation and microbial inactivation during ozonation. Water Res 46, 6257–6272. https://doi.org/10.1016/j.watres.2012.08.037.

Gyürek, L.L., Finch, G.R., 1998. Modeling Water Treatment Chemical Disinfection Kinetics. J. Environ. Eng. 124, 783–793.

Gyurek, L.L., Li, H., Belosevic, M., Finch, G.R., 1999. Ozone inactivation kinetics of cryptosporidium in phosphate buffer. J. Environ. Eng. 125, 913–924.

Haas, C.N., Kaymak, B., 2003. Effect of initial microbial density on inactivation of Giardia muris by ozone. Water Res 37, 2980–2988. https://doi.org/10.1016/S0043-1354(03)00112-X.

Harden, V.P., Harris, J.O., 1952. The isoelectric point of bacterial cells. J. Bacteriol. 65, 198–202.

Helmer, R.D., Finch, G.R., 1993. Use of MS2 coliphage as a surrogate for enteric viruses in surface waters disinfected with ozone. Ozone Sci. Eng. 15, 279–293. https://doi.org/10.1080/01919519308552490.

Hoigné, J., 1994. Characterization of water quality criteria for ozonation processes. part i:minimal set of analytical data. Ozone Sci. Eng. 16, 113–120. https://doi.org/10.1080/01919519408552416.

Hoigne, J., Bader, H., 1994. Characterization of water quality criteria for ozonation processes. part ii: lifetime of added ozone. Ozone Sci. Eng. 16, 121–134. https://doi.org/10.1080/01919519408552417.

Hoigné, J., Bader, H., 1975. Ozonation of water : role of hydroxyl radicals as oxidizing intermediates. Science 190, 782–784, 80-.

Hrudey, S.E., Payment, P., Huck, P.M., Gillham, R.W., Hrudey, E.J., 2003. A fatal waterborne disease epidemic in Walkerton, Ontario: Comparison with other waterborne outbreaks in the developed world. Water Sci. Technol. 47, 7–14. https://doi.org/10.2166/wst.2003.0146.

Hsu, B.M., Huang, C., 2002. Influence of ionic strength and pH on hydrophobicity and zeta potential of Giardia and Cryptosporidium. Colloids Surfaces A Physicochem. Eng. Asp. 201, 201–206. https://doi.org/10.1016/S0927-7757(01)01009-3.

Huber, M.M., Canonica, S., Park, G.Y., von Gunten, U., 2003. Oxidation of pharmaceuticals during ozonation and advanced oxidation processes. Environ. Sci. Technol. 37, 1016–1024. https://doi.org/10.1021/es025896h.

ICTV, 2020. Virus taxonomy: The ICTV report on virus classification and taxon nomenclature [WWW Document]. Int. Comm. Virus Taxon. URL https://talk.ictvonline.org/ictv-reports/ictv_online_report/.

Jenkins, M.B., Eaglesham, B.S., Anthony, L.C., Kachlany, S.C., Bowman, D.D., Ghiorse, W.C., 2010. Significance of wall structure, macromolecular composition, and surface polymers to the survival and transport of Cryptosporidium parvum oocysts. Appl. Environ. Microbiol. 76, 1926–1934. https://doi.org/10.1128/AEM.02295-09.

Kim, C.K., Gentile, D.M., Sproul, O.J., 1980. Mechanism of ozone inactivation of bacteriophage f2. Appl. Environ. Microbiol. 39, 210–218. https://doi.org/10.1128/aem.39.1.210-218.1980.

Kimball, A.W., 1953. The fitting of multi-hit survival curves. Biometrics 9, 201–211.

Labatiuk, C.W., Belosevic, M., Finch, G.R., 1994. Inactivation of giardia muris using ozone and ozone-hvdrogen peroxide. Ozone Sci. Eng. 16, 67–78. https://doi.org/10.1080/01919519408552381.

Labatiuk, C.W., Belosevic, M., Finch, G.R., 1992a. Evaluation of high level ozone inactivation of giardia muris using an animal infectivity model. Ozone Sci. Eng. 14, 1–12. https://doi.org/10.1080/01919519208552314.

Labatiuk, C.W., Belosevic, M., Finch, G.R., 1992b. Factors influencing the infectivity of Giardia muris cysts following ozone inactivation in laboratory and natural waters. Water Res 26, 733–743. https://doi.org/10.1016/0043-1354(92)90004-N.

Labatiuk, C.W., Schaefer, F.W., Finch, G.R., Belosevic, M., 1991. Comparison of animal infectivity, excystation, and fluorogenic dye as measures of Giardia muris cyst inactivation by ozone. Appl. Environ. Microbiol. 57, 3187–3192. https://doi.org/10.1128/aem.57.11.3187-3192.1991.

Leclerc, H., Schwartzbrod, L., Dei-Cas, E., 2002. Microbial agents associated with waterborne diseases. Crit. Rev. Microbiol. 28, 371–409. https://doi.org/10.1080/1040-840291046768.

Lee, Y., Gerrity, D., Lee, M., Bogeat, A.E., Salhi, E., Gamage, S., Trenholm, R.A., Wert, E.C., Snyder, S.A., von Gunten, U., 2013. Prediction of micropollutant elimination during ozonation of municipal wastewater effluents: use of kinetic and water specific information. https://doi.org/10.1021/es400781r.

Lee, Y., von Gunten, U., 2016. Advances in predicting organic contaminant abatement during ozonation of municipal wastewater effluent: reaction kinetics, transformation products, and changes of biological effects. Environ. Sci. Water Res. Technol. 2, 421–442. https://doi.org/10.1039/c6ew00025h.

Lewin, N., Craik, S., Li, H., Smith, D.W., Belosevic, M., 2001. Sequential inactivation of Cryptosporidium using ozone followed by free chlorine in natural water. Ozone Sci. Eng. 23, 411–420. https://doi.org/10.1080/01919510108962024.

Li, H., Gyurek, L.L., Finch, G.R., Smith, D.W., Belosevic, M., 2001. EFFECT of temperature on ozone inactivation of cryptosporidium parvum in oxidant demand-free phosphate buffer. J. Environ. Eng. 127, 456–467.

Li, Y., Smith, D.W., Belosevic, M., 2004. Morphological changes of Guardia lamblia cysts after treatment with ozone and chlorine. J. Environ. Eng. Sci. 3, 495–506.

Lim, M.Y., Kim, J.M., Lee, J.E., Ko, G., 2010. Characterization of ozone disinfection of murine norovirus. Appl. Environ. Microbiol. 76, 1120–1124. https://doi.org/10.1128/AEM.01955-09.

Mac Kenzie, W.R., Hoxie, N.J., Proctor, M.E., Gradus, M.S., Blair, K.A., Peterson, D.E., Kazmierczak, J.J., Addiss, D.G., Fox, K.R., Rose, J.B., Davis, J.P., 1994. A massive outbreak in milwaukee of cryptosporidium transmitted through the public water supply. N. Engl. J. Med. 331, 161–167.

Mesquita, M.M.F., Stimson, J., Chae, G.T., Tufenkji, N., Ptacek, C.J., Blowes, D.W., Emelko, M.B., 2010. Optimal preparation and purification of PRD1-like bacteriophages for use in environmental fate and transport studies. Water Res 44, 1114–1125. https://doi.org/10.1016/j.watres.2009.11.017.

Michen, B., Graule, T., 2010. Isoelectric points of viruses. J. Appl. Microbiol. 109, 388–397. https://doi.org/10.1111/j.1365-2672.2010.04663.x.

Oppenheimer, J.A., Aieta, M.E., Trussell, R.R., Jacangelo, J.G., Najm, I.., 2000. Evaluation of cryptosporidium inactivation in natural waters.

Owens, J.H., Miltner, R.J., Rice, E.W., Johnson, C.H., Dahling, D.R., Schaefer, F.W., Shukairy, H.M., 2000. Pilot-scale ozone inactivation of cryptosporidium and other microorganisms in natural water. Ozone Sci. Eng. 22, 501–517. https://doi.org/10.1080/01919510009408793.

Rakness, K.L., 2015. Ozone in drinking water treatment: process design, operation, and optimization. American Water Works Association.

Rakness, K.L., Najm, I., Elovitz, M., Rexing, D., Via, S., 2005. Cryptosporidium log-inactivation with ozone using effluent CT10, geometric mean CT10, extended integrated CT10 and extended CSTR calculations. Ozone Sci. Eng. 27, 335–350. https://doi.org/10.1080/01919510500250267.

Rennecker, J.L., Mariñas, B.J., Owens, J.H., Rice, E.W., 1999. Inactivation of cryptosporidium parvum oocysts with ozone. Water Res 33, 2481–2488. https://doi.org/10.1016/S0043-1354(99)00116-5.

Righetti, P.G., Caravaggio, T., 1976. Isoelectric points and molecular weights of proteins. J. Chromatogr. 127, 1–28.

Roy, D., Chian, E.S.K., Engelbrecht, R.S., 1982. Mathematical model for enterovirus inactivation by ozone. Water Res 16, 667–673. https://doi.org/10.1016/0043-1354(82)90089-6.

Roy, D., Wong, P.K.Y., Engelbrecht, R.S., Chian, E.S.K., 1981. Mechanism of enteroviral inactivation by ozone. Appl. Environ. Microbiol. 41, 718–723.

Sella, S.R.B.R., Vandenberghe, L.P.S., Soccol, C.R., 2014. Life cycle and spore resistance of spore-forming Bacillus atrophaeus. Microbiol. Res. 169, 931–939. https://doi.org/10.1016/j.micres.2014.05.001.

Sigmon, C., Shin, G.A., Mieog, J., Linden, K.G., 2015. Establishing surrogate - virus relationships for ozone disinfection of wastewater. Environ. Eng. Sci. 32, 451–460. https://doi.org/10.1089/ees.2014.0496.

Sigstam, T., Gannon, G., Cascella, M., Pecson, B.M., Wigginton, K.R., Kohn, T., 2013. Subtle differences in virus composition affect disinfection kinetics and mechanisms. Appl. Environ. Microbiol. 79, 3455–3467. https://doi.org/10.1128/AEM.00663-13.

Smith, H.V., Nichols, R.A.B., Grimason, A.M., 2005. Cryptosporidium excystation and invasion: Getting to the guts of the matter. Trends Parasitol 21, 133–142. https://doi.org/10.1016/j.pt.2005.01.007.

Soller, J.A., Eftim, S.E., Warren, I., Nappier, S.P., 2017. Microbial risk analysis evaluation of microbiological risks associated with direct potable reuse 5, 3–14. https://doi.org/10.1016/j.mran.2016.08.003.

Staehelin, J., Hoigne, J., 1985. Decomposition of ozone in water in the presence of organic solutes acting as promoters and inhibitors of radical chain reactions. Environ. Sci. Technol. 19, 1206–1213. https://doi.org/10.1021/es00142a012.

Stockdale, C.J., Adriaenssens, E.M., Kuhn, J.H., Pallen, M., Rumnieks, J., Shkoporov, A., Draper, L.A., Ross, R.P., Hill, C., 2020. Rename one class (Leviviricetes - formerly Allassoviricetes), rename one order (Norzivirales - formerly Levivirales), create one new order (Timlovirales), and expand the class to a total of six families, 420 genera and 883 species. Int. Comm. Taxon. Viruses.

Torii, S., Itamochi, M., Katayama, H., 2020. Inactivation kinetics of waterborne virus by ozone determined by a continuous quench flow system. Water Res 186, 116291. https://doi.org/10.1016/j.watres.2020.116291.

Torii, S., Miura, F., Itamochi, M., Haga, K., Katayama, K., Katayama, H., 2021. Impact of the heterogeneity in free chlorine, uv254, and ozone susceptibilities among coxsackievirus b5 on the prediction of the overall inactivation efficiency. Environ. Sci. Technol. 55, 3156–3164. https://doi.org/10.1021/acs.est.0c07796.

Torrey, J., von Gunten, U., Kohn, T., 2019. Differences in viral disinfection mechanisms as revealed by quantitative transfection of echovirus 11 genomes. Appl. Environ. Microbiol. 85, 1–14. https://doi.org/10.1128/AEM.00961-19.

USEPA, 2006. Long term 2 enhanced surface water treatment rule. United States Environ. Prot. Agency 1–375.

USEPA, 1999. Alternative disinfectants and oxidants guidance manual. United States Environ. Prot. Agency 1–328.

USEPA, 1998. National primary drinking water regulations: interim enhanced surface water treatment. United States Environ. Prot. Agency 69478–69521. https://doi.org/10.1016/0196-335x(80)90058-8.

USEPA, 1991. Guidance manual for compliance with the filtration and disinfection requirements for public water systems using surface water sources. United States Environ. Prot. Agency 1–580.

van Regenmortel, M.H.V., Fauquet, C.M., Bishop, D.H.L., Carstens, E.B., Estes, M.K., Lemon, S.M., Maniloff, J., Mayo, M.A., McGeoch, D.J., Pringle, C.R., Wickner, R.B., 2000. Virus taxonomy. Seventh report of the international committee on taxonomy of viruses, international committee on virus taxonomy.

von Gunten, U., 2018. Oxidation processes in water treatment: are we on track? Environ. Sci. Technol. 52, 5062–5075. https://doi.org/10.1021/acs.est.8b00586.

von Gunten, U., 2003a. Ozonation of drinking water : part II . disinfection and by-product formation in presence of bromide , iodide or chlorine. Water Res 37, 1469–1487.

von Gunten, U., 2003b. Ozonation of drinking water: part i. oxidation kinetics and product formation. Water Res 37, 1443–1467. https://doi.org/10.1016/S0043-1354(02)00457-8.

von Gunten, U., Hoigne, J., 1994. Bromate formation during ozonization of bromide-containing waters: interaction of ozone and hydroxyl radical reactions. Environ. Sci. Technol. 28, 1234–1242. https://doi.org/10.1021/es00056a009.

von Sonntag, C., von Gunten, U., 2012. Chemistry of ozone in water and wastewater treatment: from basic principles to applications, chemistry of ozone in water and wastewater treatment. From Basic Principles Appl. https://doi.org/10.2166/9781780400839.

Wickramanayake, G.B., Rubin, A.J., Sproul, O.J., 1985. Effects of ozone and storage temperature on Giardia cysts. J. /Am. Water Work. Assoc. 77, 74–77. https://doi.org/10.1002/j.1551-8833.1985.tb05591.x.

Wohlsen, T., Stewart, S., Aldridge, P., Bates, J., Gray, B., Katouli, M., 2007. The efficiency of ozonated water from a water treatment plant to inactivate cryptosporidium oocysts during two seasonal temperatures. J. Water Health 5, 433–440. https://doi.org/10.2166/wh.2007.039.

Wolf, C., Pavese, A., von Gunten, U., Kohn, T., 2019. Proxies to monitor the inactivation of viruses by ozone in surface water and wastewater effluent. Water Res 166, 115088. https://doi.org/10.1016/j.watres.2019.115088.

Wolf, C., von Gunten, U., Kohn, T., 2018. Kinetics of inactivation of waterborne enteric viruses by ozone. Environ. Sci. Technol. 52, 2170–2177. https://doi.org/10.1021/acs.est.7b05111.

Young, S., Torrey, J., Bachmann, V., Kohn, T., 2020. Relationship between inactivation and genome damage of human enteroviruses upon treatment by UV254, free chlorine, and ozone. Food Environ. Virol. 12, 20–27. https://doi.org/10.1007/s12560-019-09411-2.

Young, S.B., Setlow, P., 2004. Mechanisms of bacillus subtilis spore resistance to and killing by aqueous ozone. J. Appl. Microbiol. 96, 1133–1142. https://doi.org/10.1111/j.1365-2672.2004.02236.x.

Appendix C. Evaluation of preformed monochloramine for bromate control in ozonation for potable reuse

Pearce, R., Hogard, S., Buehlmann, P., Salazar-Benites, G., Wilson, C., & Bott, C. (2022). Evaluation of preformed monochloramine for bromate control in ozonation for potable reuse. Water Research, 211, 118049. https://doi.org/10.1016/j.watres.2022.118049

9 pages

Water Research 211 (2022) 118049

Contents lists available at ScienceDirect

Water Research

journal homepage: www.elsevier.com/locate/watres

Evaluation of preformed monochloramine for bromate control in ozonation for potable reuse

Robert Pearce [a,b,*], Samantha Hogard [a,b], Peter Buehlmann [c], Germano Salazar-Benites [b], Christopher Wilson [b], Charles Bott [b]

[a] Virginia Tech Department of Civil and Environmental Engineering, 750 Drillfield Dr, 200 Patton Hall, Blacksburg, VA 24061, United States
[b] Hampton Roads Sanitation District, 1434 Air Rail Ave, Virginia Beach, VA 23455, United States
[c] Brown and Caldwell, 1725 Duke St, Unit 250, Alexandria, VA 22314, United States

ARTICLE INFO

Keywords:
Ozonation
Bromate
Potable reuse
1,4-dioxane

ABSTRACT

Bromate, a regulated disinfection byproduct, forms during the ozonation of bromide through reactions with both ozone and hydroxyl radical. In this study, preformed monochloramine was evaluated for use as a bromate suppression method in pilot testing of wastewater reuse with an average bromide concentration of 422±20 μg/L. A dose of 3 mg/L NH_2Cl-Cl_2 decreased bromate formation by an average of 82% and was sufficient to keep bromate below the MCL at ozone doses up to 8.6 mg/L (1.2 O_3:TOC). Removal of 1,4-dioxane through ozonation decreased with increasing NH_2Cl dose, confirming that monochloramine suppresses bromate formation, at least in part, by acting as a hydroxyl radical scavenger. This may negatively impact oxidation objectives of ozonation in reuse applications. Increasing monochloramine contact time did not improve bromate suppression, indicating that monochloramine probably did not mask bromide as NHBrCl or other haloamines prior to ozonation. However, NHBrCl and NH_2Br may be formed from reactions between HOBr and NH_2Cl and excess free ammonia during ozonation. NDMA was formed by ozonation at concentrations up to 79 ng/L and was not enhanced by NH_2Cl addition.

1. Introduction and background

Ozonation coupled with biofiltration has recently emerged as a promising alternative to membrane-based processes for potable reuse applications. This process offers significant cost savings in terms of both capital and operating costs as well as eliminating the need to handle concentrated brine streams which are a concern for inland locations (Gerrity et al., 2014). In this process ozone provides bulk organics degradation, assimilable organic carbon (AOC) generation, and transforms trace organic contaminants (TOrCs) into more readily biodegradable transformation products, while also providing a barrier against pathogens (Arnold et al., 2018; Knopp et al., 2016; Reungoat et al., 2012; Wert et al., 2007).

Ozone is a powerful oxidant which also leads to the generation of hydroxyl (*OH) and other radicals through reactions with dissolved organic matter (DOM). Hydroxyl radical is nonselective and extremely fast reacting. While transient concentrations and exposures are very low, it is considered the strongest oxidant available for water treatment. Ozone decomposition follows multiphasic kinetics; in the initial phase (t < ~30 s) rapid ozone decomposition takes place due to fast direct reactions with organics that generate large amounts of *OH. After the most reactive DOM has been consumed, the ozone decay rate stabilizes in the second phase and can be approximated by first order decay kinetics (von Gunten, 2003a). Due to the higher concentration and reactivity of the organic matter in wastewater effluent, ozonation can generate hydroxyl radical concentrations greater than those found in advanced oxidation process (AOP) applications in natural waters (Buffle et al., 2006).

Bromate (BrO_3^-) is formed through the ozonation of bromide containing waters and is the primary disinfection byproduct (DBP) of ozonation. A maximum contaminant level for bromate of 10 μg/L was set by the USEPA following a World Health Organization report which classified it as a potential human carcinogen (EPA, 1998; WHO, 1993). Conventional drinking water treatment wisdom states that bromate formation may be an issue if bromide concentrations are greater than 50 μg/L (von Gunten, 2003b). Bromate is formed through a complex series

* Corresponding author at: Virginia Tech Department of Civil and Environmental Engineering, 750 Drillfield Dr, 200 Patton Hall, Blacksburg, VA 24061, United States.
E-mail address: probe93@vt.edu (R. Pearce).

https://doi.org/10.1016/j.watres.2022.118049
Received 12 October 2021; Received in revised form 30 December 2021; Accepted 5 January 2022
Available online 9 January 2022

of both ozone and hydroxyl radical reactions (Fig. 1) (Pinkernell and von Gunten, 2001). In the direct pathway ozone oxidizes bromide to hypobromous acid, HOBr. Only OBr^- is then further oxidized by ozone to form $BrO_2^-$and BrO_3^-. In the direct-indirect pathway HOBr and OBr^- react with hydroxyl radical to form BrO* which disproportionates to BrO_2^- which is then oxidized to BrO_3^-. The majority of bromate formation occurs through this pathway during drinking water treatment conditions (Qi et al., 2016; von Gunten, 2003b).The indirect-direct pathway is most important during the initial phase where hydroxyl radical concentrations are highest and is likely responsible for much of the bromate formation in wastewater ozonation. In this pathway, bromide is radicalized by *OH, reacts with ozone to form BrO*, and then proceeds following the latter half of the direct-indirect pathway (Pinkernell and von Gunten, 2001; Qi et al., 2016; Soltermann et al., 2017).

There are several common chemical bromate control strategies. pH suppression shifts the HOBr/OBr^- equilibrium towards hypobromous acid, thus decreasing bromate formation through the direct pathways as well as possibly decreasing *OH generation. Hydrogen peroxide addition rapidly converts ozone into *OH, decreasing overall ozone exposure and can also catalytically reduce hypobromous acid (von Gunten and Oliveras, 1998). Ammonia can be added to form bromamine (NH_2Br) from hypobromous acid which masks bromide from further oxidation (Table 1 Reaction 1). In the chlorine-ammonia process, free chlorine is used to pre-oxidize bromide to hypobromous acid then ammonia is added to mask bromide as NH_2Br prior to ozonation. Monochloramine may also be formed from excess free chlorine and acts as a radical scavenger (Table 1 Reaction 3), as such the NH_3-Cl_2 has also been used to control bromate. Hydroxyl radical scavenging was hypothesized to be the primary benefit of monochloramine over ammonia addition alone (Buffle et al., 2004). Similar to ammonia, monochloramine can react with HOBr to form bromochloramine, NHBrCl (Table 1 Reaction 2). Recently Ling et al. (2020) claimed that bromochloramine and dibromamine, $NHBr_2$, were formed prior to ozonation (Table 1 Reactions 4 and 5) in the NH_3-Cl_2 process. Six minutes of monochloramine contact time was provided to mask the majority of bromide as NHBrCl and $NHBr_2$. These compounds were also found to be more resistant to ozonation than NH_2Br.

Hampton Roads Sanitation District's (HRSD) SWIFT Research Center (SRC) is a 3.8 MLD demonstration scale advanced water treatment facility located in Suffolk, Virginia. The facility treats secondary effluent from the Nansemond Treatment Plant (5-stage Bardenpho process with methanol addition) to drinking water standards for recharge into the Potomac Aquifer. The treatment train consists of coagulation, flocculation, and sedimentation followed by ozonation, biofiltration, granular activated carbon adsorption, and UV disinfection. The facility also houses a similarly configured pilot scale (4 L/min) treatment plant for experimental work. Due to the low lying, coastal nature of HRSD's collection system, bromide concentrations of 400 μg/L or higher are often present due to saltwater infiltration as well as specific industrial sources such as landfill leachate.

Table 1
Relevant reactions for bromate suppression by monochloramine.

Reaction	Rate Constant	Citation	Number
$HOBr + NH_3 \rightarrow NH_2Br$	$k = 7.5(10^7)$ $M^{-1}s^{-1}$	Wajon and Morris (1982)	(1)
$HOBr + NH_2Cl \rightarrow NHBrCl$	$k = 2.86(10^5)$ $M^{-1}s^{-1}$	Gazda and Margerum (1994)	(2)
$NH_2Cl + {}^*OH \rightarrow NHCl^*$	$k = 5(10^8)$ $M^{-1}s^{-1}$	Poskrebyshev et al. (2003)	(3)
$2\ NH_2Cl + Br^- \rightarrow NHBrCl + NH_3 + Cl^-$	$k = 3.54(10^6)$ $M^{-2}s^{-1}$ at pH 7	Trofe et al. (1980)	(4)
$2\ NHBrCl + Br^- \rightarrow NHBr_2$	$k = 565\ M^{-1}s^{-1}$	Luh and Mariñas (2014)	(5)
$O_3 + NH_2Cl \rightarrow NO_3^- + Cl^- + H^+$	$k = 26\ M^{-1}s^{-1}$	Haag and Hoigné (1983)	(6)

During initial testing, pH suppression was found to be impractical on the pilot scale and cost prohibitive for full scale implementation due to the high alkalinity in the wastewater effluent (data not shown). Hydrogen peroxide was not considered due to the project requirement to achieve an ozone residual for disinfection CT credit. Ammonia addition was tested briefly but could not effectively keep bromate below the MCL (Buehlmann et al., 2017). Preformed monochloramine, where monochloramine is formed using sodium hypochlorite and ammonium sulfate fed into softened carrier water, was selected for bromate control. This was chosen due to the ease of control and decreased chemical demand over the NH_3-Cl_2 or Cl_2-NH_3 with somewhat variable NH_4^+ and NO_2^-in the wastewater effluent, and the desire to minimize production of free chlorine DBPs (when NH_4^+ is low). Preformed monochloramine also decreases the possibility of n-Nitrosodimethylamine (NDMA) formation by dichloramine (Hogard et al., 2021; Mitch et al., 2005; Schreiber and Mitch, 2005).

Of particular concern is 1,4-dioxane, a trace contaminant and potential human carcinogen commonly found in wastewater effluents due to its use in industry and household supplies such as detergents (Tanabe and Kawata, 2008). Influent concentrations typically range from 0.5 to 1 μg/L at the SWIFT Research Center and it has a 10^{-6} lifetime cancer risk associated with a concentration of 0.35 μg/L (EPA, 2013). It is not readily biodegradable or well adsorbed and through ozonation it is only removed by *OH oxidation, in which case radical scavenging by NH_2Cl may decrease its removal (Hogard et al., 2021).

The objectives of this study were to determine the efficacy of preformed monochloramine for bromate control during ozonation of a high bromide reuse water. Secondary effects of monochloramine addition on *OH exposure, ozone demand, decay, and disinfection credit were also analyzed as well as NDMA formation through ozonation. While determining the mechanisms of bromate suppression by monochloramine was not the objective of this study, results and the implications on treatment performance were analyzed in light of these mechanisms.

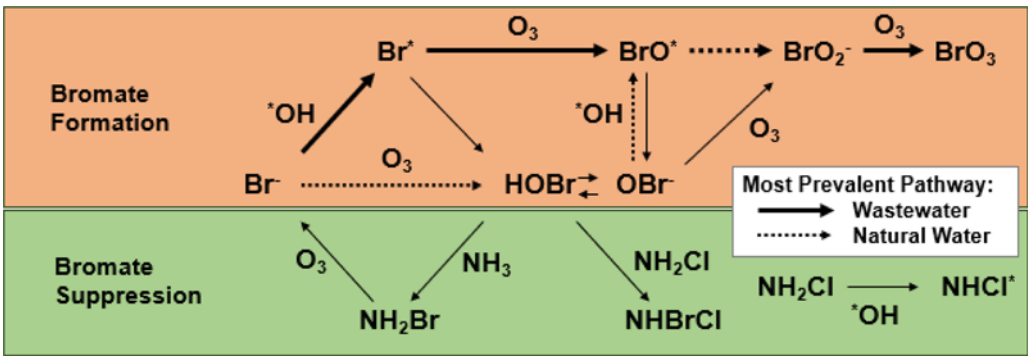

Fig. 1. Bromate formation pathways and suppression mechanisms. After Pinkernell and von Gunten (2001).

2. Materials and methods

2.1. Plant description

Pilot tests were conducted at HRSD's SRC at the Nansemond Treatment Plant (Suffolk, VA). Nansemond Treatment Plant is a 114 MLD (30 MGD), fully nitrifying and denitrifying plant utilizing a 5-stage bardenho treatment process with methanol addition for denitrification. 3.8 MLD (1 MGD) of the secondary clarifier effluent is fed into the SRC. The treatment train includes coagulation, flocculation, and sedimentation, followed by ozonation, biofiltration, granular activated carbon adsorption, and UV disinfection prior to deep well aquifer recharge. The plant operation has been described extensively elsewhere (Hogard et al., 2021).

Settled water from the SRC was fed to a pilot feed tank with a chiller to control the temperature to 20±0.8 °C, however for each test temperature stayed within a 1 °C range. Influent water quality is summarized in Table 2. A pipeline chloramine contactor was used upstream of the ozonation pilot to test the effects of monochloramine contact time as shown in Figure 2. The ozone pilot used was a modified Intuitech 2nd generation ozone pilot (Intuitech Inc, Salt Lake City, USA) operated at 3.94 L/min. The pilot ozone contactor consisted of one counter current dissolution column with a retention time of 1.5 min, followed by five contact columns also with a retention time of 1.5 min each. Each of the contact columns had a series of sample ports to measure ozone residuals along the contactor. Ozone was generated from oxygen from the onboard oxygen concentrator. Ozone gas concentrations ranged from 3.4 to 9.8% (w/w) as the lowest ozone doses required the gas flow rates to be increased for the oxygen/ozone mass flow controllers to control the dose well. Measured ozone transfer efficiency was >99%. However, in the above configuration the gas flow rates (0.15–0.3 SLPM) were below the optimal gas flow rates for the off gas analyzer. In previous testing with higher gas flow rates and lower gas concentrations, transfer efficiency was still typically >95%. Applied ozone doses were selected by taking a grab-sample for TOC and nitrite and adjusting the dose for the desired O_3:TOC ratio, all O_3:TOC ratios referenced herein are nitrite corrected. A TOC sample was also collected and sent to HRSD's Central Environmental Laboratory at the beginning of each test, the grab samples on the online instrument (Shimadzu TOC 4200) were found to read slightly higher than the laboratory instrument so the lab values were used. Influent UV absorbance changed by less than 5% over the course of each testing day so TOC was assumed to be constant for each test. Fig. 2

Preformed monochloramine stock was collected from the preformed monochloramine system at the SRC. In this system tap water is fed through GAC to dechlorinate and remove TOC which then followed by softening via ion exchange. Sodium hypochlorite followed by ammonium sulfate are then added to the carrier water using static mixers. The carrier water flow rate is set to target a 50x dilution to prevent heat buildup and chemicals are dosed for a 4.5:1 Cl_2:N ratio for optimal monochloramine formation. Monochloramine stock was collected daily during testing and fed using a peristaltic pump which was calibrated each time the chloramine addition point was changed. Monochloramine stock was kept on ice to prevent decay and used within four hours of collection. The stock concentration was measured each time it was collected and at the end of each testing day, never decaying more than 5%.

2.2. Analytical methods

Monochloramine, total chlorine, and free ammonia were measured using a Hach SL1000 Portable Parallel Analyzer (Hach, Loveland CO). Total ammonia, nitrite and nitrate were measured by TNT methods 830, 839, and 835, respectively, and quantified on a Hach DR 3900 spectrophotometer. Ozone residuals were measured by the gravimetric indigo method, Standard Methods 4500B-O_3, with malonic acid addition to mask and free chlorine from chloramination or any oxidized bromide species which may be present. Indigo absorbance at 600 nm as well as UV254 absorbance of the water samples were measured on a Genesys 180 UV–Vis spectrophotometer (Thermo Scientific, Waltham, MA).

Bromide and bromate were analyzed by ion chromatography via EPA methods 300 and 300.1, respectively. Bromate samples were preserved with EDA. In order to calculate total organic bromine, TOBr, ozone effluent bromide samples were also collected. The effluent bromide concentration was corrected for the bromide converted to bromate and compared to the influent after the method of Buffle et al. (2004). Ozone effluent bromide samples were quenched with 2 mM sodium bisulfite within one minute of sample collection.

NDMA and 1,4-dioxane were measured on an Agilent 7010B GC/MS Triple Quadrupole by EPA methods 521 and 522 with some slight modification. Notably, both samples were collected it the same 500 mL sample container preserved with 50 mg/L sodium sulfite and 1 g/L sodium bisulfate to dechlorinate and acidify the sample. Magnesium sulfate was used in place of sodium sulfate to dry the extract. Other slight deviations were as reported by Vaidya et al. (2021).

3. Results and discussion

3.1. Bromate formation

Without monochloramine addition, bromate formation increased from 0.3 to 39.9 μg/L by increasing the ozone dose from 0.31 to 1.18 O_3:TOC (3.75 to 9.6 mg/L applied O_3) as shown in Fig. 3. Bromide conversion to bromate of 2.9% at 0.86 O_3:TOC is in line with the bench testing results reported by Soltermann et al. (2016). With monochloramine addition immediately before ozonation, bromate formation was decreased by as much as 90% with 5 mg/L-Cl_2 NH_2Cl. A dose of 1 mg/L NH_2Cl reduced bromate formation by 68% on average, while 3 and 5 mg/L decreased it by 84% and 87%, respectively. Increasing monochloramine contact time to 8 min had no effect on bromate control and is discussed further below.

At the lowest ozone doses, targeting 0.3 O_3:TOC, there was no dose response observed (all bromate values were <1 μg/L) between monochloramine and bromate formed. In these tests, there was very little measured ozone residual in the effluent of the dissolution column. Other studies have shown very little BrO_3 formation at ozone doses below 0.4 O_3:TOC as there is very little ozone available to oxidize Br* and HOBr/OBr^- to form bromate (Soltermann et al., 2016).

As shown in Figs. 3and 4, there was minimal improvement in bromate by increasing monochloramine dose from 3 to 5 mg/L. Similar to both ammonia addition and the chlorine/ammonia based strategies, preformed monochloramine addition likely has a point of diminishing return where increasing dose has limited or no effect on controlling the bromate formation process (Buffle et al., 2004; Pinkernell and von

Table 2
Influent Water Quality Summary.

Parameter	pH	Temp	Alkalinity	TOC	Bromide	1,4-dioxane	NH_4	NO_2	NO_3
Unit		°C	mg/L-$CaCO_3$	mg/L	mg/L	μg/L	mg/L-N	mg/L-N	mg/L-N
Mean	7.14	20.0	178.3	6.60	0.422	0.52	0.36	0.122	2.27
Standard Deviation	0.05	0.8	7.51	0.31	0.020	0.04	0.22	0.145	0.46
Min	7.08	19.3	174	6.12	0.397	0.49	0.06	0.000	1.13
Max	7.23	22.4	184	6.9	0.457	0.56	0.519	0.498	2.80

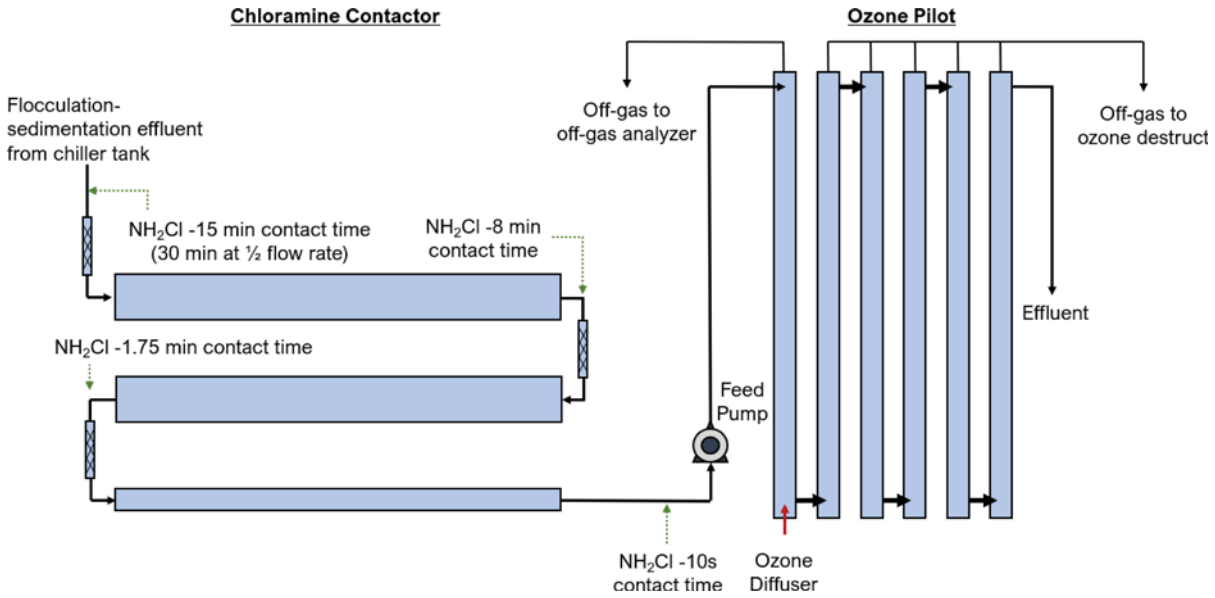

Fig. 2. Ozone pilot and chloramine contactor schematic.

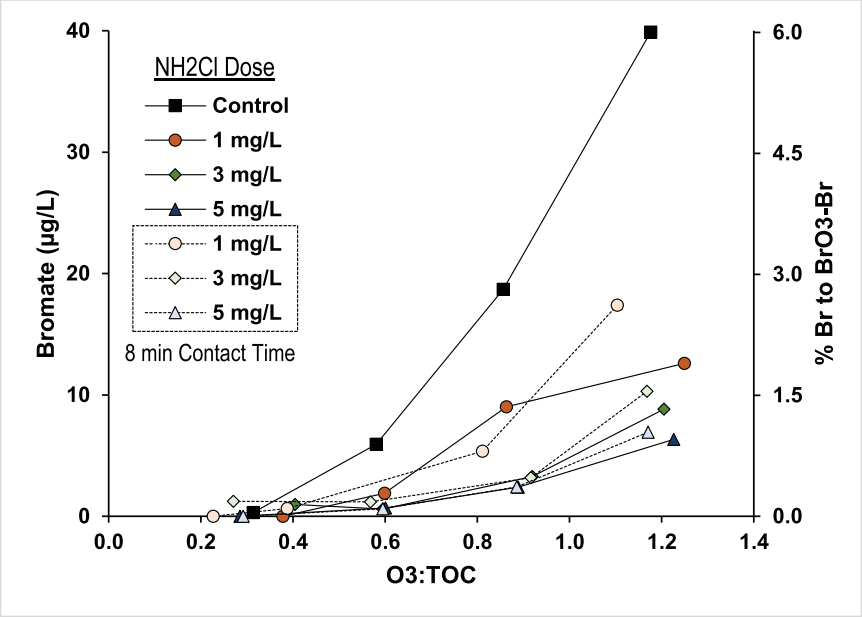

Fig. 3. Bromate formation with increasing ozone dose at various monochloramine doses added either immediately before ozonation (solid symbols) or with eight minutes of contact time (open symbols) before ozonation. Br: 414 µg/L, TOC: 6.9 mg/L.

Gunten, 2001). The location of this point is most likely water quality dependent. Benotti et al. (2011) saw no additional bromate suppression from increasing NH_2Cl from 1 mg/L to 2 mg/L, while Ikehata et al. (2013)observed a significant improvement. Interestingly, Ikehata et al. had 35% lower bromide but higher pH and TOC which may have increased their *OH generation and bromate formation for similar ozone doses. While some water quality parameters fluctuated over the course of testing, mainly NO_2^-, it is assumed that the nature and reactivity of DOM did not change.

3.2. Monochloramine as a *OH scavenger

1,4-dioxane removal decreased from 49% to 33% by increasing monochloramine dose from 0 to 5 mg/L at a fixed ozone dose of 7 mg/L (Fig. 4). This demonstrates that monochloramine is acting as a hydroxyl radical scavenger as 1,4-dioxane is ozone resistant and only removed by *OH (k_{O3}= <1 $M^{-1}s^{-1}$, k_{*OH} = 3(10^9) $M^{-1}s^{-1}$) (von Sonntag and von Gunten, 2012). This is particularly important for wastewater ozonation where more bromate is formed through the indirect *OH pathways (Soltermann et al., 2017).

1,4-dioxane samples were also collected with the control and 5 mg/L NH_2Cl in the test matrix shown in Fig. 3, and 1,4-dioxane removal decreased by roughly half (Fig. S1). A similar result was observed during ozonation at the 3.8 MLD scale by Hogard et al. (2021). Change in UV absorbance at 254 nm has been shown to be a good surrogate measure for *OH exposure and 1,4-dioxane removal (Gerrity et al., 2012; Wert et al., 2009). UV absorbance measurements were taken for all tests and were well correlated with 1,4-dioxane removal. These results show that *OH scavenging is occurring by monochloramine in all cases (Figs. S2–S4).

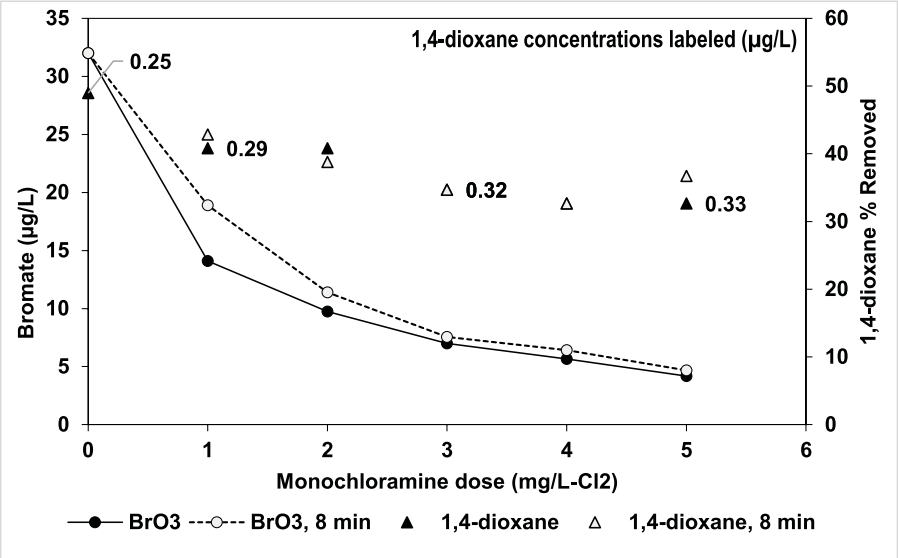

Fig. 4. Bromate formation and 1,4-dioxane removed with increasing monochloramine at a fixed ozone dose of 7 mg/L. 397 µg/L Bromide, 0.49 µg/L initial 1,4-dioxane.

Decreasing hydroxyl radical exposure by as much as 40 percent reduces bromate formation but it may also significantly reduce the oxidation capacity of the system. If non-biodegradable, ozone recalcitrant compounds such as 1,4-dioxane, atrazine, or meprobamate are an issue (or MIB and geosmin in drinking water), use of monochloramine for bromate suppression may be problematic. High ozone doses are often required to get sufficient removal of these compounds, in which case monochloramine use for bromate control is counterproductive. Some compounds with moderate reactivity with ozone, such as gemfibrozil and atenolol, are removed by both ozone and hydroxyl radicals (Lee et al., 2013). With monochloramine addition, ozone dose may need to be increased in order to account for the lower *OH exposure to remove these compounds. Additionally, increasing chloramine doses also increase the chemical dose required to quench monochloramine before biofiltration, and the addition of nitrogen with preformed monochloramine may require increased nitrogen removal in the wastewater treatment plant to meet total nitrogen or nitrate limits. On the other hand, many trace organic contaminants are oxidized quickly by molecular ozone at low ozone doses. Compounds such as diclofenac or sulfamethoxazole with $k_{O3}>10^4\ M^{-1}s^{-1}$ are primarily removed by ozone despite their high reactivity with *OH.

3.3. Monochloramine contact time

Increasing monochloramine contact time upstream of ozonation was tested to determine if bromochloramine formation (Table 1 Reaction 4) prior to ozonation further decreases bromate formation. Two conditions were tested including (1) monochloramine addition directly before the pilot feed pump, approximately 10 s before entering the ozone contactor, and (2) monochloramine addition eight minutes upstream using a small pipeline contactor for the tests shown in Figs. 3and 4. Eight minutes of chloramine contact prior to ozonation did not result in decreased bromate formation. Contact times up to 30 min were also tested (Fig. 5) and no decrease in bromate formation was observed.

Ling et al. (2020) showed ~92% masking of bromide as NHBrCl, $NHBr_2$, and NH_2Br with six minutes of NH_3—Cl_2 pretreatment and even greater with 10 min. This was said to be occurring through reactions with NH_2Cl suggesting preformed monochloramine should behave similarly. Ideally, masking of bromide prior to ozonation would improve bromate suppression allowing the chemical doses to be decreased. This

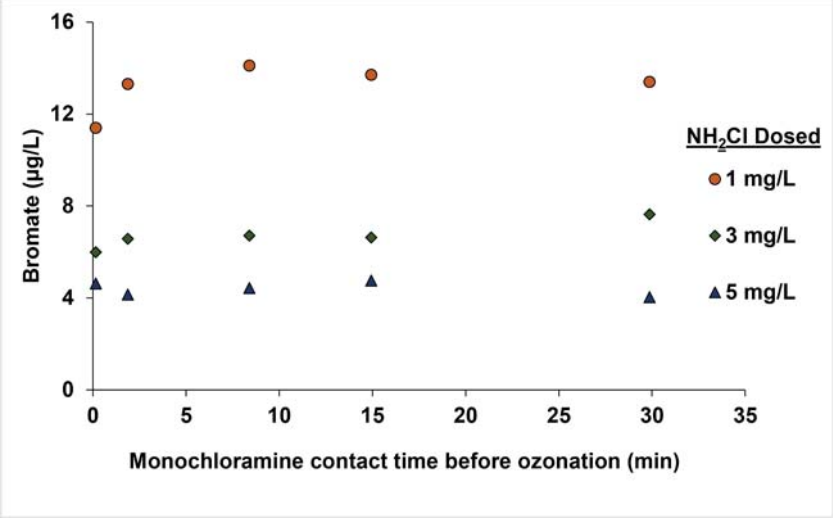

Fig. 5. Bromate formed as a function of monochloramine contact time prior to ozonation at a fixed ozone dose of 7 mg/L. Br: 413 µg/L.

would, in turn, decrease radical scavenging by NH_2Cl and improve 1, 4-dioxane removal. However, that was not the case for this study. Luh and Mariñas (2014) claimed that the Trofe et al. (1980) mechanism (Table 1 Reaction 4) was inaccurate and showed that it would take several hours for bromochloramine to form at NH_2Cl and Br^- concentrations relevant to water treatment. Ling et al. (2020) and Luh and Mariñas (2014) both use spectrophotometric methods in pure waters; however, they assume different absorbance peaks for NHBrCl measurement. Unfortunately, in real water samples with the background absorbance of the water matrix, these methods are not applicable. The DPD total chlorine and indophenol monochloramine methods used in this study cannot distinguish between the various haloamine species.

In either case, there does not appear to be any practical benefit of increasing monochloramine contact time for bromate control. In many of the tests (Figs. 3and 4), it appeared that the slight decay in NH_2Cl over the contact time resulted in decreased bromate suppression. At the SWIFT Research Center, preformed monochloramine is added to the ozone sidestream immediately before the venturi injector. This effectively doubles the monochloramine dose in the sidestream with a ~50/50 sidestream flow split and decreases bromate formation by several μg/L (data not shown). This arrangement would not be feasible with increased monochloramine contact time to the entire flow.

3.4. Intermediate masking

Fig. 4 shows a significant decrease in bromate formation with the addition of 1 mg/L NH_2Cl followed by a more gradual decrease with increasing dose thereafter. 1,4-dioxane removal shows a gradual decrease throughout. *OH radical exposure, calculated using 1,4-dioxane as a probe compound with $k_{*OH} = 3(10^9)$ $M^{-1}s^{-1}$, was decreased by 22% at 1 mg/L NH_2Cl and 41% at 5 mg/L NH_2Cl while bromate was reduced by 56 and 87 percent, respectively. This suggests that *OH radical scavenging is not the only method of bromate suppression by monochloramine. While it does not appear that NHBrCl is forming prior to ozonation, it can be formed from HOBr and NH_2Cl during ozonation (Table 1 Reaction 2). Additionally, some free ammonia was always fed with the monochloramine stock solution to ensure only monochloramine was formed. Therefore, NH_2Br can also be formed during ozonation via Reaction 1 (Table 1). As HOBr only reacts with the nonionic form, NH_3, the effective rate constant between HOBr and total ammonia (NH_3 & NH_4^+) at pH 7 is similar to that of bromochloramine formation, so both compounds are likely to form as intermediates.

3.5. Ozone demand, decay, and disinfection credit

Fig. 6 shows ozone decay with increasing monochloramine dose with a 7 mg/L applied ozone dose. The first ozone residual measurement was excluded from the decay rate calculations as it does not fit the linearized 1st order ozone decay curves. This first point was taken at the outlet of the dissolution column, approximately 2.5 s after the ozone diffuser where the initial/instantaneous demand phase of ozone decay would not yet be complete. Increasing monochloramine dose had no effect on ozone decay rate. This shows that ozone decay and *OH generation is controlled by direct reactions with DOM rather than by radical chain reaction and not affected by the addition of a radical scavenger. In another study, and previous testing with this pilot at a different HRSD treatment plant, an increase in ozone decay rate was observed with monochloramine addition (Pearce et al., 2018; Benotti et al., 2011). This was hypothesized to be due to monochloramine oxidation to nitrate by ozone via Reaction 5 in Table 1. Some monochloramine decay was observed through ozonation (data not shown). Benotti et al. (2011) had to increase their ozone dose by approximately 15 percent to achieve the same *Cryptosporidium* CT credit in river water when adding 1 mg/L monochloramine. However, that does not appear to be the case in the present study. This indicates that slower reacting compounds with rate constants on the order of 26 $M^{-1}s^{-1}$ do not control ozone decay rate.

Overall, ozone decay rate decreased with increasing ozone dose and was unaffected by monochloramine addition as shown in Fig. 7a. Initial or instantaneous ozone demand (IOD) is operationally defined as the difference between the transferred ozone dose and the measured residual at the outlet of the dissolution column. IOD increased linearly with increasing dose but decreased as a fraction of the transferred dose (Fig. 7b). Even at the highest ozone dose, IOD was still greater than 50% of the transferred ozone dose. IOD was also unaffected by monochloramine addition as direct reactions with DOM control ozone decay during this phase and play a larger role in wastewater ozonation (Buffle et al., 2006). Table 3 shows the calculated virus and *Cryptosporidium* log-inactivation credits. For viruses, CT was calculated using the maximum of the single point CT from the measured ozone residual samples multiplied by the retention time from the outlet of the dissolution column to the respective sample port. In wastewater with high ozone decay rates, the measured single point CT can vary significantly for the same ozone residual profile depending on where the residual is measured. Even when optimized the single point CT method is extremely conservative and significantly underestimates the true ozone exposure in the system. Despite this, all but the lowest doses tested were sufficient for significant viral inactivation credit as shown in Table 3. One-log virus credit was given for dissolution column effluent ozone residuals >0.1 mg/L. For *Cryptosporidium* CT was calculated by integrating the first order ozone residual decay curves. This is approximately equivalent to the Extended CSTR or Extended T_{10} methods typically used to achieve *Cryptosporidium* CT credit (Rakness et al., 2005). A baffle

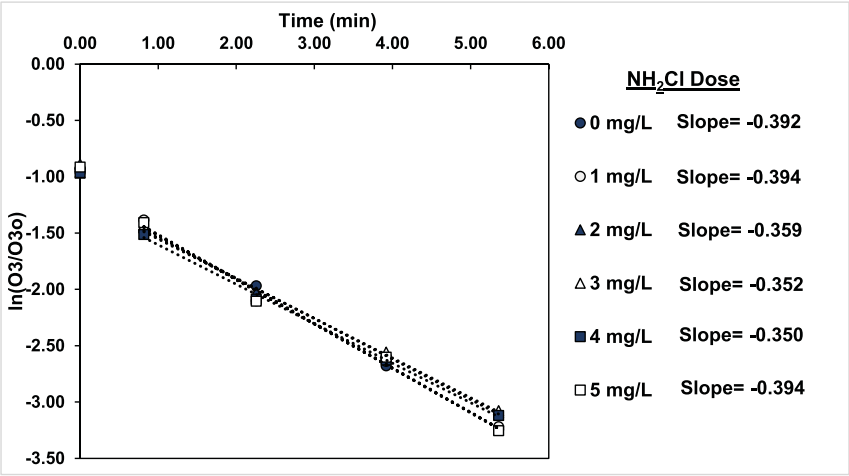

Fig. 6. Linearized first order ozone decay curves at a fixed ozone dose of 7 mg/L.

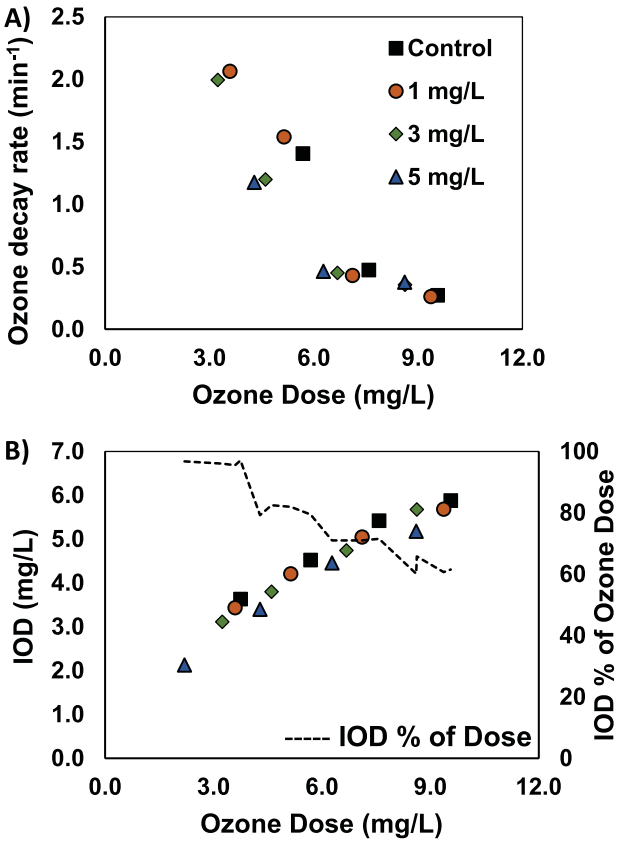

Fig. 7. A) ozone decay rate and B) initial ozone demand, IOD, vs. ozone dose at varying monochloramine doses.

factor of 0.9 was applied in all cases to approximate the pipeline contactor at the SRC.

The calculated log-inactivation credit from the chemical dose matrix decreases with increasing monochloramine dose. However, this is likely due to the ozone doses being increased during the control test for nitrite demand which decreased throughout the testing day while monochloramine doses were increased. With a fixed ozone dose of 7 mg/L (1.07 O_3:TOC), increasing monochloramine dose had no effect on the calculated *Cryptosporidium* LRV. HRSD currently operates the ozone system at the SWIFT Research Center to achieve 3-log virus inactivation credit using a single-point CT calculation in a pipeline contactor. From these pilot tests, this target would be achieved around 0.6 to 0.8 O_3:TOC which is consistent with full-scale operation (Hogard et al., 2021). Two-log *Cryptosporidium* inactivation credit would require an ozone dose of approximately 1:1 O_3:TOC (when using an integrated CT method). A dose of 3 mg/L-Cl_2 preformed monochloramine was able to keep bromate below the MCL at ozone doses as high as this. In terms of contaminant oxidation, ozone doses this high are mostly beneficial for the removal of more ozone recalcitrant compounds whose removal may be negatively affected by hydroxyl radical scavenging by monochloramine. Unless ozone CT is necessary for a secondary barrier to *Cryptosporidium*, it may be easier to achieve this removal elsewhere as many O_3-BAF based reuse treatment trains utilize membrane filtration or downstream UV disinfection (Gerrity et al., 2013).

3.6. NDMA and brominated organics

Fig. 8 shows the ozone effluent NDMA with and without monochloramine addition. These samples were taken during the control and 5 mg/L NH_2Cl conditions shown in Figs. 3 and S1. NDMA formation increased with increasing ozone dose until it plateaued around 0.6 O_3:TOC which is consistent with previous results on this water and other literature results (Hogard et al., 2021; Snyder et al., 2015).

Monochloramine addition did not increase NDMA formation. While both monochloramine and ozone can form NDMA, they are formed by distinctly different groups of precursors (Sgroi et al., 2018). Many NH_2Cl-NDMA precursors are well removed by ozonation (Lee et al., 2007). NDMA formation potential tests conducted on this water by Vaidya et al. (2021) showed an average of 780 ng/L NDMA formed with 140 mg/L-Cl_2 NH_2Cl after 10 days of contact. An ozone dose of 0.6 O_3:TOC decreased formation potential by approximately 90%. In previous testing by Hogard et al. (2021), increased ozone effluent NDMA was observed at 2 mg/L O_3 with 3 mg/L preformed monochloramine. This indicated that 2 mg/L ozone was insufficient to remove the NH_2Cl-NDMA precursors and that monochloramine could form NDMA in the eight-minute contact time of the ozone contactor. However, that did not appear to be the case here.

A dose of 5 mg/L-Cl_2 preformed monochloramine was added to the settled water and NDMA was sampled over 90 min (Table S1). No NDMA formation was observed, which is not unexpected as NDMA formation by monochloramine is typically quite slow, on the order of days in drinking water distribution systems. Preforming monochloramine should also minimize the risk of NDMA formation by dichloramine (Schreiber & Mitch, 2006). Even at the lowest ozone doses, NDMA was greater than most drinking water regulatory limits of 10 ng/L, indicating that removal by downstream biofiltration or UV photolysis would be required.

The formation of brominated organic disinfection byproducts is also a concern with chlorination and chloramination of bromide containing waters. Though most of these compounds are unregulated, they are thought to be more toxic than their chlorinated counterparts (Sharma et al., 2014). Buffle et al. (2004) showed significant total organic bromine (TOBr) formed during the Cl_2—NH_3 process. As much as 30% of the of the initial bromide ended up as TOBr, and this was reduced to approximately 15% with increased background ammonia causing NH_2Cl formation.

In this study, effluent bromide was measured on select samples with ozonation and chloramination (Table S2). TOBr, estimated as "missing" bromide between the ozone influent and effluent and corrected for bromate, was always less than 5% which is well within the range of analytical error and influent bromide fluctuation. Brominated organic formation does not appear to be a concern here. Similar to NDMA formation, it may take more time for these compounds to form. Ozonated samples were quenched with bisulfite within one minute of sample

Table 3
Calculated virus and *Cryptosporidium* log-reduction values.

Test	Chemical Dose Matrix								NH_2Cl Dose Curve
LRV	Virus LRV				*Cryptosporidium LRV*				*Crypto LRV*
O_3:TOC	0.3	0.6	0.9	1.2	0.3	0.6	0.9	1.2	1.07
0 mg/L NH_2Cl	1.1	3.3	13.1	40.5	0.02	0.35	2.1	5.6	2.9
1 mg/L NH_2Cl	1.1	2.6	11.1	32.4	0.02	0.27	2.0	5.5	3.0
2 mg/L NH_2Cl									3.2
3 mg/L NH_2Cl	1.1	2.1	9.6	23.8	0.01	0.24	1.7	3.7	3.1
4 mg/L NH_2Cl									2.9
5 mg/L NH_2Cl	1.0	2.3	9.2	23.0	0.01	0.27	1.6	3.8	3.0

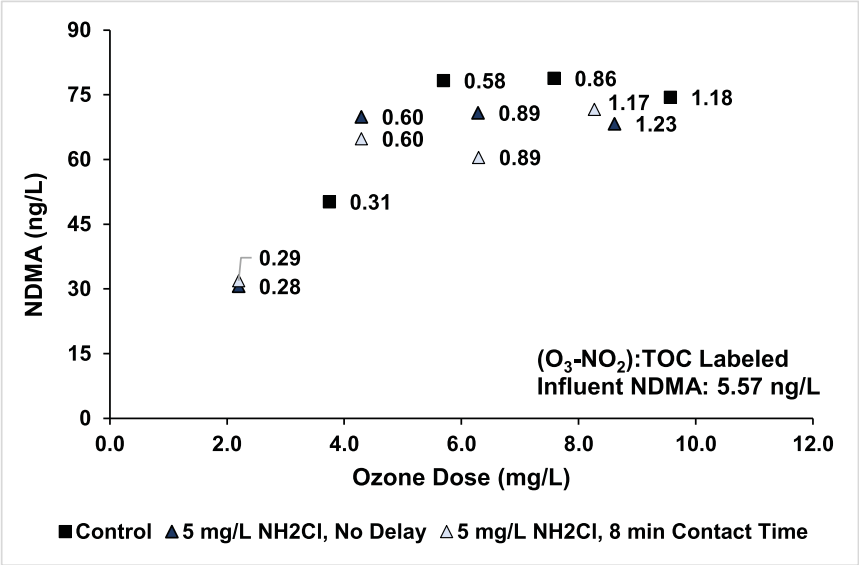

Fig. 8. Ozone effluent NDMA vs. ozone dose with and without preformed monochloramine addition.

collection giving a maximum contact time of 8 min with monochloramine plus 10 min through the ozone contactor and sample collection. Bromide samples were also collected with NDMA with up to 90 min of monochloramine contact time (Table S1) and again, no brominated organic formation was observed, at least within the sensitivity of the difference in the bromate-corrected bromide concentrations.

4. Conclusions

- With a bromide concentration of 414 μg/L, bromate exceeded the MCL of 10 μg/L at specific ozone doses greater than ~0.7 O_3:TOC. Monochloramine doses of 3 or 5 mg/L-Cl_2 NH_2Cl were able to control bromate formation to below the MCL at ozone doses up to 1.2:1 O_3:TOC and suppress bromate formation by as much as 90%. There was little improvement by increasing the monochloramine dose from 3 to 5 mg/L-Cl_2.
- Monochloramine is acting as a hydroxyl radical scavenger as evidenced by diminished 1,4-dioxane removal with increasing monochloramine dose. Use of monochloramine is a tradeoff between radical scavenging for bromate control and decreased removal of ozone resistant compounds which are removed through *OH oxidation alone. Removal of the most ozone reactive trace contaminants should be unaffected. Use of monochloramine for bromate control should come with serious evaluation of oxidation objectives.
- Increasing monochloramine contact time upstream of ozonation did not improve bromate control, indicating that bromide is not being masked as haloamines prior to ozonation. Monochloramine should be added as soon before ozonation as possible as monochloramine decay over longer contact times appeared to decrease bromate suppression.
- Monochloramine addition did not have any effect on ozone demand, decay rate, or calculated disinfection credit which is counter to previous drinking water results. This shows that ozone decay is unaffected by a radical terminator and that slow reactions between ozone and compounds such as monochloramine do not play much of a role in wastewater effluent. Though this may be water quality dependent.
- NDMA formation increased with increasing ozone dose until ~0.6 O_3:TOC where it plateaued at 60–75 ng/L. NDMA formation through ozonation was not affected by monochloramine addition for bromate control. It is likely that the short contact time before ozonation is insufficient for NDMA formation by monochloramine. However, the precursors may not have been present during these tests as precursor concentrations can be dependent on the source water and upstream treatment plant operation.
- Brominated organic formation does not appear to be a concern through ozonation either with or without monochloramine addition as there was a near perfect mass balance on bromide when accounting for bromide converted to bromate.

Declaration of Competing Interest

The authors declare that they have no known competing financial interests or personal relationships that could have appeared to influence the work reported in this paper.

Acknowledgments

The authors would like to thank the operators and staff at HRSD's Nansemond Treatment Plant as well as the analysts in HRSD's Central Environmental laboratory who made this work possible. Funding for this work was provided by HRSD.

Supplementary materials

Supplementary material associated with this article can be found, in the online version, at doi:10.1016/j.watres.2022.118049.

References

Arnold, M., Batista, J., Dickenson, E., Gerrity, D., 2018. Use of ozone-biofiltration for bulk organic removal and disinfection byproduct mitigation in potable reuse applications. Chemosphere 202, 228–237. https://doi.org/10.1016/j.chemosphere.2018.03.085.

Benotti, M.J., Wert, E.C., Snyder, S.A., Owen, C., Cheng, R., 2011. Role of Bromamines on DBP Formation and Impact on Chloramination and Ozonation [Project # 4159]. Water Research Foundation.

Buehlmann, P., Salazar-Benites, G., Wilson, C., Bott, C., 2017. Ozonation of domestic wasteater for indirect potable reuse: bromate control and related issues. In: Proceedings of the IOA World Congress. Washington DC, United States.

Buffle, M.O., Galli, S., von Gunten, U., 2004. Enhanced bromate control during ozonation: the chlorine-ammonia process. Environ. Sci. Technol. 38, 5187–5195. https://doi.org/10.1021/es0352146.

Buffle, M.O., Schumacher, J., Meylan, S., Jekel, M., von Gunten, U., 2006. Ozonation and advanced oxidation of wastewater: effect of O_3 dose, pH, DOM and HO.-scavengers on ozone decomposition and HO.generation. Ozone Sci. Eng. 28, 247–259. https://doi.org/10.1080/01919510600718825.

EPA, 1998. National primary drinking water regulations: disinfectants and disinfection byproducts: 40 CFR 9, 141, 142. Fed. Regist. 63, 69390–69476.

EPA, 2013. *1,4-dioxane* (CASRN 123-91-1). US EPA National Center for Environmental Assessment. https://cfpub.epa.gov/ncea/iris/iris_documents/documents/subst/0326_summary.pdf.

Gazda, M., Margerum, D.W., 1994. Reactions of Monochloramine with Br_2, Br_{3-}, HoBr, OBr-: formation of bromochloramines. Inorg. Chem. 33, 118–123. https://doi.org/10.1021/ic00079a022.

Gerrity, D., Gamage, S., Jones, D., Korshin, G.V., Lee, Y., Pisarenko, A., Trenholm, R.A., von Gunten, U., Wert, E.C., Snyder, S.A., 2012. Development of surrogate correlation models to predict trace organic contaminant oxidation and microbial inactivation during ozonation. Water Res. 46, 6257–6272. https://doi.org/10.1016/j.watres.2012.08.037.

Gerrity, D., Owens-Bennett, E., Venezia, T., Stanford, B.D., Plumlee, M.H., Debroux, J., Trussell, R.S., 2014. Applicability of ozone and biological activated carbon for potable reuse. Ozone Sci. Eng. 36, 123–137. https://doi.org/10.1080/01919512.2013.866886.

Gerrity, D., Pecson, B., Shane Trussell, R., Rhodes Trussell, R., 2013. Potable reuse treatment trains throughout the world. J. Water Supply Res. Technol. AQUA 62, 321–338. https://doi.org/10.2166/aqua.2013.041.

Haag, W.R., Hoign, J., 1983. Ozonation of water containing chlorine or chloramines. Water Res. 17, 1397–1402. https://doi.org/10.1016/0043-1354(83)90270-1.

Hogard, S., Salazar-Benites, G., Pearce, R., Nading, T., Schimmoller, L., Wilson, C., Heisig-Mitchell, J., Bott, C., 2021. Demonstration-scale evaluation of ozone–biofiltration–granular activated carbon advanced water treatment for managed aquifer recharge. Water Environ. Res. 1–16. https://doi.org/10.1002/wer.1525.

Ikehata, K., Wang, L., Nessl, M.B., Komor, A.T., Cooper, W.J., McVicker, R.R., 2013. Effect of ammonia and chloramine pretreatment during the ozonation of a colored groundwater with elevated bromide. Ozone Sci. Eng. 35, 438–447. https://doi.org/10.1080/01919512.2013.815105.

Knopp, G., Prasse, C., Ternes, T.A., Cornel, P., 2016. Elimination of micropollutants and transformation products from a wastewater treatment plant effluent through pilot scale ozonation followed by various activated carbon and biological filters. Water Res. 100, 580–592. https://doi.org/10.1016/j.watres.2016.04.069.

Lee, C., Schmidt, C., Yoon, J., Von Gunten, U., 2007. Oxidation of N-nitrosodimethylamine (NDMA) precursors with ozone and chlorine dioxide: kinetics and effect on NDMA formation potential. Environ. Sci. Technol. 41, 2056–2063. https://doi.org/10.1021/es062484q.

Lee, Y., Gerrity, D., Lee, M., Bogeat, A.E., Salhi, E., Gamage, S., Trenholm, R.A., Wert, E.C., Snyder, S.A., Von Gunten, U., 2013. Prediction of micropollutant elimination during ozonation of municipal wastewater effluents: use of kinetic and water specific information. Environ. Sci. Technol. 47, 5872–5881. https://doi.org/10.1021/es400781r.

Ling, L., Deng, Z., Fang, J., Shang, C., 2020. Bromate control during ozonation by ammonia-chlorine and chlorine-ammonia pretreatment: roles of bromine-containing haloamines. Chem. Eng. J. 389, 123447 https://doi.org/10.1016/j.cej.2019.123447.

Luh, J., Mariñas, B.J., 2014. Kinetics of bromochloramine formation and decomposition. Environ. Sci. Technol. 48, 2843–2852. https://doi.org/10.1021/es4036754.

Mitch, W.A., Oelker, G.L., Hawley, E.L., Deeb, R.A., Sedlak, D.L., 2005. Minimization of NDMA formation during chlorine disinfection of municipal wastewater by application of pre-formed chloramines. Environ. Eng. Sci. 22, 882–890. https://doi.org/10.1089/ees.2005.22.882.

Pearce, R., Buehlmann, P., Vaidya, R., Salazar-Benites, G., Nading, T., Wilson, C., Bott, C., 2018. Comparing the effects of ozone dissolution systems of bromate formation and control in high bromide reuse waters: a pilot study. In: Proceedings of the IOA-PAG Conference. Las Vegas, NV, United States.

Pinkernell, U., von Gunten, U., 2001. Bromate minimization during ozonation: mechanistic considerations. Environ. Sci. Technol. 35, 2525–2531. https://doi.org/10.1021/es001502f.

Poskrebyshev, G.A., Huie, R.E., Neta, P., 2003. Radiolytic reactions of monochloramine in aqueous solutions. J. Phys. Chem. A 107, 7423–7428. https://doi.org/10.1021/jp030198k.

Qi, S., Mao, Y., Lv, M., Sun, L., Wang, X., Yang, H., Xie, Y.F., 2016. Pathway fraction of bromate formation during O_3 and O_3/H_2O_2 processes in drinking water treatment. Chemosphere 144, 2436–2442. https://doi.org/10.1016/j.chemosphere.2015.11.022.

Rakness, K.L., Najm, I., Elovitz, M., Rexing, D., Via, S., 2005. Cryptosporidium log-inactivation with ozone using effluent CT10, geometric mean CT10, extended integrated CT10and extended CSTR calculations. Ozone Sci. Eng. 27, 335–350. https://doi.org/10.1080/01919510500250267.

Reungoat, J., Escher, B.I., Macova, M., Argaud, F.X., Gernjak, W., Keller, J., 2012. Ozonation and biological activated carbon filtration of wastewater treatment plant effluents. Water Res. 46, 863–872. https://doi.org/10.1016/j.watres.2011.11.064.

Schreiber, I.M., Mitch, W.A., 2005. Influence of the order of reagent addition on NDMA formation during chloramination. Environ. Sci. Technol. 39, 3811–3818. https://doi.org/10.1021/es0483286.

Sgroi, M., Vagliasindi, F.G.A., Snyder, S.A., Roccaro, P., 2018. N-Nitrosodimethylamine (NDMA) and its precursors in water and wastewater: a review on formation and removal. Chemosphere 191, 685–703. https://doi.org/10.1016/j.chemosphere.2017.10.089.

Sharma, V.K., Zboril, R., McDonald, T.J., 2014. Formation and toxicity of brominated disinfection byproducts during chlorination and chloramination of water: a review. J. Environ. Sci. Health Part B Pestic. Food Contam. Agric. Wastes 49, 212–228. https://doi.org/10.1080/03601234.2014.858576.

Snyder, S.A., von Gunten, U., Amy, G., Debroux, J., Gerrity, D., 2015. Use of Ozone in Water Reclamation for Contaminant Oxidation. WateReuse Research Foundation.

Soltermann, F., Abegglen, C., Götz, C., Von Gunten, U., 2016. Bromide sources and loads in swiss surface waters and their relevance for bromate formation during wastewater ozonation. Environ. Sci. Technol. 50, 9825–9834. https://doi.org/10.1021/acs.est.6b01142.

Soltermann, F., Abegglen, C., Tschui, M., Stahel, S., von Gunten, U., 2017. Options and limitations for bromate control during ozonation of wastewater. Water Res. 116, 76–85. https://doi.org/10.1016/j.watres.2017.02.026.

Tanabe, A., Kawata, K., 2008. Determination of 1,4-dioxane in household detergents and cleaners. J. AOAC Int. 91, 439–444. https://doi.org/10.1093/jaoac/91.2.439.

Trofe, T.W., Inman, G.W., Donald Johnson, J., 1980. Kinetics of monochloramine decomposition in the presence of bromide. Environ. Sci. Technol. 14, 544–549. https://doi.org/10.1021/es60165a008.

Vaidya, R., Wilson, C.A., Salazar-Benites, G., Pruden, A., Bott, C., 2021. Factors affecting removal of NDMA in an ozone-biofiltration process for water reuse. Chemosphere 264, 128333. https://doi.org/10.1016/j.chemosphere.2020.128333.

von Gunten, U., 2003a. Ozonation of drinking water: part I. Oxidation kinetics and product formation. Water Res. 37, 1443–1467. https://doi.org/10.1016/S0043-1354(02)00457-8.

von Gunten, U., 2003b. Ozonation of drinking water: part II. Disinfection and by-product formation in presence of bromide, iodide or chlorine. Water Res. 37, 1469–1487. https://doi.org/10.1016/S0043-1354(02)00458-X.

von Gunten, U., Oliveras, Y., 1998. Advanced oxidation of bromide-containig waters: bromate formation mechanisms. Environ. Sci. Technol. 32, 63–70. https://doi.org/10.1021/es970477j.

von Sonntag, C., von Gunten, U., 2012. Chemistry of ozone in water and wastewater treatment: from basic principles to applications 10.2166/9781780400839.

Wajon, J.E., Morris, J.C., 1982. Rates of formation of N-bromo amines in aqueous solution. Inorg. Chem. 21, 4258–4263. https://doi.org/10.1021/ic00142a030.

Wert, E.C., Rosario-Ortiz, F.L., Drury, D.D., Snyder, S.A., 2007. Formation of oxidation byproducts from ozonation of wastewater. Water Res. 41, 1481–1490. https://doi.org/10.1016/j.watres.2007.01.020.

Wert, E.C., Rosario-Ortiz, F.L., Snyder, S.A., 2009. Using ultraviolet absorbance and color to assess pharmaceutical oxidation during ozonation of wastewater. Environ. Sci. Technol. 43, 4858–4863. https://doi.org/10.1021/es803524a.

WHO, 1993. Guidelines for drinking-water quality. Geneva.

Appendix D. Critical Review on Bromate Formation during Ozonation and Control Options for Its Minimization

Morrison, C. M., Hogard, S., Pearce, R., Mohan, A., Pisarenko, A. N., Dickenson, E. R. V., von Gunten, U., & Wert, E. C. (2023). Critical Review on Bromate Formation during Ozonation and Control Options for Its Minimization. Environmental Science and Technology. https://doi.org/10.1021/acs.est.3c00538

17 pages

Environmental Science & Technology

pubs.acs.org/est

Critical Review

Critical Review on Bromate Formation during Ozonation and Control Options for Its Minimization

Christina M. Morrison, Samantha Hogard, Robert Pearce, Aarthi Mohan, Aleksey N. Pisarenko, Eric R. V. Dickenson, Urs von Gunten,* and Eric C. Wert*

Cite This: *Environ. Sci. Technol.* 2023, 57, 18393−18409

Read Online

ACCESS | Metrics & More | Article Recommendations | Supporting Information

ABSTRACT: Ozone is a commonly applied disinfectant and oxidant in drinking water and has more recently been implemented for enhanced municipal wastewater treatment for potable reuse and ecosystem protection. One drawback is the potential formation of bromate, a possible human carcinogen with a strict drinking water standard of 10 μg/L. The formation of bromate from bromide during ozonation is complex and involves reactions with both ozone and secondary oxidants formed from ozone decomposition, i.e., hydroxyl radical. The underlying mechanism has been elucidated over the past several decades, and the extent of many parallel reactions occurring with either ozone or hydroxyl radicals depends strongly on the concentration, type of dissolved organic matter (DOM), and carbonate. On the basis of mechanistic considerations, several approaches minimizing bromate formation during ozonation can be applied. Removal of bromate after ozonation is less feasible. We recommend that bromate control strategies be prioritized in the following order: (1) control bromide discharge at the source and ensure optimal ozone mass-transfer design to minimize bromate formation, (2) minimize bromate formation during ozonation by chemical control strategies, such as ammonium with or without chlorine addition or hydrogen peroxide addition, which interfere with specific bromate formation steps and/or mask bromide, (3) implement a pretreatment strategy to reduce bromide and/or DOM prior to ozonation, and (4) assess the suitability of ozonation altogether or utilize a downstream treatment process that may already be in place, such as reverse osmosis, for post-ozone bromate abatement. A one-size-fits-all approach to bromate control does not exist, and treatment objectives, such as disinfection and micropollutant abatement, must also be considered.

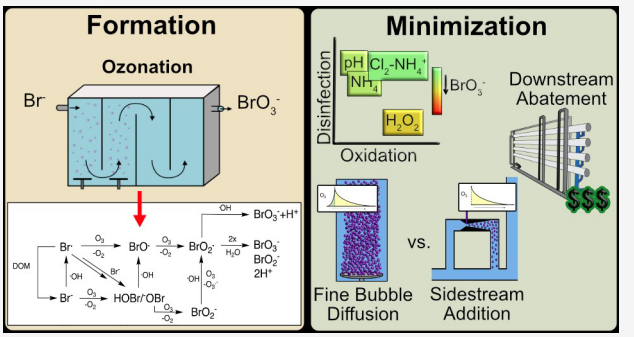

KEYWORDS: *bromate, ozonation, human carcinogen, dissolved organic matter*

INTRODUCTION

Ozone is applied as a disinfectant and oxidant during drinking water treatment, with hundreds of full-scale treatment plants worldwide.[1] As interest in water reuse and ecological protection of waterways grows in the United States and Europe, ozonation is increasingly included in advanced wastewater treatment processes for the oxidation of micropollutants by ozone and hydroxyl radicals (•OH).[1,2] During ozonation of bromide-containing waters, oxidation of bromide by ozone and •OH leads to bromate formation, which is a human and ecological health concern.

This Critical Review of the current knowledge of bromate will cover the following aspects: (i) toxicity of bromate, (ii) sources of bromide in natural waters and wastewaters, (iii) analytical methods for bromate determination, (iv) kinetics and mechanisms of bromate formation, (v) theoretical and empirical modeling of bromate formation, and (vi) bromate mitigation strategies implemented before, during, and after ozonation.

TOXICOLOGICAL ASPECTS OF BROMATE

Bromate was classified as a possible human carcinogen in the 1990s and is regulated to a maximum contaminant level of 10 μg/L by several regulatory agencies.[3,4] This stringent limit is based on toxicological studies conducted on rodents[5−7] and subsequent risk assessments conducted by the U.S. Environmental Protection Agency (USEPA) and the World Health Organization (WHO).[8,9] These studies have shown that exposure to bromate may result in cancer in kidneys, thyroid, and testicular mesothelium of rats.[7] Although bromate is regulated as a probable genotoxic carcinogen, there is evidence of a nongenotoxic mode of action.[10,11] Genotoxic effects have

Special Issue: Oxidative Water Treatment: The Track Ahead

Received: January 24, 2023
Revised: May 23, 2023
Accepted: May 24, 2023
Published: June 26, 2023

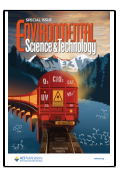

been shown to result from oxidative damage to DNA at relatively high levels of exposure to bromate, whereas nongenotoxic effects, including apoptosis (cell death) and mutation, can result at lower bromate concentrations.[10] Studies have also shown the reduction of bromate to bromide in simulated gastric solutions, suggesting that regulatory limits might be set conservatively low.[12] The strict human health standard for bromate has limited the applicability of ozone for disinfection/oxidation in both water and enhanced wastewater treatment.

Bromate has also demonstrated potential ecological impacts. Lethal concentrations (LC_{50}) of bromate in the range of 31−2258 mg/L for different fish species have been reported.[13,14] With a safety factor of 10, a long-term bromate exposure limit of 3 mg/L was proposed to protect the most sensitive aquatic organisms.[13] Bromate exposure tests with *Ceriodaphnia dubia* resulted in a more stringent acute and chronic standard of 50 μg/L.[15,16]

BROMIDE OCCURRENCE AND SOURCES

Bromide is naturally occurring in geological structures such as limestone, granite, and shale, at concentrations ranging between 0.3 and 24 mg/kg.[17] Typically, bromide in surface water results from geogenic sources,[17] but other sources include seawater intrusion and anthropogenic sources.[18,19] Anthropogenic sources of bromide include industrial point discharges, municipal waste incinerators, landfills, chemical plants, coal-fired power plants, private swimming pools, and hydraulic fracturing.[19−22] Median bromide levels in drinking water sources (groundwaters and surface waters) were in the range of 30−80 μg/L on the basis of U.S. surveys; however, concentrations have been observed in the range of hundreds of microgram to milligrams per liter.[23,24]

A bromide concentration threshold of ∼100 μg/L was proposed for drinking water disinfection with ozone to avoid a violation of the drinking water standard for bromate.[25] This is only a rough estimate, because bromate formation largely depends on other treatment goals and the water matrix.[26] In a specific water source, the bromide threshold level may be significantly different, and therefore, site specific tests should be performed.[26] Bromide levels in wastewater effluents can be significantly higher, with median levels reported around 230 μg/L,[23] and higher levels of ≤50 mg/L have been reported.[22] The elevated bromide levels in wastewaters magnify the challenges pertaining to bromate control during ozonation for potable reuse applications and ecosystem protection scenarios. A full summary of bromide occurrence is outside the scope of this review; however, this topic has been evaluated in numerous previous studies.[17,20,22−24,27−32]

BROMATE MEASUREMENT

Bromate is primarily analyzed by ion chromatography with conductivity detection (IC-CD) with method reporting limits (MRL) of 4−5 μg/L.[33−37] Detection of bromate by postcolumn reactions followed by ultraviolet (UV) measurement (IC-PCR) avoids interference from chloride and sulfate and increases sensitivity. An MRL of ≲1 μg/L is possible with this approach.[38−40] Other methods use ion chromatography coupled with inductively coupled plasma mass spectrometry (IC-ICP-MS), (tandem) mass spectrometry (IC-MS and IC-MS/MS), or liquid chromatography-tandem triple quadrupole mass spectrometry (LC-MS/MS).[40−44] MS-based methods have sub-microgram per liter MRLs. For laboratory studies on bromate formation, or monitoring in practice, IC-PCR or IC/LC-MS methods should be applied to have MRLs far below the drinking water standard of 10 μg/L. There has been limited success for online bromate measurements. One approach, which utilizes fluorescence detection of trifluoperazine (TFP), has been examined and showed promise; however, further long-term experience is needed with such systems.[45,46]

For sample collection, oxidant quenching should be carried out to avoid continuing bromate formation during storage. Quenching agents, such as indigo trisulfonate, thiosulfate, sulfite, buten-3-ol, or cinnamic acid, can be applied.[42,47] Proper preservation and the proper storage temperature (<6 °C) result in holding times of approximately one month without sample deterioration.[34]

BROMATE FORMATION DURING OZONATION

Overview of Pathways.

Ozone Reactions. Acidic solutions containing ozone and bromide were investigated in the 1940s with the goal of measuring Br_2 formation.[48] This reaction was confirmed at circumneutral pH with the formation of HOBr/OBr^-, which is the hydrolysis product of Br_2.[49,50] This is the first step in bromate formation with ozone (eq 1):

$$O_3 + Br^- \rightarrow OBr^- + O_2 \quad (1)$$

Two second-order rate constants for reaction 1 were reported: k = 160 M^{-1} s^{-1} at 20 °C[49] or k = 258 M^{-1} s^{-1} at 25 °C.[50] With these moderate second-order rate constants, calculated half-life times of bromide are in the range of 2−4 min for an ozone concentration of 1 mg/L. Therefore, for disinfection processes with a substantial ozone exposure, significant extents of OBr^- can be formed. During oxidation of micropollutants, often no or low ozone residual concentrations are present and therefore OBr^- formation will be minor.[22]

OBr^- is in equilibrium with HOBr with a pK_a of 8.8[51] (eq 2):

$$OBr^- + H^+ \rightleftarrows HOBr \quad (2)$$

This high pK_a of HOBr is crucial for bromate formation with ozone, because HOBr reacts very slowly with ozone ($k \leq 10^{-2}$ M^{-1} s^{-1}[49]), whereas OBr^- has a moderate reactivity (k = 100 M^{-1} s^{-1} at 20 °C[49]) (eq 3):

$$O_3 + OBr^- \rightarrow BrO_2^- + O_2 \quad (3)$$

In addition to reaction 3, the attack of ozone on OBr^- can also proceed through a second faster reaction, which is a reduction of OBr^- back to bromide (k = 330 M^{-1} s^{-1} at 20 °C[49]) (eq 4):

$$O_3 + OBr^- \rightarrow Br^- + 2^1O_2 \quad (4)$$

Paradoxically, this is a reductive process occurring during ozonation. Similar reactions occur during the ozonation of OCl^- and Mn^{2+}.[52,53]

The last reaction en route to bromate is an oxidation of bromite (BrO_2^-), which has been suggested to be an oxygen-transfer reaction ($k > 10^5$ M^{-1} s^{-1} at 20 °C[49]) (eq 5):

$$O_3 + BrO_2^- \rightarrow BrO_3^- + O_2 \quad (5)$$

However, more recently it was demonstrated that reaction 5 proceeds via an electron transfer (k = 8.9 × 10^4 M^{-1} s^{-1} at 25 °C[54]) (eq 6):

$$O_3 + BrO_2^- \rightarrow BrO_2^{\bullet} + O_3^{\bullet -} \quad (6)$$

Bromine dioxide ($BrO_2^{\bullet}$) undergoes a self-reaction and a disproportionation[54,55] according to eqs 7 and 8:

https://doi.org/10.1021/acs.est.3c00538
Environ. Sci. Technol. 2023, 57, 18393−18409

$$2BrO_2^{\bullet} \rightleftarrows Br_2O_4 \quad (7)$$

$$Br_2O_4 + H_2O \rightarrow BrO_2^- + BrO_3^- + H_2O \quad (8)$$

An overall second-order rate constant from bromine dioxide to bromate has been estimated as $k = 5 \times 10^7\ M^{-1}\ s^{-1}$ at 10 °C.[54]

Hydroxyl Radical Reactions. In the original studies on bromate formation, the role of $^{\bullet}OH$ was not considered.[49] However, it can play a major role at various levels of bromate formation during ozonation.[56]

Bromide can be oxidized by $^{\bullet}OH$ to bromine radicals ($Br^{\bullet}$) in a two-step reaction with an equilibrium[57] (eqs 9 and 10):

$$^{\bullet}OH + Br^- \rightleftarrows BrOH^{\bullet -} \quad (9)$$

$$BrOH^{\bullet -} \rightleftarrows Br^{\bullet} + {}^-OH \quad (10)$$

The second-order rate constant for reaction 9 is $1.06 \times 10^{10}\ M^{-1}\ s^{-1}$;[58] however, due to the equilibrium character of eqs 9 and 10, an overall second-order rate constant of $k = 1.1 \times 10^9\ M^{-1}\ s^{-1}$ for the net reaction of bromide to $Br^{\bullet}$ can be estimated for bromide concentrations of ≤1 mg/L[59] (eq 11):

$$^{\bullet}OH + Br^- \rightarrow Br^{\bullet} + {}^-OH \quad (11)$$

One of the main sinks of $Br^{\bullet}$ is its reaction with bromide, with a second-order rate constant (k) of $\approx 10^{10}\ M^{-1}\ s^{-1}$ for the forward and $6.6 \times 10^3\ M^{-1}\ s^{-1}$ for the reverse reaction[1] (eq 12):

$$Br^{\bullet} + Br^- \rightleftarrows Br_2^{\bullet -} \quad (12)$$

$Br_2^{\bullet -}$ can lead to the formation of Br_2 over several equilibria and disproportionation reactions,[1] and Br_2 is then hydrolyzed to HOBr under typical water treatment conditions.[51] This pathway is also crucial for bromate formation in systems with only $^{\bullet}OH$ (without ozone) as was demonstrated with γ-radiolysis experiments.[60,61] Because $HOBr/OBr^-$ is a decisive intermediate, bromate is not formed in UV-based advanced oxidation in the presence of hydrogen peroxide (H_2O_2) (e.g., UV/H_2O_2), because H_2O_2 reduces $HOBr/OBr^-$ back to bromide. This is not the case for ozone-based advanced oxidation (see Hydrogen Peroxide).[62] Also, $BrOH^{\bullet -}$, which is formed from the reaction of $^{\bullet}OH$ with Br^- (eq 9), reacts with bromide, leading to $Br_2^{\bullet -}$ and the ensuing reactions.[1,57]

$HOBr/OBr^-$, which is formed from the oxidation of bromide with ozone or $^{\bullet}OH$, can further react with $^{\bullet}OH$ with second-order rate constants of $2 \times 10^9\ M^{-1}\ s^{-1}$ ($k_{OH,HOBr}$) and $4.5 \times 10^9\ M^{-1}\ s^{-1}$ (k_{OH,OBr^-})[63] (eqs 13 and 14):

$$^{\bullet}OH + HOBr \rightarrow BrO^{\bullet} + H_2O \quad (13)$$

$$^{\bullet}OH + OBr^- \rightarrow BrO^{\bullet} + {}^-OH \quad (14)$$

Bromine monoxide ($BrO^{\bullet}$) can also be formed from the reaction of hypobromite with carbonate radicals ($k = 4.3 \times 10^7\ M^{-1}\ s^{-1}$[63]). This reaction is relevant, because of the higher steady-state concentrations of carbonate radicals compared to that of $^{\bullet}OH$.[64]

$BrO^{\bullet}$ undergoes disproportionation with the formation of hypobromite and bromite ($k = 4.9 \times 10^9\ M^{-1}\ s^{-1}$[63]) (eq 15):

$$2BrO^{\bullet} + H_2O \rightarrow OBr^- + BrO_2^- + 2H^+ \quad (15)$$

Bromite, which also reacts with ozone (see above), can react further with $^{\bullet}OH$ to afford bromine dioxide ($BrO_2^{\bullet}$) ($k = 1.9 \times 10^9\ M^{-1}\ s^{-1}$[63]) (eq 16):

$$BrO_2^- + {}^{\bullet}OH \rightarrow BrO_2^{\bullet} + {}^-OH \quad (16)$$

An analogues reaction (eq 16) also occurs with the carbonate radical ($k = 1.1 \times 10^8\ M^{-1}\ s^{-1}$[63]). Bromine dioxide can then react further to afford bromate according to reactions 7 and 8 or with $^{\bullet}OH$ ($k = 2 \times 10^9\ M^{-1}\ s^{-1}$[65]) (eq 17):

$$BrO_2^{\bullet} + {}^{\bullet}OH \rightarrow BrO_3^- + H^+ \quad (17)$$

Bromine Radical Reactions. Bromine radicals (see eqs 9 and 10) can undergo the following reactions: (i) oxidation by ozone, (ii) reaction with bromide, and (iii) reaction with dissolved organic matter (DOM).

(i) On the basis of a combination of γ-radiolysis and tailored ozonation experiments, it was estimated by kinetic modeling that $Br^{\bullet}$ reacts with ozone to afford bromine monoxide ($BrO^{\bullet}$) with a k of $\approx 1.5 \times 10^8\ M^{-1}\ s^{-1}$[61] (eq 18), the same product that is also formed by eqs 13 and 14:

$$O_3 + Br^{\bullet} \rightarrow BrO^{\bullet} + O_2 \quad (18)$$

Bromine monoxide then disproportionates according to eq 15. This pathway can lead to bromate during the O_3/H_2O_2 advanced oxidation process (AOP).

(ii) According to eq 12, $Br^{\bullet}$ is in equilibrium with $Br_2^{\bullet -}$ as a potential sink. Figure S1 shows the $Br^{\bullet}/Br_2^{\bullet -}$ equilibrium concentration ratios as a function of bromide concentration. For a bromide concentration of 1 μM (80 μg/L), ~87% is present as $Br^{\bullet}$ and ~13% as $Br_2^{\bullet -}$. The $Br^{\bullet}/Br_2^{\bullet -}$ concentration ratio is ~1 at 500 μg/L bromide. Therefore, for low to moderate bromide levels, $Br^{\bullet}$ will always dominate and therefore contribute to further reactions with ozone.

(iii) Another important sink for $Br^{\bullet}$ is DOM, with second-order rate constants (k) in the range of $1.4–4.2 \times 10^8\ M_C^{-1}\ s^{-1}$ for DOM isolates and real waters.[66,67] Experiments with a preozonated DOM isolate showed that the second-order rate constant with $Br^{\bullet}$ did not change significantly, which implies a constant consumption of $Br^{\bullet}$ by DOM during ozonation.[67]

Reactions of $Br^{\bullet}$ with organic compounds proceed mainly by electron transfer,[66−68] shown for DOM in eq 19:

$$Br^{\bullet} + DOM \rightarrow Br^- + DOM^{\bullet +} \quad (19)$$

It has been demonstrated that a minor fraction may proceed by an addition of bromine to the ensuing brominated products.[67]

On the basis of the second-order rate constants for the reactions of $Br^{\bullet}$ with ozone and DOM, the initial fraction of $Br^{\bullet}$ reacting with either constituent can be calculated as a function of the specific ozone dose (milligrams of O_3 per milligram of DOC) (eq 20 and Figure 1):

$$f(O_3 + Br^{\bullet}) = \frac{k_{O_3+Br^{\bullet}}[O_3]}{k_{O_3+Br^{\bullet}}[O_3] + k_{DOM+Br^{\bullet}}[DOC]} \quad (20)$$

Figure 1 shows that for typically applied specific ozone doses (0.2−1.0 g of O_3/g of DOC), the initial fraction of $Br^{\bullet}$ reacting with ozone can account for ≤50% (DOC = 5 mg/L).

Bromate Formation Mechanism. On the basis of the reactions discussed above, a bromate formation mechanism including both ozone and $^{\bullet}OH$ can be compiled (Figure 2).

It is evident from Figure 2 that bromate formation is a complex reaction mechanism occurring during ozonation, because of the relevance of both ozone and $^{\bullet}OH$ at most reaction steps. The mechanism is compiled on the basis of

https://doi.org/10.1021/acs.est.3c00538
Environ. Sci. Technol. 2023, 57, 18393−18409

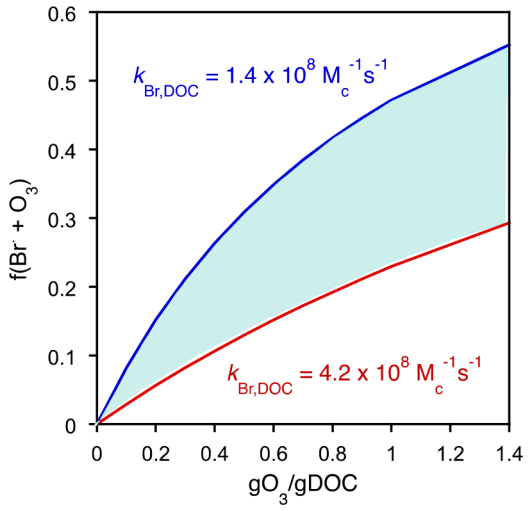

Figure 1. Fraction of the reaction of ozone with the bromine radical as a function of the specific ozone dose (the initial ozone dose is taken for the calculations). The blue and red curves represent the lower and higher limits, respectively, of the second-order rate constant for the reaction of $Br^{\bullet}$ with DOM. The colored area represents the range of the fraction $f(Br^{\bullet} + O_3)$ (eq 20) for the lower or higher second-order rate constants for the $Br^{\bullet}$–DOM reaction (second-order rate constants were obtained from ref 66) (DOC = 5 mg/L).

several key papers[47,49,56,59,61,69−72] and was also discussed in a previous publication.[1] This reaction mechanism was previously categorized into three main pathways. (i) The direct−direct (O_3) pathway consists of ozone-controlled bromate formation. (ii) The direct−indirect ($^{\bullet}OH$) pathway comprises an oxidation of bromide to $HOBr/OBr^-$ by ozone followed by a further oxidation by $^{\bullet}OH$. (iii) The indirect−indirect pathway consists of a $^{\bullet}OH$-dominated pathway.[73] Even though this approach can help as an orientation in the mechanism, it neglects that most reaction steps depend on the $^{\bullet}OH/O_3$ concentration ratio and the corresponding second-order rate constants. This ratio is water specific and depends on the specific ozone dose. To overcome this problem, the R_{ct} concept was developed, which allows for the determination of the $^{\bullet}OH/O_3$ concentration ratio by a relatively simple procedure.[74−77] This approach has also been applied to determine the ozonation transformation products of micropollutants.[78,79] During ozonation, typical concentration ratios (R_{ct}) of $^{\bullet}OH$ and O_3 are on the order of 10^{-6}–10^{-9}. Figure 3 shows the fractions of reactions proceeding by O_3 or $^{\bullet}OH$ for various bromine species (Br^-, $HOBr/OBr^-$, and BrO_2^-) as a function of R_{ct}.

Figure 3 illustrates that during the initial phase (second range) of ozonation (R_{ct} values as high as 10^{-6}[80]), reactions of $^{\bullet}OH$ with bromide and $HOBr/OBr^-$ dominate over ozone reactions. For the later phases of ozonation ($R_{ct} > 10^{-7}$), bromide oxidation occurs mainly by ozone and, depending on the pH, the fraction of the further reaction of $HOBr/OBr^-$ with ozone making up between 10% and 80%. For bromite, ozone always outcompetes $^{\bullet}OH$ for the further oxidation to bromate.

Water Quality Considerations. *Role of pH.* pH plays a decisive role in bromate formation; first and most importantly, it is crucial for ozone chemistry. At low pH, ozone is more stable and the formation of $^{\bullet}OH$ is slow, which is demonstrated by 40 times lower R_{ct} values at pH 6 than at pH 9.[1,74] Such conditions are ideal for disinfection because high levels of ozone exposure are achieved with limited formation of $^{\bullet}OH$. Under such conditions, mainly HOBr is formed from the reaction of ozone with bromide, and it is not further oxidized by ozone due to the low reactivity of HOBr with ozone (see above). Even though the oxidation of HOBr by $^{\bullet}OH$ has a reasonable second-order rate

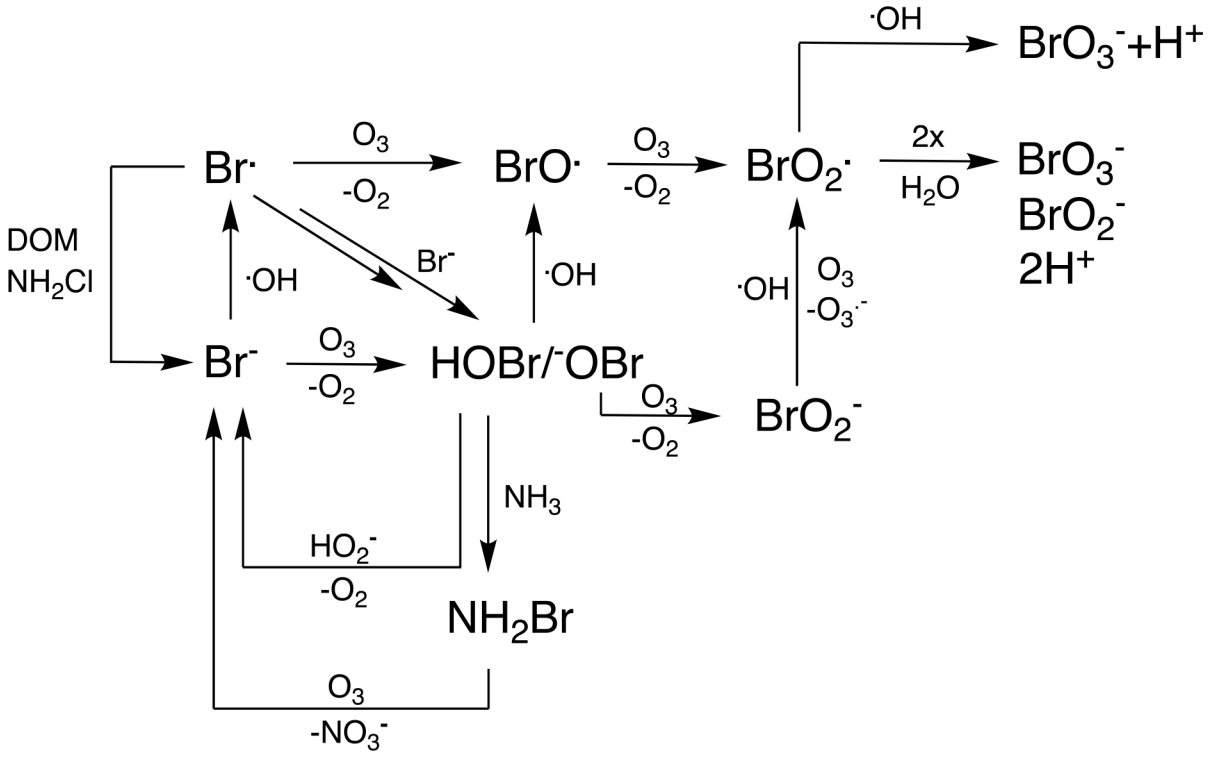

Figure 2. Simplified mechanism for bromate formation during ozonation of bromide-containing waters. Adapted from and expanded on the basis of a previous study.[1] Reactions of $HOBr/OBr^-$ with hydrogen peroxide and ammonia are also included.

https://doi.org/10.1021/acs.est.3c00538
Environ. Sci. Technol. 2023, 57, 18393−18409

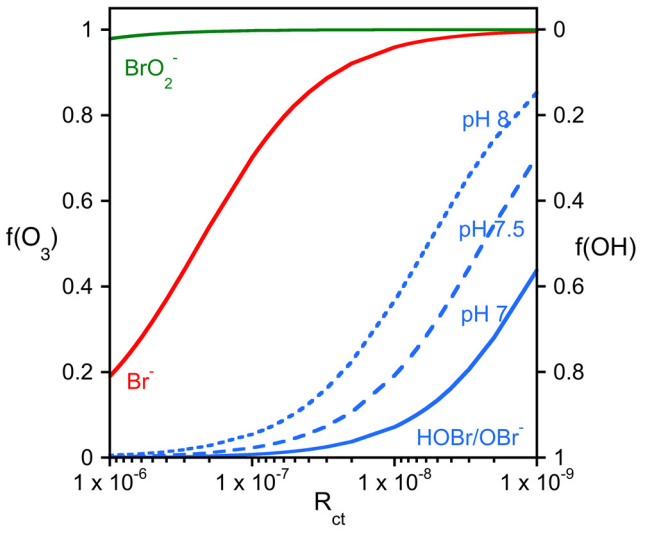

Figure 3. Fractions of reactions of Br^-, $HOBr/OBr^-$, and BrO_2^- occurring with ozone or $^\bullet OH$ as a function of R_{ct} in the range of 10^{-6}–10^{-9} ($^\bullet OH/O_3$ concentration ratio). Note that the *X*-axis and the second *Y*-axis are reversed.

constant, its oxidation by this pathway is slow because of the low transient $^\bullet OH$ concentrations at low pH.[47,74] The effect of pH on bromate formation has been demonstrated (e.g., during the ozonation of Seine River water with a bromide concentration of 60 μg/L) for which bromate concentrations of 4 and 9 μg/L were obtained at pH 6 ($R_{ct} = 2.9 \times 10^{-9}$) and pH 8 ($R_{ct} = 9.0 \times 10^{-9}$), respectively, for an ozone exposure of 10 mg L^{-1} min^{-1}.[47] pH depression can be applied as a bromate mitigation strategy during disinfection with ozone; at lower pH values, a better disinfection efficiency can be achieved with a lower level of bromate formation (see Mitigation).

Temperature. Temperature affects bromate formation at two levels: (i) faster reactions of bromide and transient bromine species[50] with ozone and $^\bullet OH$ and (ii) faster decomposition of ozone.[74] The only information about the effect of temperature on the oxidation of bromine species is related to the oxidation of bromide by ozone, with second-order rate constants of 258 and 97 M^{-1} s^{-1} at 25 and 5 °C, respectively.[50] The effect of temperature on R_{ct} is quite significant with an approximately 10-fold increase from 6.0×10^{-9} to 8.5×10^{-8} from 5 to 35 °C, respectively, for the ozonation of Lake Zurich water at pH 8. For a given ozone exposure, this leads to much higher level of bromate formation at higher temperatures, if the enhanced inactivation of microorganisms at higher temperatures is not considered.[81] Therefore, a temperature correction for disinfection should be implemented for ozone dosage control to achieve an ozone exposure, which guarantees a certain inactivation of target organisms.[82] This approach helps to save on ozone production and mitigates bromate formation. The overall benefit is difficult to predict, because only a few activation energies of the involved reactions (bromate formation, ozone decay, and inactivation of microorganisms) are known.

Dissolved Organic Matter. The effect of DOM on bromate formation is threefold: (i) quenching transient bromine species, (ii) scavenging ozone and $^\bullet OH$, and (iii) influencing the R_{ct}.

(i) HOBr can react with DOM moieties, such as phenols, β-dicarbonyl compounds, and amines.[47,51,83,84] Except for the amines, ozone also reacts quickly with such HOBr-quenching moieties, and therefore, they will not persist to react with HOBr.[1,85] It has been shown that the concentration of Br(+I) (sum of HOBr and bromamines) remains fairly constant during ozonation.[47] The reactivities of organic bromamines that might be present are 2–3 orders of magnitude lower with phenolic moieties than with HOBr, and therefore, the formation of bromoorganic compounds is also not expected from this pathway.[84]

(ii) Scavenging of ozone and $^\bullet OH$ is a major factor affecting ozonation processes. However, because ozonation has a certain oxidation/disinfection target, typical ozone doses are adapted to DOC concentrations to compensate for the oxidant demand. In this context, the specific ozone dose (milligrams of O_3 per milligram of DOC) is decisive for bromate formation. It has been demonstrated during wastewater ozonation that bromate formation is initiated at specific ozone doses of $\gtrsim$0.5 mg of O_3/mg of DOC.[22] Under these conditions, the ozone residual is high enough for reactions with bromide and $Br^\bullet$, and therefore, bromate can be formed.

(iii) The effect of DOM type on R_{ct} is probably the most important factor influencing bromate formation. In a study of 12 groundwaters and lake waters, it was shown that the R_{ct} values vary over 2 orders of magnitude.[75] Part of this effect is also due to varying carbonate levels (see the next section). Nevertheless, this shows that the indirect effect of DOM on bromate formation can be very significant.

Carbonate Alkalinity. Carbonate/bicarbonate reacts moderately with $^\bullet OH$ to afford carbonate/bicarbonate radicals.[86,87] This reaction can influence bromate formation on two levels, (i) reactions of carbonate radical with bromine species and (ii) quenching of $^\bullet OH$, thereby influencing R_{ct}.

(i) $^\bullet OH$ scavenging by carbonate depends on the pH ($k_{OH,HCO_3^-} = 8.5 \times 10^6$ M^{-1} s^{-1}; $k_{OH,CO_3^{2-}} = 3.9 \times 10^8$ M^{-1} s^{-1})[86,87] and the DOC concentration, because DOM is typically the main $^\bullet OH$ scavenger during the ozonation of real waters. Basically, carbonate scavenging affects the R_{ct}, and this in turn has a significant effect on bromate formation (see above). It has been shown during the ozonation of Lake Zurich water by varying the carbonate levels at pH 8 (15 °C) from 0 to 2.5 mM that R_{ct} decreases from 1.25×10^{-7} to 1.5×10^{-8}.[74] The influence of such changes on bromate formation is difficult to assess, because of the role of carbonate radicals as oxidants, which increase, while R_{ct} decreases. More systematic studies are necessary to assess these counteracting effects.

(ii) It has been reported that carbonate radicals can react with bromide with a second-order rate constant of $<5 \times 10^5$ M^{-1} s^{-1}:[88]

$$Br^- + CO_3^{\bullet-} \rightarrow Br^\bullet + CO_3^{2-} \quad (21)$$

This reaction is in equilibrium with the back reaction with second-order rate constants of 2×10^6 and 1×10^6 M^{-1} s^{-1} for carbonate and bicarbonate, respectively:[88]

$$Br^\bullet + CO_3^{2-} \rightarrow Br^- + CO_3^{\bullet-} \quad (22)$$

$$Br^\bullet + HCO_3^- \rightarrow Br^- + HCO_3^\bullet \quad (23)$$

Because the bicarbonate concentration in natural waters is typically in the millimolar range, the first-order rate constant for the back reaction will be orders of magnitude higher than that for

https://doi.org/10.1021/acs.est.3c00538
Environ. Sci. Technol. 2023, 57, 18393−18409

the forward reaction, and therefore, oxidation of bromide by carbonate radical is negligible.

Oxidation of OBr^- by the carbonate radical occurs with a second-order rate constant of $4.3 \times 10^7\ M^{-1}\ s^{-1}$:[86]

$$OBr^- + CO_3^{\bullet -} \rightarrow BrO^{\bullet} + CO_3^{2-} \quad (24)$$

This reaction seems to be relevant, because significant differences in bromate formation in the absence and presence of carbonate have been observed during the ozonation of bromide-containing waters under standardized oxidant conditions.[56]

MODELING

Mechanistic Models. Kinetic models for the prediction of bromate formation during ozonation are set up by a combination of all of the relevant chemical equations with the corresponding rate constants in an equation system that may contain 100−200 reactions. Available codes such as Kintecus can be used to solve such coupled differential equations.[89]

Bromate modeling is one of the most challenging endeavors in environmental oxidation chemistry. The challenges are related to the roles of ozone and •OH at various levels of the bromate formation pathway and also require modeling of the complex ozone chemistry in aquatic systems.

Kinetic Modeling of Ozone Decomposition. Even though rate constants for the inorganic reactions involved in ozone decomposition and the ensuing •OH formation are available in the literature, there are two main challenges:

(i) Second-order rate constants for individual ozone decomposition reactions have been measured individually by different researchers, and large differences can be expected between different laboratories.[1] Therefore, ozone decomposition modeling has a high level of uncertainty.

(ii) The DOM can react with ozone and •OH with second-order rate constants that vary from one type of DOM to another.[1,75] Furthermore, the fraction of promotion and inhibition of the radical chain reaction upon reaction of •OH with DOM is not *a priori* known and has to be determined by fitting procedures.[76,90]

On the basis of these factors, ozone modeling in real waters has high levels of uncertainty. Several attempts to kinetically model ozone decomposition were made, but fitting of some of the rate constants was typically necessary to match the ozone evolution.[91,92] Transient •OH formation was not even assessed in these models, and therefore, there is only limited application of such modeling exercises in real systems.

To overcome these inherent problems with ozone modeling, the experimentally determined ratios of the concentrations of •OH and O_3 discussed above, R_{ct} has been applied to model bromate formation under well-defined conditions during ozonation and advanced oxidation with O_3/H_2O_2. This enabled a fitting of the second-order rate constant for the reaction of O_3 with Br• ($k = 1.5 \times 10^8\ M^{-1}\ s^{-1}$).[61]

Kinetic Modeling of Bromate Formation. Modeling of bromate formation was established first for ozonation systems in which •OH radicals were scavenged. Such models can be set up with only a few kinetic equations and were successfully applied for a trend analysis of bromate formation for varying parameters in ultrapurified water.[18] If both O_3 and •OH are included in such bromate formation models, >40 reactions are needed.[56,61,93] In addition, DOM may play an important role in quenching transient bromine species, such as HOBr and Br•.[47,66,72] Similar to the ozone decomposition models, this approach also has the inherent problem of second-order rate constants that were determined by different research groups. One case in point is the reaction of ozone with bromide, for which the two values in the literature differ by a factor of 1.6 [160 and 258 $M^{-1}\ s^{-1}$ (see above)].[49,50] This example for a second-order rate constant that can be easily determined illustrates clearly the challenges of bromate formation models. Furthermore, if the >40 equations for bromate formation during ozonation of bromide-containing water are combined with the ozone decomposition chemistry, the level of uncertainty increases even more.

Nevertheless, kinetic bromate formation models can still yield useful information related to (i) relative bromate formation for changing water quality parameters (pH, ammonium, alkalinity, etc.), (ii) the contribution of a certain pathway to bromate formation, (iii) estimation of unknown rate constants for the reactions of transient bromine species with O_3 and •OH, and (iv) planning of tailored experiments to elucidate well-defined partial reaction systems. Bromate formation modeling has been extensively performed to support mechanistic studies for which relative changes in bromate are important and can be translated into mitigation strategies at full scale.[56,93]

Empirical Models. Since the early 1990s, nonmechanistic, empirical correlations have been applied to model bromate formation during ozonation of water and wastewater.[94,95] These can be generally categorized into three model types: linear regression, multilinear regression (MLR), and models based on artificial neural networks (ANNs).[26,96−106] Table S1 provides a list of various models, including their corresponding boundary conditions.

Applying real world data to several different models demonstrated a large variability, which is an inherent weakness of empirical models.[105] At their best, they were able to predict the trend of bromate formation with varying water quality parameters; however, the inaccuracy of the predicted bromate concentration was large. It appears that these models are highly water specific and should be used with caution, and not without prior model validation.

MITIGATION

Bromate control is challenging because of the need for micropollutant abatement and/or disinfection by ozone and/or •OH, which in turn leads to the formation of bromate. Several strategies can be applied before, during, or after ozonation to minimize the level of bromate in finished waters while maintaining the treatment goals (Figure 4). Strategies applied before or during ozonation aim to minimize the formation of bromate, whereas post-ozonation treatments focus on the abatement of bromate.

Bromate Minimization before Ozonation. Pretreatment strategies include processes located before ozonation aimed at bromide or DOC removal (Figure 4).

Bromide Removal. Electrochemical processes can remove ≤35% of bromide from natural waters in laboratory batch and continuous flow systems.[107,108] During the process, bromide is oxidized to bromine, which could potentially lead to formation of brominated compounds. Nevertheless, this may be offset by minimized brominated compound formation associated with lower bromide levels during oxidative post-treatment processes. Because bromate formation during ozonation is roughly proportional to the initial bromide concentration, this approach could partially mitigate bromate. However, for electrochemical

https://doi.org/10.1021/acs.est.3c00538
Environ. Sci. Technol. 2023, 57, 18393−18409

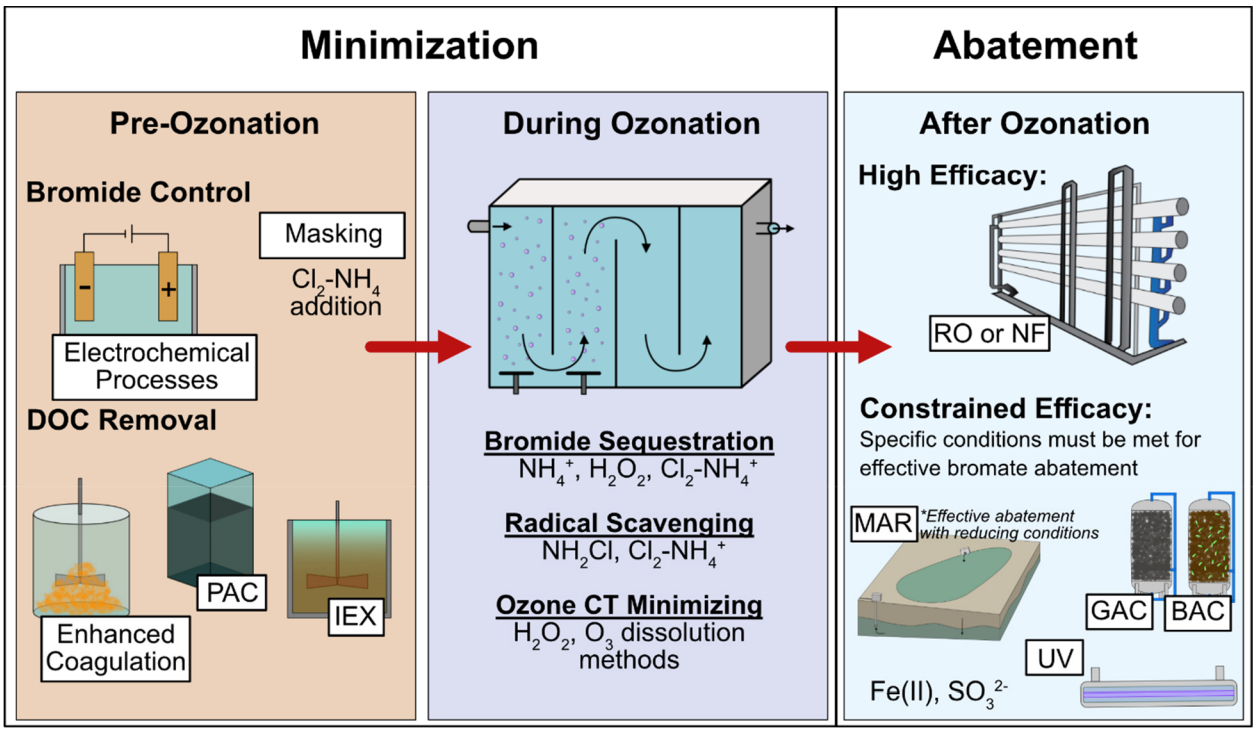

Figure 4. Overview of bromate mitigation strategies during pretreatment, ozonation, and post-treatment.

processes, up-scaling and cost/energy effectiveness lead to a limited applicability of this process in full-scale systems.[109]

A more promising bromide sequestration approach is the sequential addition of chlorine and NH_4^+,[110] and due to the multiple bromate suppression mechanisms that occur both before and during ozonation, it is described in greater detail in subsequent sections (see Ammonium- and Chloramine-Based Approaches).

DOC Removal. Treatments for DOC removal may inadvertently reduce bromate formation by decreasing the ozone demand to achieve target ozone exposures. This may be particularly relevant for waters with higher concentrations of DOC, such as wastewater.

Anion exchange resin has been demonstrated to remove ≤50−60% of bromide and DOC from natural waters.[111,112] Generally, bromate minimization occurred primarily from DOC rather than bromide removal.[113] During pilot-scale testing, magnetic ion exchange pretreatment removed 30% of the influent DOC and reduced the ozone dose requirements by 15−25% to meet CT requirements, which subsequently reduced the level of bromate formation by 35%.[114] Despite these promising results, this approach has not been readily implemented in full for bromate control.

Pretreatment by powdered activated carbon (PAC) can remove DOC. As a pretreatment step, it was shown to reduce the bromate yield at relatively large PAC doses (50−100 mg/L, >40% DOC removal), most likely due to the smaller doses of ozone needed to meet target micropollutant abatement.[95] However, for PAC doses in the range of 10−20 mg/L, an increased bromate yield was observed, potentially due to changes in electron-donating capacity of the DOM.[95] Because this behavior is not fully understood, more tests are needed before a broader application of this method will be possible.

DOC removal can also be achieved during enhanced coagulation, with optimal conditions based on coagulant type, pH, hydraulic conditions, etc.[115] In a study of three wastewaters, enhanced coagulation with 10−30 mg/L ferric chloride removed 10−47% of the DOC, which subsequently reduced the ozone dose by a similar percentage to meet treatment objectives.[116] This reduction in the applied ozone dose would likely reduce the level of bromate formation; however, further evaluation is necessary.

Bromate Minimization during Ozonation. There are several methods for minimizing bromate formation during ozonation, including reactor design and operation and chemical interventions (Table 1).

Process Design and Operation. Because reactor hydraulics should approach plug flow for efficient disinfection and oxidation, there is limited room for changes. However, one factor that can influence bromate formation is the ozone mass-transfer (i.e., dissolution of gaseous ozone in water) method and design.[117,118] There are two major methods for ozone mass transfer: (i) fine bubble diffusion (FBD) and (ii) addition of a concentrated ozone solution through a sidestream. Alternative ozone injection methods, such as injection through membranes or as micro/nanobubbles, have been developed, though their ability to minimize bromate formation has not yet been evaluated.

(i) In FBD systems, the first chamber of an ozone contactor is used for ozone gas−liquid transfer (Figure 5a). The ozone exposure (CT) in this dissolution zone (i.e., dissolution CT) is not included in regulatory disinfection credit (i.e., compliance CT). Therefore, the FBD chamber may contribute to bromate formation without any regulatory disinfection credit. When a treatment plant operates at design flow, the residence time in the FBD chamber can be minimized (often <2 min), which minimizes bromate formation in the ozone-transfer zone. However, during routine operation, flow rates can range from 25% to 60% of the design flow rate, resulting in longer contact times in

https://doi.org/10.1021/acs.est.3c00538
Environ. Sci. Technol. 2023, 57, 18393−18409

Table 1. Summary of Chemical Bromate Control Strategies

method	bromate minimization mechanism	bromate minimization efficiency	disinfection efficiency	oxidation efficiency	feasibility
pH depression	shifting $HOBr/OBr^-$ equilibrium, decreasing R_{ct} (increased O_3 stability)	pH 8 to 6 in drinking water, 50−91%[47,120]	enhanced (stabilized ozone)	potentially diminished for O_3 recalcitrant micropollutants (lower R_{ct})	expensive, requires storage of caustic chemicals, not applicable for medium/high-alkalinity water
NH_3 addition	HOBr quenching (NH_2Br formation)	42−73% (surface water, pH 8, 100−900 μg of NH_3-N/L)[47,120,123,124]	unaltered from conventional ozonation	unaltered from conventional ozonation	$^{\bullet}OH$ pathway not affected, removal of excess ammonium in biological postfiltration
preformed NH_2Cl	decreasing R_{ct} (radical scavenging), HOBr and $Br^{\bullet}$ quenching	68−87% (wastewater, 1−5 mg of NH_2Cl as Cl_2/L)[129]	unaltered, although lower levels of ozone exposures have been demonstrated	potentially diminished for O_3 recalcitrant micropollutants (lower R_{ct})	monochloramine must be produced on site, removal of excess ammonium in biological postfiltration
chlorine−ammonium	bromide sequestration (NH_2Br formation), HOBr quenching	44−94% (surface water, 0.25−1.0 mg/L Cl_2 and 100−500 μg of NH_3-N/L)[123−125]	unaltered from ozone alone or slightly enhanced	unaltered from ozone alone	formation of chlorinated/brominated DBPs
H_2O_2	reduced lifetime of ozone, reaction with HOBr	~130% to 60% (surface water, 0.5−1.5 mol of H_2O_2/mol of O_3),[133] −50% to 67% (wastewater, 0.14−4.2 mol of H_2O_2/mol of O_3)[95,134,135]	diminished (low level of or no O_3 exposure)	enhanced (increased level of radical production)	residual H_2O_2 removal in biological postfiltration

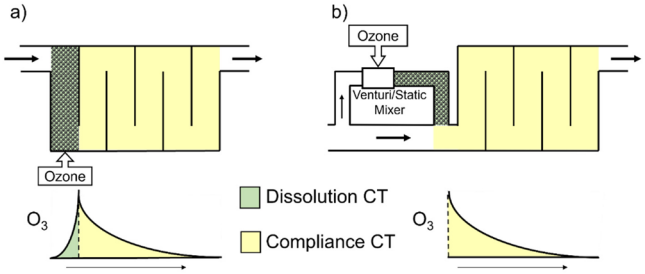

Figure 5. Comparisons of dissolution CT and compliance CT for different ozone mass-transfer systems: (a) conventional fine bubble diffuser and (b) sidestream addition.

the mass-transfer zone and thus higher levels of ozone exposure, leading to higher levels of bromate formation (2−7-fold in a pilot study).[117] Multiple contactor systems can take contactors out of service to minimize the residence time and the corresponding bromate production in the ozone mass-transfer zone.[117] This aspect of FBD should be considered when designing an ozonation process.

(ii) In sidestream systems, ozone gas is added to a sidestream water flow (10−20%) using venturi or static mixers and subsequently blended with the main water flow rate (80−90%) to achieve a target ozone dose entering the disinfection zone (Figure 5b),[82,117] which can minimize the dissolution zone CT compared to that of FBD systems. However, a nearly 5-fold larger ozone dose than in FBD is required in the sidestream to meet target dosages after blending. Hence, the residence time of the sidestream can influence the bromate concentration in the mainstream. Sidestream residence times increased bromate levels from 3−6 μg/L at 5 s to 40−140 μg/L at a residence time of >30 s.[117] Therefore, for the minimization of ozone decomposition and bromate formation, design guidance recommends that the residence time in the sidestream should not exceed 5 s, although time allowance for gas/liquid mass transfer should also be considered.[117]

pH Depression. Decreasing the pH influences both ozone stability and bromate formation (Table 1). A lower pH minimizes the amount of OBr^- available for oxidation by ozone (see Figure 2). However, because both HOBr and OBr^- are oxidized by $^{\bullet}OH$ with similar second-order rate constants (eqs 13 and 14), another major benefit of a decrease in pH is increased ozone stability with a lower transient $^{\bullet}OH$ concentration and a lower R_{ct}.[47] A decrease in pH from 8 to 6 typically results in a 50−60% decrease in the level of bromate formation in drinking water,[47,119] though a bromate minimization of >90% has also been demonstrated.[120] This approach allows for bromate minimization while meeting disinfection objectives. However, the chemical costs associated with pH depression, and subsequently increasing pH downstream, are in the range of 2−9 times higher than for ozone generation, depending on the water quality.[120] Because of this, pH depression is impractical for waters with moderate to high alkalinity, such as many drinking waters and wastewaters. Additionally, the decreased level of $^{\bullet}OH$ generation caused by pH depression should also be considered, as it may be counterproductive to a desired oxidation of micropollutants.[95]

Ammonium- and Chloramine-Based Approaches. The literature refers to ammonium-based strategies as "ammonia"/

https://doi.org/10.1021/acs.est.3c00538
Environ. Sci. Technol. 2023, 57, 18393−18409

"NH_3" rather than "ammonium"/"NH_4^+". It should be noted that we are choosing to henceforth refer to these strategies as "ammonium", as this is the applied form. Ammonium addition suppresses bromate formation by forming monobromamine, NH_2Br, from hypobromous acid and ammonia (k = 5.5−7.5 × 10^7 M^{-1} s^{-1}):[84,121]

$$HOBr + NH_3 \rightarrow NH_2Br + H_2O \quad (25)$$

preventing HOBr from being further oxidized to bromate. NH_2Br is oxidized by ozone to nitrate, releasing bromide again (k = 40 M^{-1} s^{-1}):[122]

$$NH_2Br + 3O_3 \rightarrow NO_3^- + Br^- + 3O_2 + 2H^+ \quad (26)$$

While the second-order rate constant for the reaction between hypobromous acid and ammonia is high, it should be noted that the reaction is between the two nonionic species. With pK_a values of 8.8 and 9.3 for $HOBr/OBr^-$ and NH_4^+/NH_3, respectively, neither can be the dominant species simultaneously. With the pH in the general range for drinking water or wastewater (6−8), the apparent second-order rate constant decrease by 1−2 orders of magnitude compared to the species specific second-order rate constant in eq 25.[121] While an increasing pH can increase the rate of NH_2Br formation, this leads to a lower ozone stability and potentially offsets the benefit of ammonium addition due to larger ozone doses required to meet disinfection objectives.[120] Regardless, in surface waters at pH ∼8, the level of bromate was decreased by 40−73% (Table 1 and Table S2) across a wide range of ozone doses with ∼200 μg of NH_4^+-N/L.[47,120,123,124] Because of the fast consumption of HOBr by ammonia, reaction 25 dominates the consumption of HOBr at 200 μg of NH_4^+-N/L (k' = 28 s^{-1}) over its further reaction with ozone ($k' \approx 3.2 \times 10^{-4}$ s^{-1} at 1 mg/L O_3) and $^\bullet$OH ($k' \approx 5 \times 10^{-4}$ s^{-1} for an R_{ct} of 10^{-8}) by orders of magnitude.

Bromate initiated by the oxidation of bromide with $^\bullet$OH is not efficiently mitigated by ammonium addition because HOBr is only a minor product of this pathway. Hence, the efficiency of ammonium addition for bromate mitigation depends strongly on the water characteristics and the importance of the main bromide oxidation pathway. This is also illustrated by the fact that bromate formation cannot be completely suppressed by ammonium addition, with often a maximum mitigation to 50−70%.[120,123] Because ammonium addition minimizes bromate through sequestration of bromine and not through the alteration of ozone and/or $^\bullet$OH exposure, the efficiency of ozone for either disinfection or oxidation is not affected (Table 1).

The chlorine−ammonium process was developed to provide enhanced bromate control beyond what is possible with ammonium addition alone.[119,124,125] In this process, chlorine is added upstream of ozonation to oxidize bromide to HOBr (k = 1550 M^{-1} s^{-1}):

$$HOCl + Br^- \rightarrow HOBr + Cl^- \quad (27)$$

Five to seven minutes of chlorine contact before ammonium addition is typical, though contact times as short as 1 min have been investigated.[119,124,125] Ammonium is then added to form NH_2Br prior to ozonation (reaction 25). Via the formation of NH_2Br prior to ozonation, the chlorine−ammonium process masks bromine and, in contrast to ammonium addition, can suppress bromate formation initiated by both O_3 and $^\bullet$OH. The level of bromate formation has been demonstrated to be reduced by 44−94%[119,123−125] depending on the treatment conditions (Table 1 and Table S3).

In addition to HOBr formation and quenching, the chlorine−ammonium process affects ozone performance in several ways. Preoxidation with chlorine decreases the ozone consumption rate and the level of $^\bullet$OH formation by altering the DOM.[125] This was also confirmed at pilot- and full-scale, where a decreased ozone demand and decay rate were observed, largely due to chlorine preoxidation, with a significantly increased level of ozone exposure at the same ozone dose.[124] Additionally, monochloramine is formed by the reaction of residual HOCl with NH_3. It is a weak $^\bullet$OH scavenger, which can partly suppress $^\bullet$OH reactions and stabilize dissolved ozone (k = 5.2−5.7 × 10^8 M^{-1} s^{-1}):[126,127]

$$NH_2Cl + {}^\bullet OH \rightarrow NHCl^\bullet + H_2O \quad (28)$$

In one study, there was no difference in bromate formation for prechlorination contact times 1 or 5 min prior to ammonium addition. This is an indication that monochloramine alone may also play an important role in bromate suppression.[119]

On the basis of this observation, the options and limitations of NH_2Cl for bromate mitigation were investigated. To this end, it has been demonstrated that the ammonium−chlorine processes, in which mostly NH_2Cl is formed prior to ozonation, has a bromate mitigation effect similar to that of the chlorine−ammonium process. In this configuration, bromide will not be masked as bromamine prior to ozonation. Instead, bromochloramine can be formed during ozonation (k = 2.86 × 10^5 M^{-1} s^{-1}):[128]

$$NH_2Cl + HOBr \rightarrow NHBrCl + H_2O \quad (29)$$

However, similar to the addition of ammonium, this does not quench the bromine radical pathway. In a comparative study, the ammonium−chlorine process reduced the level of bromate formation from 17 to 3−4 μg/L compared to a value of 2 μg/L for the chlorine−ammonium process.[119] Nevertheless, the ammonium−chlorine process was selected for bromate control because it resulted in a lower level of formation of trihalomethanes (THMs).

As a variant of the ammonium−chlorine process, preformed monochloramine has been added to wastewater to control bromate formation;[98] 5 mg/L NH_2Cl (as Cl_2) (∼130 μM NH_2Cl) could reduce the level of bromate formation by ≤92%, depending on the specific ozone dose (Table 1 and Table S4). This dose is larger than what is commonly utilized in drinking water [1−2 mg of NH_2Cl/L (as Cl_2) (∼15−30 μM NH_2Cl)]; however, the purpose of NH_2Cl addition is not disinfection of the distribution system but mitigation of bromate. Similar to ammonium addition, an optimum monochloramine concentration exists beyond which bromate minimization cannot be further enhanced.[81,125] Monochloramine minimizes bromate formation by several mechanisms: (i) quenching of $^\bullet$OH (see above), (ii) formation of bromochloramine, and (iii) quenching of $Br^\bullet$.

(i) As an $^\bullet$OH scavenger, monochloramine should stabilize ozone decay in drinking water. However, a certain increase in the ozone decay rate was observed in the presence of monochloramine both in river water and during water reuse.[129] This may be due to the reaction of monochloramine with ozone (k = 26 M^{-1} s^{-1}):[52]

$$NH_2Cl + O_3 \rightarrow NO_3^- + Cl^- + 2H^+ \quad (30)$$

The $^\bullet$OH scavenging of NH_2Cl not only mitigates bromate formation but also may reduce the rate of

https://doi.org/10.1021/acs.est.3c00538
Environ. Sci. Technol. 2023, 57, 18393−18409

oxidation of ozone-resistant compounds, such as 1,4-dioxane.[129]

(ii) Even though the formation of bromochloramine from the reaction of NH_2Cl and Br^- is often mentioned as a mitigation effect for bromate, this is not very likely. The apparent second-order rate constant at circumneutral pH for the formation of bromochloramine from the reaction of NH_2Cl with Br^- is low ($k = 1.4 \times 10^{-1}$ M^{-1} s^{-1}):[130]

$$NH_2Cl + Br^- \rightarrow \text{products} \quad (31)$$

For a NH_2Cl concentration of 5 mg/L as Cl_2 (~130 μM NH_2Cl), an ozone concentration of 1 mg/L, and an R_{ct} of 10^{-8}, the fractions of Br^- reacting with NH_2Cl, O_3, and $^{\bullet}OH$ are 0.3%, 94%, and 5.7%, respectively. This shows clearly that reaction 31 is not an efficient sink for bromide.

(iii) It has been shown that $Br^{\bullet}$ reacts with a k of 4.4×10^9 M^{-1} s^{-1} with NH_2Cl.[67] An addition of 15 μM NH_2Cl (~1 mg/L as Cl_2) can reduce the contribution of the O_3–$Br^{\bullet}$ reaction (eq 18) from 8–15% to 2–4%, and therefore, the NH_2Cl–$Br^{\bullet}$ and NH_2Cl–HOBr reactions contribute roughly equally to the reduction of the level of bromate formation.[67]

Hydrogen Peroxide. The addition of hydrogen peroxide (H_2O_2) during ozonation leads to an advanced oxidation process (AOP), which can maintain micropollutant abatement and mitigate bromate formation compared to conventional ozonation with the same ozone dose.[61,95]

Ozone reacts only with HO_2^- (eq 32), which is present in only a minor fraction at neutral pH ($pK_{a,H_2O_2} = 11.6$).[131] The reaction of O_3 with HO_2^- ($k = 5.5 \times 10^6$ M^{-1} s^{-1}; $k_{app,pH7} = 140$ M^{-1} s^{-1}) produces $^{\bullet}OH$ with a yield of ~50% through a complex mechanism, which is discussed elsewhere (eq 32).[1,55,131]

$$O_3 + HO_2^- \rightarrow \rightarrow 0.5^{\bullet}OH \quad (32)$$

O_3/H_2O_2 can influence bromate formation on two levels: (i) reduction of the lifetime of ozone and (ii) quenching of HOBr.[132]

(i) Enhanced transformation of O_3 to $^{\bullet}OH$ in the O_3/H_2O_2 process results in a shift toward the formation of $Br^{\bullet}$ (eqs 9 and 10). Under these conditions, $Br^{\bullet}$ will primarily react with DOM back to bromide (eq 19) due to the resulting shorter lifetime and lower transient concentration of O_3.

(ii) Reduction of HOBr by H_2O_2 ($k = 7.6 \times 10^8$ M^{-1} s^{-1}) proceeds by eq 33:[62]

$$HOBr + HO_2^- \rightarrow Br^- + H_2O + O_2 \quad (33)$$

with an apparent second-order rate constant of ~2×10^4 M^{-1} s^{-1} at pH 7. For a H_2O_2 concentration of 1 mg/L, the half-life of HOBr is ~1 s at pH 7.

The performance of H_2O_2 for bromate suppression is quite variable (Table 1 and Table S5); an 85% decrease and a 110% increase in the level of bromate formation have been reported in bench testing and in full-scale systems relative to conventional ozonation.[95,133−135] These differences are largely due to different operational conditions, with either constant ozone doses or constant ozone residual, for conventional ozonation and the O_3/H_2O_2 process, respectively, although the water matrix can also impact the efficacy of H_2O_2.[135] If a constant ozone dose is applied for the two processes, the level of ozone exposure decreases in the O_3/H_2O_2 process and therefore the level of bromate formation decreases. For a constant ozone residual, the ozone exposures for the two processes are similar, while in the O_3/H_2O_2 process, the level of $^{\bullet}OH$ exposure increases, which leads to a higher level of bromate formation. Therefore, O_3/H_2O_2 should not be used for treatment objectives that include disinfection of bacteria and protozoa due to the necessity to maintain an ozone residual. A significant inactivation of viruses can still be with the O_3/H_2O_2 process, despite there being no measurable CT.[136] This is caused by the high second-order rate constants for virus inactivation with ozone.[81,137]

Several novel approaches to ozone contactor design have been developed to maximize $^{\bullet}OH$ exposure while minimizing bromate formation in the presence of H_2O_2 by multiple smaller doses (for more details, see section S.1 of the Supporting Information).[109,132,138,139] A serial O_3/H_2O_2/LP UV process approach allowed for application of optimized ozone doses and demonstrated minimal bromate formation while achieving significant abatement of micropollutants.[140]

Alternative Chemical Control Strategies. Preoxidation processes with various oxidants, such as chlorine, chlorine dioxide, and permanganate, may affect ozone and $^{\bullet}OH$ chemistry, and thus potentially bromate formation, through changes in DOM properties. Typically, this leads to a higher ozone stability and allows the partial mitigation of bromate formation, while a certain disinfection target can be reached.[124,141] Heterogenous catalytic ozonation in which a catalyst, such as metal oxides (e.g., FeOOH), is added to enhance ozone transformation to $^{\bullet}OH$[142] have been demonstrated to reduce the level of bromate formation by ≤91%.[143] However, there are numerous issues related to heterogeneous processes and large doses of catalysts are required, which have prevented full-scale applications so far.[109] In a preliminary study, a very low level of bromate formation with effective abatement of micropollutants was achieved by ozonation in the activated sludge reactor instead of the clarified secondary effluent.[144]

Post-Treatment for Bromate Abatement. Abatement of bromate downstream of ozone treatment has largely proven to be unsuccessful, with the exception of high-pressure membrane treatment such as reverse osmosis (RO) and nanofiltration (NF). It has been demonstrated that 96–97% of bromate can be removed in pilot- and full-scale RO systems after ozonation,[145,146] whereas NF membranes have been demonstrated to remove 45–77% with rejection increasing at high pH and ionic strength and decreasing in the presence of DOM.[147] This is especially relevant in the context of wastewater reuse that typically has DOC concentrations higher than those of natural waters. However, RO and NF may not be viable options or cost-effective for some systems (i.e., inland communities) employing upstream ozone, but RO and NF could be particularly useful for an integrated process train with multiple water quality goals, if both ozone and RO are necessary for potential regulatory requirements (e.g., California's Draft Criteria for Direct Potable Reuse).[148] Other post-ozone treatment processes have demonstrated limited success in the abatement of bromate, such as granular activated carbon and biofiltration,[149−161] ion exchange,[162−168] managed aquifer recharge,[169−174] ferrous iron and sulfite,[175−178] and UV irradiation.[179−181]

PRACTICAL CONSIDERATIONS

A one-size-fits-all approach to bromate mitigation is difficult to achieve. Absolute bromate concentrations will depend on both the water matrix composition, including bromide levels, and treatment goals. Only once bromate levels are demonstrated with a particular water and particular treatment conditions can a

https://doi.org/10.1021/acs.est.3c00538
Environ. Sci. Technol. 2023, 57, 18393−18409

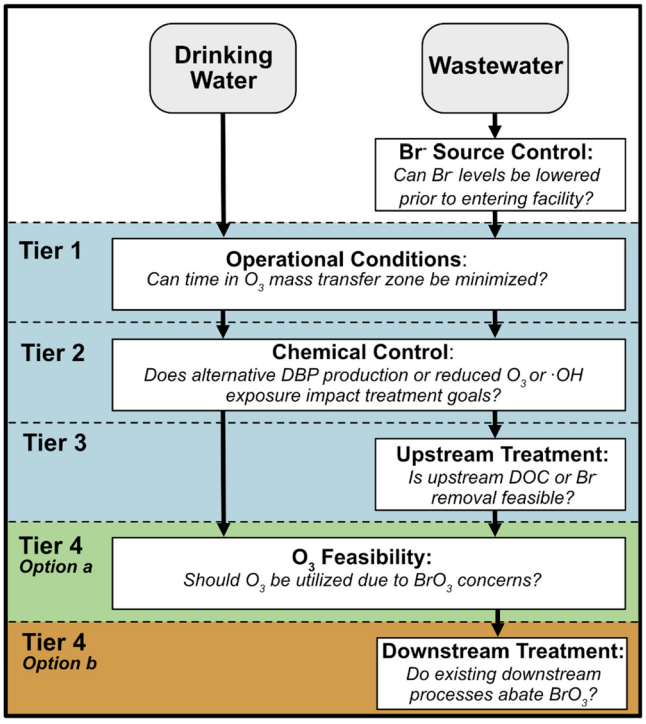

Figure 6. Tiered approach for the assessment of bromate control strategies based on the results of this work. In the blue area, the focus should primarily be on removing bromide from entering the ozonation process and on minimizing bromate formation through optimizing ozone dissolution, adding specific chemicals that sequester bromide, and/or disrupting bromate formation reactions. In the green area, if these solutions are not viable, then the question of whether ozone should be used should be assessed. The brown area shows options and limitations of downstream treatment for bromate abatement.

mitigation strategy be chosen for application. An approach for making such decisions is suggested in Figure 6. Outside of approaches that can be taken by the utility, an additional option worth mentioning is bromide source control. In the case in which there is a known bromide point source, elimination via diverting this waste stream, or eliminating bromide via treatment prior to discharge, could lead to reduced bromide levels entering the treatment facility and thus a reduced level of bromate formation.[22] This approach is not feasible for most drinking water utilities but could be considered, if necessary, for wastewater treatment facilities.

Tier One. Ideally, operational conditions affecting the extent of ozone transfer versus regulatory CT should first be considered, for both drinking water and wastewater treatment approaches. The ozone exposure should be minimized in portions of the contactor where no ozone CT credit is measured or assigned. This can be achieved by the selection (e.g., FBD and SSI) and optimization of the dissolution method (e.g., distributed ozone diffusion and reduction of sidestream residence time), which can reduce the level of bromate formation and overall cost.

Tier Two. If bromate levels are still increased after the optimization of operational conditions, a chemical control during ozonation should be considered. The chemical strategy of choice should be based on the specific treatment objectives for the ozone process, as many of the chemical strategies can affect ozone and •OH exposures. In these cases, practitioners are often challenged with balancing treatment goals with bromate formation. For instance, if ozone is implemented for disinfection purposes, it is not appropriate to utilize hydrogen peroxide as a bromate control strategy as it greatly reduces the level of ozone exposure (CT). However, this strategy would still allow for micropollutant oxidation. Furthermore, addition of chloramine or hydrogen peroxide may require the management of residuals during downstream treatment processes, such as biofiltration. Table 1 provides an overview of the different chemical addition strategies.

Tier Three. If bromate levels are still an issue, then upstream treatment minimizing either bromide or DOC, such as enhanced coagulation or PAC, could be considered. However, on the basis of the inconclusive results for different DOC removal options, such an approach should be used with caution. Preliminary bench- or pilot-scale testing with the specific source water and specific upstream treatment should be evaluated to demonstrate the extent, if any, of bromate mitigation. Such upstream treatments, if successful, also have the added benefit of reducing the size of the ozone doses necessary to achieve treatment goals, particularly in wastewater. This could potentially lower overall ozone costs, although this analysis is outside the scope of this work. DOC removal is less relevant for drinking water treatment due to the lower DOC levels compared to those of wastewater.

Tier Four. A majority of post-ozonation bromate abatement strategies are generally ineffective; therefore, relying on such an approach for bromate mitigation is not recommended. A universal promising approach to the abatement of bromate appears to be RO; however, it is cost-prohibitive if it is not already utilized for other treatment objectives and is not typically realistic for drinking water treatment facilities. The lack of post-ozonation bromate abatement options highlights the necessity of focusing efforts on minimizing bromate formation during ozonation. However, abstaining from an ozone-based process altogether may be the most feasible option for a challenging matrix. In these cases, alternate treatment processes may be desirable depending on the treatment objectives. For example, If disinfection and micropollutant abatement are desired, the AOP UV/H_2O_2 system may be an option,[60,109] whereas if treatment is solely targeting micropollutant abatement, activated carbon (GAC, PAC, etc.) could be utilized.[182,183]

RESEARCH NEEDS

This Critical Review has highlighted several current research needs, which are particularly important considering the continued interest in using ozone for drinking water treatment or enhanced wastewater treatment for potable reuse, irrigation, or ecosystem protection:

- Better mechanistic understanding of the mitigation strategies based on chlorine and ammonia, including remeasurement of some of the second-order rate constants.
- Better mechanistic understanding of bromate mitigation during heterogeneous ozonation in the presence of metal oxides.
- Further development of analytical methods for online determination of bromate concentrations to adapt treatment for changing water qualities.
- Process optimization to better control the balance between treatment objectives and bromate formation (i.e., multiple-point peroxide addition, multistage mass transfer, and novel ozone-transfer systems).

https://doi.org/10.1021/acs.est.3c00538
Environ. Sci. Technol. 2023, 57, 18393−18409

- Standardized reporting of ozone and •OH exposures during bromate control studies, including determination methods. This would allow a better evaluation of the trade-offs between bromate control and other treatment objectives (i.e., oxidation and/or disinfection).
- Further evaluations of the ability of upstream treatments that aim to remove DOC to minimize bromate formation during ozonation. Certain upstream treatments, such as enhanced coagulation, may allow for several water quality changes that can impact bromate formation, such as DOC concentration, pH, and alkalinity reduction.
- Determinations for the need to manage chemical residuals, i.e., chloramine and hydrogen peroxide, for downstream treatment processes, such as biofiltration.
- Field demonstration for the reduction of the level of bromate in managed aquifer recharge systems for potable reuse applications.

■ ASSOCIATED CONTENT

Supporting Information

The Supporting Information is available free of charge at https://pubs.acs.org/doi/10.1021/acs.est.3c00538.

Details on $Br^{\bullet}/Br_2^{\bullet-}$ concentrations as a function of bromide; summary of bromate formation models; and water quality data demonstrating the performance of ammonium, chlorine−ammonia, preformed monochloramine, and hydrogen peroxide for bromate control (PDF)

■ AUTHOR INFORMATION

Corresponding Authors

Urs von Gunten − *Eawag, Swiss Federal Institute of Aquatic Science and Technology, CH-8600 Dubendorf, Switzerland; School of Architecture, Civil and Environmental Engineering (ENAC), Ecole Polytechnique Fédérale de Lausanne (EPFL), 1015 Lausanne, Switzerland;* orcid.org/0000-0001-6852-8977; Email: vongunten@eawag.ch

Eric C. Wert − *Southern Nevada Water Authority (SNWA), Las Vegas, Nevada 89193-9954, United States;* orcid.org/0000-0001-5587-4635; Email: eric.wert@snwa.com

Authors

Christina M. Morrison − *Southern Nevada Water Authority (SNWA), Las Vegas, Nevada 89193-9954, United States;* orcid.org/0000-0001-8145-428X

Samantha Hogard − *Hampton Roads Sanitation District, Virginia Beach, Virginia 23471-0911, United States; The Charles Edward Via, Jr. Department of Civil and Environmental Engineering, Virginia Polytechnic Institute and State University, Blacksburg, Virginia 24061, United States;* orcid.org/0000-0001-9364-7257

Robert Pearce − *Hampton Roads Sanitation District, Virginia Beach, Virginia 23471-0911, United States; The Charles Edward Via, Jr. Department of Civil and Environmental Engineering, Virginia Polytechnic Institute and State University, Blacksburg, Virginia 24061, United States*

Aarthi Mohan − *Southern Nevada Water Authority (SNWA), Las Vegas, Nevada 89193-9954, United States;* orcid.org/0000-0002-1540-7757

Aleksey N. Pisarenko − *Trussell Technologies, Inc., Solana Beach, California 92075, United States*

Eric R. V. Dickenson − *Southern Nevada Water Authority (SNWA), Las Vegas, Nevada 89193-9954, United States;* orcid.org/0000-0003-2341-4997

Complete contact information is available at: https://pubs.acs.org/10.1021/acs.est.3c00538

Notes

The authors declare no competing financial interest.

■ ACKNOWLEDGMENTS

This review was funded by The Water Research Foundation Project Number 5035: Impact of Bromate Control Measures on Ozone Oxidation/Disinfection and Downstream Treatment Processes in Potable Reuse.

■ REFERENCES

(1) von Sonntag, C.; von Gunten, U. *Chemistry of Ozone in Water and Wastewater Treatment: From Basic Principles to Applications*; IWA Publishing, 2012.

(2) Oneby, M. A.; Bromley, C. O.; Borchardt, J. H.; Harrison, D. S. Ozone treatment of secondary effluent at U.S. municipal wastewater treatment plants. *Ozone Sci. Eng.* **2010**, *32*, 43−55.

(3) Stage 1 Disinfectants and Disinfection Byproduct Rule (Stage 1 DBPR) 63 FR 69390. U.S. Environmental Protection Agency, 1998; *63*, No. 241.

(4) *Guidelines for Drinking Water Quality*, 4th ed. (incorporating the first and second addenda); World Health Organization: Geneva, 2022.

(5) Kurokawa, Y.; Aoki, S.; Matsushima, Y.; Takamura, N.; Imazawa, T.; Hayashi, Y. Dose-response studies on the carcinogenicity of potassium bromate in F344 rats after long-term oral administration. *J. Natl. Cancer Inst.* **1986**, *77*, 977−982.

(6) Kurokawa, Y; Takayama, S; Konishi, Y; Hiasa, Y; Asahina, S; Takahashi, M; Maekawa, A; Hayashi, Y Long-term in vivo carcinogenicity tests of potassium bromate, sodium hypochlorite, and sodium chlorite conducted in Japan. *Environ. Health Perspect.* **1986**, *69*, 221−235.

(7) DeAngelo, A. B.; George, M. H.; Kilburn, S. R.; Moore, T. M.; Wolf, D. C. Carcinogenicity of potassium bromate administered in the drinking water to male B6C3F1 mice and F344/N rats. *Toxicol. Pathol.* **1998**, *26*, 587−594.

(8) Health Risk Assessment/Characterization of the Drinking Water Disinfection Byproduct Bromate. U.S. Environmental Protection Agency, 1998.

(9) *Bromate in Drinking Water*; World Health Organization: Geneva, 2003.

(10) Bull, R. J.; Cotruvo, J. A. Nongenotoxic mechanisms involved in bromate-induced cancer in rats. *J. Am. Water Works Assoc* **2013**, *105*, E709−E720.

(11) Kolisetty, N.; Delker, D. A.; Muralidhara, S.; Bull, R. J.; Cotruvo, J. A.; Fisher, J. W.; Cummings, B. S. Changes in mRNA and protein expression in the renal cortex of male and female F344 rats treated with bromate. *Arch. Toxicol.* **2013**, *87*, 1911−1925.

(12) Cotruvo, J. A.; Keith, J. D.; Bull, R. J.; Pacey, G. E.; Gordon, G. Bromate reduction in simulated gastric juice. *J. Am. Water Works Assoc.* **2010**, *102*, 77−86.

(13) Hutchinson, T. H.; Hutchings, M. J.; Moore, K. W. A review of the effects of bromate on aquatic organisms and toxicity of bromate to oyster (Crassostrea gigas) embryos. *Ecotoxicol. Environ. Saf.* **1997**, *38*, 238−243.

(14) Butler, R.; Godley, A.; Lytton, L.; Cartmell, E. Bromate environmental contamination: Review of impact and possible treatment. *Crit. Rev. Environ. Sci. Technol.* **2005**, *35*, 193−217.

(15) Santiago, S. Study to support the derivation of environmental quality standard for bromate ecotoxicity of sodium bromate on reproduction of *Ceriodaphnia dubia* and on other freshwater organisms. 2015. https://www.ecotoxcentre.ch/projects/risk-assessment/ecotoxicological-assessment-of-bromate (accessed 2022-08-15).

(16) Ecotox Centre of Switzerland. Proposals for Quality Criteria for Surface Waters. 2015. https://www.ecotoxcentre.ch/expert-service/quality-criteria/quality-criteria-for-surface-waters (accessed 2022-08-15).
(17) Flury, M.; Papritz, A. Bromide in the Natural Environment: Occurrence and Toxicity. *J. Environ. Qual* **1993**, *22*, 747−758.
(18) von Gunten, U.; Hoigné, J. Factors controlling the formation of bromate during ozonation of bromide-containing waters. *J. Water Supply: Res. Technol.—AQUA* **1992**, *41*, 299−304.
(19) Winid, B. Bromine and water quality- Selected aspects and future perspectives. *Appl. Geochem.* **2015**, *63*, 413−435.
(20) Mctigue, N. E.; Cornwell, D. A.; Graf, K.; Brown, R. Occurrence and consequences of increased bromide in drinking water sources. *J. Am. Water Works Assoc* **2014**, *106*, E492−E508.
(21) Harkness, J. S.; Dwyer, G. S.; Warner, N. R.; Parker, K. M.; Mitch, W. A.; Vengosh, A. Iodide, bromide, and ammonium in hydraulic fracturing and oil and gas wastewaters: Environmental implications. *Environ. Sci. Technol.* **2015**, *49*, 1955−1963.
(22) Soltermann, F.; Abegglen, C.; Götz, C.; von Gunten, U. Bromide Sources and Loads in Swiss Surface Waters and Their Relevance for Bromate Formation during Wastewater Ozonation. *Environ. Sci. Technol.* **2016**, *50* (18), 9825−9834.
(23) Westerhoff, P. Occurrence Survey of Bromide and Iodide in Water Supplies. Water Research Foundation Project 4711. 2022. https://www.waterrf.org/research/projects/occurrence-survey-bromide-and-iodide-water-supplies (accessed 2022-08-15).
(24) Obolensky, A.; Singer, P. C.; Shukairy, H. M. Information Collection Rule Data Evaluation and Analysis to Support Impacts on Disinfection By-Product Formation. *J. Environ. Eng.* **2007**, *133*, 53−63.
(25) Siddiqui, M. S.; Amy, G. L. Factors Affecting DBP Formation During Ozone-Bromide Reactions. *J. Am. Water Works Assoc.* **1993**, *85*, 63−72.
(26) Ozekin, K.; Amy, G. L. Threshold Levels for Bromate Formation in Drinking Water. *Ozone Sci. Eng.* **1997**, *19*, 323−337.
(27) Regli, S.; Chen, J.; Messner, M.; Elovitz, M. S.; Letkiewicz, F. J.; Pegram, R. A.; Pepping, T. J.; Richardson, S. D.; Wright, J. M. Estimating Potential Increased Bladder Cancer Risk Due to Increased Bromide Concentrations in Sources of Disinfected Drinking Waters. *Environ. Sci. Technol.* **2015**, *49*, 13094−13102.
(28) Amy, G.; Siddiqui, M.; Zhai, W.; Debroux, J.; Odem, W. Survey of bromide in drinking water and impacts on DBP formation. Water Research Foundation Project 825; 1994. https://www.waterrf.org/research/projects/survey-bromide-drinking-water-and-impacts-dbp-formation.
(29) Lundström, U.; Olin, Å. Bromide concentration in Swedish precipitation, surface and ground waters. *Water Res.* **1986**, *20*, 751−756.
(30) Magazinovic, R. S.; Nicholson, B. C.; Mulcahy, D. E.; Davey, D. E. Bromide levels in natural waters: its relationship to levels of both chloride and total dissolved solids and the implications for water treatment. *Chemosphere* **2004**, *57*, 329−335.
(31) Davis, S. N.; Fabryka-Martin, J. T.; Wolfsberg, L. E. Variations of bromide in potable ground water in the United States. *Ground Water* **2004**, *42*, 902−909.
(32) von Gunten, U.; Salhi, E. Bromate in drinking water: A problem in Switzerland? *Ozone Sci. Eng.* **2003**, *25*, 159−166.
(33) Wagner, H. P.; Pepich, B. V.; Hautman, D. P.; Munch, D. J. Performance evaluation of a method for the determination of bromate in drinking water by ion chromatography (EPA Method 317.0) and validation of EPA Method 324.0. *J. Chromatogr. A* **2000**, *884*, 201−210.
(34) Wagner, H. P.; Pepich, B. V.; Hautman, D. P.; Munch, D. J. US EPA Method 317: Determination of inorganic oxyhalide disinfection by-products in drinking water using ion chromatography with the addition of a postcolumn reagent for trace bromate analysis. 2001.
(35) Wagner, H. P.; Pepich, B. V.; Hautman, D. O.; Munch, D. J.; Salhi, E.; von Gunten, U. US EPA Method 326.0 Determination of Inorganic Oxyhalide Disinfection By-Products in Drinking Water Using Ion Chromatography Incorporating the Addition of a Suppressor Acidified Postcolumn Reagent for Trace Bromate Analysis Revision 1.0. 2002.
(36) Wagner, H. P.; Pepich, B. V.; Pohl, C.; Srinivasan, K.; De Borba, B.; Lin, R.; Munch, D. J. US EPA Method 302.0 : Determination of Bromate in Drinking Water Using Two-Dimensional Ion Chromatography With Suppressed Conductivity Detection. 2009.
(37) Pfaff, J. US EPA Method 300.1. Revision 1.0: Determination of Inorganic Anions in Drinking Water by Ion Chromatography. 1993.
(38) Salhi, E.; von Gunten, U. Simultaneous determination of bromide, bromate and nitrite in low ug/L levels by ion chromatography without sample pretreatment. *Water Res.* **1999**, *33*, 3239−3244.
(39) Weinberg, H. S.; Yamada, H. Post-Ion-Chromatography Derivatization for the Determination of Oxyhalides at Sub-PPB Levels in Drinking Water. *Anal. Chem.* **1998**, *70*, 1−6.
(40) Creed, J. T.; Brockhoff, C. A.; Martin, T. D. US EPA Method 321.8: Determination of bromate in drinking waters by ion chromatography inductively coupled plasma-mass spectrometry. 1997.
(41) Snyder, S. A.; Vanderford, B. J.; Rexing, D. J. Trace analysis of bromate, chlorate, iodate, and perchlorate in natural and bottled waters. *Environ. Sci. Technol.* **2005**, *39*, 4586−4593.
(42) Shah, A. D.; Liu, Z. Q.; Salhi, E.; Hofer, T.; Werschkun, B.; von Gunten, U. Formation of disinfection by-products during ballast water treatment with ozone, chlorine, and peracetic acid: influence of water quality parameters. *Environ. Sci. Water Res. Technol.* **2015**, *1*, 465−480.
(43) Young, T. R.; Cheng, S.; Li, W.; Dodd, M. C. Rapid, high-sensitivity analysis of oxyhalides by non-suppressed ion chromatography-electrospray ionization-mass spectrometry: application to ClO_4^-, ClO_3^-, ClO_2^-, and BrO_3^- quantification during sunlight/chlorine advanced oxidation. *Environ. Sci. Water Res. Technol.* **2020**, *6*, 2580−2596.
(44) Zaffiro, A. D.; Pepich, B. V.; Slingsby, R. W.; Pohl, J.; Pohl, C. A.; Munch, D. J. US EPA Method 557: Determination of Haloacetic Acids, Bromate, and Dalapon in Drinking Water by Ion Chromatography Electrospray Ionization Tandem Mass Spectrometry (IC-ESI-MS/MS). 2009.
(45) Ohtomo, T.; Yatabe, R.; Tanaka, Y.; Kato, J.; Igarashi, S. Fluorescence Detection-FIA for ppb Levels of Bromate with Trifluoperazine. *J. Flow Injection Anal.* **2009**, *26*, 127−131.
(46) Fujioka, T.; Boivin, S.; Takeuchi, H. Online monitoring of bromate in treated wastewater: implications for potable water reuse. *Environ. Sci.: Water Res. Technol.* **2022**, *8*, 2034−2039.
(47) Pinkernell, U.; von Gunten, U. Bromate minimization during ozonation: Mechanistic considerations. *Environ. Sci. Technol.* **2001**, *35*, 2525−2531.
(48) Taube, H. Reactions in Solutions Containing O_3, H_2O_2, H^+ and Br^-. The Specific Rate of the Reaction $O_3 + Br^-$. *J. Am. Chem. Soc.* **1942**, *64*, 2468−2474.
(49) Haag, W. R.; Hoigné, J. Ozonation of Bromide-Containing Waters: Kinetics of Formation of Hypobromous Acid and Bromate. *Environ. Sci. Technol.* **1983**, *17*, 261−267.
(50) Liu, Q.; Schurter, L. M.; Muller, C. E.; Aloisio, S.; Francisco, J. S.; Margerum, D. W. Kinetics and mechanisms of aqueous ozone reactions with bromide, sulfite, hydrogen sulfite, iodide, and nitrite ions. *Inorg. Chem.* **2001**, *40*, 4436−4442.
(51) Heeb, M. B.; Criquet, J.; Zimmermann-Steffens, S. G.; von Gunten, U. Oxidative treatment of bromide-containing waters: Formation of bromine and its reactions with inorganic and organic compounds - A critical review. *Water Res.* **2014**, *48*, 15−42.
(52) Haag, W. R.; Hoigné, J. Ozonation of water containing chlorine or chloramines. *Reaction products and kinetics. Water Res.* **1983**, *17*, 1397−1402.
(53) Reisz, E.; Leitzke, A.; Jarocki, A.; Irmscher, R.; von Sonntag, C. Permanganate formation in the reactions of ozone with Mn(II): a mechanistic study. *J. Water Supply Res. Technol.* **2008**, *57*, 451−464.
(54) Odeh, I. N.; Nicoson, J. S.; Huff Hartz, K. E.; Margerum, D. W. Kinetics and mechanisms of bromine chloride reactions with bromite and chlorite ions. *Inorg. Chem.* **2004**, *43*, 7412−7420.

https://doi.org/10.1021/acs.est.3c00538
Environ. Sci. Technol. 2023, 57, 18393−18409

(55) Fischbacher, A.; Löppenberg, K.; von Sonntag, C.; Schmidt, T. C. A New Reaction Pathway for Bromite to Bromate in the Ozonation of Bromide. *Environ. Sci. Technol.* **2015**, *49*, 11714−11720.
(56) von Gunten, U.; Hoigné, J. Bromate formation during ozonation of bromide-containing waters: Interaction of Ozone and Hydroxyl Radical Reactions. *Environ. Sci. Technol.* **1994**, *28*, 1234−1242.
(57) Klaning, U.; Wolff, T. Laser Flash Photolysis of HClO, ClO^-, HBrO, and BrO^- in Aqueous Solution. Reactions of Cl^- and Br^- Atoms. *Ber. Bunsen-Ges.* **1985**, *89*, 243−245.
(58) Zehavi, D.; Rabani, J. The oxidation of aqueous bromide ions by hydroxyl radicals. A pulse radiolytic investigation. *J. Phys. Chem.* **1972**, *76*, 312−319.
(59) von Gunten, U.; Hoigné, J. Ozonation of bromide-containing waters: Bromate formation through ozone and hydroxyl radicals. In *Disinfection By-Products in Water Treatment*; Minear, R. A., Amy, G. L., Eds.; CRC Press: Boca Raton, FL, 1996; pp 187−206.
(60) Symons, J. M.; Zheng, M. C. H. H. Technical Note: Does hydroxyl radical oxidize bromide to bromate? *J. Am. Water Works Assoc* **1997**, *89*, 106−109.
(61) von Gunten, U.; Oliveras, Y. Advanced Oxidation of Bromide-Containing Waters: Bromate Formation Mechanisms. *Environ. Sci. Technol.* **1998**, *32*, 63−70.
(62) von Gunten, U.; Oliveras, Y. Kinetics of the reaction between hydrogen peroxide and hypobromous acid: Implication on water treatment and natural systems. *Water Res.* **1997**, *31*, 900−906.
(63) Buxton, G. V.; Dainton, F. Radical and Molecular Yields in the γ-Radiolysis of Water. V. The Sodium Hypobromite System. *Proc. R. Soc. A* **1968**, *304*, 441−447.
(64) Canonica, S.; Kohn, T.; Mac, M.; Real, F. J.; Wirz, J.; von Gunten, U. Photosensitizer method to determine rate constants for the reaction of carbonate radical with organic compounds. *Environ. Sci. Technol.* **2005**, *39*, 9182−9188.
(65) Field, R. J.; Raghavan, N. V.; Brummer, J. G. A pulse radiolysis investigation of the reactions of $BrO_2\cdot$ with $Fe(CN)_6^{4-}$, Mn(II), phenoxide ion, and phenol. *J. Phys. Chem.* **1982**, *86*, 2443−2449.
(66) Lei, Y.; Lei, X.; Westerhoff, P.; Tong, X.; Ren, J.; Zhou, Y.; Cheng, S.; Ouyang, G.; Yang, X. Bromine Radical (Br• and $Br_2^{\bullet-}$) Reactivity with Dissolved Organic Matter and Brominated Organic Byproduct Formation. *Environ. Sci. Technol.* **2022**, *56*, 5189−5199.
(67) Lim, S.; Barrios, B.; Minakata, D.; von Gunten, U. Reactivity of Bromine Radical with Dissolved Organic Matter Moieties and Monochloramine: Effect on Bromate Formation during Ozonation. *Environ. Sci. Technol.* **2023**, DOI: 10.1021/acs.est.2c07694.
(68) Lei, Y.; Lei, X.; Yu, Y.; Li, K.; Li, Z.; Cheng, S.; Ouyang, G.; Yang, X. Rate Constants and Mechanisms for Reactions of Bromine Radicals with Trace Organic Contaminants. *Environ. Sci. Technol.* **2021**, *55*, 10502−10513.
(69) Song, R. Ozone-Bromide-NOM interactions in water treatment. Ph.D. Dissertation, University of Illinois at Urbana-Champaign, Urbana, IL, 1996.
(70) von Gunten, U.; Bruchet, A.; Costentin, E. Bromate formation in advanced oxidation processes. *J. Am. Water Works Assoc* **1996**, *88*, 53−65.
(71) Westerhoff, P.; Song, R.; Amy, G.; Minear, R. Numerical Kinetic Models for Bromide Oxidation To Bromine And Bromate. *Water Res.* **1998**, *32*, 1687−1699.
(72) Westerhoff, P.; Song, R.; Amy, G.; Minear, R. NOM's role in bromine and bromate formation during ozonation. *J. Am. Water Works Assoc* **1998**, *90*, 82−94.
(73) Song, R.; Westerhoff, P.; Minear, R.; Amy, G. Bromate minimization during ozonation. *J. Am. Water Works Assoc* **1997**, *89*, 69−78.
(74) Elovitz, M. S.; von Gunten, U.; Kaiser, H. P. Hydroxyl radical/ozone ratios during ozonation processes. II. The effect of temperature, pH, alkalinity, and DOM properties. *Ozone Sci. Eng.* **2000**, *22*, 123−150.
(75) Elovitz, M. S.; von Gunten, U.; Kaiser, H.-P. The Influence of Dissolved Organic Matter Character on Ozone Decomposition Rates and R_{ct}. *Natural Organic Matter and Disinfection By-Products*; American Chemical Society: Washington, DC, 2000; pp 248−269.
(76) Elovitz, M. S.; von Gunten, U. Hydroxyl radical/ozone ratios during ozonation processes. I. The R_{ct} concept. *Ozone Sci. Eng.* **1999**, *21*, 239−260.
(77) Yong, E. L.; Lin, Y. P. Incorporation of initiation, promotion and inhibition in the Rct concept and its application in determining the initiation and inhibition capacities of natural water in ozonation. *Water Res.* **2012**, *46*, 1990−1998.
(78) Gulde, R.; Clerc, B.; Rutsch, M.; Helbing, J.; Salhi, E.; McArdell, C. S.; von Gunten, U. Oxidation of 51 micropollutants during drinking water ozonation: Formation of transformation products and their fate during biological post-filtration. *Water Res.* **2021**, *207*, 117812.
(79) Gulde, R.; Rutsch, M.; Clerc, B.; Schollee, J.; von Gunten, U.; McArdell, C. S. Formation of transformation products during ozonation of secondary wastewater effluent and their fate in post-treatment: From laboratory- to full-scale. *Water Res.* **2021**, *200*, 117200.
(80) Buffle, M.-O.; Schumacher, J.; Meylan, S.; Jekel, M.; von Gunten, U. Ozonation and Advanced Oxidation of Wastewater: Effect of O_3 Dose, pH, DOM and HO• Scavengers on Ozone Decomposition and HO• Generation. *Ozone Sci. Eng.* **2006**, *28*, 247−259.
(81) Morrison, C. M.; Hogard, S.; Pearce, R.; Gerrity, D.; von Gunten, U.; Wert, E. C. Ozone disinfection of waterborne pathogens and their surrogates: A critical review. *Water Res.* **2022**, *214*, 118206.
(82) Kaiser, H. P.; Koster, O.; Gresch, M.; Perisset, P. M. J.; Jaggi, P.; Salhi, E.; von Gunten, U. Process Control for Ozonation Systems: A Novel Real-Time Approach. *Ozone Sci. Eng.* **2013**, *35*, 168−185.
(83) Dickenson, E. R. V.; Summers, R. S.; Croué, J. P.; Gallard, H. Haloacetic acid and trihalomethane formation from the chlorination and bromination of aliphatic β-Dicarbonyl acid model compounds. *Environ. Sci. Technol.* **2008**, *42*, 3226−3233.
(84) Heeb, M. B.; Kristiana, I.; Trogolo, D.; Arey, J. S.; von Gunten, U. Formation and reactivity of inorganic and organic chloramines and bromamines during oxidative water treatment. *Water Res.* **2017**, *110*, 91−101.
(85) Houska, J.; Salhi, E.; Walpen, N.; von Gunten, U. Oxidant-reactive carbonous moieties in dissolved organic matter: Selective quantification by oxidative titration using chlorine dioxide and ozone. *Water Res.* **2021**, *207*, 117790.
(86) Buxton, G. V.; Elliot, A. J. Rate constant for reaction of hydroxyl radicals with bicarbonate ions. Int. J. Radiat. *Appl. Instrumentation. Part* **1986**, *27*, 241−243.
(87) Buxton, G. V.; Greenstock, C. L.; Helman, W. P.; Ross, A. B. Critical Review of Rate Constants for Reactions of Hydrated Electrons, Hydrogen Atoms and Hydroxyl Radicals in Aqueous Solutions. *J. Phys. Chem. Ref. Data* **1988**, *17*, 513−5486.
(88) Matthew, B. M.; Anastasio, C. A chemical probe technique for the determination of reactive halogen species in aqueous solution: Part 1 - Bromide solutions. *Atmos. Chem. Phys.* **2006**, *6*, 2423−2437.
(89) Ianni, J. C. *Kintecus*, ver. 6.51; 2018.
(90) Staehelin, J.; Hoigné, J. Decomposition of Ozone in Water in the Presence of Organic Solutes Acting as Promoters and Inhibitors of Radical Chain Reactions. *Environ. Sci. Technol.* **1985**, *19*, 1206−1213.
(91) Tomiyasu, H.; Fukutomi, H.; Gordon, G. Kinetics and Mechanism of Ozone Decomposition in Basic Aqueous Solution. *Inorg. Chem.* **1985**, *24*, 2962−2966.
(92) Westerhoff, P.; Song, R.; Amy, G.; Minear, R. Applications of ozone decomposition models. *Ozone Sci. Eng.* **1997**, *19*, 55−73.
(93) Westerhoff, P.; Song, R.; Amy, G.; Minear, R. Numerical kinetic models for bromide oxidation to bromine and bromate. *Water Res.* **1998**, *32*, 1687−1699.
(94) Li, W. T.; Cao, M. J.; Young, T.; Ruffino, B.; Dodd, M.; Li, A.-M.; Korshin, G. Application of UV absorbance and fluorescence indicators to assess the formation of biodegradable dissolved organic carbon and bromate during ozonation. *Water Res.* **2017**, *111*, 154−162.
(95) Soltermann, F.; Abegglen, C.; Tschui, M.; Stahel, S.; von Gunten, U. Options and limitations for bromate control during ozonation of wastewater. *Water Res.* **2017**, *116*, 76−85.

(96) Siddiqui, M.; Amy, G.; Ozekin, K.; Westerhoff, P. Empirically and Theoretically-Based Models for Predicting Brominated Ozonated by-Products. *Ozone: Sci. Eng.* **1994**, *16*, 157−178.
(97) Aljundi, I. H. Bromate formation during ozonation of drinking water: A response surface methodology study. *Desalination* **2011**, *277*, 24−28.
(98) Moslemi, M.; Davies, S. H.; Masten, S. J. Empirical modeling of bromate formation during drinking water treatment using hybrid ozonation membrane filtration. *Desalination* **2012**, *292*, 113−118.
(99) Song, R.; Donohoe, C.; Minear, R.; Westerhoff, P.; Ozekin, K.; Amy, G. Empirical Modeling of Bromate Formation During Ozonation of Bromide-Containing Waters. *Water Res.* **1996**, *30*, 1161−1168.
(100) Galey, C.; Sohn, J.; Amy, G.; Cavard, J. Modeling Bromate Formation at the Full Scale: A Comparison of Three Ozonation Plants. Amererican Water Works Association Water Quality and Technology Conference. 1997.
(101) Sohn, J.; Amy, G.; Cho, J.; Lee, Y.; Yoon, Y. Disinfectant decay and disinfection by-products formation model development: Chlorination and ozonation by-products. *Water Res.* **2004**, *38*, 2461−2478.
(102) Legube, B.; Parinet, B.; Gelinet, K.; Berne, F.; Croue, J. P. Modeling of bromate formation by ozonation of surface waters in drinking water treatment. *Water Res.* **2004**, *38*, 2185−2195.
(103) Van Der Helm, A. W. C.; Smeets, P. W. M. H.; Baars, E. T.; Rietveld, L. C.; Van Dijk, J. C. Modeling of ozonation for dissolved ozone dosing. *Ozone Sci. Eng.* **2007**, *29*, 379−389.
(104) Mizuno, T.; Tsuno, H.; Yamada, H. A simple model to predict formation of bromate ion and hypobromous acid/hypobromite ion through hydroxyl radical pathway during ozonation. *Ozone Sci. Eng.* **2007**, *29*, 3−11.
(105) Jarvis, P.; Parsons, S. A.; Smith, R. Modeling bromate formation during ozonation. *Ozone Sci. Eng.* **2007**, *29*, 429−442.
(106) Civelekoglu, G.; Yigit, N. O.; Diamadopoulos, E.; Kitis, M. Prediction of bromate formation using multi-linear regression and artificial neural networks. *Ozone Sci. Eng.* **2007**, *29*, 353−362.
(107) Kimbrough, D. E.; Suffet, I. H. Electrochemical removal of bromide and reduction of THM formation potential in drinking water. *Water Res.* **2002**, *36*, 4902−4906.
(108) Kimbrough, D. E.; Suffet, I. H. Electrochemical process for the removal of bromide from California state project water. *J. Water Supply Res. Technol.—AQUA* **2006**, *55*, 161−167.
(109) von Gunten, U. Oxidation Processes in Water Treatment: Are We on Track? *Environ. Sci. Technol.* **2018**, *52*, 5062−5075.
(110) Haag, W. R.; Hoigné, J.; Bader, H. Improved ammonia oxidation by ozone in the presence of bromide ion during water treatment. *Water Res.* **1984**, *18*, 1125−1128.
(111) Hsu, S.; Singer, P. C. Removal of bromide and natural organic matter by anion exchange. *Water Res.* **2010**, *44*, 2133−2140.
(112) Singer, P. C.; Schneider, M.; Edwards-Brandt, J.; Budd, G. C. MIEX for removal of DBP precursors: Pilot-plant findings. *J. Am. Water Work. Assoc.* **2007**, *99*, 128−139.
(113) Johnson, C. J.; Singer, P. C. Impact of a magnetic ion exchange resin on ozone demand and bromate formation during drinking water treatment. *Water Res.* **2004**, *38*, 3738−3750.
(114) Wert, E. C.; Edwards-Brandt, J. C.; Singer, P. C.; Budd, G. C. Evaluating magnetic ion exchange resin (MIEX)® pretreatment to increase ozone disinfection and reduce bromate formation. *Ozone Sci. Eng.* **2005**, *27*, 371−379.
(115) Sun, Y.; Zhou, S.; Chiang, P.-C.; Shah, K. J. Evaluation and optimization of enhanced coagulation process: Water and energy nexus. *Water-Energy Nexus* **2019**, *2*, 25−36.
(116) Wert, E. C.; Gonzales, S.; Dong, M. M.; Rosario-Ortiz, F. L. Evaluation of enhanced coagulation pretreatment to improve ozone oxidation efficiency in wastewater. *Water Res.* **2011**, *45*, 5191−5199.
(117) Wert, E. C.; Lew, J.; Rakness, K. L. Effect of ozone dissolution systems on ozone exposure and bromate formation. *J. Am. Water Works Assoc.* **2017**, *109*, E302−E312.
(118) Rakness, K. L.; Hunter, G.; Lew, J.; Mundy, B.; Wert, E. C. Design Considerations for Cost-Effective Ozone Mass Transfer in Sidestream Systems. *Ozone Sci. Eng.* **2018**, *40*, 159−172.
(119) Liang, S.; Yun, T. I.; Krasner, S. W.; Yates, R. S. Evaluation of Emerging Bromate Control Strategies. *Water Pract. Technol.* **2010**, *5* (3), wpt2010064.
(120) Williams, M. D.; Coffey, B. M.; Krasner, S. W. Evaluation of pH and ammonia for controlling bromate during *Cryptosporidium* disinfection. *J. Am. Water Works Assoc.* **2003**, *95*, 82−93.
(121) Wajon, J. E.; Morris, J. C. Rates of Formation of N-Bromo Amines in Aqueous Solution. *Inorg. Chem.* **1982**, *21*, 4258−4263.
(122) Haag, W. R.; Hoigné, J. Kinetics and products of the reactions of ozone with various forms of chlorine and bromine in water. *Ozone Sci. Eng.* **1984**, *6*, 103−114.
(123) Ikehata, K.; Wang, L.; Nessl, M. B.; Komor, A. T.; Cooper, W. J.; McVicker, R. R. Effect of Ammonia and Chloramine Pretreatment during the Ozonation of a Colored Groundwater with Elevated Bromide. *Ozone Sci. Eng.* **2013**, *35*, 438−447.
(124) Wert, E. C.; Neemann, J. J.; Johnson, D.; Rexing, D.; Zegers, R. Pilot-scale and full-scale evaluation of the chlorine-ammonia process for bromate control during ozonation. *Ozone Sci. Eng.* **2007**, *29*, 363−372.
(125) Buffle, M.-O.; Galli, S.; von Gunten, U. Enhanced Bromate Control during Ozonation: The Chlorine-Ammonia Process. *Environ. Sci. Technol.* **2004**, *38*, 5187−5195.
(126) Gleason, J. M.; McKay, G.; Ishida, K. P.; Mezyk, S. P. Temperature dependence of hydroxyl radical reactions with chloramine species in aqueous solution. *Chemosphere* **2017**, *187*, 123−129.
(127) Poskrebyshev, G. A.; Huie, R. E.; Neta, P. Radiolytic Reactions of Monochloramine in Aqueous Solutions. *J. Phys. Chem. A* **2003**, *107*, 7423−7428.
(128) Gazda, M.; Margerum, D. W. Reactions of Monochloramine with Br_2, Br_3^-, HOBr, OBr^-: Formation of Bromochloramines. *Inorg. Chem.* **1994**, *33*, 118−123.
(129) Pearce, R.; Hogard, S.; Buehlmann, P.; Salazar-Benites, G.; Wilson, C.; Bott, C. Evaluation of preformed monochloramine for bromate control in ozonation for potable reuse. *Water Res.* **2022**, *211*, 118049.
(130) Luh, J.; Mariñas, B. J. Kinetics of bromochloramine formation and decomposition. *Environ. Sci. Technol.* **2014**, *48*, 2843−2852.
(131) Staehelin, J.; Hoigné, J. Decomposition of Ozone in Water: Rate of Initiation by Hydroxide Ions and Hydrogen Peroxide. *Environ. Sci. Technol.* **1982**, *16*, 676−681.
(132) Merle, T.; Pronk, W.; von Gunten, U. MEMBRO$_3$X, a novel combination of a membrane contactor with advanced oxidation (O_3/H_2O_2) for simultaneous micropollutant abatement and bromate minimization. *Environ. Sci. Technol. Lett.* **2017**, *4*, 180−185.
(133) Yu, J.; Wang, Y.; Wang, Q.; Wang, Z.; Zhang, D.; Yang, M. Implications of bromate depression from H_2O_2 addition during ozonation of different bromide-bearing source waters. *Chemosphere* **2020**, *252*, 126596.
(134) Hübner, U.; Zucker, I.; Jekel, M. Options and limitations of hydrogen peroxide addition to enhance radical formation during ozonation of secondary effluents. *J. Water Reuse Desalin.* **2015**, *5*, 8−16.
(135) Lee, Y.; Gerrity, D.; Lee, M.; Gamage, S.; Pisarenko, A.; Trenholm, R. A.; Canonica, S.; Snyder, S. A.; von Gunten, U. Organic Contaminant Abatement in Reclaimed Water by UV/H_2O_2 and a Combined Process consisting of O_3/H_2O_2 followed by UV/H_2O_2: Prediction of abatement efficiency, energy consumption, and by-product formation. *Environ. Sci. Technol.* **2016**, *50* (7), 3809−3819.
(136) Gamage, S.; Gerrity, D.; Pisarenko, A. N.; Wert, E. C.; Snyder, S. A. Evaluation of Process Control Alternatives for the Inactivation of Escherichia coli, MS2 Bacteriophage, and Bacillus subtilis Spores during Wastewater Ozonation. *Ozone Sci. Eng.* **2013**, *35*, 501−513.
(137) Wolf, C.; von Gunten, U.; Kohn, T. Kinetics of Inactivation of Waterborne Enteric Viruses by Ozone. *Environ. Sci. Technol.* **2018**, *52*, 2170−2177.
(138) Bowman, R. H. HiPOx Advanced Oxidation of TBA and MTBE in Groundwater. In *Contaminated Soils, Sediments, and Water: Science in the Real World*; Calabrese, E. J., Kostecki, P. T., Dragun, J., Eds.; Springer US, 2005; pp 299−213.
(139) Bourgin, M.; Borowska, E.; Helbing, J.; Hollender, J.; Kaiser, H.-P.; Kienle, C.; McArdell, C. S.; Simon, E.; von Gunten, U. Effect of

https://doi.org/10.1021/acs.est.3c00538
Environ. Sci. Technol. 2023, 57, 18393−18409

operational and water quality parameters on conventional ozonation and the advanced oxidation process O_3/H_2O_2: Kinetics of micropollutant abatement, transformation product and bromate formation in a surface water. *Water Res.* **2017**, *122*, 234−245.
(140) Lekkerkerker-Teunissen, K.; Knol, A. H.; van Altena, L. P.; Houtman, C. J.; Verberk, J. Q. J. C.; van Dijk, J. C. Serial ozone/peroxide/low pressure UV treatment for synergistic and effective organic micropollutant conversion. *Sep. Purif. Technol.* **2012**, *100*, 22−29.
(141) Antoniou, M. G.; Sichel, C.; Andre, K.; Andersen, H. R. Novel pre-treatments to control bromate formation during ozonation. *J. Hazard. Mater.* **2017**, *323*, 452−459.
(142) Legube, B. Catalytic ozonation: a promising advanced oxidation technology for water treatment. *Catal. Today* **1999**, *53*, 61−72.
(143) Li, W.; Lu, X.; Xu, K.; Qu, J.; Qiang, Z. Cerium incorporated MCM-48 (Ce-MCM-48) as a catalyst to inhibit bromate formation during ozonation of bromide-containing water: Efficacy and mechanism. *Water Res.* **2015**, *86*, 2−8.
(144) De Franceschi, L.; Heiniger, B.; Murillo, A.; Mende, K.; Baumgarten, S.; Bornemann, C.; Fischer, F.; Hachenberg, M.; Taudien, Y.; Kolisch, G. A bromate-free solution to remove micropollutants. IOA Conference and Exhibition. 2022.
(145) Gyparakis, S.; Diamadopoulos, E. Formation and reverse osmosis removal of bromate ions during ozonation of groundwater in coastal areas. *Sep. Sci. Technol.* **2007**, *42*, 1465−1476.
(146) Van Der Hoek, J. P.; Rijnbende, D. O.; Lokin, C. J. A.; Bonne, P. A. C.; Loonen, M. T.; Hofman, J. A. M. H. Electrodialysis as an alternative for reverse osmosis in an integrated membrane system. *Desalination* **1998**, *117*, 159−172.
(147) Lin, D.; Liang, H.; Li, G. Factors affecting the removal of bromate and bromide in water by nanofiltration. *Environ. Sci. Pollut. Res.* **2020**, *27*, 24639−24649.
(148) Marron, E. L.; Mitch, W. A.; von Gunten, U.; Sedlak, D. L. A Tale of Two Treatments: The Multiple Barrier Approach to Removing Chemical Contaminants during Potable Water Reuse. *Acc. Chem. Res.* **2019**, *52*, 615−622.
(149) Siddiqui, M.; Zhai, W.; Amy, G.; Mysore, C. Bromate ion removal by activated carbon. *Water Res.* **1996**, *30*, 1651−1660.
(150) Kirisits, M. J.; Snoeyink, V. L.; Kruithof, J. C. The reduction of bromate by granular activated carbon. *Water Res.* **2000**, *34*, 4250−4260.
(151) Bourgin, M.; Beck, B.; Boehler, M.; Borowska, E.; Fleiner, J.; Salhi, E.; Teichler, R.; von Gunten, U.; Siegrist, H.; McArdell, C. S. Evaluation of a full-scale wastewater treatment plant upgraded with ozonation and biological post-treatments: Abatement of micro-pollutants, formation of transformation products and oxidation by-products. *Water Res.* **2018**, *129*, 486−498.
(152) Zimmermann, S. G.; Wittenwiler, M.; Hollender, J.; Krauss, M.; Ort, C.; Siegrist, H.; von Gunten, U. Kinetic assessment and modeling of an ozonation step for full-scale municipal wastewater treatment: Micropollutant oxidation, by-product formation and disinfection. *Water Res.* **2011**, *45*, 605−617.
(153) Hollender, J.; Zimmermann, S. G.; Koepke, S.; Krauss, M.; McArdell, C. S.; Ort, C.; Singer, H.; von Gunten, U.; Siegrist, H. Elimination of organic micropollutants in a municipal wastewater treatment plant upgraded with a full-scale post-ozonation followed by sand filtration. *Environ. Sci. Technol.* **2009**, *43*, 7862−7869.
(154) Bao, M. L.; Griffini, O.; Santianni, D.; Barbieri, K.; Burrini, D.; Pantani, F. Removal of bromate ion from water using granular activated carbon. *Water Res.* **1999**, *33*, 2959−2970.
(155) Huang, W. J.; Chen, L. Y. Assessing the effectiveness of ozonation followed by GAC filtration in removing bromate and assimilable organic carbon. *Environ. Technol.* **2004**, *25*, 403−412.
(156) Zhang, Y. Q.; Wu, Q. P.; Zhang, J. M.; Yang, X. H. Removal of bromide and bromate from drinking water using granular activated carbon. *J. Water Health* **2015**, *13*, 73−78.
(157) Asami, M.; Aizawa, T.; Morioka, T.; Nishijima, W.; Tabata, A.; Magara, Y. Bromate removal during transition from new granular activated carbon (GAC) to biological activated carbon (BAC). *Water Res.* **1999**, *33*, 2797−2804.
(158) Chen, W.-f.; Zhang, Z. Y.; Li, Q.; Wang, H. Y. Adsorption of bromate and competition from oxyanions on cationic surfactant-modified granular activated carbon (GAC). *Chem. Eng. J.* **2012**, *203*, 319−325.
(159) Kirisits, M. J.; Snoeyink, V. L. Reduction of bromate in a BAC filter. *J. Am. Water Works Assoc.* **1999**, *91*, 74−84.
(160) Kirisits, M. J.; Snoeyink, V. L.; Inan, H.; Chee-Sanford, J. C.; Raskin, L.; Brown, J. C. Water quality factors affecting bromate reduction in biologically active carbon filters. *Water Res.* **2001**, *35*, 891−900.
(161) Kirisits, M. J.; Snoeyink, V. L.; Chee-Sanford, J. C.; Daugherty, B. J.; Brown, J. C.; Raskin, L. Effects of operating conditions on bromate removal efficiency in BAC filters. *J. Am. Water Works Assoc.* **2002**, *94*, 182−193.
(162) Matos, C. T.; Velizarov, S.; Reis, M. A. M.; Crespo, J. G. Removal of bromate from drinking water using the ion exchange membrane bioreactor concept. *Environ. Sci. Technol.* **2008**, *42*, 7702−7708.
(163) Wiśniewski, J. A.; Kabsch-Korbutowicz, M. Bromate removal in the ion-exchange process. *Desalination* **2010**, *261*, 197−201.
(164) Chubar, N. I.; Samanidou, V. F.; Kouts, V. S.; Gallios, G. G.; Kanibolotsky, V. A.; Strelko, V. V.; Zhuravlev, I. Z. Adsorption of fluoride, chloride, bromide, and bromate ions on a novel ion exchanger. *J. Colloid Interface Sci.* **2005**, *291*, 67−74.
(165) Mestri, S.; Dogan, S.; Tizaoui, C. Bromate Removal from Water Using Ion Exchange Resin: Batch and Fixed Bed Column Performance. *Ozone: Sci. Eng.* **2023**, *45*, 291−304.
(166) Naushad, M.; Alothman, Z. A.; Khan, M. R.; Wabaidur, S. M. Removal of Bromate from Water Using De-Acidite FF-IP Resin and Determination by Ultra-Performance Liquid Chromatography-Tandem Mass Spectrometry. *Clean - Soil, Air, Water* **2013**, *41*, 528−533.
(167) Wisniewski, J. A.; Kabsch-Korbutowicz, M.; Łakomska, S. Removal of bromate ions from water in the processes with ion-exchange membranes. *Sep. Purif. Technol.* **2015**, *145*, 75−82.
(168) Chen, R.; Yang, Q.; Zhong, Y.; Li, X.; Liu, Y.; Li, X.-M.; Du, W.-X.; Zeng, G.-M. Sorption of trace levels of bromate by macroporous strong base anion exchange resin: Influencing factors, equilibrium isotherms and thermodynamic studies. *Desalination* **2014**, *344*, 306−312.
(169) Hübner, U.; Kuhnt, S.; Jekel, M.; Drewes, J. E. Fate of bulk organic carbon and bromate during indirect water reuse involving ozone and subsequent aquifer recharge. *J. Water Reuse Desalin.* **2016**, *6*, 413−420.
(170) Wang, F.; van Halem, D.; Ding, L.; Bai, Y.; Lekkerkerker-Teunissen, K.; van der Hoek, J. P. Effective removal of bromate in nitrate-reducing anoxic zones during managed aquifer recharge for drinking water treatment: Laboratory-scale simulations. *Water Res.* **2018**, *130*, 88−97.
(171) Hijnen, W. A. M.; Jong, R.; Van Der Kooij, D. Bromate removal in a denitrifying bioreactor used in water treatment. *Water Res.* **1999**, *33*, 1049−1053.
(172) Wang, F.; Salgado, V.; van der Hoek, J. P.; van Halem, D. Bromate reduction by iron(II) during managed aquifer recharge: A laboratory-scale study. *Water (Basel, Switz.)* **2018**, *10*, 370.
(173) Demirel, S.; Uyanik, I.; Yurtsever, A.; çelikten, H.; Uçar, D. Simultaneous bromate and nitrate reduction in water using sulfur-utilizing autotrophic and mixotrophic denitrification processes in a fixed bed column reactor. *Clean - Soil, Air, Water* **2014**, *42*, 1185−1189.
(174) Chairez, M.; Luna-Velasco, A.; Field, J. A.; Ju, X.; Sierra-Alvarez, R. Reduction of bromate by biogenic sulfide produced during microbial sulfur disproportionation. *Biodegradation* **2010**, *21*, 235−244.
(175) Listiarini, K.; Tor, J. T.; Sun, D. D.; Leckie, J. O. Hybrid coagulation-nanofiltration membrane for removal of bromate and humic acid in water. *J. Membr. Sci.* **2010**, *365*, 154−159.
(176) Gordon, G.; Gauw, R. D.; Emmert, G. L.; Walters, B. D.; Bubnis, B. Chemical Reduction Methods for Bromate Ion Removal. *J. Am. Water Works Assoc.* **2002**, *94*, 91−98.

https://doi.org/10.1021/acs.est.3c00538
Environ. Sci. Technol. 2023, 57, 18393−18409

(177) Qiao, J.; Feng, L.; Dong, H.; Zhao, Z.; Guan, X. Overlooked Role of Sulfur-Centered Radicals during Bromate Reduction by Sulfite. *Environ. Sci. Technol.* **2019**, *53*, 10320−10328.
(178) Siddiqui, M.; Amy, G.; Ozekin, K.; Zhai, W.; Westerhoff, P. Alternative strategies for removing bromate. *J. Am. Water Works Assoc.* **1994**, *86*, 81−96.
(179) Farkas, L.; Klein, F. S. On the photo-chemistry of some ions in solution. *J. Chem. Phys.* **1948**, *16*, 886−893.
(180) Siddiqui, M. S.; Amy, G. L.; McCollum, L. J. Bromate destruction by UV irradiation and electric arc discharge. *Ozone Sci. Eng.* **1996**, *18*, 271−290.
(181) Peldszus, S.; Andrews, S. A.; Souza, R.; Smith, F.; Douglas, I.; Bolton, J.; Huck, P. M. Effect of medium-pressure UV irradiation on bromate concentrations in drinking water, a pilot-scale study. *Water Res.* **2004**, *38*, 211−217.
(182) Altmann, J.; Ruhl, A. S.; Zietzschmann, F.; Jekel, M. Direct comparison of ozonation and adsorption onto powdered activated carbon for micropollutant removal in advanced wastewater treatment. *Water Res.* **2014**, *55*, 185−193.
(183) Ruhl, A. S.; Zietzschmann, F.; Hilbrandt, I.; Meinel, F.; Altmann, J.; Sperlich, A.; Jekel, M. Targeted testing of activated carbons for advanced wastewater treatment. *Chem. Eng. J.* **2014**, *257*, 184−190.

https://doi.org/10.1021/acs.est.3c00538
Environ. Sci. Technol. 2023, 57, 18393−18409